THE UNIVERSITY
OF BIRMINGHAM

Bioleaching of chalcopyrite

By
Woranart Jonglertjunya

A thesis submitted to
The University of Birmingham
For the degree of
DOCTOR OF PHILOSOPHY

Department of Chemical Engineering
School of Engineering
The University of Birmingham
United Kingdom
April 2003

Abstract

This research is concerned with the bioleaching of chalcopyrite ($CuFeS_2$) by *Thiobacillus ferrooxidans* (ATCC 19859), which has been carried out in shake flasks (250 ml) and a 4-litre stirred tank bioreactor. The effects of experimental factors such as initial pH, particle size, pulp density and shake flask speed have been studied in shake flasks by employing cell suspensions in the chalcopyrite concentrate with the ATCC 64 medium in the absence of added ferrous ions. The characterisation of *T. ferrooxidans* on chalcopyrite concentrate was examined by investigating the adsorption isotherm and electrophoretic mobility. Subsequently, a mechanism for copper dissolution was proposed by employing relevant experiments, including the chemical leaching of chalcopyrite by sulphuric acid and ferric sulphate solutions, bioleaching of chalcopyrite in the presence of added ferric ions, and cell attachment analysis by scanning electron microscopy. Following the above, the work then focused on the bioleaching of the chalcopyrite concentrate in a stirred tank bioreactor for the purpose of scaling up, and investigated the effects of agitation speeds. Finally, the bioleaching of low-grade copper ores has been briefly studied.

The results show that the rate of copper dissolution has a positive relationship with bacterial growth, particularly with respect to bacterial attachment, which has an important role based on adsorption isotherm and scanning electron microscopy studies. However, it is not only bacteria that play an important role in copper dissolution; also the strength of sulphuric acid can influence copper solubility. For example, copper dissolution can be achieved using a sulphuric acid solution of pH 1.5, giving a concentration of about 1 g/l copper after 25 days.

The results obtained from the adsorption isotherm of *T. ferrooxidans* and the electrophoretic mobility of chalcopyrite particles before and after interaction with each other has proved the fact that the changes in surface chemistry occurred when bacterial interactions on the mineral surface took place.

Furthermore, agitation speed have a significant influence on cell growth, metal dissolution and cell adsorption ratio when carried out in shake flasks and a stirred tank bioreactor. The bioleaching results for different shake flask speeds (i.e. 100, 200 and 300 rpm) in shake flasks displayed that shake flask speed above 100 rpm was detrimental to bacterial growth and thus copper dissolution. For the bioreactor experiments, agitation was performed within a rotor speed range of 50, 100, 150 and 200 rpm. A rotor speed of 150 rpm represents the most suitable conditions for bacterial growth and the percent extraction of copper dissolution amongst those considered.

In conclusion, the concentration of copper dissolution for all pulp densities reached its maximum at a concentration of 4.8 ± 0.2 g/l after 30 days leaching time. This indicted that copper dissolution has a limited solubility; this may be because the chalcopyrite particle surface was covered by mineral and bacterial deposits over the period of bioleaching time as described in the SEM analysis of the bioleaching surface.

Finally, this work attempted to extract copper from a low-grade ore using bioleaching techniques. However, initial bioleaching tests proved that *T. ferrooxidans* could not leach copper and iron from the low-grade copper ores due to the chemical composition of the gangue minerals (mainly carbonates). This is due to the neutralising action of carbonates, which create an environment in which the pH is too high for the acidophilic bacteria to grow.

Acknowledgements

I would like to express my thanks to my supervisors, Dr. Neil Rowson and Dr. Caroline McFarlane for their guidance, encouragement, support and invaluable help throughout this project. I would also like to thank H. Jennings, E. Mitchell, D. French and P. Plant for their technical assistance, as well as L. Draper for her clerical assistance.

I would also like to thank my colleagues for their comments, cheerfulness and friendship. I would also like to express my thanks to Dimitra, Fosco, Anya, Frank, Eng Seng for their unstinting and enjoyable friendship.

Special thanks also go to my parents, T. Jonglertjanya and S. Sapayatosok, for their unconditional love and support. Finally, I would like to thank my sister, Fon, for her understanding, patience and love.

Table of Contents

List of Figures

List of Tables

CHAPTER 1 Introduction

1.1 Copper extraction

The percentage of copper consumption worldwide has grown by about one or two percent per year since 1980 and has been projected to grow continually at this rate, because of population growth and increased world trade (Biswas and Davenport, 1994). Copper demand in the future is projected to increase because of its application in new marine uses such as ship hulls and sheathing of offshore platforms, electric vehicles, earth-coupled heat pumps, solar energy, fire sprinkler systems and nuclear waste disposal canisters (Copper Organisation, 2001 a). The increased use of copper due to its electrical conductivity, corrosion resistance, thermal conductivity and new applications has gradually led to a decrease in exploitable ore reserves. More efficient mining and extraction will ensure the continued availability of copper into the future (Biswas and Davenport, 1994).

The methods of copper extraction can be classified as either pyro-metallurgical or hydro-metallurgical (Figure 1.1). The conventional method of copper extraction is the pyro-metallurgical process (Copper Organisation, 2001 b; Moody, 2001; BHP Copper, 1996). After mining, the ore is crushed and roll milled into a fine pulp, which is then concentrated by flotation using chemical reagents. The concentrate formed is smelted and electrolytically refined. Copper cathodes of 99.9% purity may be shipped as melting stock to mills or foundries. Cathodes may also be cast into wire rod, billets, cakes or ingots, generally, as pure copper or alloyed with other metals (Copper Organisation, 2001 b). However, the smelting and refining process has been criticised over many years because of environmental concerns. Firstly the process results in

impurities (primarily toxic metals) in the waste, secondly, because of the pollution potential of the chemical reagents, and thirdly, for the vast amounts of SO_2 produced from sulphide ores during smelting (Moody, 2001).

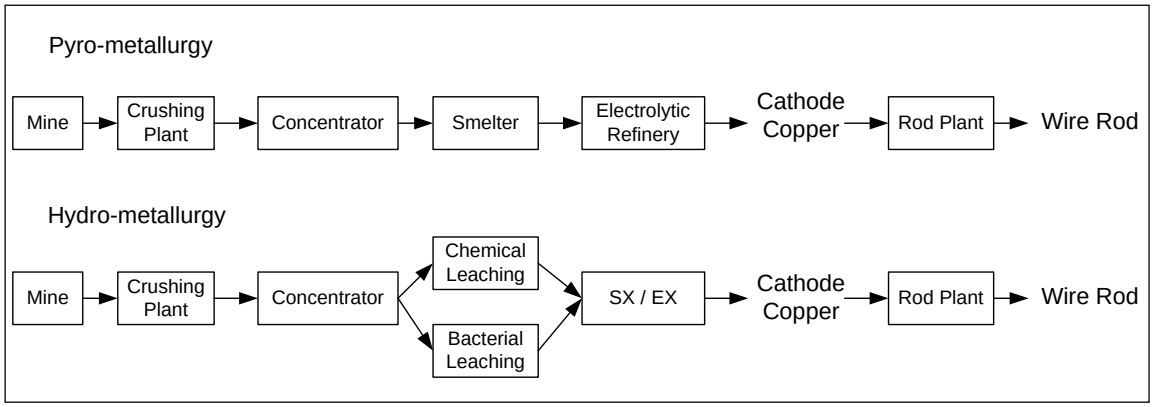

Figure 1.1 Copper extraction and concentration processes

The other method of copper extraction is the hydro-metallurgical process. In this process the ore concentrate is leached either by bacterial or by chemical methods. This is followed by the use of various techniques to concentrate the metal using ion exchange or solvent extraction and electro-winning to deliver a high-grade copper cathode (Moody, 2001). Chemical leaching may include the use of (i) gaseous oxygen at high pressures and temperatures (pressure oxidation), (ii) chlorine, (iii) nitric acid or (iv) sulphuric acid. However all of these methods with the exception of sulphuric acid leaching suffer from plant complexity and non-competitive economics (Barrett *et al.*, 1993), since the severe conditions of pressure oxidation demand a high standard of plant design and materials.

The application of bacterial oxidation processes to extract copper from copper sulphide ores offers the opportunity to develop economic, pollution-free and energy-efficient processes (Barrett *et al*., 1993). Since its origins in the mid 1960s, advocates have claimed that biohydrometallurgy is a cleaner, more environmentally friendly means of copper production (Moody, 2001).

1.2 Bioleaching

Bioleaching is the extraction of metals from ores using the principal components of water, air and microorganisms (Billiton, 2001), all of which are found readily within the environment. In the case of ores containing iron and sulphur e.g. pyrite and chalcopyrite, bioleaching is brought about by bacteria such as *Thiobacillus ferrooxidans*, *Leptospirillum ferrooxidans*, *Thiobacillus thiooxidans*, *Sulfolobus* species and others. These microorganisms derive energy from the oxidation of ferrous ions, the oxidation of sulphur and the fixation of carbon dioxide.

There are two dominant mechanisms, which are considered to be involved in bioleaching. In the first mechanism, the catalytic action of the microorganisms is responsible for the dissolution of the mineral. Most researchers have proposed that the microorganisms interact with the mineral surface directly, enhancing the rate of dissolution. Through a bacterial oxidation, the bacteria then change the metal sulphide particles into soluble sulphates therefore dissolving the metals. The first mechanism is referred to as the direct mechanism. In the second mechanism, the microbial action results in the oxidation of ferrous ions to ferric ions, and the ferric ions then chemically oxidise the sulphide minerals. This is referred to as the indirect mechanism.

Mining companies may be able to use bioleaching as a way to exploit low-grade ores and mineral resources located in areas that would otherwise be too expensive to mine. Additionally, there are several perceived advantages to using bioleaching such as (a) the use of naturally occurring key components (microorganisms, water and air), (b) the use of atmospheric pressure and ambient temperature conditions and (c) the avoidance of generation of dust and SO_2 (Billiton, 2001). Orr (2000) states that bioleaching technologies can deliver significant environmental benefits when compared to traditional smelting and other treatment methods and also capital and operating cost advantages over smelting. NRCan Biotechnology (2002) also support the assertion that bioleaching has a less harmful impact on the environment than conventional extraction methods, because it uses less energy and does not produce SO_2 emissions.

Bacterial oxidation methods for the extraction of copper have been used for the commercial production of copper. For example, one of the biggest dump leaching sites at the Kennecott Bingham Canyon Mine in Utah, USA has produced as much as 200 tonnes of copper per day which accounts for approximately 25 percent of the world's copper production (Holmes and Debus, 1991; Barrett *et al*., 1993; Bosecker, 1997). Some ore that is lower than 0.2-0.3 % copper is dumped to waste piles. In the 1950s, it was noticed that there was some blue solutions leaking from these waste piles that contained copper sulphide. After investigation, it was found that naturally occurring bacteria were oxidising the copper ore to soluble copper sulphate. These bacteria were given the name 'ferrooxidans' for their role in oxidising iron sulphides, and 'thiooxidans' for their role in oxidising sulphur. Thus, the Bingham Canyon's dump began the commercial application of bacterial leaching (Dresher, 2001). The copper was

extracted by spraying the middle of dump with bacteria, principally of the genus *Thiobacillus*. The copper rich leachate was then typically concentrated by solvent extraction and electrowinning.

Over recent years, interest in this technology has increased. The South African company Gencor pioneered commercial bioleaching reactors for refractory gold bearing sulphide concentrates. They implemented the world's first such plant at the Fairview gold mine in South Africa during 1986, which was known as BIOX® plant (Billiton, 2001). The BIOX® process utilises a mixed population of *Thiobacillus ferrooxidans*, *Thiobacillus thiooxidans* and *Leptospirillum ferrooxidans* to oxidise sulphide ore at a temperature of 40 °C. BIOX® plants for gold recovery have been commissioned with five plants still operating today. These are Fairview (South Africa), Sao Bento (Brazil), Wiluna (Western Australia), Ashanti (Ghana), and Tamboraque (Peru). BIOX® company has expanded to BioNIC™, BioCOP™ and BioZINC™ for nickel, copper, and zinc recovery respectively (Billiton, 2001).

In recent years, the use of bioleaching of copper in the industry has come of age. The most significant current application of microorganisms in this field is heap bioleaching as well as aerated stirred tank reactors. Table 1.1 summarises the commercial applications of bioleaching of copper and lists ore type, technology, microorganisms, temperature, status, and effectiveness. BioCOP™ has been operating a pilot plant process in Chile since the end of 1997 using mesophiles on concentrates of both copper oxide and copper sulphide ores (Billiton, 2001). Aerated, stirred tank bioleaching of chalcopyrite concentrates was conducted at Mt Lyell in Tasmania using a moderate

thermophile operating at 48 °C. This resulted in a 96.4 % copper extraction and 30,000 tonnes of cathode copper per year. In 2001 Mintek and BacTech launched a project involving tank bioleaching technology of copper sulphide concentrates and more particularly, of those containing chalcopyrite, which is notoriously difficult to bioleach (Pinches, 2001). In 2002, Mintek, BacTech and Peñoles joined forces in a venture to commercialise base-metal bioleaching technology at Monterrey, Mexico, with the emphasis on treating mixed sulphide and chalcopyrite–bearing concentrates. At present the plant is processing about 0.5 tonnes per day of copper concentrates in order to demonstrate the viability of the bioleaching process and to test various novel bioreactor designs that could significantly reduce costs (Pinches, 2001). However, there is a lack of specific details in the literature about organisms and conditions used in industrial applications.

In addition, a simplified flowsheet for the commercial bioleaching of chalcopyrite is shown in Figure 1.2 (Miller *et al.*, 1999). The figure below also shows the integration of bioleaching with the necessary upstream and downstream operations.

Table 1.1 Commercial application of bioleaching of copper

Project	Type	Technology	Microorganisms	Temp	Status	Effectiveness	Refs.
BioCop ™, in Chile (Chuquicamata mine)	Copper concentrate	heap bioleaching, followed by electrowinning	Mesophile, BIOX® culture	-	Commissioned 1997, In operation	n/a	Billiton, 2001
Mintek-BacTech, in Mt Lyell, Tasmania	Chalcopyrite concentrate	Aerated stirred tanks, followed by electrowinning	Moderate thermohile	48℃	Commissioned 1999, In operation	Produce 30,000 tonnes of cathode copper per year	Anthony, *et al.*, 2002
BioCop-Codelco, in Chile (Mansa Mina)	Low grade copper ore	Aerated stirred tanks, followed by electrowinning	Thermohile	n/a	Commissioned 2000, In operation	Produce 20,000 tonnes of cathode copper per year	Anthony, *et al.*, 2002, Billiton, 2001
Mintek-BacTech-Peñoles, in Monterrey, Mexico	Mixed sulphide concentrate	Aerated stirred tanks, followed by electrowinning	Moderate thermohile	n/a	Commissioned 2001, In operation	Process 0.5 tonnes/day copper concentrate	Pinches, 2001
Titan BioHeap™-China's Jinchua Corp., in Western Australia	Low grade copper and nickel ore	heap bioleaching, followed by electrowinning	Salt tolerant bacteria (several strains)	-	Commissioned 2002, In operation	Produce 800 tonnes of cathode copper from the first 5000 tonne heap	Ryan, 2002

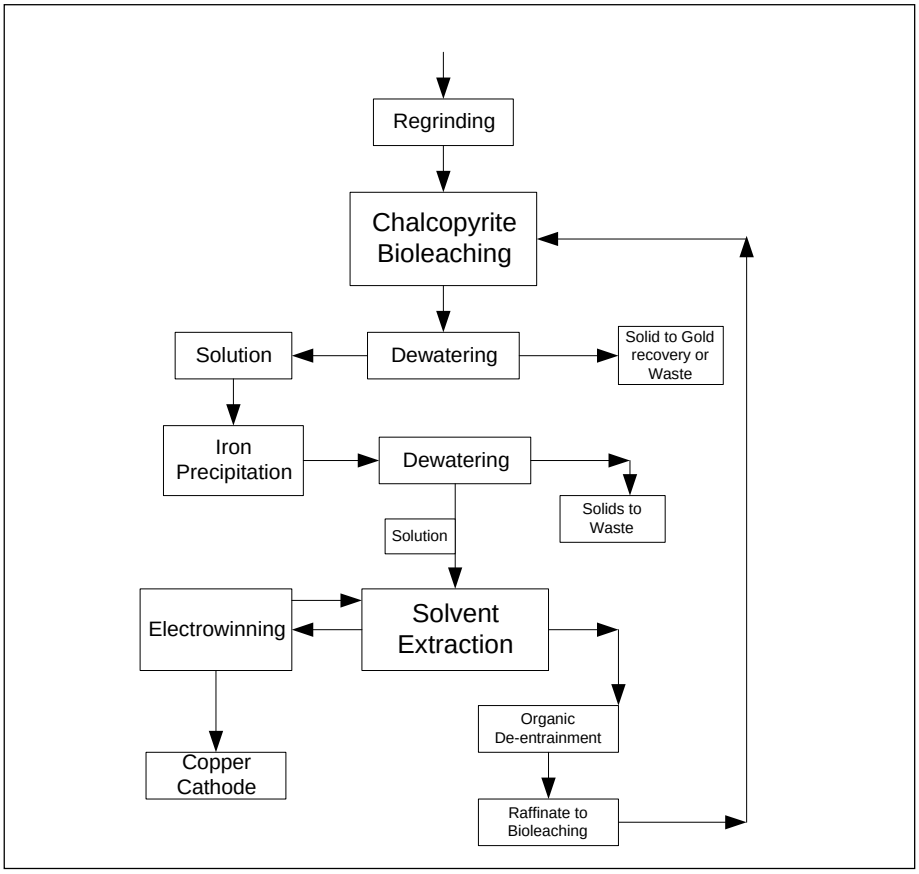

Figure 1.2 Simplified flowsheet of an integrated circuit for the bioleaching of chalcopyrite concentrate (reprinted from Miller *et al.*, 1999)

1.3 Motivation for the research

The bacterial oxidation of ores has been recognised as contributing to extraction of metal since the discovery of *Thiobacillus ferrooxidans* in 1947 (Barrett *et al.*, 1993). Although bioleaching has been studied more than 50 years, there are a number of outstanding issues that remain. For example, the bioleaching process is still slower than conventional techniques (i.e. pyro-metallurgical process), which may increase the cost. Not all ore types even those containing sulphur can be bioleached. NRCan Biotechnology (2002) points out that in some cases it is not clear how to make the bacteria stop extracting the minerals once they have started. This would be relevant to problems of acid mine drainage and reflects the lack of biochemical understanding of the leaching process. Additionally, a key success factor is the ability to control microbial growth, which is influenced by many variables: types of microorganisms, ore types, type and quantity of metal, nutrient addition, oxygen supply, pH, temperature, pulp density and agitator shear rate. The bioleaching of a given ore from different sources and/or different types of ores also requires test studies to be conducted, despite the success of metal extraction by the same bacteria in other ores. Consequently, it is necessary to find an optimum condition for a particular case.

The choice of *T. ferrooxidans* for the bioleaching of chalcopyrite is explained in the following sections:

1.3.1 Selecting *T. ferrooxidans*

A variety of chemolithotrophic bacteria, which are capable of oxidising iron- or sulphur-containing ores, can be readily isolated from the ore itself. *T. ferrooxidans* are

capable of oxidising both iron and sulphur ores, whereas some bacteria such as *L. ferrooxidans* and *T. thiooxidans* are primarily iron-oxidising and sulphur-oxidising microorganisms respectively.

Since the discovery of *T. ferrooxidans*, much research has been done. Studies on the bacteria have been conducted in several areas e.g. mechanism of bioleaching, effect of process variables, effect of genetic modification. For many years *T. ferrooxidans* were considered to be the most important microorganisms in commercial bioleaching and biobeneficiation that operate at 40 °C or less (Rawlings *et al.*, 1999).

Some researchers have studied bioleaching using pure cultures and mixed cultures, and then compared their efficiency in terms of metal dissolution. Studies have shown that oxidation of ore by mixed cultures of bacteria takes place at a higher rate than by using pure cultures (Battaglia *et al*., 1998). However, it is very complex to explain how consortia of bacteria appear to work, compared to pure culture. Thus far, no one has proposed any bioleaching model of mixed cultures. In contrast there have been some recently published new bioleaching models for individual bacterial strains, e.g. *T. ferrooxidans, L. ferrooxidans* (Tributsch, 2001; Sand *et al.,* 2001; Blight *et al.*, 2000). These recent studies have enhanced understanding of the bioleaching mechanisms.

Several researchers have shown that thermophiles can enhance achievement in the bioleaching of sulphide concentrate, particularly chalcopyrite (Billiton, 2001; Konishi *et al.,* 1999). For mining operations located in hot climates it may be worthwhile to use moderate thermophiles or extreme thermophiles in terms of energy cost, however, in

cold or temperate climates (e.g. Canada) has been shown thermophile bioleaching is not cost efficient (NRCan Biotechnology, 2002). *T. ferrooxidans* (which are mesophiles) are able to oxidise iron sulphide ore at low temperatures. Norris (1990) states that *T. ferrooxidans* can oxidise pyrite at temperatures as low as 10 °C, although temperatures about 30-35 °C are considered to be optimal (Rawlings *et al*., 1999).

In summary, the reasons for selecting *T. ferrooxidans* for this study are: (i) the bacteria can oxidise both iron- or sulphur- containing ores, (ii) there is detailed understanding of how *T. ferrooxidans* work, and (iii) *T. ferrooxidans* represents the hope for bioleaching application in cold climates.

1.3.2 Bioleaching of chalcopyrite

There are many deposits of low-grade chalcopyrite ores worldwide that are notoriously difficult to bioleach, and more particularly, those ores cannot be exploited by existing heap bioleaching methods. Additionally, it would be uneconomic to upgrade copper concentration by flotation to produce concentrates (Pinches, 2001). Successful development of the aerated stirred tank will enable the bioleaching of chalcopyrite, by way of providing improved technology in already existing copper bioleaching projects. The bioleaching process by *T. ferrooxidans* is critically dependent on successful bacterial growth under optimum conditions. Although the cell growth rate is improved by the addition of ferrous ions as the energy source, the leachates gain more iron concentrate. The presence of iron will lead to the reduction in purity of copper leachate. Although the bio-leachate solution passing through the downstream iron precipitation unit (Figure 1.2) lead to a higher overall copper purification, it also caused a 1% copper

loss in term of overall plant recovery of copper (Miller *et al.,* 1999). On the whole, the downstream iron precipitation unit increased costs. Eichrom industries developed the iron control process for copper electrolyte in order to provide copper mining facilities with an ion exchange system, which would operate with Eichrom's Diphonix® resin. The overall capacity of resin is 6-8 g of iron per litre of resin, resulting in an iron stripping efficiency of 70-80 % (Eichrom, 2002). The ion exchange system, which is extremely expensive, extracts iron from copper electrolyte before the solvent extraction-electrowinning (SX/EW) process. (Eichrom, 2002; Grotefend, 2001).

Overall, the development of a process that enhances copper dissolution but not iron dissolution from chalcopyrite would reduce the problem of the dissolved iron presence in copper leachates. Specifically, the bacteria should grow using iron from the ore itself instead of adding ferrous ions. This would minimise the amount of iron dissolution during the bioleaching process and would be less expensive than the iron precipitation process or the ion exchange process.

1.3.3 Research on the bioleaching of chalcopyrite

Much literature has been published on the bioleaching and biobeneficiation of ores. Studies have considered factors such as variables affecting bacterial growth and/or bacterial leaching, kinetic models, bacterial leaching mechanisms, reactor designs, and other related areas. According to BIDS ISI Data Service, from 1984 to 2002 approximately 200 papers have been published on the bioleaching of various mineral particles of these; 25 have studied bioleaching of chalcopyrite. Most of these consider the use of *T. ferrooxidans* and *Sulfolobus* sp. Some researchers have used selected and

isolated microbial strains from mines. Some researchers have used the bacteria that are obtained from a collection company such as the American Type Culture Collection (ATCC). These studies are summarised in Table 1.2. However only about 15 papers have been published on the optimisation of growth and bioleaching conditions (e.g. particle size, solid concentration, culture media). In some papers electrophoretic mobilities, isoelectric point, adsorption isotherm, and SEM microscopy have been used to investigate the surface characteristics of the mineral particles before and after bioleaching processes. The rest of the papers were studies on kinetic models and model simulation of the process. Consequently, some more research should be carried out in order to increase the knowledge of chalcopyrite bioleaching.

1.3.4 Industrial relevance

This work was sponsored by Rio Tinto Research & Development Division, Bristol, England. Their interest was in optimising the leaching kinetics and selectivity (for copper) of the bacterial leaching process on Chalcopyrite ores.

Key issues in the economic processing of copper sulphide ores include the time scale of the process and the simplification of the downstream processing after the bioleach stage. A fast, copper selective leaching stage with a minimal dissolution of elemental iron to complicate the downstream processing (e.g. solvent extraction, electrowinning) would give Rio Tinto a clear industrial advantage over other copper production methods.

Table 1.2 Studies on the bioleaching of chalcopyrite

Refs.	Type of bacteria	Copper content in ores	Study areas
Bhattacharya *et al.,* 1990	*T. ferrooxidans*	0.75 % Cu	Mathematical kinetic equation
Blancarte-Zurita *et al*., 1986	*T. ferrooxidans*	27.8 % Cu	Effect of particle size
Cardone *et al*., 1999	*T. ferrooxidans*	33% Cu	SEM microscopy
Devasia *et al*., 1996	*T. ferrooxidans*	50% chalcopyrite	Electrophoretic mobilites, IEP Particle size
Elzeky and Attia, 1995	*T. ferrooxidans*	100% chalcopyrite	Bacterial adaptation
Escobar *et al.,* 1996	*T. ferrooxidans*	99% chalcopyrite	measure attached bacteria using bacteria grown with radioactive (C_{14}) $NaHCO_3$
Gericke *et al*., 2001	Extreme thermophiles	66% chalcopyrite	Pilot plant: 3 stage bioleaching with 121 reactors
Gómez *et al.,* 1996 a	*Sulfolobus rivotincti*	27 % Cu	SEM microscopy
Gómez *et al.,* 1997 b	Microorganisms from mine	35% Cu	SEM microscopy and X-ray analysis in the presence of Ag^+, Hg^{2+}, Bi^{3+}
Gómez *et al.,* 1999 c	Moderate thermophiles from mine	19 % Cu	Effect of Ag^+ Effect of temperature
Hiroyoshi *et al*., 1999	*T. ferrooxidans*	29 % Cu	Effect of ferrous sulphate
Konishi *et al*., 1999	*Acidianus brierleyi*	29 % Cu	Absorption isotherm Effect of ferric ions Effect of total cell concentration Effect of solid concentration
Konishi *et al*., 2001	*Acidianus brierleyi*	29 % Cu	Bioleaching in Batch reactor and model simulation for CSTRs
Lorenzo *et al.,* 1997	Microorganisms from mine	19 % Cu	Iron oxidation rate by different type of bacteria
Mier *et al.,* 1995	*Sulfolobus* BC	22 % Cu	The influence of several metal ions
Nakazawa *et al.,* 1998	*T. ferrooxidans*	20 % Cu	Effect of activated carbon Effect of initial pH
Paponetti *et al.,* 1991	*T. ferrooxidans*	83% chalcopyrite	Effect of solid concentration
Sato *et al*., 2000	*T. ferrooxidans*	20% Cu	Effect of silver
Shrihari *et al.,* 1991	*T. ferrooxidans*	22% Cu	Effect of particle size
Stott *et al*., 2000	*S. thermosulfidooxidans*	64% chalcopyrite	The role of iron-hydroxy precipitation
Sukla *et al*., 1990	*T. ferrooxidans*	23% Cu	Effect of silver Effect of particle size
Third *et al.,* 2000	Mixed culture from mine	88% chalcopyrite	Effect of inoculum Effect of Ferrous ions Effect of Ferric ions
Third *et al.,* 2002	Mixed culture from mine	88% chalcopyrite	Control redox potential by O_2 limitation
Witne and Phillips, 2001	*T. ferrooxidans* *Sulfobacillus acidophilus* *Sulfolobus* BC65	20% Cu	Effect of air addition (O_2, CO_2) Effect of solid concentration
Yuehua *et al.,* 2002	Mixed isolated culture *T. ferrooxidans* + *T. thioooxidans* + *L. ferrooxidans*	30% Cu	Effect of silver ion

1.4 Aims and objectives

This study was concerned with the bioleaching of chalcopyrite concentrate by *Thiobacillus ferrooxidans* in the absence of added ferrous ions with the aim of enhancing copper dissolution. Initially, experiments were carried out in a shake flask in order to investigate the effects of experimental factors such as initial pH, particle size, pulp density and shake flask agitation speed on cell growth, copper and iron dissolution as a function of time. The characterisation of *T. ferrooxidans* on chalcopyrite concentrate was examined by investigating the adsorption isotherm of *T. ferrooxidans* and the electrophoretic mobility of chalcopyrite particles before and after bioleaching. Then, the mechanism of copper dissolution was proposed by employing relevant experiments including chemical leaching of chalcopyrite by sulphuric acid and ferric sulphate solutions, bioleaching of chalcopyrite in the presence of added ferric ions, and cell attachment by scanning electron microscopy.

Following the above, the work then focused on the scale up capabilities of the bioleaching, concentrating especially on the agitation rate. Ultimately the aim of this research was to apply the bioleaching techniques to extract copper from low-grade ore.

1.5 Layout of thesis

The literature review is reported in chapter 2. Firstly, an introduction to the microorganisms used in bioleaching processes (section 2.1) is presented followed by details of *Thiobacillus ferrooxidans* in section 2.2. The general mechanisms of bioleaching are then discussed in section 2.3. Finally, the operating conditions used to effect bacteria growth and metal dissolution are reviewed in section 2.4.

The experimental work is treated in chapters 3 to 7. Chapter 3 investigates the effects of operating conditions in shake flask cultures i.e. shake flask speed, particle size, initial pH and pulp density, on bioleaching of chalcopyrite concentrate. Chapter 4 is concerned with the characterisation of the interaction of *Thiobacillus ferrooxidans* with the chalcopyrite particle and includes adsorption isotherms and electrophoretic mobility measurements. The mechanisms of copper dissolution are then considered in Chapter 5. In this chapter, chemical leaching, ferric sulphate leaching and scanning electron microscopy are used to propose the mechanisms. Chapter 6 then describes work conducted on the effect of agitation speed on cell growth and bioleaching of chalcopyrite concentrate in a 4 L (working volume) stirred tank vessel. Finally, Chapter 7 includes experiments using copper low-grade for chemical leaching and bioleaching techniques in shake flask conditions. The overall conclusions of the work are then summarized in Chapter 8 together with suggestions for future work. Details of the growth of *Thiobacillus ferrooxidans*, bacterial preparation, and growth media are given in Appendix I to III respectively. Chalcopyrite concentrate and copper low-grade mineralogy reports are also presented in the Appendix IV and V respectively. Moreover, metal precipitation, buffer and adsorption results are presented in the subsequent appendices (Appendix VI to VIII).

CHAPTER 2 Literature review

2.1 Microorganisms in bioleaching processes

Microbial leaching is a procedure that refers to the natural ability of some microorganisms to solubilise some mineral constituents of rock or ore. Microbial leaching may therefore manifest itself in the extraction or mobilisation of valuable metal from an ore. When microbial attack of an ore results in metal solubilisation, the process is referred to as bioleaching. When the microbial attack of an ore influences the partial or total removal of one or more ore constituents that interfere with the extraction of the valuable metal from an ore, this process is referred to as biobeneficiation (Ehrlich, 1995). Bioleaching and biobeneficiation are aspects of biohydrometallurgy.

Two main families of microorganisms are involved in biohydrometallurgy. The first of which are chemolithotrophic bacteria, for example *Thiobacillus ferrooxidans* (*T. ferrooxidans*) and closely related species, the second are heterotrophic microbes, including bacteria, fungi and yeast, such as *Bacillus mucilaginosus*, *Aspergillus niger* and related species. Table 2.1 lists some chemolithotrophic bacteria and Table 2.2 lists some heterotrophic microbes, each with biohydrometallurgy potential.

The chemolithotrophic bacteria currently used in biohydrometallurgy are acidophiles, growing at pH values from 1.5 to 4 and autotrophs, getting their energy from the oxidative attack of the metal sulphides that they solubilise. The chemolithotrophic bacteria get their carbon for assimilation from CO_2 and their nitrogen from inorganic compounds. In contrast, the heterotrophic microbes use organic compounds as their

energy and carbon source. They also require appropriate growth conditions such as pH, and a nitrogen source.

Table 2.1 Some chemolithotrophic bacteria with biohydrometallurgy potential

Organism	Ore minerals	Refs
T. ferrooxidans	Chalcopyrite concentrate	Nakazawa *et al*, 1998
	ZnS concentrate	Blancarte-Zurita *et al*., 1986
	Pyrite concentrate	Fowler *et al*., 2001
	Covellite concentrate (CuS)	Curutchet and Donati, 2000
	Chalcopyrite low grade	Bhattacharya *et al*, 1990
	Heazelwoodite (Ni_3S_2)	Giaveno and Donati, 2001
	Sphalerite concentrate	Bállester *et al.,* 1990
T. thiooxidans	Pyrrhotite	Veglió *et al.,* 2000
T. caldus	Arsenopyrite	Dopson and Lindstrom, 1999
L. ferrooxidans	Pyrite concentrate	Boon and Heijnen, 1998
Arthrobacter sp.	Pyrolusite (MnO_2) concentrate	Cardone *et al.,* 1999
Acidianus brierleyi	Chalcopyrite concentrate	Konishi *et al.*, 1999
	Pyrite concentrate	Konishi *et al.*, 1997
Sulfobacillus thermosulfidooxidans	Pyrite and Arsenopyrite concentrate	Clark and Norris, 1996
Sulfolobus rivotincti	Chalcopyrite concentrate	Gómez *et al.,* 1999 b
Sulfolobus metallicus (BC)	Pyrite concentrate	Nemati and Harrison, 2000
Metallosphaera sedula	Pyrite concentrate	Han and Kelly, 1998

There are three main groups of the chemolithotrophic bacteria. The first of which are mesophiles, which function near 30 ºC, such as the genera *Thiobacillus* and *Leptospirillum*, the second are moderate thermophiles, which function at elevated temperatures in the range of 40 ºC to 60 ºC, such as the genus *Sulfobacillus*, the final are extreme thermophiles, which growth in the temperature range of 60 ºC to 90 ºC, such as the genera *Sulfolobus*, *Acidanus*, *Metallosphaera* and *Sulfurococcus*.

Table 2.2 Some heterotrophic microbes with biohydrometallurgy potential

Organism	Ore minerals	Refs
Bacteria		
Paenibacillus polymyxa	Low-grade bauxite	Vasan *et al.,* 2001
Fungi		
Aspergillus sp. + Penicillium *sp.*	Low-grade nickel-cobalt oxide ores	Agatzini and Tzeferis, 1997
	Low-grade Laterite ores	Valix *et al.,* 2001
	Aluminosilicate (95% spodumene)	Rezza *et al.,* 2001
Aspergillus niger	Zinc and nickel silicates	Castro *et al.,* 2000
Yeast		
Rhodotorula rubra	Aluminosilicate (95% spodumene)	Rezza *et al.,* 2001

2.1.1 *Thiobacillus*

Thiobacillus is mainly known for its ability to oxidise elemental sulphur and sulphur containing compounds, but the conditions required (such as pH, temperature) may vary depending on the physiology of each species. Bacteria of the genera *Thiobacillus* are normally strict aerobes and are either obligate or facultative chemolithotrophs or are mixotrophs. They grow in media of pH values between 0.5 and 10. Some are acidophiles, others can grow at neutral pH values. *Thiobacillus* are mesophiles having optimum temperatures for growth at around 30 °C, however, they can grow and oxidise inorganic substrates within a wide temperature range between 2 to 37 °C (Barrett *et al.*, 1993). Some *Thiobacillus* are moderately thermophilic bacteria such as *Thiobacillus caldus* (sulphur-oxidiser). These bacteria oxidise sulphur above 40 °C and have been used in bioleaching of gold from pyrite and arsenopyrite (Suzuki, 2001).

Chemolithotrophic bacteria including the genus *Thiobacillus*, can oxidise a range of sulphur compounds (i.e. S^{2-}, S°, S_2O_4, $S_2O_3^{2-}$, SO_4^{2-}). Some of the oxidation reactions are listed below.

$$H_2S + 2O_2 \rightarrow H_2SO_4$$

$$2H_2S + O_2 \rightarrow 2S° + 2H_2O$$

$$2S° + 3O_2 + 2H_2O \rightarrow 2H_2SO_4$$

$$Na_2S_2O_3 + 2O_2 + H_2O \rightarrow Na_2SO_4 + H_2SO_4$$

Moreover, some *Thiobacillus* species can derive energy from ferrous ions oxidation as follows:

$$2FeS_2 + 7O_2 + 2H_2O \rightarrow 2FeSO_4 + 2H_2SO_4$$

$$4FeSO_4 + O_2 + 2H_2SO_4 \rightarrow 2Fe_2(SO_4)_3 + 2H_2O$$

There are five main species of *Thiobacillus*, which are *Thiobacillus thioparus*, *Thiobacillus dentrificans*, *Thiobacillus thiooxidans*, *Thiobacillus intermedius*, and *Thiobacillus ferrooxidans*. The genus *Thiobacillus* can be divided into two groups on the basis of pH values for growth (Wentzel, 2001). The first of these are the species that can grow only in neutral pH values. The two species that fit this type are *T. thioparus* and *T. dentrificans*. Wentzel (2001) state that *T. thioparus* is responsible for the oxidation of sulphur ($N\text{-}C\text{-}S^- + 2O_2 + 2H_20 \rightarrow SO_4^{-2} + NH_4^+ + CO_2 + 220$ kcal/moleO_2) and *T. dentrificans* uses the same kind of reaction as *T. thioparus* except that instead of O_2, it uses NO_3^- as the terminal electron acceptor ($5S + 6KNO_3 + 2CaCO_3 \rightarrow 2CaSO_4 + 3\ K_2SO_4 + 2CO_2 + N_2$).

The second type of *Thiobacillus* are the species that grow at lower pH values, for example *T. thiooxidans*, *T. intermedius*, and *T. ferrooxidans*. *T. thiooxidans* grows

best in an acidic pH, can oxidise only sulphur and can be used for removal of accumulating sulphur from minerals during indirect leaching or in direct leaching of minerals in the absence of iron, e.g. $ZnS + 2O_2 \rightarrow Zn^{2+} + SO_4^{2-}$ (Suzuki, 2001). *T. intermedius* is a facultative chemolithotroph with a pH range of 3 to 7 and its growth is powered by $S_2O_3^{2-}$ as an electron donor (Wentzel, 2001). *T. ferrooxidans* is the dominant organism in the biohydrometallurgy field. *T. ferrooxidans* can use either ferrous ions or sulphur as an energy source and has been studied extensively as the agent of bacterial leaching (Suzuki, 2001). Since *T. ferrooxidans* is relevant to the thesis, it will be considered in detail in subsequent sections (section 2.2).

2.1.2 *Leptospirillum*

Leptospirillum ferrooxidans (*L. ferrooxidans*) is a moderately thermophilic iron-oxidiser (Johnson, 2001). *L. ferrooxidans* can oxidise only ferrous ions, but can grow at higher temperatures than the genus *Thiobacillus*, which have an optimum temperature of around 30 °C, and also at stronger acidity levels. *L. ferrooxidans* has a higher affinity for Fe^{2+} than *T. ferrooxidans* (apparent K_m 0.25 mM Fe^{2+} versus 1.34 mM for *T. ferrooxidans*, where K_m is the Michaelis constant for reactant Fe^{2+}) and a lower affinity for Fe^{3+}, a competitive inhibitor. These qualities make *L. ferrooxidans* suitable for mineral leaching under conditions of high temperature, low pH, and high Fe^{3+}/Fe^{2+} ratio. However, *T. ferrooxidans* has a faster growth rate than *L. ferrooxidans* during the initial stages of a mixed batch culture when the redox potential is low (Rawlings *et al.,* 1999), and is likely to be the dominant iron-oxidising bacterium in such a system (Rawlings *et al.,* 1999).

L. ferrooxidans also tolerates higher concentrations of uranium, molybdenum and silver than *T. ferrooxidans*, but it is more sensitive to copper and unable to oxidise sulphur or sulphur compounds by itself (Bosecker, 1997). This can be done together with sulphur-oxidising acidophiles (e.g. *T. caldus*, *T. ferrooxidans*, or *T. thiooxidans*). For example, the BIOX® plant use a mixed culture of *Thiobacillus* and *Leptospirillum* to oxidise sulphidic refractory gold concentrate (Brierley and Brierley, 2001).

2.1.3 Thermophilic bacteria

Thermophilic iron-oxidising bacteria can be divided into moderate and extreme thermophiles. Temperature optimum for growth and metal leaching are in the range between 65 and 85 °C for extreme thermophiles and about 40 to 60 °C for moderate thermophiles. A variety of thermophilic microorganisms, especially *Sulfolobus* species, have been enriched and isolated from bioleaching environments (Brandl, 2001). In general the bacteria grow chemolithotrophically at the expense of iron. Some of the bacteria are facultative autotrophs, which require the presence of small amounts of yeast extract, cysteine, or glutathione for growth.

A moderately thermophilic bacterium, *Sulfobacillus thermosulfidooxidans*, is a gram-positive, nonmotile, sporeforming, rod-shaped eubacterium. Its temperature range for growth is 28-60 °C, with an optimum around 50 °C. The bacteria are facultative autotrophs in that bacterial growth is stimulated by a trace (0.01-0.05 % (w/v)) of yeast extract, but 0.1 % (w/v) yeast extract is inhibitory (Ehrlich, 1990). The bacteria can grow autotrophically on Fe (II), S°, or metal sulphide as energy source. In summary the characteristics of *S. thermosulfidooxidans* are: (1) the bacteria incorporates CO_2 in the

presence of yeast extract, (2) no CO_2 is fixed when grown on $FeSO_4$ + yeast extract, (3) optimal growth requires yeast extract and (4) the bacteria can oxidise $FeSO_4$, CuS, FeS_2, $CuFeS_2$, NiS, or $S_4O_6^{-2}$ (Chan, 2001).

Well-studied examples of the extreme thermophiles within acidophilic iron-oxidising bacteria are *Sulfolobus acidocaldarius* and *Acidianus brierleyi* (Ehrlich, 1990; Konishi *et al*, 1999). Both are in the genera *Archaebacteria*. There are four of these genera, which are *Sulfolobus*, *Acidanus*, *Metallosphaera*, and *Sulfurococcus* (Barrett *et al.*, 1993). They are all aerobic, extremely thermophilic and acidophilic bacteria oxidising ferrous ions, elemental sulphur and sulphide minerals (Bosecker, 1997). Their temperature range of growth is between 55 and 90 °C, with an optimum in the range 70-75 °C. They grow between pH 1 and 5, with optimum growth around pH 3.0 (Gulley, 1999). All the species are facultatively chemolithotrophic and grow under autotrophic, mixotrophic or heterotrophic conditions. The organisms grow more rapidly in the presence of 0.01-0.02 % (w/v) yeast extract (Barrett *et al.*, 1993) and grow heterotrophically with yeast extract at high concentration (Ehrlich, 1990).

2.1.4 Heterotrophic microorganisms

A series of heterotrophic microorganisms (bacteria, fungi, and yeast) are also part of microbial leaching communities. In the case of oxide, carbonate and silicate ores, the use of *Thiobacillus* sp is limited because of its poor ability to extract metal (Bosecker, 1997). For such ores, research is being carried out on the use of heterotrophic bacteria and fungi. Of the heterotrophic bacteria, the genus *Bacillus* is the most effective in metal solubilisation whilst with regard to fungi the genera *Aspergillus* and *Penicillium*

are the most important ones (Bosecker, 1997). Some examples of the application of heterotrophic microorganisms in microbial leaching are the removal of silica from bauxite by using *Bacillus mucilaginosus* and *Bacillus polymyxa*, and the solubilisation of aluminum from alumino-silicates by *Asperillus niger* (Vasan *et al.*, 2001).

The heterotrophic microorganisms require organic molecules as energy sources. For example, a medium of culture *Bacillus* sp. contains 0.5 % (w/v) sucrose, essential salts, yeast extract as nitrogen source and $CaCO_3$ (Vasan *et al.*, 2001). In addition, the microorganisms also require maintenance of a pH nearer neutrality and a mesophilic temperature.

The extraction of a mineral from an ore by heterotrophic bacteria involves enzymatic reduction (Ehrlich, 1995). Several heterotrophs can contribute to metal extraction by the excretion of organic acids, for example *Bacillus megaterium* excrete citrate, *Pseudomonas putida* excrete citrate and gluconate, or *Aspergillus niger* excrete citrate, gluconate, oxalate, malate, tartrate and succinate (Brandl, 2001).

2.2 Thiobacillus ferrooxidans

2.2.1 Characteristics and physiology

Thiobacillus ferrooxidans, synonym *Ferrobacillus ferrooxidans*, appears to be the most widely studied organism in the oxidation of metal sulphides (Johnson, 2001; Ehrlich, 1990; Ehrlich, 2001; Brandl, 2001). Cells of *T. ferrooxidans* are gram-negative and rod-shaped, ranging in diameter from 0.3 to 0.8 micrometers (μm) and in length from 0.9 to 2 μm (Barrett *et at*., 1993). The bacteria are usually 0.5 by 1 to 1.5 μm and occur singly

or in pairs. Cell mobility is achieved by means of a single polar flagellum (Ehrlich, 1990). *T. ferrooxidans* are generally characterised by five main properties (Nemati *et al.*, 1998):

- Chemolithotrophic- growth and maintenance energy is derived from the oxidation of ferrous ions or reduced sulphur compounds,
- Autotrophic- carbon dioxide is used as a cellular carbon source and nitrogen and phosphorus are also needed as nutrients for growth and synthesis along with the trace minerals K, Mg, Na, Ca and Co,
- Aerobic- oxygen is essential as an electron acceptor and by contact with ambient air can provide oxygen and carbon dioxide,
- Mesophilic- bacterial growth and iron oxidation occurs at temperatures between 20 °C and 40 °C, and
- Acidophilic- bacterial growth occurs at a pH in the range of 1.5 to 6.0.

T. ferrooxidans are regarded as being obligate chemolithotrophs which derive energy for growth and maintenance from the oxidation of ferrous ions to ferric ions and the oxidation of reduced sulphur compounds. They assimilate carbon in the form of carbon dioxide via a biosynthetic cycle, namely, the Calvin-Benson cycle. Although the bacteria are classified as being obligate aerobic, i.e., oxygen is essential as a final electron acceptor in aerobic respiration, it can also grow on elemental sulphur or metal sulphides (covellite, CuS) under anaerobic condition using ferric ions as the electron acceptor (Donati *et al.*, 1997; Brandl, 2001). Oxygen and carbon dioxide can be provided by ambient air (Nagpal *et al.*, 1993). The bacteria have an optimum pH range

of 1.5 to 4 and an optimum temperature of 20 to 35 °C for growth (Nemati *et al.*, 1998).

2.2.2 Energy consideration

Iron-oxidising bacteria derive energy from the oxidation of ferrous ions ($2Fe^{2+} + ½ O_2 + 2H^+ \rightarrow 2Fe^{3+} + H_2O$), or sulphur ($S^o + 1½ O_2 + H_2O \rightarrow H_2SO_4$) and metal sulphide and also they derive carbon from CO_2 by the Calvin cycle. The overall reduction process is presented by the half-reaction ($O_2 + 4H^+ + 4e^- \rightarrow 2H_2O$).

A currently accepted model for iron-oxidising systems for *T. ferrooxidans* is shown in Figure 2.1 (Ehrlich, 1990). Regarding the model, ferrous ions are oxidised to ferric ions at the cell envelope of *T. ferrooxidans* (Ehrlich, 1990; Barrett *et al.*, 1993; Norris, 1990; Tuovinen, 1990). The electrons from this oxidation process are transferred and passed to a copper plasmic protein (rusticyanin and periplasmic cytochrome C). The reduced cytochrome C binds to the outer surface of the plasma member. Electron transfer then occurs across the membrane to cytochrome oxidase which is located on the inside surface of the plasma membrane. The reduced cytochrome oxidase reacts with O_2 and leads to the formation of water.

Energy coupling in iron oxidation by *T. ferrooxidans* is understood in terms of a chemiosmotic mechanism (Barrett *et al.*, 1993; Norris, 1990; Tuovinen, 1990). A proton motive force is set up across the plasma membrane due to charge separation on the two sides of the membrane (Figure 2.1). The proton motive force results from the pH gradient from the high proton concentration in the periplasm to the lower concentration in the cytosol and from a transmembrane electrical potential. Moreover, the electron

transport system (i.e. electron transfer to O_2) results in the movement of protons (in the form of water) from the cytoplasm into the periplasm. Energy coupling (i.e. ATP synthesis is mediated by adenosine 5′-triphosphate (ATP ase) which is anchored in the membrane with a proton channel, which allows passage of protons. Proton transport results in the synthesis of ATP (ADP + Pi $\rightarrow$ ATP).

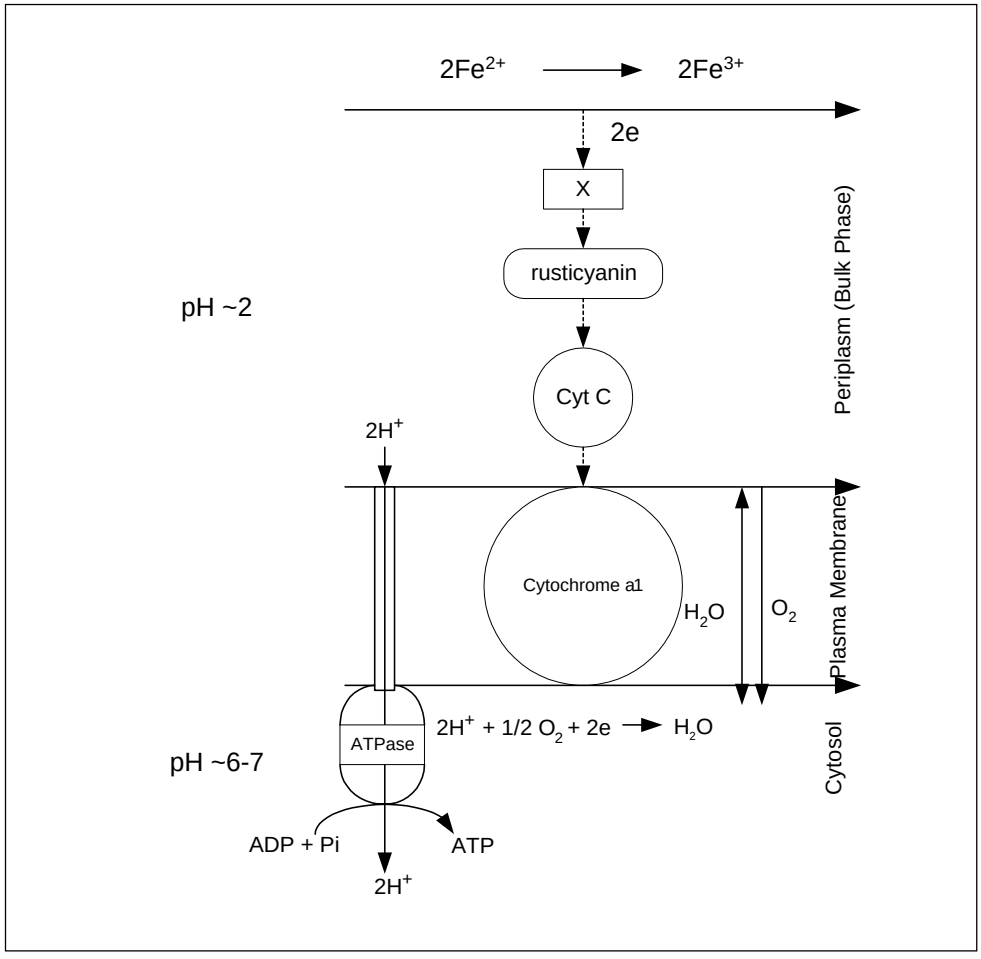

Figure 2.1 Bioenergetics of iron oxidation in *Thiobacillus ferrooxidans* (reprinted from Ehrlich, 1990)

The assimilation of CO_2 by *T. ferrooxidans* requires a source of reducing power (Fe^{2+}). Ferrous ions have a dual function in the nutrition of the bacteria, namely as a source of

energy and a source of reducing power. The mechanism of CO_2 assimilation in *T. ferrooxidans* involves the Calvin-Benson cycle (Ehrlich, 1990). CO_2 is fixed by Ribulose 1, 5-bisphosphate obtained from Ribulose 5-phosphate (Figure 2.2). The overall mechanism generates glucose ($6CO_2$ +18 ATP + 12 NADPH + $12H_2O \rightarrow C_6H_{12}O_6$ + 18ADP +18 Pi +12 $NADP^+$ + $6H^+$).

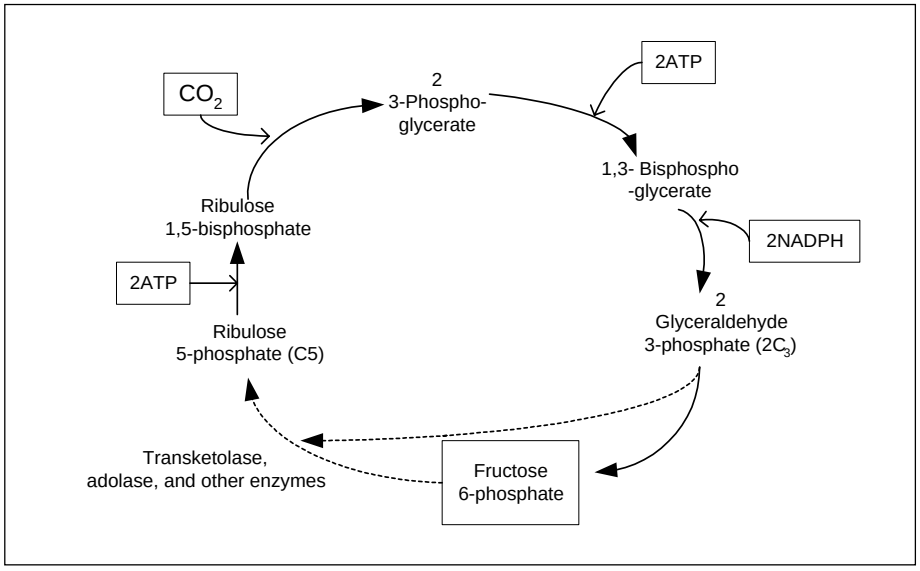

Figure 2.2 CO_2 assimilation by *Thiobacillus ferrooxidans* (reprinted from Hallick, 2001)

2.3 The general mechanisms of bioleaching

Silverman and Lundgren (1959) originally proposed a model with two different mechanisms for the bioleaching of metals. Firstly, direct leaching in which the bacterial membrane directly interacts with the sulphide surface using enzymatic mechanisms. Thus direct leaching is observed only if the cells attach to the mineral surface. Cell attachment to suspended mineral particles takes place within minutes or hours with cell preferentially occupying irregularities of the surface structure (Brandl, 2001).

Secondly, the oxidation of reduced metal through the indirect mechanisms is mediated by ferric ions (Fe^{3+}) generated from the microbial oxidation of ferrous ions (Fe^{2+}) compounds present in the mineral. Ferric ion is an oxidising agent, can oxidise metal sulphides and is chemically reduced to ferrous ions. Ferrous ions can be microbially oxidised to ferric ions again. In this case, iron has a role as electron carrier. It has been proposed that no direct physical contact is needed for the oxidation of iron (Brandl, 2001).

The following equations describe the direct and indirect mechanism for the oxidation of metal sulphides. Detailed descriptions of the two mechanisms are given by Tuovinen, 1990; Haddadin *et al.*,1995; Nemati *et al.*, 1998.

Direct mechanism:

In this process, metal sulphides can be directly oxidised by *T. ferrooxidans* to soluble metals sulphates according to equation 2.1.

$$MS + 2O_2 \xrightarrow{T.\,ferrooxidans} M^{2+} + SO_4^{2-} \qquad (2.1)$$

Because the metal sulphides exist in an insoluble form and the metal sulphate (MSO_4) is usually water soluble, this reaction is able to transform a solid phase to a liquid one to which further treatment can be provided to recover the metal. Theoretically, the mechanism can be continued until all the substrate (MS) is converted to product (MSO_4). Examples of the direct mechanism are as follows:

Pyrite : $4FeS_2 + 15O_2 + 2H_2O \rightarrow 2Fe_2(SO_4)_3 + 2H_2SO_4$

Chalcopyrite : $4CuFeS_2 + 17O_2 + 2H_2SO_4 \rightarrow 4CuSO_4 + 2Fe_2(SO_4)_3 + 2H_2O$

Chalcocite : $2Cu_2S + 5O_2 + 2H_2SO_4 \rightarrow 4CuSO_4 + 2H_2O$

Covellite : $CuS + 2O_2 \rightarrow CuSO_4$

Sphalerite : $ZnS + 2O_2 \rightarrow ZnSO_4$

Indirect mechanism

$$4FeSO_4 + 2H_2SO_4 + O_2 \xrightarrow{Thiobacillus} 2Fe_2(SO_4)_3 + 2H_2O \quad (2.2)$$

$$MS + Fe_2(SO_4)_3 \rightarrow MSO_4 + 2FeSO_4 + S° \quad (2.3)$$

The indirect mechanism is represented by the oxidation of sulphide minerals by ferric ions. Reaction (2.2) takes place under the action of *Thiobacillus*, whereas reaction (2.3) occurs chemically without any association of bacteria. The oxidation of elemental sulphur (according to equation 2.4) also occurs by *Thiobacillus*.

$$2S^o + 3O_2 + 2H_2O \xrightarrow{Thiobacillus} 4H^+ + 2SO_4^{2-} \quad (2.4)$$

Therefore, metal dissolution occurs by a cyclic process between reaction 2.2 and 2.3 and the formation of H^+ during the sulphur oxidation (equation 2.4) enhances the overall efficiency. Examples of chemical oxidation processes are as follows:

Pyrite : $FeS_2 + Fe_2(SO_4)_3 \rightarrow 3FeSO_4 + 2S°$

Chalcopyrite : $CuFeS_2 + 2Fe_2(SO_4)_3 \rightarrow CuSO_4 + 5FeSO_4 + 2S°$

Chalcocite : $Cu_2S + 2Fe_2(SO_4)_3 \rightarrow 2CuSO_4 + 4FeSO_4 + S°$

Covellite : $CuS + Fe_2(SO_4)_3 \rightarrow CuSO_4 + 2FeSO_4 + S°$

Sphalerite : $ZnS + Fe_2(SO_4)_3 \rightarrow ZnSO_4 + 2FeSO_4 + S°$

The model of direct and indirect metal leaching is still under discussion, especially the hypothesis of the direct mechanism. New insights have been derived from recent research, with more advanced techniques for the analysis of degradation products

occurring in the bioleaching process and the analysis of extracellular polymeric substances.

Recently, two indirect mechanisms have been proposed whereas no evidence for a direct enzymatically mediated process has been found (Schippers and Sand, 1999; Sand *et al*, 2001). Thiosulphate and polysulphide have been found as intermediates during the oxidation of galena, sphalerite, chalcopyrite, hauerite, orpiment, or realgar. One mechanism is based on the oxidative attack of iron (III) ions on the acid-insoluble metal sulphides FeS_2, MoS_2, and WS_2 with thiosulphate as an intermediate. The second mechanism deals with metal dissolution by the attack of ferric ions and/or by protons in which case the main sulphur intermediate is polysulphide and elemental sulphur (Figure 2.3). The following equations summarise the two mechanisms (Schippers and Sand, 1999; Sand *et al*, 2001):

Thiosulphate mechanism (for FeS_2, MoS_2, WS_2):

$$FeS_2 + 6Fe^{3+} + 3H_2O \rightarrow S_2O_3^{2-} + 7Fe^{2+} + 6H^+ \quad (2.5)$$

$$S_2O_3^{2-} + 8Fe^{3+} + 5H_2O \xrightarrow{bacteria} 2SO_4^{2-} + 8Fe^{2+} + 10H^+ \quad (2.6)$$

Polysulphide mechanism (for ZnS, $CuFeS_2$, PbS):

$$MS + Fe^{3+} + H^+ \rightarrow M^{2+} + 0.5\,H_2S_n + Fe^{2+} \; (n \geq 2) \quad (2.7)$$

$$0.5H_2S_n + Fe^{3+} \xrightarrow{bacteria} 0.125\,S_8 + Fe^{2+} + H^+ \quad (2.8)$$

$$0.125\,S_8 + 1.5\,O_2 + H_2O \xrightarrow{bacteria} SO_4^{2-} + 2H^+ \quad (2.9)$$

The main characteristic of these two mechanisms is the hypothesis that ferric ions and/or protons are the only chemical agents involved in dissolving a metal sulphide. The bacteria have the functions to regenerate the ferric ions and/or protons and then

concentrate them at the interface between sulphide surface/water or sulphide surface/bacteria cell in order to enhance the metal leaching processes (Sand *et al*, 2001). The three species of microorganisms that are implicated in this model are: *T. ferrooxidans*, *T. thiooxidans* and *L. ferrooxidans*. The determining factor is the exopolymer layer surrounding the cells in which the chemical processes take place (Sand *et al*, 2001).

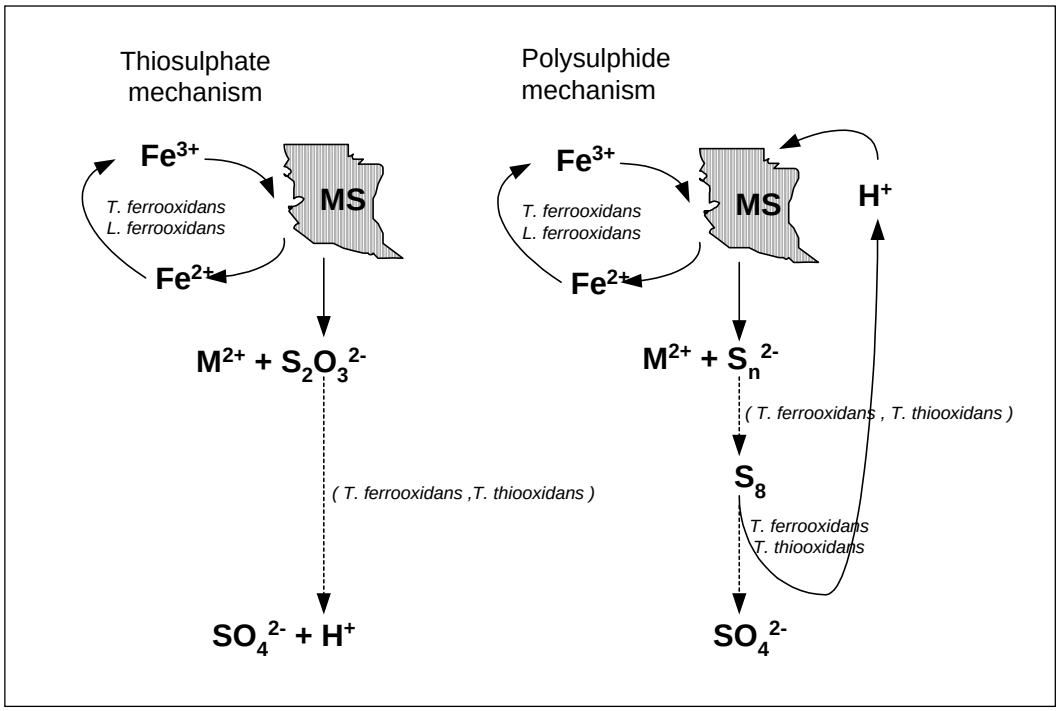

Figure 2.3 Bioleaching proceeds by two different indirect mechanisms via thiosulphate or via polysulphide and sulphur and is based on the properties of metal sulphides (MS). Dashed lines indicate occurrence of intermediate sulphur compounds (reprinted from Schippers and Sand, 1999).

By the time the thiosulphate and polysulphide model had been presented, another bacteria leaching model had been proposed. In this model three multiple patterns of bacterial leaching coexist, including indirect leaching, contact leaching, and cooperative

leaching (Tributsch and Rojas-Chapana, 2000; Tributsch, 2001). The following equation presents the overall mechanism (Tributsch, 2001):

$$MS + 2X + 2O_2 \xrightarrow{bacteria,\ chemicals} M^{2+} + 2X + SO_4^{2-} \qquad (2.10)$$

where $X = H^+$ (acid leaching), $X = Fe^{3+}$ (ferric ions leaching), and $2X = Y^+ + H^+$ (polysulphide carrier [Y-SH] mechanism).

The dissolution of metal sulphides is controlled by the $[H^+]$ concentration of the solution and bacterial forming products (i.e. the ferric ions $[Fe^{3+}]$ and the polysulphide carriers [Y-SH]). These polysulphide carriers contribute to a disruption of sulphide chemical bonds (Tributsch, 2001). Tributsch indicated metal dissolution involves (1) extraction of electrons and bond breaking by $[Fe^{3+}]$, (2) extraction of sulphur by polysulphide and iron complexes forming reactants $[Y^+]$, and (3) electrochemical dissolution by polarisation of the sulphide [high Fe^{3+} concentration]. *T. ferrooxidans* use an extracellular polymeric layer (Figure 2.4) to extract sulphur in the form of colloids and use a polysulphide forming intermediate (with a thiol-group, SH^-) to disrupt the pyrite, whereas, *L. ferrooxidans* (which can only oxidise Fe^{2+}) appears to dissolve pyrite by electrochemical dissolution. Transmission electron microscope (TEM) pictures (Figure 2.4) enabled visualisation of the extracellular polymeric layer, which contained sulphur colloids in case (a) and pyrite fragments in case (b).

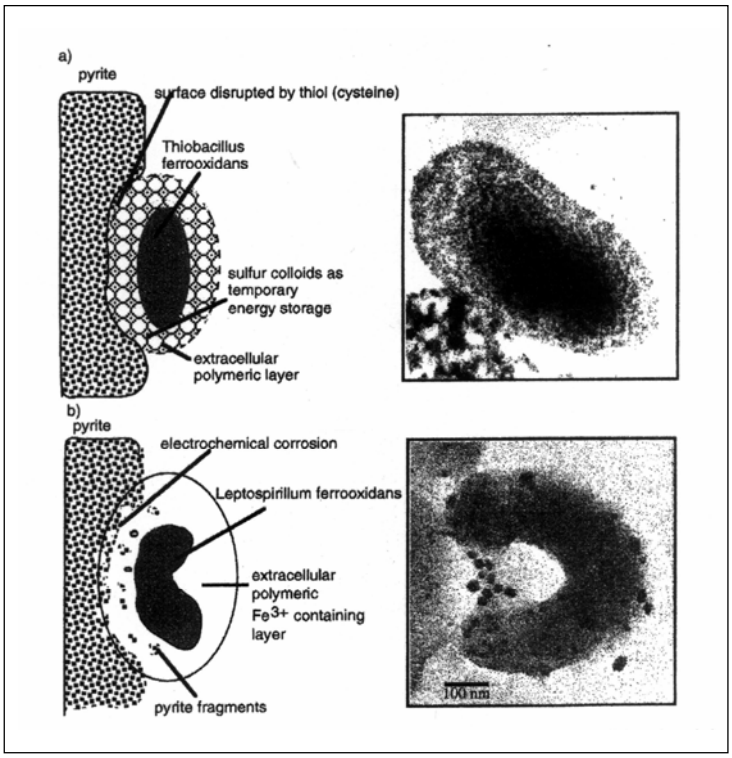

Figure 2.4 Contact leaching during which bacteria actively condition the FeS_2 interface by providing an extracellular polymeric layer: (a) *T. ferrooxidans*, (b) *L. ferrooxidans* (reprinted from Tributsch, 2001).

Silverman and Lundgren (1959) originally proposed the hypothesis of indirect leaching operating concurrently with direct leaching. In direct leaching the bacteria are thought to attach to the sulphide surface. Recently, the term 'contact leaching' has been introduced by Tributsch (2001). Contact leaching describes a situation in which the sulphide is conditioned to facilitate the dissolution process. There is no evidence to support that bacterial membrane directly interacts with the sulphide using enzymatic mechanisms (Tributsch, 2001; Rojas-Chapana *et al.*, 1998; Blight *et al.*, 2000; Schippers and Sand, 1999). In cooperative leaching (Rojas-Chapana *et al.*, 1998), the contact leaching bacteria produce a soluble and particulate sulphide species, which in turn are consumed by bacteria in the surrounding electrolyte. The schemes showing

three patterns of bacterial leaching: indirect leaching, contact leaching, and cooperative leaching are also given in Figure 2.5.

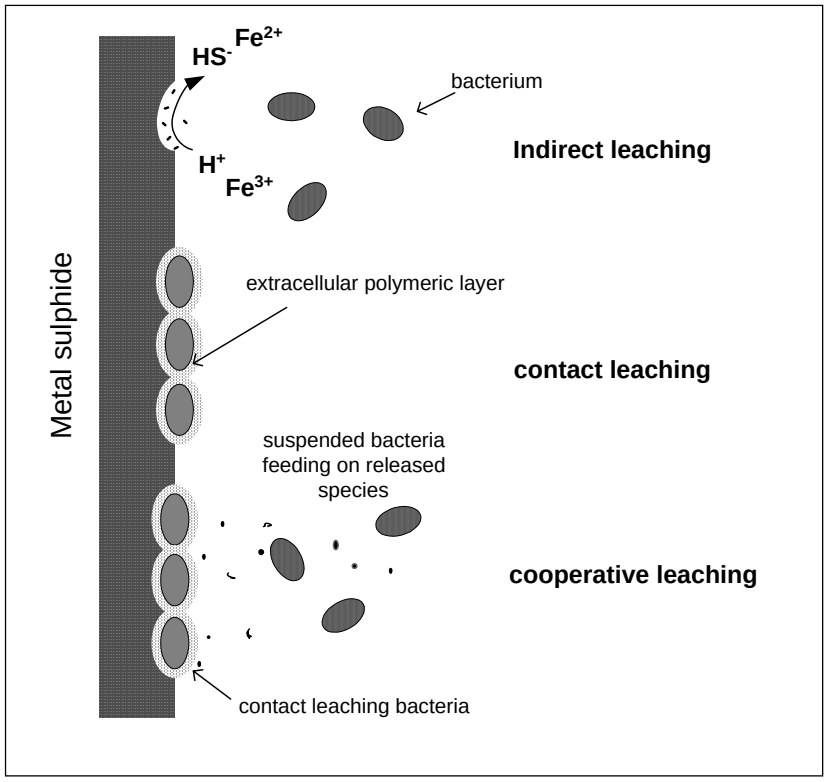

Figure 2.5 Scheme visualising indirect leaching, contact leaching, and cooperative leaching of sulphide (reprinted from Tributsch, 2001).

Another recent bioleaching model is that of Blight *et al.*, (2000) who considered the bio-oxidation of pyrite using *T. ferrooxidans*. Their hypotheses were: (i) when the cells attach themselves to the oxide/sulphide, cell reproduction will occur, extracellular polysaccharides are produced, and iron oxyhydroxides are formed, (ii) iron species act as a mediator, the iron is oxidised at the level of cell attachment and reduced at the oxide/sulphide interface, (iii) sulphur species produced by the action of the mediator at the oxide/sulphide interface diffuses through the surface layers and is either metabolised

or passes into the bulk solution. A schematic view of the model of Blight *et al*., (2000) is shown in Figure 2.6.

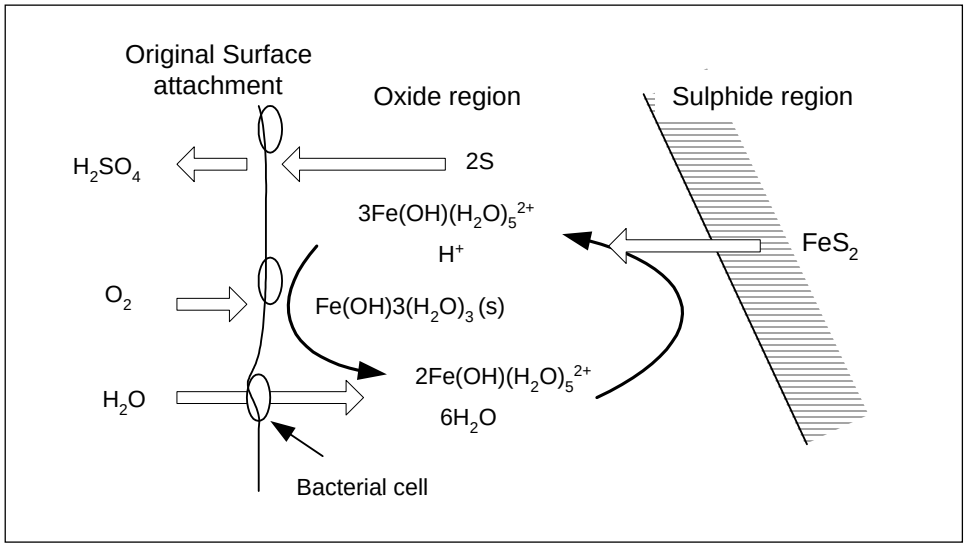

Figure 2.6 Schematic diagram of bioleaching model (reprinted from Blight *et al.*, 2000)

The proposed stoichiometry are as follows:

At the oxide/sulphide interface:

$$2FeS_2 + 2\ H_2O \rightarrow 2Fe(OH)^+ + S_4^- + 2H^+ + 3e^- \quad (2.11)$$

At the bio-film:

$$S_4^- + 16\ H_2O \rightarrow 4\ SO_4^{2-} + 32\ H^+ + 25\ e^- \quad (2.12)$$

$$2Fe(OH)^+ + 4\ H_2O \rightarrow 2Fe(OH)_3\ (s) + 4H^+ + 2e^- \quad (2.13)$$

Reductive reaction at the bio-film:

$$7.5O_2 + 30H^+ + 30\ e^- \rightarrow 15\ H_2O \quad (2.14)$$

The mediator reaction:

$$Fe^{2+} \leftrightarrow Fe^{3+} + e^- \quad (2.15)$$

Overall stoichiometry:

$$2FeS_2 + 7H_2O + 7.5\ O_2 \rightarrow 2Fe(OH)_3\,(s) + 4\ SO_4^{2-} + 8H^+ \qquad (2.16)$$

To summarise, the model of metal bioleaching is still under discussion. Different hypotheses have been put forward to explain how bacteria can dissolve metal from either metal sulphides or metal oxides, and new observations may be derived from new research in the future.

2.4 Factors affecting bacterial leaching

The rate and efficiency of bacterial leaching of mineral ores depends upon a number of different factors. Brandl, (2001) has summarised these factors, which can be seen in Table 2.3. Physico-chemical as well as microbiological factors of the leaching environment affect bioleaching rates and efficiencies. Moreover, the properties of the mineral ores and the manner in which they are processed are also significant since they also affect bioleaching rates and efficiencies. The influence of different microbiological, mineralogical, physicochemical and process parameters on the oxidation of mineral ores has been reviewed by many researchers, for example, Barrett *et al*., 1993; Ehrlich, 1990; Norris, 1990; Rawlings, 1997.

Unfortunately whilst much has been published in this field, results are sometimes conflicting and often the conditions used are not described in much detail. Given the inherent variability of the systems used it is difficult to get consistent results. Some of the main parameters affecting bioleaching are discussed in more detail below.

Table 2.3 Factors and parameters influencing bacterial mineral oxidation (reprinted from Brandl, 2001).

Factor	Parameter	
Physicochemical parameters of a bioleaching environment	Temperature pH redox potential oxygen content and availability carbon dioxide content mass transfer	nutrient availability iron (II) concentration light pressure surface tension presence of inhibitors
Microbiological parameters of a bioleaching environment	Microbial diversity Population diversity Spatial distribution of microorganisms	Metal tolerance Adaptation abilities of microorganisms
Properties of the minerals to be leached	mineral type mineral composition mineral dissemination grain size surface area	porosity hydrophobicity galvanic interactions formation of secondary minerals
Processing	Leaching mode (in situ, heap, dump, or tank leaching) Pulp density	Stirring rate (in case of tank leaching operaions) Heap geometry (in case of heap leaching)

2.4.1 Type of microorganisms

Bioleaching experiments have been conducted using pure strain or mixed strains, characterised or uncharacterised strains, and mesophiles or thermophiles. *T. ferrooxidans* is one of the dominant mesophilic microorganisms used in bioleaching processes. Many researchers have studied either the pure strain obtained from a collection company or the isolated strain from a mine. *T. ferrooxidans* has been used to oxidise a wide range of metal sulphur compounds such as pyrite (FeS_2), chalcopyrite ($CuFeS_2$), covellite (CuS), arsenopyrite (FeAsS), chalcocite (Cu_2S), sphalerite (ZnS), heazelwoodite (Ni_3S_2), pyrrhotite ($Fe_{1-x}S$, $_{x=0-0,17}$). The oxidation of sulphide ores by

T. ferrooxidans was found to be influenced by various parameters such as properties of the mineral ores, pulp density, temperature, particle size and other factors. For example copper dissolution from covellite by *T. ferrooxidans* was observed in the presence of ferrous ions (9 g/l) as energy source (Porro *et al*., 1997). The best oxidation of chalcopyrite by *T. ferrooxidans* was achieved at low particle size (+45, -53 μm) and in the presence of 50 mg/l silver ions (Sukla *et al*., 1990). Battaglia *et al*. (1998) found that the cobalt dissolution rate from cobaltiferous pyrite was increased in the mixed culture of *T. ferrooxidans* and *L. ferrooxidans*, compared with a pure culture. The best leaching rates were obtained when *T. ferrooxidans*, *T. thiooxidans*, and *L. ferrooxidans* were all present.

Variations in bioleaching characteristics of two strains of the same bacteria have been observed (Sampson *et al*., 2000 a). After 350 hours of leaching *T. ferrooxidans* (DSM 583) were able to solubilise 24, 40, and 38 % iron from pyrite concentrate (pyrite + quartz), chalcopyrite concentrate (chalcopyrite + pyrite + pyrrhotite), and arsenopyrite concentrate (arsenopyrite + loëllingite + quartz) respectively, while *T. ferrooxidans* (ATCC 23270) were able to solubilise 42, 40, and 61 % iron from pyrite concentrate, chalcopyrite concentrate, and arsenopyrite concentrate respectively.

A few researchers have studied the comparison of metal dissolution using mesophiles and thermophiles. For example, Clark and Norris (1996) have reported that the rate of pyrite/arsenopyrite concentrate oxidation obtained from moderate thermophiles microorganisms was faster than that of mesophiles. They also found that the percentage of copper dissolution from complex sulphide was almost 100 % when using a

Sulfolobus-like strain at 80 °C. However, Yahya and Johnson (2002) reported that the rate of pyrite concentrate oxidation obtained from *T. ferrooxidans* was faster than that of *Sulfobacillus* sp. at the same initial pH of 2.5 and temperature of 35 °C. A few researchers have also shown that extreme thermophiles can significantly increase rate of bioleaching in case of chalcopyrite. Konishi *et al*. (2001) studied the kinetics of chalcopyrite leaching by *Acidianus brierleyi* at 65 °C, pH 1.2, +38, -53 μm particle size, and 0.5 % (w/v) pulp density in a batch stirred tank reactor. Almost 100 % copper dissolution was achieved within 10 days in comparison with *T. ferrooxidans* which took about 10 days to achieve 20 % dissolution with the same sample. The final percentage of copper given from Konishi *et al*. (2001) show good agreement with Gericke *et al*. (2001) who studied bioleaching of chalcopyrite concentrate using an extremely thermophilic microorganism isolated from a hot sulphur-rich coal dump. A final extraction of 98 % copper (18.8 g/l Cu) and 96 % iron (10 g/l Fe) were achieved (Gericke *et al*., 2001).

Although it has been found that thermophiles show a good copper dissolution there is also a high simultaneous dissolution of iron, which as mentioned previously reduces the purity of copper in the leachate. This is deemed to be the distinct disadvantage of using thermophiles.

2.4.2 The type of mineral ores

Metal dissolution (either by chemical or by bacterial methods) depends upon the nature of the mineral ores, i.e. its precise chemical composition, and for a given type of ore its origin. Hiroyoshi *et al*. (1997) highlighted how different sources of chalcopyrite

samples have different leaching efficiency (Figure 2.7). In their study the effects of ferrous sulphate and ferric sulphate additions on copper extraction were compared for four chalcopyrite samples. The copper composition of the samples were 28.7, 20.6, 33.3 and 29.3 wt % for Akenobe, Zhezkent, Unknown, and Ohmine, respectively. Although, all samples are high-grade chalcopyrite, the rates of copper dissolution were very different. In particular, the amount of extracted copper in the Akenobe sample was significantly larger than the other samples.

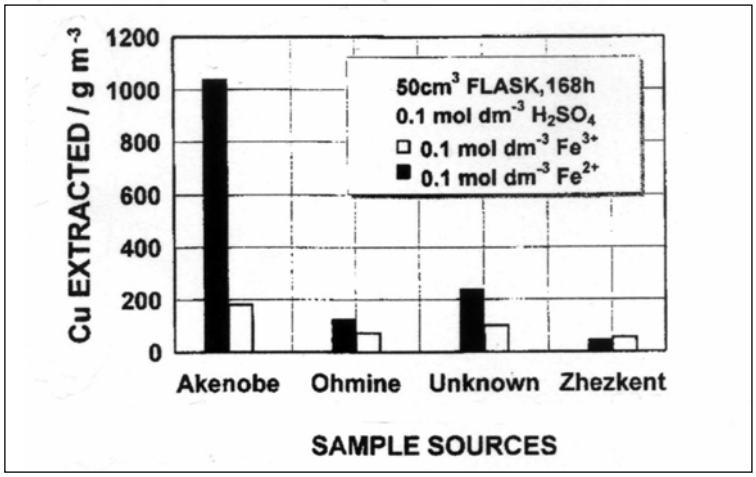

Figure 2.7 Amount of extracted copper with four chalcopyrite samples leached for168 h. in 0.1 mol dm^{-3} sulphuric acid solutions containing 0.1 mol dm^{-3} ferrous ions or 0.1 mol dm^{-3} ferric ions (reprinted from Hiroyoshi *et al*., 1997).

Given the problems in understanding the bioleaching process for a given ore it is not surprising that it is difficult to understand bioleaching of complex ores which contain several different minerals. Ahonen and Tuovinen (1995) studied the bacterial leaching of complex sulphide ores, containing chalcopyrite, sphalerite, pentlandite, pyrite and pyrrhotite, using uncharacterised strains from mines. The results were obscured on a number of levels. Not only did the relationships between leaching rates and pH, redox

potential and ferric ions in solution vary for each mineral, these relationships are not understood for individual ores let alone the complex ones.

2.4.3 Medium

The fundamental elements for cell growth and cell biomass are carbon, oxygen, hydrogen, nitrogen, phosphorus, sulphur and magnesium. The functional description of these elements is given by Tuovinen (1990). Oxygen in cellular compounds is derived from the elemental oxygen from air. Organic carbon may have some benefit for the bacteria if there is any toxic metal in the solution, for example yeast extract at low concentration has been shown to diminish toxicity to bacteria (Tuovinen, 1990). Hydrogen is required as a reductant for $NAD(P)^+$ in biosynthetic pathways. Ammonia appears to be the nitrogen source and phosphate or sulphate is desired in metabolic balance and growth restriction. Magnesium is used for energy-transducing enzyme activities.

Different modified media for autotrophic microorganisms have been developed and studied by different researchers. All these contain excess concentrations of phosphate, magnesium and ammonium ion, so as not to limit growth. Examples of the media used for growing *T. ferrooxidans* include 'Tuovinen and Kelly' medium, 'Thiobacillus ferrooxidans' medium, 'ATCC 2093' medium, 9K medium and ATCC 64 medium (Appendix III). The bacteria have also been cultivated in media with $FeSO_4 \cdot 7H_2O$ as the energy source.

The growth of *T. ferrooxidans* and iron oxidation is markedly influenced by the ferrous ions concentration (Nemati, 1996). The depletion of ferrous ions results in a decline of

bacterial growth. Espejo and Ruiz (1987) also suggested that growth of *T. ferrooxidans* was obtained when the amounts of available ferrous ions were about 0.35 kg/m^3 available in the environment. The maximum growth rate of *T. ferrooxidans* (μ_{max} = 0.094 h^{-1}) was achieved at 4.42 kg/m^3 Fe^{2+} (22 kg/m^3 $FeSO_4 \cdot 7H_2O$) for a pH value of 2.5 and temperature of 30 °C (Pagella *et al*., 1996). These workers examined concentrations of 22, 44, 88, and 176 kg/m^3 of $FeSO_4 \cdot 7H_2O$ at temperatures of 20 and 30 °C. Using *T. ferrooxidans* (NCIMB 9490) at concentrations of 3.25x10^7 to 1.21x10^8 cells/ml, Nemati and Webb (1997) found that the maximum iron oxidation rates were achieved in solutions containing 0.9 to 1.85 kg/m^3 of Fe^{2+}. In addition, Fowler *et al.* (1999) found that the pyrite dissolution rate increased with the addition of ferric ions in the range of 1 to 20 g/l whether or not the bacteria (*T. ferrooxidans*) were present. Hugues *et al.* (1997) studied the influence of the nitrogen source on the oxidation of pyrite. When urea solution was replaced by ammonium sulphate solution, the bacterial growth (mixed strains from mines) increased by 9% over the first four days of leaching time and the increase in pyrite oxidation achieved was found to be 18 % over the same period.

Metal oxidation by bioleaching can be inhibited by a variety of factors such as organic compounds, surface-active agents, solvents, or specific metals. The presence of organic compounds (yeast extract) was found to inhibit pyrite oxidation by *T. ferrooxidans* (Nicolau and Johnson, 1999). However, the addition of small amounts of silver ion in the presence of *T. ferrooxidans* resulted in an increased copper dissolution from chalcopyrite (Sukla *et al*., 1990; Sato *et al*., 2000). After 20 days of leaching, the copper recovery was 10%, 58%, 62%, and 65% for the 0, 27, 133, and 266 mg silver chloride

additions respectively (corresponding to a silver chloride concentration about 0, 0.135, 0.665, and 1.33 % (w/v) respectively) (Sato *et al*., 2000). Moreover, it has been demonstrated that the addition of small amounts of cysteine lead to an increased pyrite corrosion by *T. ferrooxidans* compared to controls without additions (Rojas-Chapana and Tributsch, 2000). A low concentration of cysteine (10^{-5} M) was sufficient to generate a significant increase of corrosion, but at a higher concentration of cysteine ($>>10^{-3}$ M) a toxic effect in bacteria activity was found.

2.4.4 Temperature

The optimum temperature for the growth of mesophiles is probably about 30 to 35 °C, but the upper and lower temperature limits may depend on the strain and growth conditions. The growth rate can be reduced by approximately fifty percent, for every 6 °C temperature decrease in the range of 25 to 2 °C (Norris, 1990). Some strains may be able to adapt to low temperatures. Ahonen and Tuovinen (1991) studied temperature effects on bacterial leaching of sulphide ores using uncharacterised strains from mines. Table 2.4 shows some of the results that were obtained at temperatures between 4 and 37 °C. At low temperature the rates were slow but as the temperature increased so did the rated. The initially slow rates range can be attributed to the lag phases preceding active bacterial leaching.

Increasing temperature in the range of 20 to 35 °C was found to enhance the biological oxidation rate of ferrous ions by *T. ferrooxidans* (Nemati and Webb, 1997). Deng *et al.* (2000) also studied the temperature effect in the range of 20 to 45 °C. It was observed

that the biooxidation rate of iron and arsenic using *T. ferrooxidans* was at its highest in the range of 28 to 32 °C.

Table 2.4 Kinetics parameters of copper and zinc leaching from low-grade sulphide ores (reprinted from Ahonen and Tuovinen, 1991)

Temp (°C)	Copper leaching			Zinc leaching		
	Rate constant, k (l/day)	Rate, (%/day)	t½ (day)	Rate constant, k (l/day)	Rate, (%/day)	t½ (day)
37	0.0049	0.49	142	0.1600	16	4.3
28	0.0042	0.42	164	0.0914	9.1	7.6
19	0.0026	0.26	266	0.1050	10.5	6.6
16	0.0021	0.21	329	0.0819	8.2	8.5
13	0.0017	0.17	415	0.0592	5.9	11.7
10	0.0011	0.11	624	0.0503	5	13.8
7	0.0007	0.07	1050	0.0161	1.6	43
4	0.0005	0.05	1390	0.0270	2.7	25.7

t½= estimated time to reach 50 % dissolution of low-grade sulphide ores

2.4.5 pH

T. ferrooxidans are acidophilic which means that these bacteria can grow and oxidise iron in a pH range of 2.0 to 2.5. The strain used by Silverman and Lundgren in 1959, oxidised iron at a pH between 3.0 and 3.6. The optimal pH for oxidation and cell growth can vary between strains and is also dependent on experimental conditions. In general, all strains of *T. ferrooxidans* can grow and oxidise iron around pH 2 (Ehrlich, 1990). Deng *et al*. (2000) also reported that the pH in a range of 1.5-3.0 showed the highest biooxidation rate of iron and arsenic using *T. ferrooxidans*.

Ubaldini *et al.* (1997) found that the iron extraction (mg/l) from bioleaching of arsenopyrite using *T. ferrooxidans* was not related to initial pH in the range of 2.0 - 2.5, while the arsenic extraction yield increased when the initial pH was decreased from pH 2.5 to 2.0. Moreover, Nakazawa *et al*. (1998) studied the effect of initial pH ranging

from pH 1.0 to 1.7 on the bioleaching of chalcopyrite concentrate by *T. ferrooxidans.* The results show that the dissolution rate of copper and iron increased when using an initial pH of 1.0.

2.4.6 Particle size

Ahonen and Tuovinen (1995) stated that the leaching rates for metal sulphide ores increased with a reduction in particle size and this effect was enhanced at lower pH values. In this case, the copper and nickel leaching rate approximately doubled when the particle diameter was decreased from +5, -10 mm to +1.68, -5 mm. Devasia *et al.* (1996) proposed that bacterial adhesion and hence bioleaching rates depend on the particle size of the minerals and compared a range of sizes between +38, -53 μm and +106, -150 μm. Figure 2.8 shows the results of copper and iron dissolution from these ranges of chalcopyrite particles by *T. ferrooxidans* grown on sulphur, liquid thiosulphate and ferrous ions solution in shake flask cultures. It was proposed that leaching rates were significantly higher for the smaller particle range due to the larger surface area available for bacterial attachment.

2.4.7 Pulp density

Gómez *et al.* (1999 a) studied the optimal pulp density for bioleaching complex sulphide ores using mixed characterised mesophiles from mines. The authors observed a significant decrease in metal dissolution when the pulp density was increased from 5 % to 20 % (w/v). Deng *et al.* (2000) studied the bioleaching of low-grade gold ores using *T. ferrooxidans*. They found a rapid decrease in arsenic and iron oxidation rates when the pulp density was higher than 10 % (w/v). The optimal pulp density was 10 % (w/v).

Ubaldini *et al*. (1997) affirmed that there was no significant difference in the rate of bioleaching of arsenopyrite using *T. ferrooxidans* and *T. thiooxidans* when the pulp density increases from 10 to 20 % (w/v).

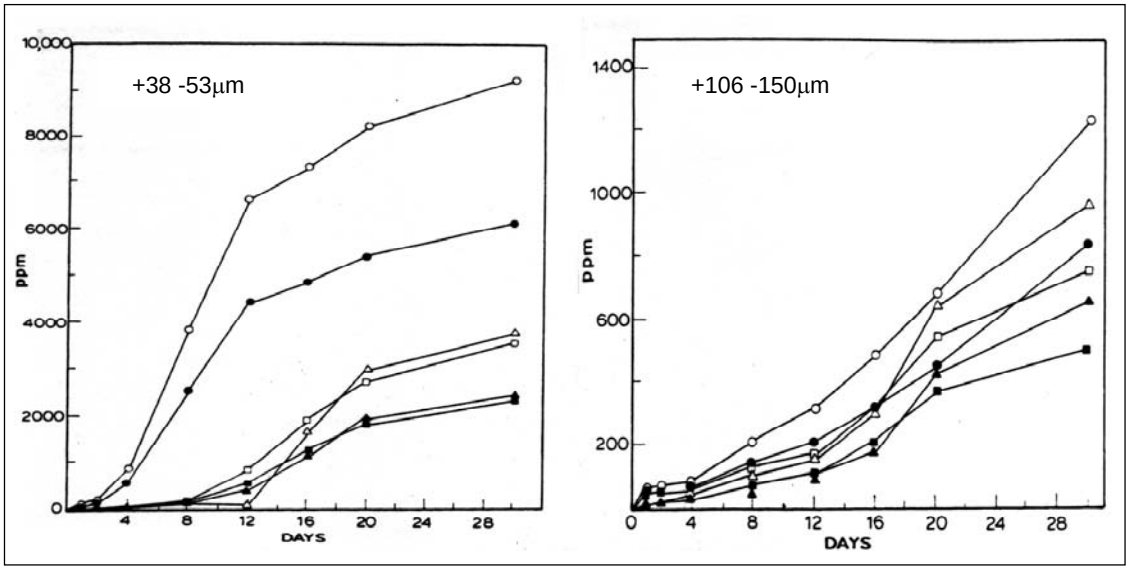

Figure 2.8 Iron and copper dissolution from chalcopyrite particles by *T. ferrooxidans* grown on ferrous ions (△, ▲), thiosulphate (□, ■), and sulphur (○, ●), respectively (reprinted from Devasia *et al*., 1996).

2.4.8 Oxygen and carbon dioxide

T. ferrooxidans assimilate carbon dioxide via the Calvin-Benson cycle to get carbon requirements for cell growth. A lack of carbon dioxide restricts the bacteria growth and can limit the rate and amount of mineral sulphide oxidation. However, carbon dioxide can also show inhibitory effects on metal leaching. Aqueous-phase carbon dioxide at concentrations of more than 10 mg/l was found to inhibit growth of *T. ferrooxidans* on pyrite-arsenopyrite-pyrrothite ore (Nagpal *et al*., 1993). Optimal concentrations of carbon dioxide were found to be in the range of 3 to 7 mg/l. However, some researchers have reported no effect in increasing in bacterial leaching rates by the

supplementation of ambient air with carbon dioxide. Gómez *et al*. (1999 a) reported that an increase in the carbon dioxide concentration (1 % v/v) showed a similar metal extraction rate to that of ambient air (0.03 % v/v).

2.4.9 Conclusion

As has already been discussed above, the metal dissolution rate will depend on many of the parameters affecting the oxidation of the ores in question, as well as there being microorganisms strain dependent factors. The nature of the mineral ores also affects bacterial growth and metal dissolution. The bioleaching of a given ore from different sources and/or different types of ores also requires test studies to be conducted, despite the success of metal extraction by the same bacteria on other ores. Consequently, it is necessary to find an optimum condition for a particular ore sample.

From the previously published literature, the results are sometimes conflicting and often the conditions used are not described in much detail. Overall, the optimum conditions for bacterial leaching of ores are (i) a medium that contains nitrogen and phosphorus is required, as nutrients for growth and synthesis along with the trace minerals K, Mg, Na, Ca and Co, (ii) the optimum temperature for the growth of mesophiles is probably about 30 to 35 °C, (iii) the pH for the cell growth of acidophilic microorganism is in the range of 1.5 to 3.0, (iv) a particle size of < 150 μm, (v) no more than 10 % (w/v) pulp density, and (vi) an adequate ambient air supply.

CHAPTER 3 Factors affecting bacterial leaching on shake flask cultures of *T. ferrooxidans*

3.1 Introduction

Shake flasks are very widely used in bioprocess projects. One reason for this may be the fact that shake flasks are mainly used in the first steps of the bioprocess development since they enable a large number of experiments to be conducted with relatively low cost (e.g. media and chemicals). Shake flask cultures are primitive systems in terms of gas transfer, mixing efficiency and continuous monitoring (Büchs, 2001) and therefore care is required in extrapolating results to stirred tank reactors. Although shake flasks are physically unrelated to stirred vessels, some information from shake flask experiments can be valuable (e.g. medium optimisation). Given these restrictions the main aim of this chapter was to evaluate the effect of a range of variables on culture growth rate and metal dissolution.

The growth rate of *T. ferrooxidans* in the shake flask culture and the metal dissolution kinetics depends on various mineralogical, microbial and process parameters, including shake flask speed, particle size, initial pH, and pulp density. A number of these are discussed in more detail in section 2.4 (Chapter 2). In order to investigate the significance of these parameters, experiments were undertaken whereby a culture of *T. ferrooxidans* was grown under various experimental conditions. This chapter describes the materials and procedures used for these experimental works. In studying each experimental parameter, a graph of bacterial growth, metal dissolution, pH value and redox potential was plotted as a function of time and comparisons were made with cell free systems. The rates of copper and total iron dissolution were calculated based on

the leaching time. Furthermore, the copper dissolution data from other literature on mineral bioleaching is compared with the work presented in this thesis.

3.2 Materials and Methods

3.2.1 Chalcopyrite concentrate

A Chalcopyrite ($CuFeS_2$) concentrate originating from the Palabora mine South Africa and supplied by Rio Tinto, Research & Development Division, Bristol, England was ground in a ball mill and screened into size ranges of –38 μm, +38, -53 μm, + 53, -75 μm, +75, -106 μm, +106, -150 μm, +150, -300 μm and +300, -2000 μm.

Table 3.1 Copper and total iron concentration (%) in the chalcopyrite concentrate size fractions

Particle size (μm)	Copper (Cu) %	Total Iron (Fe) %
-2000, +300	26.6	23.8
-300, +150	28.2	25.3
-150, +106	28.2	26.3
-106, +75	28.6	26.8
-75, +53	28.9	27.6
- 53, +38	30.4	27.6
-38	30.7	27.7

Copper and total iron assays in the different particle size ranges of chalcopyrite concentrate ($CuFeS_2$) were analysed by digesting the ore in HNO_3-HCl as described in Standard Methods for Examination of Water and Wastewater (Greenberg *et al*, 1992). The metal content of the supernatant (solubilised metal) was determined by Flame Atomic Adsorption Spectrophotometry. Table 3.1 shows the percentage of copper and total iron concentration in the chalcopyrite concentrate for the various particle sizes.

Copper and total iron concentration from the chalcopyrite concentrate was found to vary with particle size, specifically the metal concentration increased with decreasing particle size. In the chalcopyrite concentrate mineralogy report (Appendix IV), two size fractions (>150 μm and <38 μm) of a chalcopyrite concentrate were characterised using a combination of reflected light microscopy and SEM-based techniques. The copper concentrate consisted largely of chalcopyrite, a high proportion of the chalcopyrite numeral is relatively more abundant in the <38 μm fines than in the >150 μm size fraction. Gangue minerals, i.e., quartz, sericite and K-feldspar are present as impure ore minerals. Quartz is more abundant in the coarser grade of chalcopyrite concentrate. This is confirmed by the assay results presented in Table 3.1, which show that for the size range of < 38 μm, the percentage of copper and iron in the chalcopyrite concentrate were greater in comparison to that of other size ranges.

Preparing bacterial cultures requires the use of sterile techniques to guarantee that the population, which grows in the culture, is the intended bacterial population. Brickett *et al*., (1995) tested eight methods of ore sterilisation, including steam autoclaving, dry heat, tyndallisation, cobalt-60 irradiation, thymol and mercuric chloride addition using a copper ore. They found that autoclave-treated ores appeared to most closely mimic the behaviour of control ores, suggesting that relatively minor alteration of the ore occurred. Therefore, steam sterilisation in an autoclave (Scientific, Series 300, UK) was chosen in order to kill all living organisms that may be present in the chalcopyrite concentrate. Prior to all the bioleaching experiments the chalcopyrite concentrate was sterilised. 5 g of the chalcopyrite concentrate was added to a tube, which was then autoclaved at 121 °C for 15 minutes.

In order to investigate whether autoclaving had any influence on metal dissolution, an experiment was set up by preparing a series of flasks with the sterile and non-sterile chalcopyrite concentrate. The particles were added to a flask (250 ml) containing 45 ml of ATCC 64 medium (without ferrous ions) at an initial pH of 2.8. The flask was incubated in a rotary shaker at 30 °C and 200 rpm. After 7 days, the copper and total iron content in the solution was determined. The assay results indicated that sterilisation did not significantly affect copper and iron dissolution under the specified conditions (Table 3.2).

Table 3.2 Comparison of copper and iron dissolution obtained from sterile and non-sterile chalcopyrite tests

Time (day)	Sterile chalcopyrite		Non-sterile chalcopyrite	
	Copper dissolution (g/l)	Iron dissolution (g/l)	Copper dissolution (g/l)	Iron dissolution (g/l)
1	0.033	0.038	0.030	0.035
2	0.045	0.040	0.043	0.050
3	0.056	0.049	0.061	0.048
5	0.052	0.045	0.048	0.043
7	0.061	0.043	0.068	0.055

3.2.2 Microorganism and media

A *Thiobacillus ferrooxidans* culture isolated from mine waters was chosen as the base strain because it is recognised as being responsible for the oxidation of iron and inorganic sulphur compounds in areas such as a mine tailings and coal. The culture (strain NCIMB 9490) was ordered from the National Collection of Industrial and Marine Bacteria, Scotland. Due to persistent problems in growing the organism (Appendix II), the same strain was also ordered from the American Type Culture Collection (ATCC 19859).

From the results of a series of preliminary experiments (Appendix II), *T. ferrooxidans* (ATCC 19859) was selected and the ATCC 64 medium was chosen as an appropriate medium for growth. The components of this medium are shown in Appendix III. Aseptic techniques were used throughout the study.

3.2.3 Bacterial preparation

A 10 % v/v inoculum of the stock culture (Appendix II) was added to a flask (250 ml) containing 45 ml of ATCC 64 medium at an initial pH of 2.8. The flask was incubated in a rotary shaker at 30 °C and 200 rpm. The cells were harvested after they had reached the late exponential phase (96 hours) and the culture was filtered through filter paper (Whatman No. 1) to eliminate iron precipitation and other solid particles. The culture was centrifuged at 8000 rpm for 40 minutes to separate the cells and washed three times with the same medium (without ferrous ions) used for growth. The cells were then diluted to a known concentration with the medium and then used for all subsequent experiments.

3.2.4 Analysis of the solution pH, the redox potential and the free cell concentration

A pH probe that was connected to a pH/redox module was used to monitor the pH. Before monitoring, the pH probe was calibrated with standard reference buffer solutions (Sigma, UK). The redox probe used was a combination platinum/ reference (Ag/AgCl) redox cell (Sentek (UK), type 01). The redox probe was calibrated with redox buffer solutions (Mettler Toledo, UK). Whenever the monitor issued a slow reading, this was a sign that the electrode had become coated or clogged with metal ions. Accordingly, the redox probe required additional cleaning with a Diaphragmareiniger diaphragm cleaner solution (Mettler Toledo, UK).

The oxidation of metal ions was monitored by logging the redox potential (mV); the redox potential had a positive value because of an oxidising environment. The redox potential of the solution (E), according to the Nernst equation 3.1, becomes more positive due to the increase in ferric ions concentration during the bacterial oxidation of ferrous ions (Nemati and Webb, 1997).

$$E = E_0 + \frac{RT}{nF} \ln \frac{\left[Fe^{3+}\right]}{\left[Fe^{2+}\right]} \qquad (3.1)$$

where E = potential of the solution, V

E_0 = standard potential of Fe^{3+}/ Fe^{2+} couple, V

R = universal gas constant, $kJK^{-1}\ mol^{-1}$

n = number of electrons transferred per molecule

F= kJV^{-1} equiv $^{-1}$

$[Fe^{3+}]$ = molar concentration of ferric ion, kmol m^{-3}

$[Fe^{2+}]$ = molar concentration of ferrous ion, kmol m^{-3}

The free cells (bacterial cells in the surrounding solution) were diluted with sterile distilled water and immediately counted under a phase-contrast microscope using a Helber bacterial counting chamber to obtain a cell number concentration. It is important to note that the cell count was based solely on the free cells, without taking into account the attached cells on the mineral surface. Santelli *et al*., 2001 suggested that approximately 10-50 % of the cells are attached to mineral surface based on estimates from the SEM observation. Thus, an estimate of attached cells from SEM observation is not reliable, and hardly any attached cells on the mineral surface can be observed.

3.2.5 Analysis of the copper and total iron concentration

Copper and total iron content in the solution was determined by atomic absorption spectrophotometry (AAS). Calibration curves for each metal were determined using standardised metal solutions. The leaching solutions were diluted with sterile distilled water and later the same day the amounts of copper and total iron were determined by atomic absorption spectrophotometry (AAS). The rates of copper and total iron dissolution were calculated as described in the standard test method for determining the rate of bioleaching of iron from pyrite by *Thiobacillus ferrooxidans* (ASTM E1357-90).

3.2.6 Experimental procedure

In order to optimise the bioleaching process, shake flask speed, chalcopyrite concentrate particle size, initial pH, and pulp density were studied. When the influence of one of them was studied the rest were fixed at the conditions shown in Table 3.3. All experiments were carried out in a 250 ml shake flask containing 45 ml of previously

sterilised ATCC 64 medium (without ferrous ions). A 10 % v/v inoculum of the bacterial culture (section 3.2.3) and the sterile chalcopyrite concentrate (previously autoclaved at 121 °C for 15 minutes) were added to a series of flasks. Duplicate trials were conducted. The flasks were incubated in a rotary shaker at 30°C. The control experiments were set up by preparing a series of flasks with the same composition but bacteria were absent. In subsequent experiments, the growth of bacteria in the absence of chalcopyrite concentrate was also considered; a series of flasks containing the medium (without ferrous ions and chalcopyrite concentrate particles) were incubated in a rotary shaker at 30°C and 100 rpm.

Table 3.3 Operational conditions for shake flask experiments

Variable	Tested conditions	Fixed conditions		
Shake flask speed	100 rpm 200 rpm 300 rpm	Particle size +53, -75 μm	Initial pH 2.8	Pulp density 5% (w/v)
Particle size	+38, -53 μm +53, -75 μm +75, -106 μm +106, - 150 μm	Shake flask speed 100 rpm	Initial pH 2.8	Pulp density 5% (w/v)
Initial pH	pH 1.5 pH 2.0	Shake flask speed 100 rpm	Particle size +53, -75 μm	Pulp density 5% (w/v)
Pulp density	2.5% (w/v) 10 % (w/v)	Shake flask speed 100 rpm	Particle size +53, -75 μm	Initial pH 2.8

Two flasks were removed to provide duplicate samples for each data point. After determining the mass of the flasks, the loss of water due to evaporation was compensated by adding sterile distilled water (ASTM E1357-90). The leaching solution was filtered through filter paper (Whatman No. 1) to separate solid and liquid phases and the filtrate was then used for analysis of the solution pH, redox potential, free cell concentration, total iron and copper concentration.

3.3 Effect of shake flask speed on bioleaching of chalcopyrite

3.3.1 Introduction

Agitation speed have a significant influence on particle distribution and transport phenomena and hence bacterial growth and product formation in stirred bioreactors (Boswell *et al*., 2002). However, there is only one published paper on the effect of shake flask speed on the bioleaching of metal. Ubaldini *et al.* (1997) found that iron and arsenic dissolution (mg/l) from 10 and 20 % (w/v) arsenopyrite (-74 μm) using a mixed culture of *T. ferrooxidans* and *T. thiooxidans* into shake flasks (300 ml) with 100 ml of 9K media at 200 rpm were not significantly different from those at 250 rpm. Although, bacterial growth, pH, and redox potential values were not actually reported.

The aim of this work was to examine the copper and iron solubility during the bioleaching of the chalcopyrite concentrate when different shake flask speeds were used (100, 200 and 300 rpm). The effect of agitation speed in a stirred bioreactor is reported in a later chapter, chapter 6. The effect of shake flask speed was studied by employing cell suspensions containing bacterial concentrations between 3.0×10^8 to 5.0×10^8 cells/ml of the total solution, a constant particle size range (chalcopyrite concentrate) of +53, -75 μm, pulp density of 5 % (w/v), and an initial solution pH of 2.8. The effects on the free cell concentration, the solution pH, redox potential and copper and iron dissolution were investigated.

The bioleaching results for different shake flask conditions are presented in Figures 3.1-3.7. The bioleaching of the chalcopyrite concentrate at 100 rpm are shown in Figures 3.1-3.3. The control experiments (in the absence of bacteria) at the same shake

flask speed are presented in Figures 3.4 and 3.5. Furthermore, the bioleaching of the chalcopyrite concentrates at 200 rpm and 300 rpm is also shown in Figures 3.6 and 3.7, respectively. In order to compare the effect of shake flask speed on bioleaching, copper dissolution (g/l) is presented as a function of time for different shake flask speeds in Figure 3.9. Finally, the growth of *T. ferrooxidans* in the absence of ferrous ions and chalcopyrite at 100 rpm is shown in Figure 3.10, in order to confirm whether the bacteria can grow in the medium ATCC 64 without those elements.

3.3.2 Effect of shake flask speed on bacterial growth

The growth of bacteria depends on the interactions of many of the same parameters affecting the oxidation of the substrate, among which shake flask speed dependent factors play an important role. The bacteria growth curve for 100 rpm displayed a typical pattern (Figure 3.1). The lag lasted approximately 5 days and was followed by an exponential phase (5-15 days), a stationary phase (15-30 days) and then a death phase (after 30 days). In order to calculate the specific growth rate, natural logarithm of free cell concentration was plotted against time. Calculation of the gradient of the line corresponding to exponential phase growth yielded the maximum specific growth rate (μ) in units of h^{-1}. The value obtained was 0.024 h^{-1}.

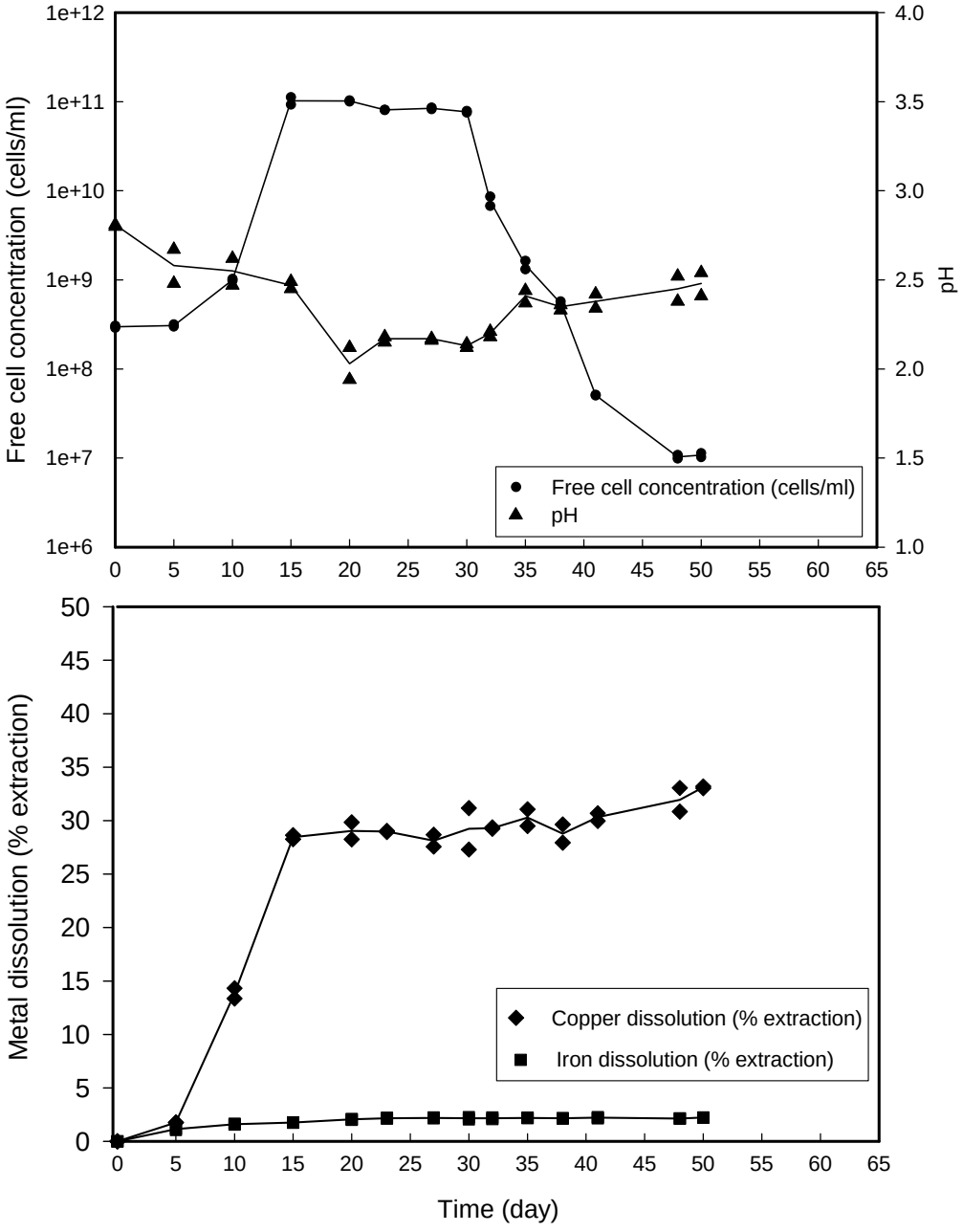

Figure 3.1 Bioleaching of chalcopyrite concentrate at 5% (w/v) pulp density, +53, -75 µm, initial pH 2.8 and 100 rpm

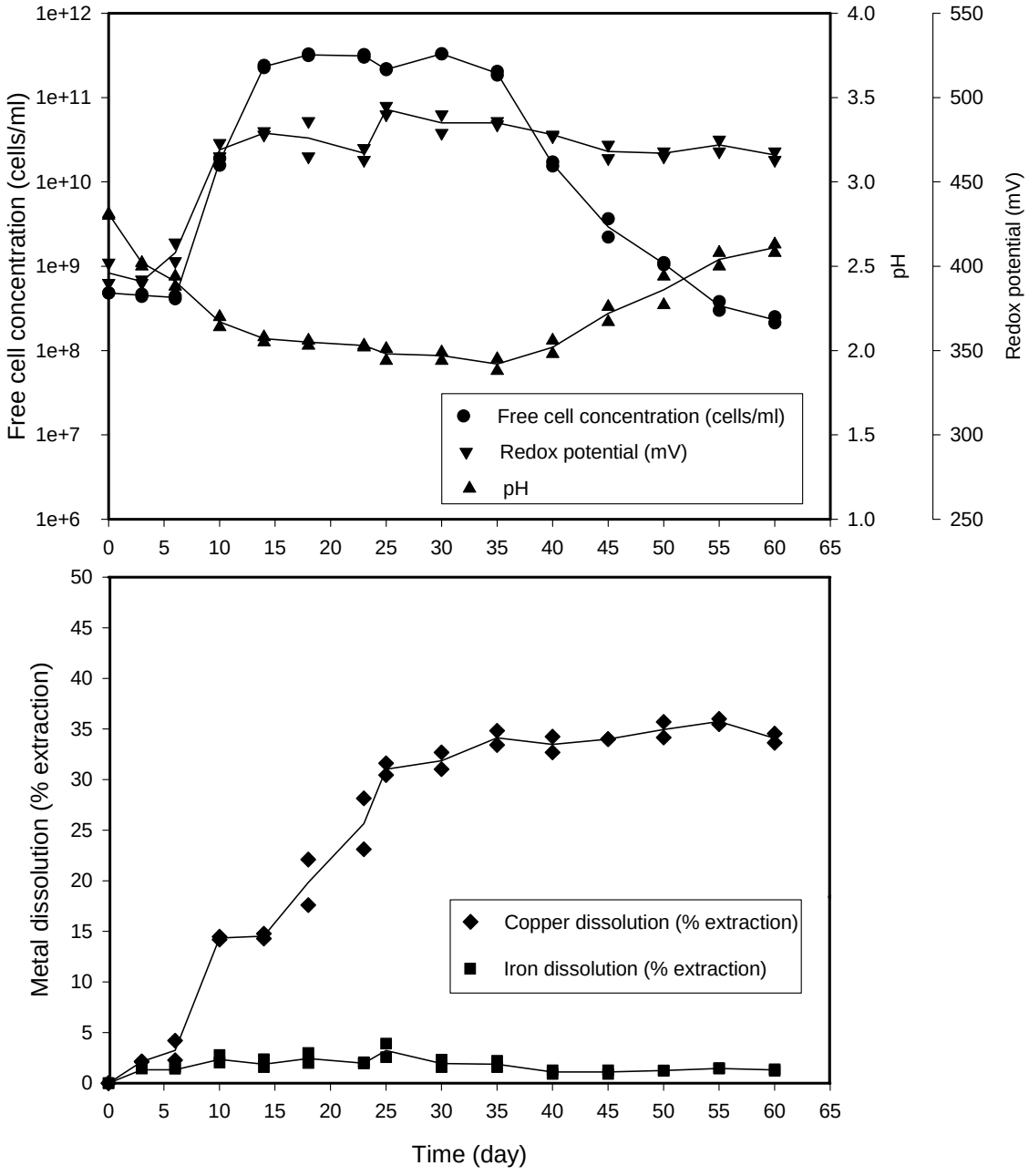

Figure 3.2 The first repeat bioleaching of chalcopyrite concentrate at 5% (w/v) pulp density, +53, -75 µm, initial pH 2.8 and 100 rpm

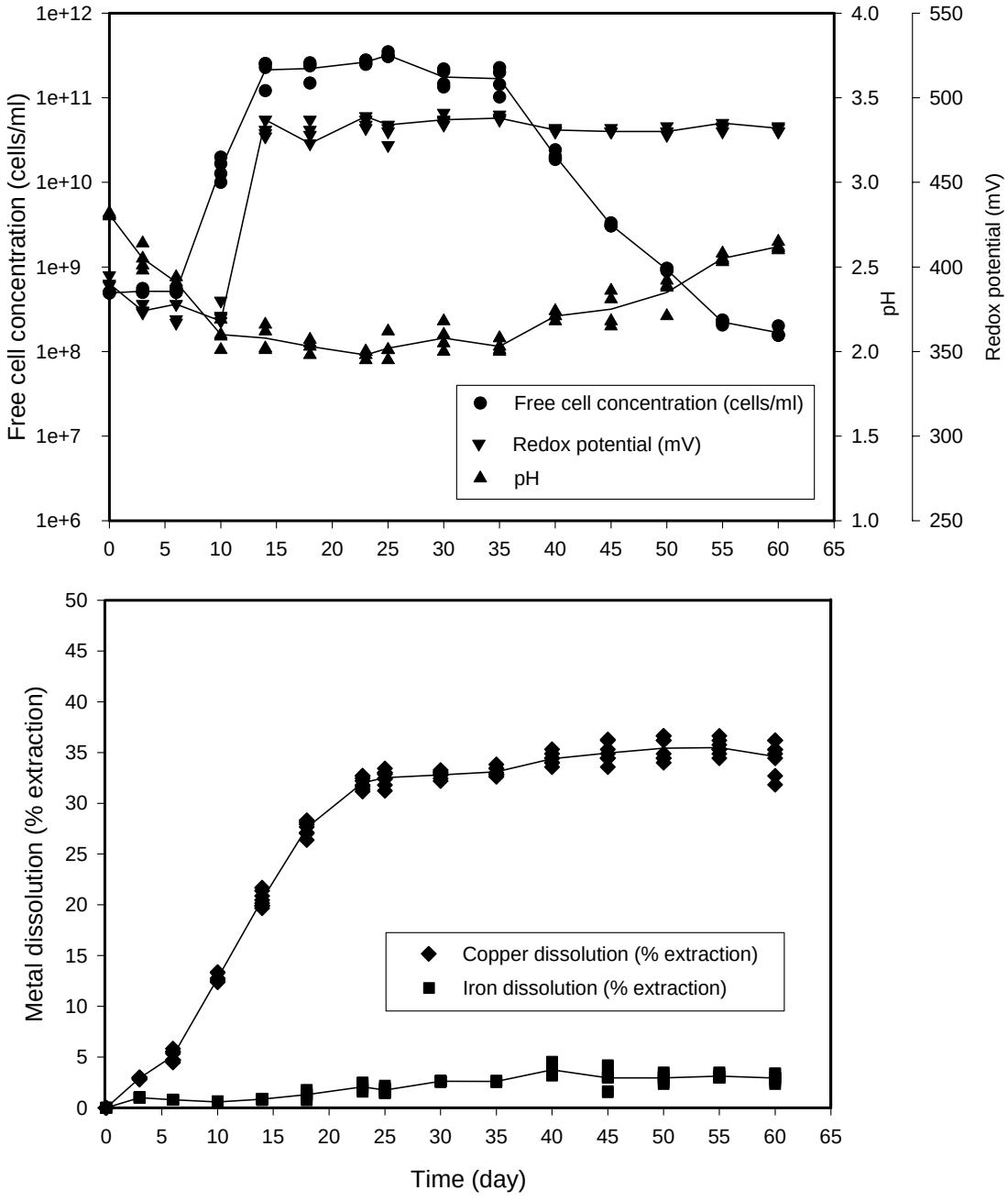

Figure 3.3 The second repeat bioleaching of chalcopyrite concentrate at 5 % (w/v) pulp density, +53, -75 μm, initial pH 2.8 and 100 rpm

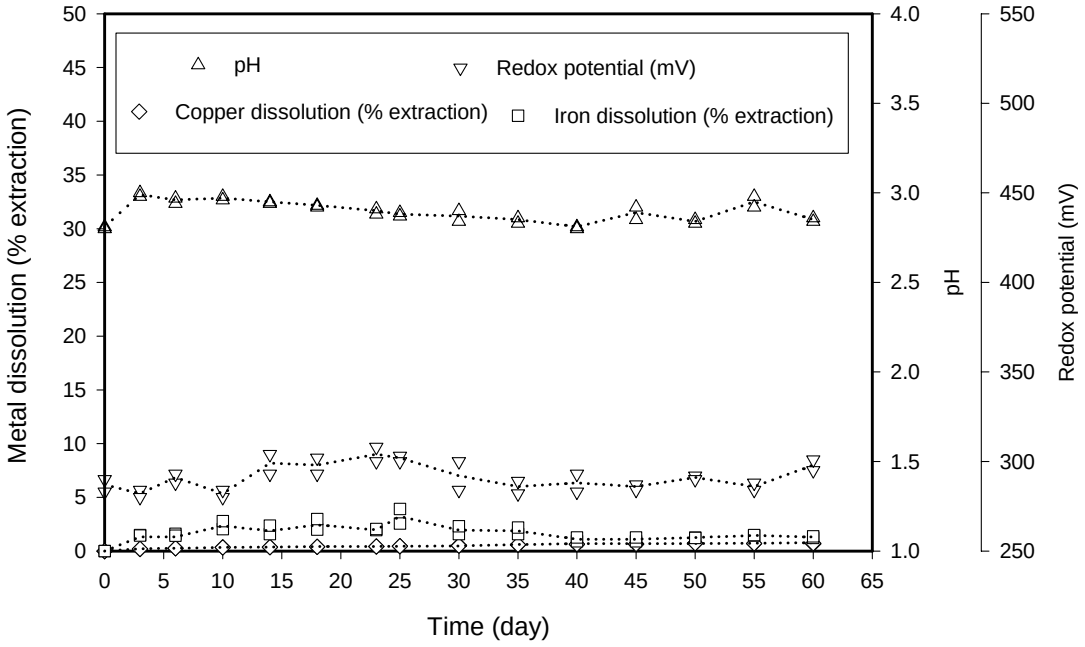

Figure 3.4 The control experiments (in the absence of bacteria) at 5% (w/v) pulp density, +53, -75 μm, initial pH 2.8 and 100 rpm

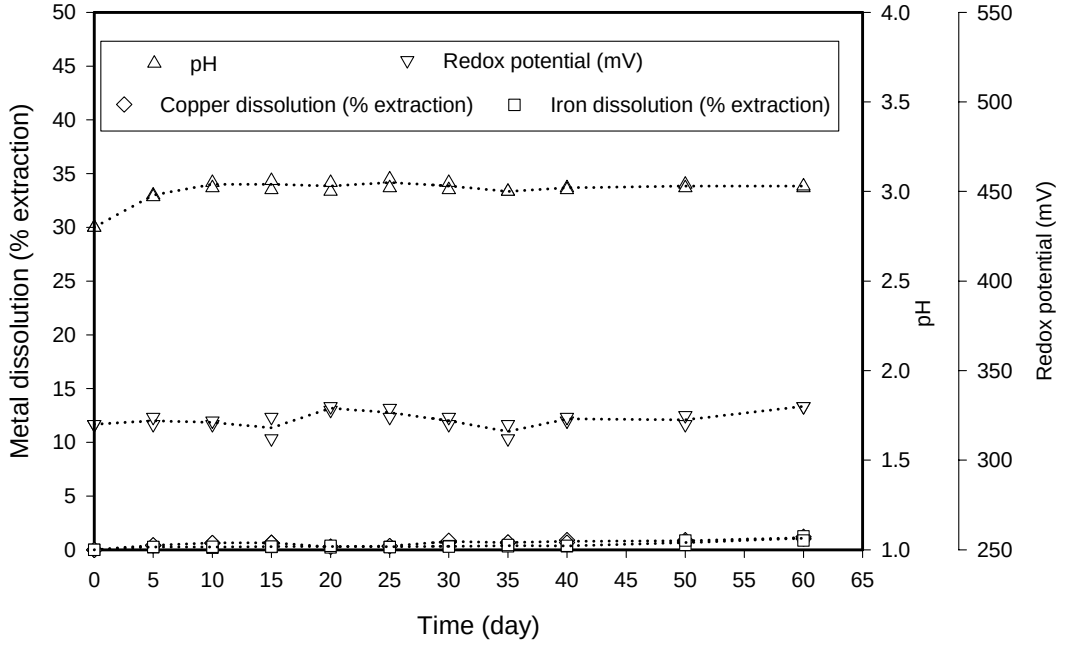

Figure 3.5 The first repeat of control experiments (in the absence of bacteria) at 5% (w/v) pulp density, +53, -75 μm, initial pH 2.8 and 100 rpm

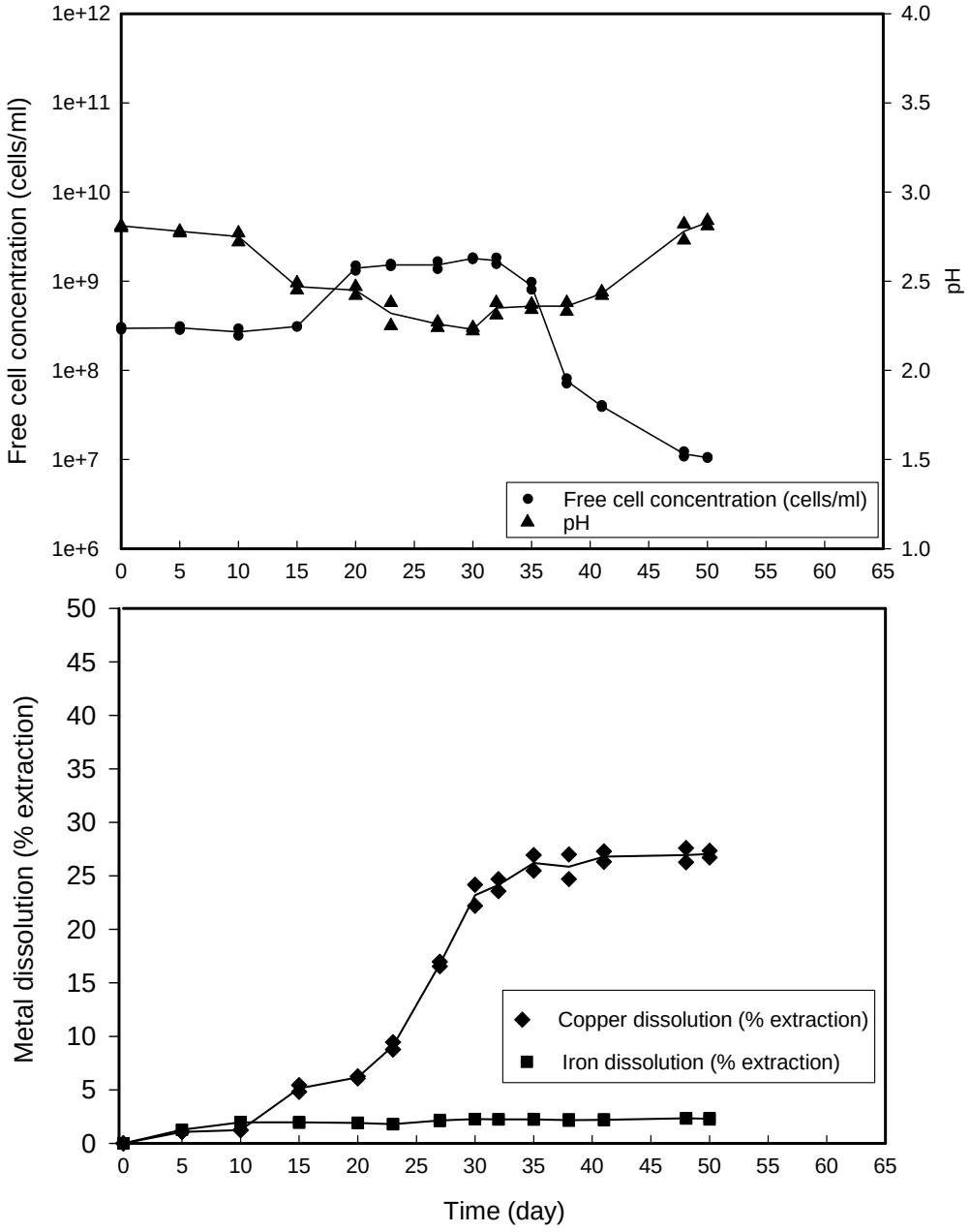

Figure 3.6 Bioleaching of chalcopyrite concentrate at 5% (w/v) pulp density, +53, -75 µm, initial pH 2.8 and 200 rpm

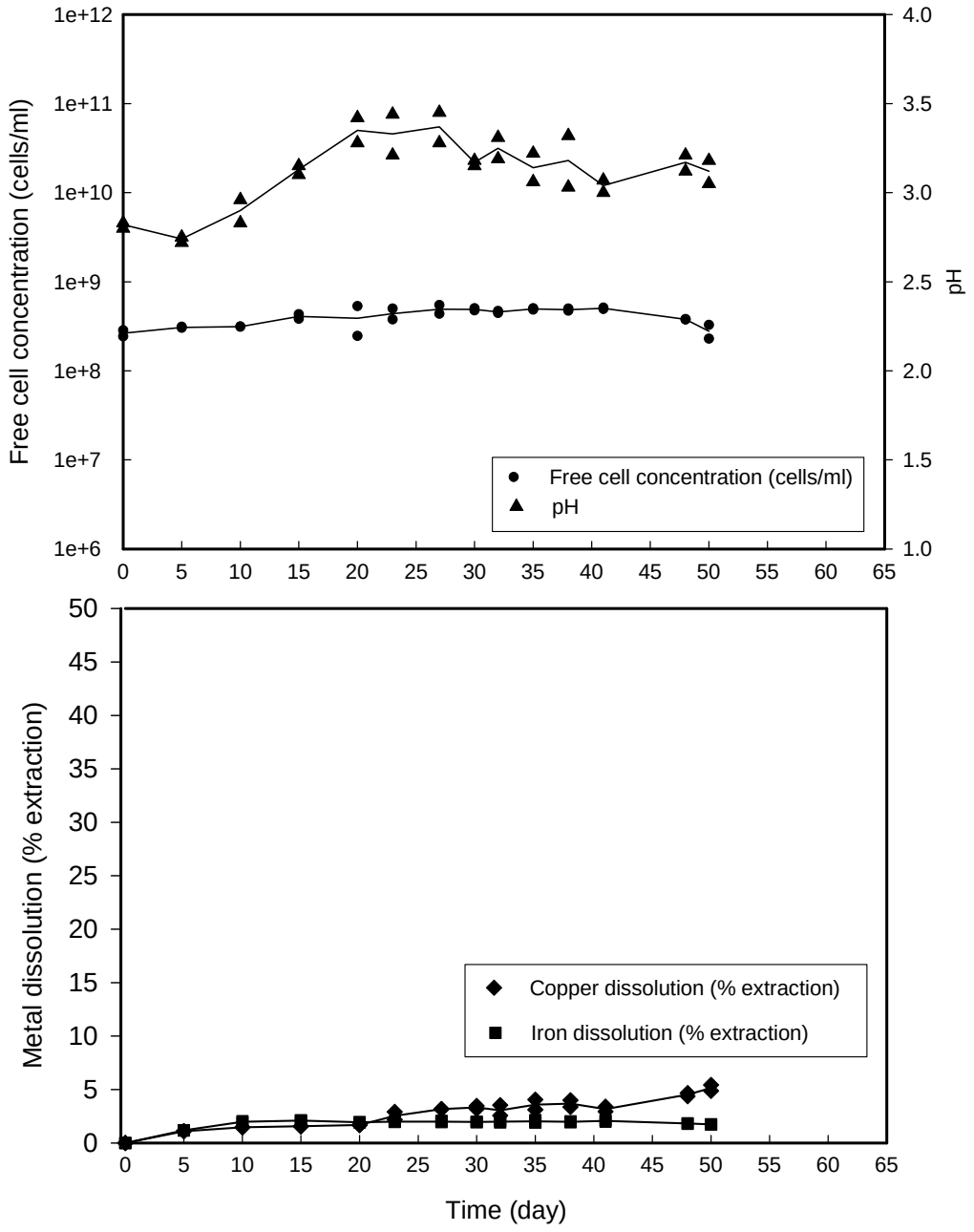

Figure 3.7 Bioleaching of chalcopyrite concentrate at 5% (w/v) pulp density, +53, -75 µm, initial pH 2.8 and 300 rpm

The growth curves from repeat experiments (Figures 3.2 and 3.3) showed good agreement with the growth curve from Figure 3.1. Those growth curves gave the maximum specific growth rate (μ_m) of 0.033 and 0.031 h^{-1}. The mean average maximum specific growth rate (μ_m) during the exponential phase was found to be 0.029±0.005 h^{-1} and the average generation time was 23.5 hours for a series of three repeat experiments. The bacterial growth rate on chalcopyrite concentrate showed an approximately three-fold decrease in comparison to growth on ferrous ions (Appendix I).

An increase of shake flask speed had a significant effect on the growth of this organism. The results for 100 and 200 rpm (Figures 3.1 and 3.6) showed an initial lag phase, which was longer at 200 rpm (i.e. 15 days in comparison to 5 days). Again, this was followed by an exponential, a stationary and then a death phase. During the exponential phase for 200 rpm, the growth curve gave the maximum specific growth rate (μ_m) of 0.009 h^{-1}, which was much lower than the growth rate at 100 rpm. In addition the generation time for 200 rpm was found to be 80 hours, almost a 3.5-fold increase in comparison to the generation time for 100 rpm. No growth was observed at 300 rpm and overall there was little change in free cell concentration (Figure 3.7).

Generally, an aerobic bioreactor is designed to achieve a higher cell concentration by promoting gas-liquid mass transfer and a relatively homogeneous distribution of nutrients cells and other components (Ju and Kankipati, 1998). Many researchers have found that increases in mechanical agitation have led to shorter fermentation times and increases in fermentation reproducibility, for example, the growth rate of

Saccharomyces cerevisiae and alcohol productivity was found to increase by increasing agitation from 150 to 600 rpm (Boswell *et al*., 2002). However in this study a high shake flask speed had contradictory effects with no growth of *T. ferrooxidans* at 300 rpm.

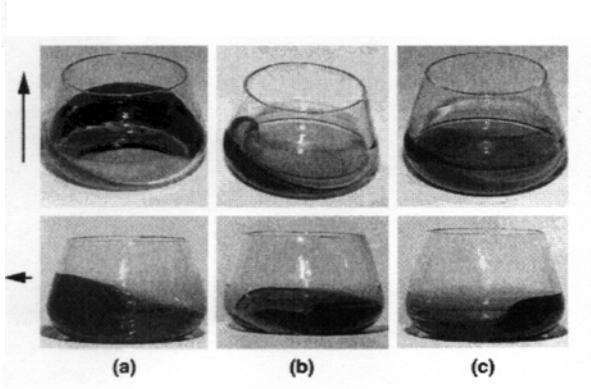

Figure 3.8 Liquid distribution in shaking flasks for a 250-ml flask at a shaking frequency of 200 L/min for: (a) a viscosity of 1 mPa·s (b) a viscosity of 75 mPa·s, and (c) a viscosity of 135 mPa·s; First row: photographs taken in the direction of the centrifugal acceleration, Second row: photographs taken perpendicular to the centrifugal acceleration, and the arrows on the left side are the direction of the centrifugal acceleration (reprinted from Büchs *et al*., 2000)

The mass flow patterns in shake flasks and bioreactors are different and unrelated to each other. The flow patterns in shake flasks are in the direction of the centrifugal acceleration (Figure 3.8, Büchs *et al*., 2000). Büchs *et al*. (2002) stated that the transition between laminar and turbulent flow can be determined at low shaking speeds (80 to 120 rpm) in unbaffled flasks (100 -2000 ml) when using low viscosity liquid. The observation that no growth occurred at 300 rpm may have been related to the turbulence in the system. Several researchers have reported the capability of *T. ferrooxidans* to attach to mineral surfaces and its growth has been found to occur primarily through attachment (Brock, 1978).

Gómez and Cantero (1998) who studied ferrous sulphate oxidation by *T. ferrooxidans* found that there was no significant difference in respect of substrate consumption when shake flask speeds were in the range of 100 and 250 rpm. Bacterial growth was also found in conditions of limiting oxygen (without agitation). Their studies concluded that the dissolved oxygen demand of *T. ferrooxidans* was very low. This finding can therefore confirm that the increase in shake flask speed did not enhance the bacterial growth. The higher shear forces at 300 rpm may have resulted in cell detachment or prevention of cell attachment in the first place.

3.3.3 Effect of shake flask speed on the solution pH and the redox potential

As can be expected bacterial activity had an effect on sulphuric acid production, which caused a reduction in the pH values during growth. The pH curve shows a decrease in pH from 2.8 to about 2.0 after 20 days (Figure 3.1), this was followed by an increase in pH to end of the experiments. The final pH of the solution was about 2.5 after 50 days, a rise of 0.5 from the minimum value. The repeat experiments (Figures 3.2 and 3.3) also showed similar pH patterns. However, the observed drop in pH appeared to be more gradual rather than replicating the pH curve of Figure 3.1. The pH values dropped from 2.8 to 2.0 after 23 days to reach a pH of about 2.6 after 60 days (repeat 1, Figure 3.2) and from an initial pH of 2.8 to about 2.0 after 18 days, followed by a slight reduction in acidity over the next 42 days to reach a pH of about 2.6 (repeat 2, Figure 3.3). This increase in pH value was presumably due to the fact that when the bacterial growth reached the stationary phase, no further cell growth occurred to produce acid ions into the solution. Moreover, the reduction in acidity was affected when the bacteria reached the dead phase, probably because of the effects of cell lysis and the

release and breakdown of cytoplasmic contents. This appeared to cause a slight increase in the pH values of the solution because the pH value of the cytoplasma is about 6-7 (Figure 2.1, Chapter 2).

The pH values for the test carried out at 200 rpm showed the same pattern as for 100 rpm, but with a more prolonged reduction in pH values. The pH values dropped from 2.8 to 2.2 after 30 days, followed by a slight increase in the pH values over the next 20 days to reach a pH of about 2.8 (Figure 3.6). However, the pH curve for 300 rpm showed a different trend to the other shake flask speeds. There was a notable increase in the pH values, with a maximum value of 3.3. This was presumably because there was no acid production since bacteria did not grow under these conditions.

The oxidation of metal ions was monitored by logging the redox potential (mV). The redox potential curves (Figures 3.2 and 3.3) show that the lag phase was about 6 days and was followed by an increase in the redox potential to reach about 480 mV, which was much higher than that obtained from the control experiments (Figures 3.4 and 3.5). After 15 days, the redox potential remained practically constant between 480 to 490 mV until the end of the experiments. These graphs show the relationship between the redox potential and iron dissolution. Higher values of the redox potential implies higher ferric to ferrous ions concentration ratio, because the redox potential monitors the oxidation of metal ions. In this case ferrous ions were oxidised by the bacteria to ferric ions and the redox potential had a positive value because of an oxidising environment.

3.3.4 Effect of shake flask speed on metal dissolution

A lag was observed before leaching occurred. For shake flask speed of 100 rpm the lag phase lasted approximately 5 days (Figure 3.1), after which the rate of copper dissolution reached 0.39 g/l per day. The rate began to level off after 15 days and reached a maximum yield of 4.78 g/l after 50 days. The final percentage of total copper dissolution was approximately 33 %. The graph shows that there was no significant increase in copper dissolution after 15 days. In contrast, the rate of iron dissolution was found to be only 0.01 g/l per day, which was significantly different from the copper dissolution rate. Iron dissolution levelled off at about 0.30 g/l and the total iron dissolution percentage was approximately 2 %. The graph shows no increase in the amount of total iron concentration before the experiment was terminated. Since the iron dissolution rate was very small but copper dissolution rate was high, it appears that this difference was significant and preferential leaching of copper was possibly occurring under these conditions.

The metal dissolution curves of the repeat experiments (100 rpm) are shown in Figures 3.2 and 3.3. These show similar metal dissolution patterns to Figure 3.1. The lag phase was a little longer at 6 days for both repeat experiments. These curves gave a copper dissolution rate of 0.20 and 0.27 g/l per day which levelled off at about 20-25 days until the end of the experiment. The final total copper dissolutions were 35 % and 35.4 % after 50 days. The average copper dissolution rate was found to be 0.29 g/l per day and the average copper percentage was 34.5 % for the three repeat experiments. Also, the iron dissolution was lower than 3 % for all the three repeat experiments.

The lag phase for the 200 rpm test (Figure 3.6) was 10 days and therefore longer than that for 100 rpm, after which the copper dissolution rate reached a maximum of 0.16 g/l per day and began to level off after about 35 days. The final yield of total copper solubilised after completion of leaching (50 days) was 3.9 g/l (27 %), a significantly lower value than that observed in the 100 rpm test. This was probably due to bacterial growth inhibition under these conditions. The maximum free cell concentration obtained from this graph was much lower than that of the 100 rpm test, being 1.8×10^9 cells/ml, compared to about 3×10^{11} cells/ml for the latter. The higher shake flask speed had an inhibitive effect on copper and iron dissolution. At 300 rpm the copper dissolution reached a concentration of 0.7 g/l (5 %) at 50 days (Figure 3.7) in line with the much reduced growth at this speed. Bioleaching at a shake flask speed of 200 and 300 rpm were found to be less effective than those at 100 rpm. Differences in cell adsorption at these speeds are discussed in chapter 4.

3.3.5 Control experiments

For the control experiments (Figures 3.4 and 3.5), the pH values remained roughly constant at pH values of 3, and again the redox potential began to level off at about 300 mV from the beginning of these experiments. Both pH and redox potential values did not significantly alter during the duration of the experiments (60 days). Copper dissolution appeared to be lower than 1 % (<0.1 g/l), whereas iron dissolution was found to be about 1-3 % (<0.4 g/l) in the absence of bacteria. The percentages of copper dissolution obtained from the above experiments in the presence of bacteria (Figures 3.1 - 3.3) were much greater than those of the control experiments. This demonstrates that the copper dissolution took place because of the influence of bacteria.

For the growth of bacteria in the absence of ferrous ions and chalcopyrite at 100 rpm (Figure 3.10), the growth curve shows that, as was expected, there was no bacterial growth. The growth rate gradually decreased until the culture could not be counted (i.e. lower than 10^6 cells/ml). The pH values increased slightly to pH 3 and remained roughly constant until the end of experiments. This was possibly because of the lack of substrate for the organism to use. The cells began to lose viability and lysis, which also caused a slight increase in the pH values. Furthermore, the solution, as expected, did not contain significant amounts of the copper and iron ions (graphs not shown).

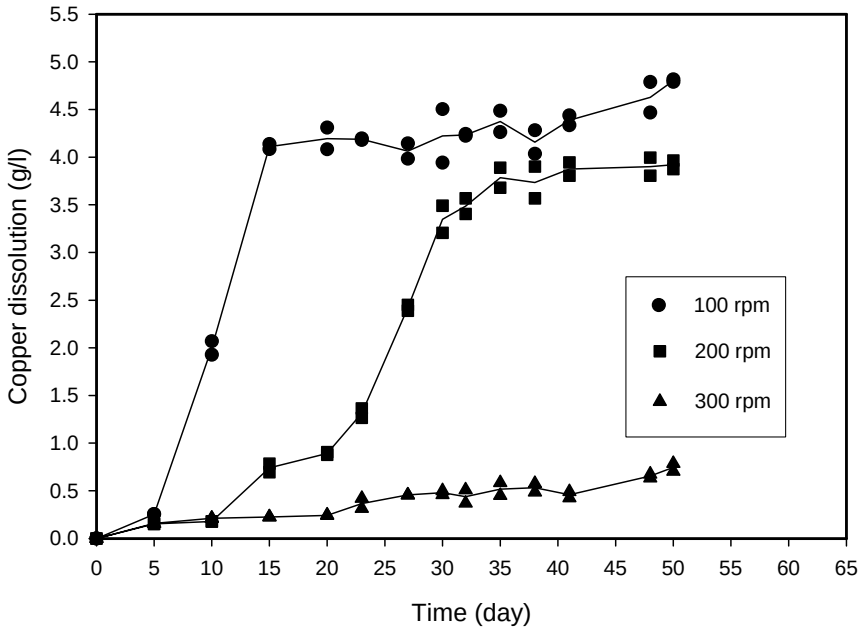

Figure 3.9 Copper dissolution (mg/l) as a function of time for bioleaching of chalcopyrite concentrate at 5% (w/v) pulp density, +53, -75 μm, initial pH of 2.8 at different shake flask speeds

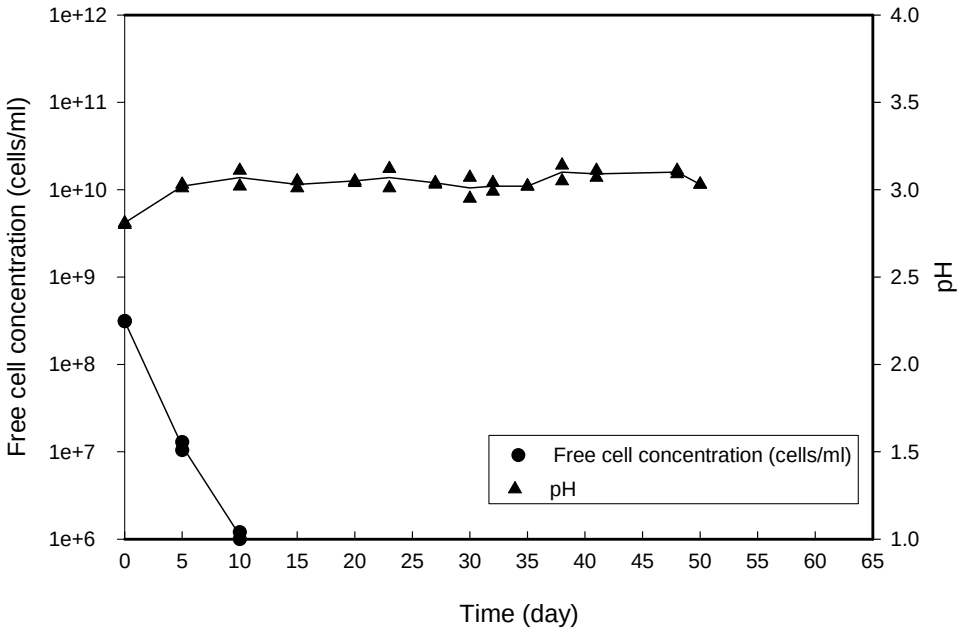

Figure 3.10 Growth of bacteria in ATCC 64 medium (in the absence of ferrous ions and the chalcopyrite) at initial pH 2.8 and 100 rpm

3.3.6 Conclusion

The copper and iron solubilisation data gave good agreement with cell growth, pH and redox potential values. As the free cell concentration increased, an increase in the dissolution of copper was observed. The rates of copper dissolution at different shake flask speeds showed that shake flask speed of above 100 rpm was detrimental. The highest rate of copper dissolution occurred at 100 rpm, whilst the lowest occurred at 300 rpm. This was presumably because the bacteria were observed to grow better at lower speeds. The rates of copper dissolution were found to be 0.29, 0.16 and 0.02 g/l per day at 100, 200 and 300 rpm respectively (Table 3.4). The final copper concentration was also found to depend on the shake flask speed. After 50 days, the percentage of total copper dissolution was found to be 33 %, 27 % and 5 % at 100, 200

and 300 rpm respectively. However, the percentages of iron dissolution were found to be only 2.2 %, 2.3 % and 1.7 % at the corresponding shake flask speeds.

Table 3.5 shows the comparison of copper solubility between thermophiles and mesophiles. The results showed some differences in rate and percentage of copper extraction. Thermophiles tended to oxidise copper concentrate ores faster than mesophiles, with the exception of the work done by Jordan *et al*. (1996). These different results are probably due to different study conditions, corresponding to different types of ores and bacteria strains. In the present work, the mesophile *T. ferrooxidans* showed a similar copper dissolution rate of 12 mg /l/hr with work done by Jordan *et al*. (1996) when using *Acidianus brierlyi*.

Table 3.4 Experimental results of bioleaching in shake flask speed tests

Shake flask speed (rpm)	Lag phase of cell growth (days)	Maximum specific growth rate, μ_m (h^{-1})	Lag time of copper dissolution (days)	Rate of copper dissolution (g/l per day)
100	5	0.03	5	0.29
200	15	0.009	10	0.16
300	No growth	No growth	20	0.02

On the whole, the relationship between bacteria growth and shake flask speed was not clear, particularly with respect to the solid substrates where other factors such as the role of attachment may have an important role. In order to verify whether the cells were attached to the surface of chalcopyrite concentrate, experiments to find the adsorption isotherm (Chapter 4) under different shake flask conditions were carried out.

Table 3.5 A comparison of copper extraction between thermophiles and mesophiles based on shake flask studies

Ref.	Ore minerals	Minerals content	Microorganism	Conditions							Results	
				Flask	Temp. (°C)	Medium	pH	Pulp density	Particle size	Shake flask speed (rpm)	Rate	% extraction
Romano *et al.*, 2001	Molybdenite concentrate	47 % Mo 3 % Cu	A mixed culture of *T. ferrooxidans*, *T. thiooxidans* and *L. ferrooxidans*	N/A	35	9K medium (without ferrous ions)	1.8	20 g/l	N/A	150	N/A	50 % Cu, 20 days
			A moderately thermophilic isolated from the drainage waters of the Rio Tinto mines (Huelva, Spain)		45	Norris medium	1.5				N/A	50 % Cu, 17 days
			Sulfolobus BC		68	Norris medium	1.5				N/A	95 % Cu, 10 days
Witne and Phillips, 2001	Copper concentrate	20 % Cu 17 % Fe 18 % S	*T. ferrooxidans* (DSM 583)	250 ml	30	Modified enriched salt solution	1.5-1.8	3 % (w/v)	A size distribution of 90 % passing 112 μm	80	7.9 mg Cu/l/hr	76 % Cu, N/A days
			Sulfobacillus acidophilus		50					160	11.6 mg Cu/l/hr	78 % Cu, N/A days
			Sulfolobus strain BC65		70					160	14.7 mg Cu/l/hr	85 % Cu, N/A days
Gomez *et al.*, 1999 b	Copper concentrate	16 % Cu 31 % Fe 7 % Zn	*S. rivotincti*	250 ml	68.5	9K medium (without ferrous ions)	2	3 % (w/v)	N/A	100	N/A	80 % Cu, 20 days
Jordan *et al.*, 1996	Copper concentrate	15 % Cu 45 % Fe 35 % S	five moderately thermophilic isolates YTF1, THWX, ALV, TH1, TH3	250 ml	50	Basal salt	1.6	3 % (w/v)	N/A	170	21-23 mg Cu/l/hr	N/A
			Sulfolobus BC		70		1.2				16 mg Cu/l/hr	N/A
			Acidianus brierlyi		70		1.2				12 mg Cu/l/hr	N/A
This work	Chalcopyrite concentrate	29 % Cu 27 % Fe	*T. ferrooxidans* (ATCC 19859)	250 ml	30	ATCC 64 medium	2.8	5 % (w/v)	-75, +53 μm	100	12 mg Cu/l/hr	32±2 % Cu, 25 days

3.4 Effect of particle size on the bioleaching of chalcopyrite

3.4.1 Introduction

Particles of different sizes have different surface areas, and hence the efficiency of bacteria attachment and metal dissolution can be expected to depend on the chalcopyrite concentrate particle size and pulp density. Many published papers indicated that leaching rates increase with a reduction in particle size, corresponding to an increase in surface area (Torma *et al*., 1972; Blankarte-Zurita *et al*., 1986; Devasia *et al*., 1996). It was also proposed that leaching rates were significantly higher for the smaller particle size range due to the larger surface area available for bacterial attachment (Devasia *et al*., 1996). In contrast, Shrihari *et al*. (1991 and 1995) found that the rate of leaching increased as the particle size increases, in spite of the lower surface area available. They stated the explanation for this increase was due to the fact that the rate of decrease in cell density in the liquid for a period of 8 h. increased with particle size, indicating the cell attachment efficiency (Shrihari *et al*., 1991). The experimental leaching conditions of some independent researchers are shown in Table 3.6.

The aim of this work was to examine the copper and iron solubility during the bioleaching of the chalcopyrite concentrate when different particle sizes were used (i.e. +38, -53 μm , +53, -75 μm , +75, -106 μm and +106, -150 μm). The effects of particle size were studied by employing cell suspensions containing a 10 % (v/v) inoculum (a bacterial concentration of about 3.0 x 10^9 cells/ml), the different particle sizes of chalcopyrite concentrate, a pulp density of 5 % (w/v) and an initial pH of the solution of 2.8. These flasks were incubated at 30 °C in a rotary shaker and 100 rpm. The effects on the free cell concentration, the solution pH, copper and iron dissolution were

investigated. The bioleaching results for different size fractions of chalcopyrite are presented in Figures 3.11 to 3.14. Finally, in order to compare the effect of particle size on bioleaching, copper dissolution (g/l) is presented as a function of time for different particle size fractions in Figure 3.15.

Table 3.6 Particle size studies by various researchers

Ref.	Minerals	Bacteria	Particle size	Conditions
Blankarte-Zurita *et al*., 1986	Chalcopyrite	*T. ferrooxidans*	$\bar{x}$ = 38 μm 181 μm 167 μm 310 μm 564 μm 674 μm	Shake flask, 10.7%w/v chalcopyrite, n/a rpm
Sukla *et al*., 1990	Chalcopyrite	*T. ferrooxidans*	+45, -53 μm +53, -75 μm +75, -106 μm +106, -150 μm	Shake flask, 1%w/v chalcopyrite, 200 rpm
Shrihari *et al*., 1991	Chalcopyrite	*T. ferrooxidans*	+63, -74 μm +150, -335 μm +699, -850 μm +1000, -1400 μm	Shake flask, 20% w/v chalcopyrite 240 rpm
Asai *et al.*, 1992	Pyrite	*T. ferrooxidans*	+53, -63 μm +63, -88 μm +149, -177 μm	Shake flask, 1 % w/v pyrite, n/a rpm
Shrihari *et al.*, 1995	Pyrite	*T. ferrooxidans*	+150, -250 μm +297, -550 μm +550, -925 μm +925, -1190 μm +1190, -2830 μm	Shake flask, 20% w/v pyrite, n/a rpm
Devasia *et al.*, 1996	Chalcopyrite	*T. ferrooxidans*	+38, -53 μm +106, -150 μm	Shake flask, 5% w/v Chalcopyrite, 240 rpm
Nemati *et al*., 2000	Pyrite	*S. metallicus*	-25 μm +25, -45 μm +75, -106 μm +106, -125 μm +125, -150 μm +150, -180 μm	Shake flask, 3% w/v pyrite, 120 rpm

3.4.2 Effect of particle size fractions on bacterial growth

The experimental data (Figures 3.11 to 3.14) demonstrate that the free cell concentration, copper dissolution, iron dissolution and solution pH are markedly affected by the size of chalcopyrite particles. The bacteria growth curve shows the typical pattern; a lag, an exponential, a stationary and then a death phase. The lag phase of cell growth curve decreased with decreasing particle size. The lag phase for a size range of +106, -150 μm was 10 days, while that of +75, -106 μm was slightly shorter (i.e. 8 days). For a size range of +53, -75 μm the lag phase showed the same length as that of +38, -53 μm, being 5 days.

During the exponential phase for the size range of +38, -53 μm, the growth curve gave a maximum specific growth rate (μ_m) of 0.045 h^{-1}, which was much greater in comparison to that of other size ranges. The maximum specific growth rates were found to be 0.030, 0.018 and 0.015 h^{-1} for the size ranges of +53, -75 μm, +75, -106 μm and +106, -150 μm, respectively. Overall, the maximum specific growth rates increased with decreasing particle size.

The overall trends in bacterial growth observed with each size fraction were similar, although the highest biomass concentration (approximately 1 x 10^{11} cells/ml) was achieved for size fractions of +38, -53 μm and +53, -75 μm. For size ranges of +75, -106 μm and +106, -150 μm, the maximum free cell concentration was lower (i.e. approximately 1 x 10^{10} cells/ml). Although the maximum specific growth rate for the size ranges of +38, -53 μm was found to be greater than that of +53, -75 μm, it was found that the highest biomass concentrations obtained from its conditions were similar.

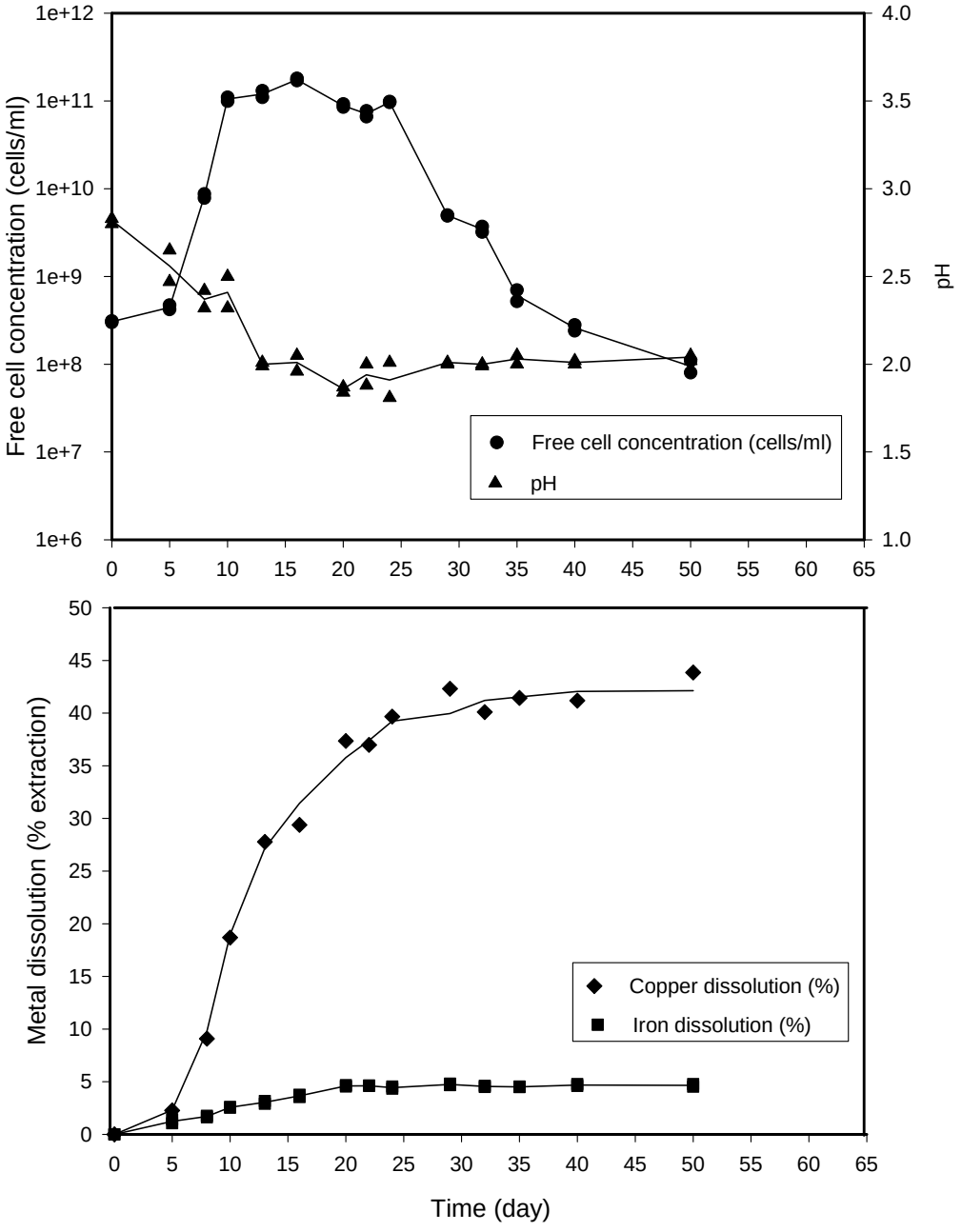

Figure 3.11 Bioleaching of chalcopyrite concentrate at 5% (w/v) pulp density, +38, -53 µm, initial pH 2.8 and 100 rpm

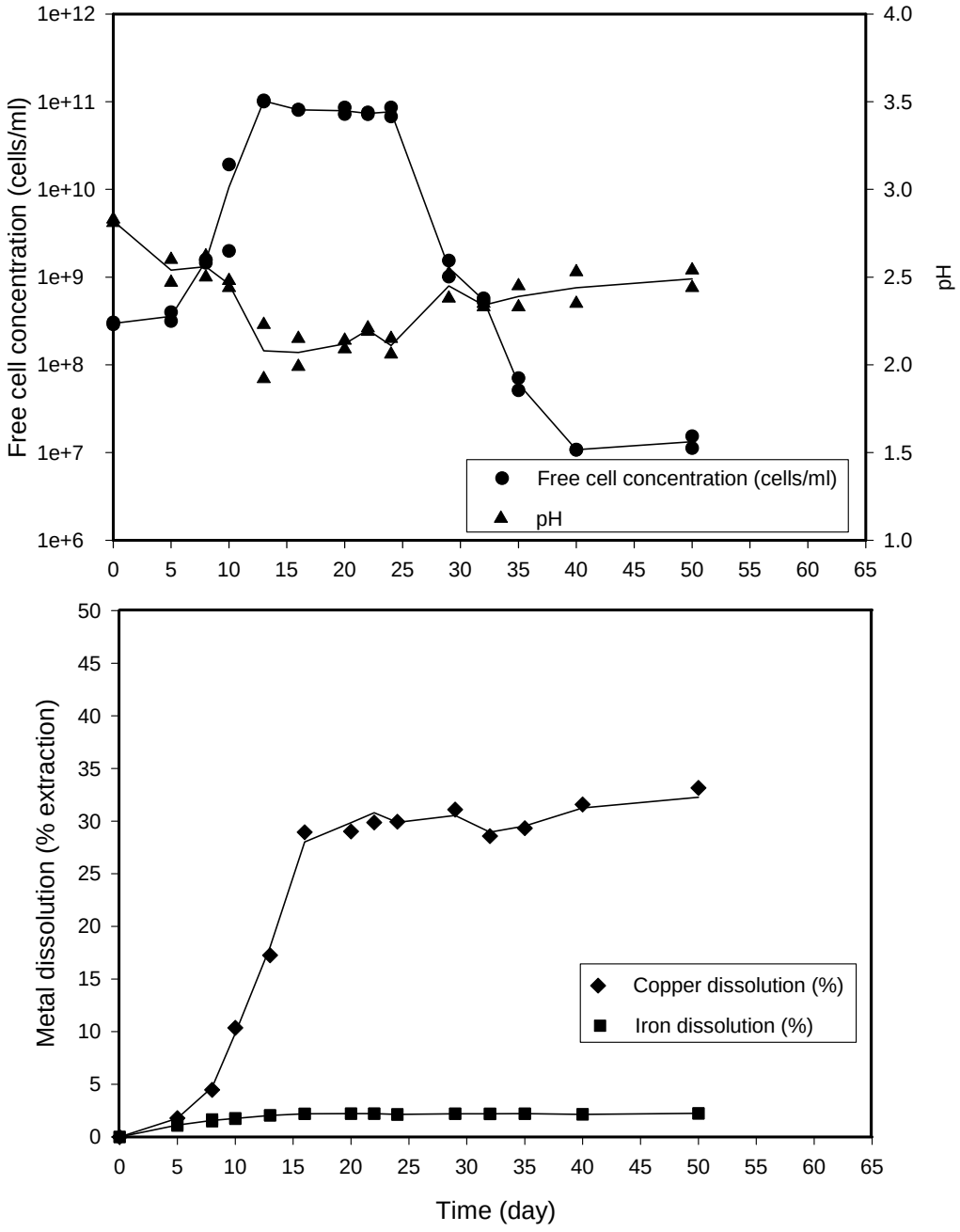

Figure 3.12 Bioleaching of chalcopyrite concentrate at 5% (w/v) pulp density, +53, -75 µm, initial pH 2.8 and 100 rpm

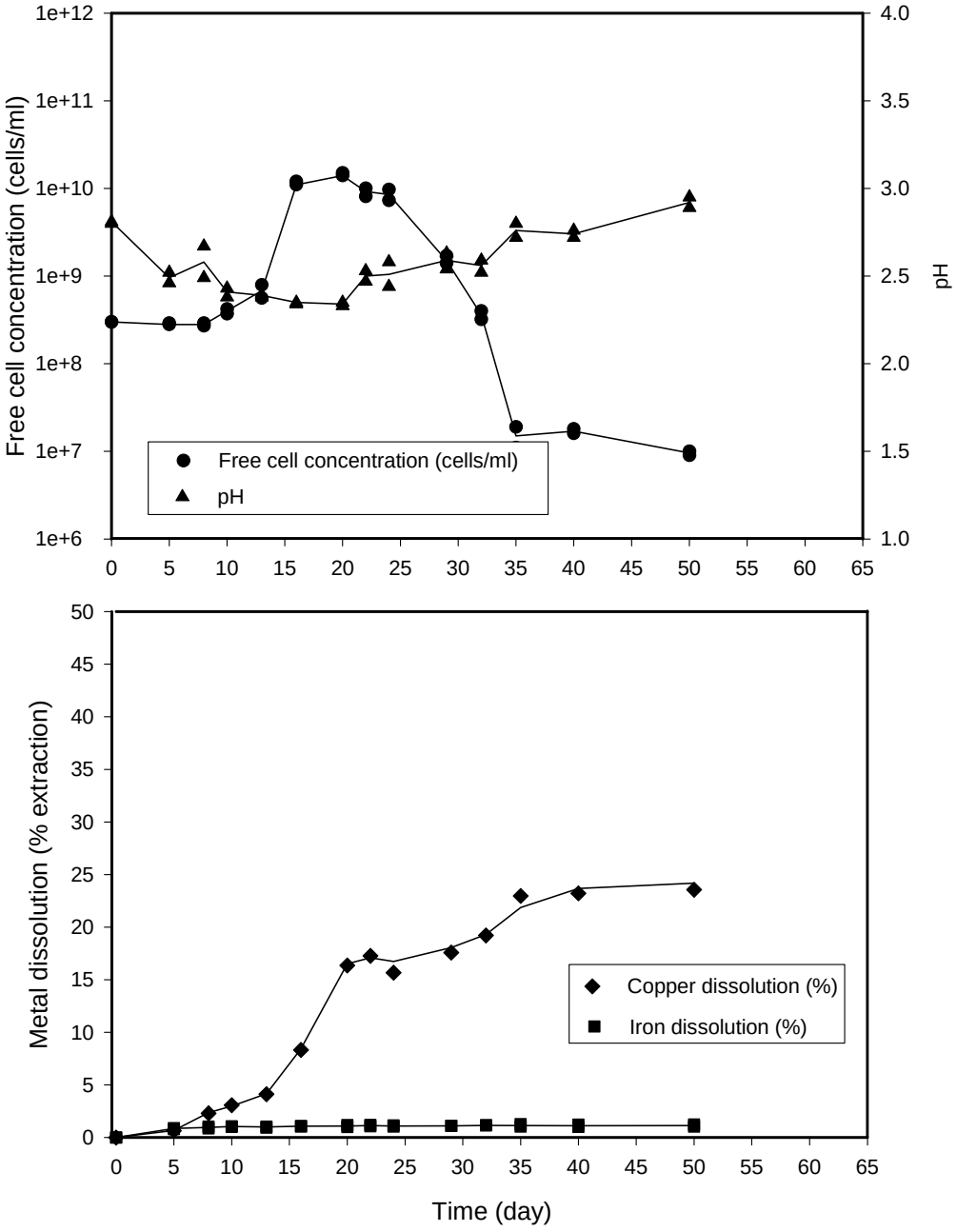

Figure 3.13 Bioleaching of chalcopyrite concentrate at 5% (w/v) pulp density, +75, -106 µm, initial pH 2.8 and 100 rpm

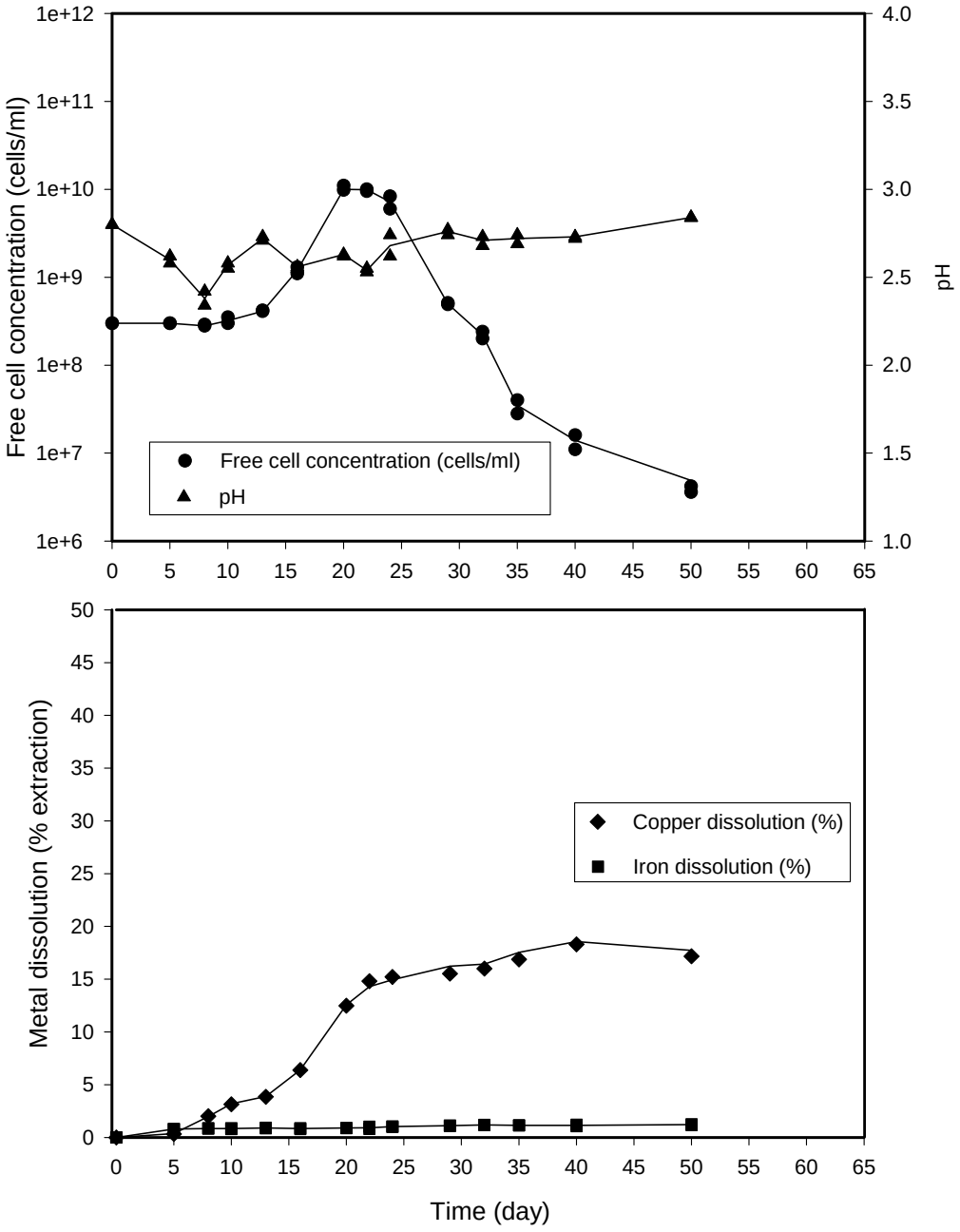

Figure 3.14 Bioleaching of chalcopyrite concentrate at 5% (w/v) pulp density, +106, -150 µm, initial pH 2.8 and 100 rpm

Since the bacterial yields from both conditions have reached the same level, the only advantage of using the finer particle size would be the shorter duration of the process. In this case, for the size ranges of +38, -53 μm, the biomass concentration reached the maximum value after 10 days, compared to 13 days for that of +53, -75 μm size fraction.

3.4.3 Effect of particle size range of chalcopyrite on solution pH

For the size range of +38, -53 μm, the pH curve shows a marked drop from 2.8 to about 2.0 after 13 days (Figure 3.11), this was then followed by a slight decrease to the minimum pH of 1.86 over the next 7 days. The final pH of the solution was 2.04 after 50 days. For the size range of +53, -75 μm (Figure 3.12) a similar pH pattern was observed. The pH decrease appeared to be gradual. The pH values dropped from 2.8 to 2.07 after 16 days and the final pH after 50 days was about 2.5. The pH values for the size range of +75, -106 μm (Figure 3.13) decreased to 2.35 after 16 days and then was followed by a slight reduction in acidity over the next 34 days to reach pH about 2.9. Finally, for the size range of +106, -150 μm, the pH curve shows that the minimum pH was 2.38 after 8 days (Figure 3.14). The final pH of this solution was about 2.8 after 50 days, a rise of 0.42 from the minimum value. These pH fluctuations were presumably due to the activities of bacteria at different stages. For example, the increase in acidity was observed when the bacteria grew; on the contrary, when no further cell growth occurred, the pH values increased.

3.4.4 Effect of particle size on metal dissolution

As can be expected, a lag phase occurred before metal dissolution began, for all the size ranges used in this study. From figures 3.11-3.14 the lag phase ranges from 5 to 15 days. For the size range of +38, -53 μm, the rate of copper dissolution reached 0.40 g/l per day. The copper dissolution rate began to level off after 25 days and reached a maximum yield of 6.05 g/l after 50 days. The final percentage of total copper dissolution was approximately 42 %. However, the rate of iron dissolution was found to be only 0.031 g/l per day, which was significantly lower when compared to the copper dissolution rate.

For the size range of +53, -75 μm similar metal dissolution patterns were found. However, the curve gave a smaller copper dissolution rate of 0.31 g/l per day and, again, the curves levelled off until the end of the experiment. The final total copper dissolution was 4.6 g/l in concentration or 32 % after 50 days. However, the total iron dissolution was found to be about 2 % after the lag phase until the end of experiments. In addition, the percentages of copper dissolution (after 50 days) were found to be approximately 24 % and 18 % for size fractions of +75, -106 and +106, -150 μm respectively, whilst the percentages of total iron dissolution were found to be around 1 % and 1 % in order of increasing size fractions.

3.4.5 Conclusion

For size fractions of +38, -53 μm, +53, -75 μm, +75, -106 μm and +106 -150 μm, the percentage of total copper dissolution (after 50 days) were found to be 42 %, 32 %, 24 % and 18 % respectively, however the percentage iron dissolution was found to be

only 4.6 %, 2.2 %, 1.1 % and 1.2 % respectively. Similarly, the rates of copper dissolution decreased with increasing particle size, i.e. 0.40, 0.31, 0.19, 0.15 g/l per day (Figure 3.15). It would appear that the explanation for this increase is that the finer particle size has more surface area, enhancing metal dissolution.

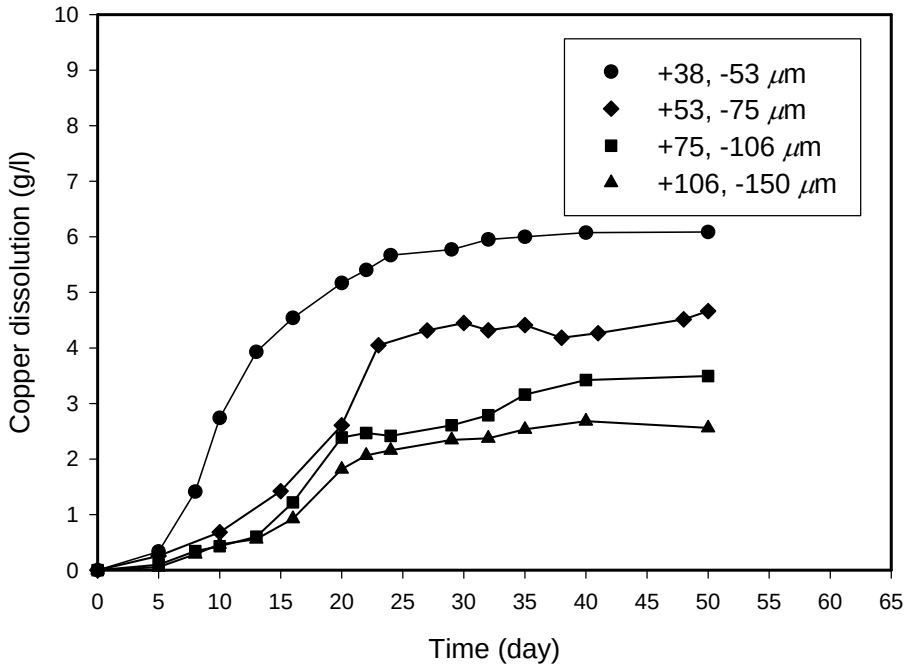

Figure 3.15 Copper dissolution (mg/l) as a function of time for bioleaching of chalcopyrite concentrate at 5% (w/v) pulp density, initial pH 2.8 and at different size fractions; +38, -53 µm, +53, -75 µm, +75, -106 µm, +106, -150 µm

An increase in copper dissolution was caused by the notable increase in the number of free cell concentration in the presence of the finer particles compared to that of the coarser particles. Although the rates and percentages of copper dissolution for the size fraction of +38, -53 μm were significantly greater than those of +53, -75 μm, both size fractions appeared to have the similar biomass concentrations. Therefore, this increase in dissolution rate was not entirely due to the number of bacterial cells: the nature of mineral particle may in fact have an important role. From the mineralogy report of the chalcopyrite concentrate (Appendix IV), the finer particle size fraction consisted of slightly more copper and less gangue minerals, especially quartz. Thus, the difficulty in bioleaching of coarser particles may have been caused by the presence of some impure elements in the chalcopyrite concentrate.

Comparison of this work with that of Asai *et al*. (1992) and Nemati *et al*. (2000), shows a good agreement. These authors also reported an increase in the rate of metal dissolution with decreasing particle size for size fractions between +53, -63 μm and +149, -177 μm (Asai *et al.*, 1992) and +25, -45 μm and +150, -180 μm at a shake flask speed of 120 rpm (Nemati *et al*., 2000). In contrast, Shrihari *et al*. (1991) reported an increase in the rate of leaching for size fractions between +63, -74 μm and +1000, -1400 μm. This is possibly due to the completely different shake flask speed (240 rpm), pulp density (20 % w/w) and large particle size examined. Shrihari *et al.* (1991) pointed out that there is increasing attachment efficiency with increasing particle size because the rate of decrease in cell density in the liquid for a period of 8 h. increased with particle size.

3.5 Effect of initial pH on bioleaching of chalcopyrite

3.5.1 Introduction

As mentioned in the literature review, *T. ferrooxidans* can be classified as an acidophilic bacterium since growth and metal oxidation takes place at a pH range of 1.0 to 4.0. The experimental leaching conditions of some independent researchers are shown in the Table 3.7. Ubaldini *et al.* (1997) found that after 7 days of treatment the iron extraction (mg/l) from arsenopyrite was not related to initial solution pH in the range of 2.0 - 2.5, whilst arsenic extraction increased from about 38 % to 50 % as the pH decreased. Deng *et al*. (2000) reported that pH in a range of 1.5-3.0 gave the highest biooxidation rate of iron and arsenic using *T. ferrooxidans*. Nakazawa *et al*. (1998) found that the copper and iron dissolution rates for chalcopyrite increased when the pH value was altered from pH 1.7 to 1.0, which is in contrast to the data of Fowler *et al*. (1999) observed a decrease in the rate of iron dissolution from pyrite with a change in pH values from pH 1.7 to 1.3. The iron dissolution was also found to be enhanced by the presence of bacteria above that achieved by chemical dissolution under the same conditions (Fowler *et al*., 1999). It is still difficult to interpret the results found from this literature, given the conflicting results obtained. These conflicting results are probably due to different study conditions, corresponding to different types of ores and bacteria strains. In addition, the small number of published papers available does not allow researchers to draw a sound conclusion; the present study may contribute to fill this apparent gap in knowledge.

The aim of this work was to examine the copper and iron solubility during the bioleaching of the chalcopyrite concentrate when different initial pH was used (i.e. pH

1.5 and pH 2.0). The effect of initial pHs was studied by employing cell suspensions containing 10 % (v/v) inoculum (corresponding to bacterial concentration about 2.5 x 10^9- 3.8 x 10^9 cells/ml), a particle size of +53, -75 μm, pulp density of 5 % (w/v) and a variety of initial pHs. These shake flasks were incubated at 30 °C and 100 rpm in a rotary shaker. The effects on the free cell concentration, the solution pH, copper and iron dissolution were investigated.

Table 3.7 Bioleaching conditions of independent researchers

Ref.	Minerals	Bacteria	Initial pH	Conditions
Ubaldini *et al.*, 1997	Arsenopyrite	Mixed culture of *T. ferrooxidans* and *T. thiooxidans*	2.0, 2.25, 2.5	Shake flask, 10-20 % (w/w), <75 μm
Fowler *et al*., 1999	Pyrite	*T. ferrooxidans*	1.3-1.7	2 litre bioreactor, 1 % (w/w), +63, -75 μm
Nakazawa *et al*., 1998	Chalcopyrite	*T. ferrooxidans*	1.0-1.7	Shake flask, 2 % (w/w), <75 μm
Deng *et al*., 2000	Gold sulphide ores	*T. ferrooxidans*	0.5-4.0	Shake flask, 10% (w/w), <150 μm

The bioleaching results and the control experiments (in the absence of bacteria) for different initial pHs are presented in Figures 3.16-3.22. The bioleaching of chalcopyrite concentrate at an initial pH of 1.5 is shown in Figure 3.16 and a repeat under the same conditions is shown in Figure 3.17. Whilst the control experiments (in the absence of bacteria) at the same initial pH are presented in Figure 3.18 and Figure 3.19. In addition, the bioleaching of chalcopyrite concentrate and the control experiments (in the absence of bacteria) at an initial pH of 2.0 are shown in Figure 3.20 a, and b respectively. A repeat of the same initial pH experiment is also shown in Figure 3.21, while the control experiment is shown in Figure 3.22. Furthermore, the results obtained

from those previous experiments at initial pH of 2.8 (Figures 3.1-3.3) are included in this discussion.

3.5.2 Effect of initial pH on bacterial growth

For an initial pH of 1.5, the growth curve (Figure 3.16) showed a lag phase of about 20 days, this was then followed by an exponential phase of about 10 days with a maximum specific growth rate of 0.014 h^{-1}. The growth curve from the repeat experiment (Figure 3.17) showed good agreement, for example, the lag phase was of the same duration and the maximum specific growth rate reached 0.013 h^{-1}. The mean average maximum specific growth rate was 0.014 h^{-1} for a series of two repeat experiments.

When data from experiments at pH 1.5 were compared to the lag phase of previous experiments (Figures 3.1-3.3), when the initial pH was set at a value of 2.8, a difference of an extra 15 days was observed in the lag phase. Also the maximum specific growth rate during the exponential phase decreased by more than a half from ~0.030 h^{-1}. In addition the generation time at an initial pH of 1.5 was found to be 52 hours, a 2.2-fold increase in comparison to the generation time for the initial pH of 2.8. Although both experiments had approximately the same initial free cell concentration, the maximum of free cell concentration reached was only 5×10^{10} cells/ml, compared to 3×10^{11} cells/ml for the higher pH.

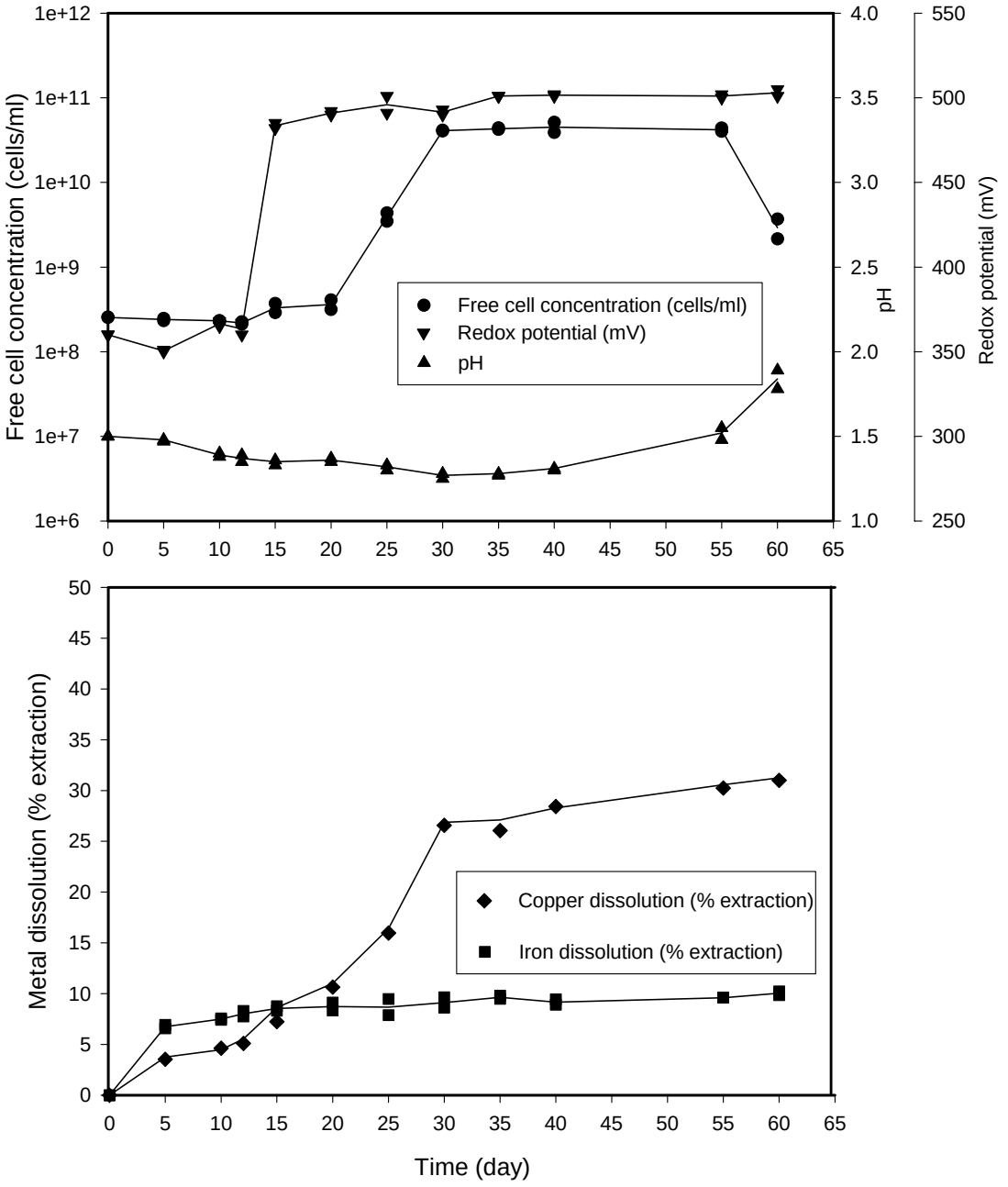

Figure 3.16 Bioleaching of chalcopyrite concentrate at 5% (w/v) pulp density, +53, -75 µm, initial pH 1.5 and 100 rpm

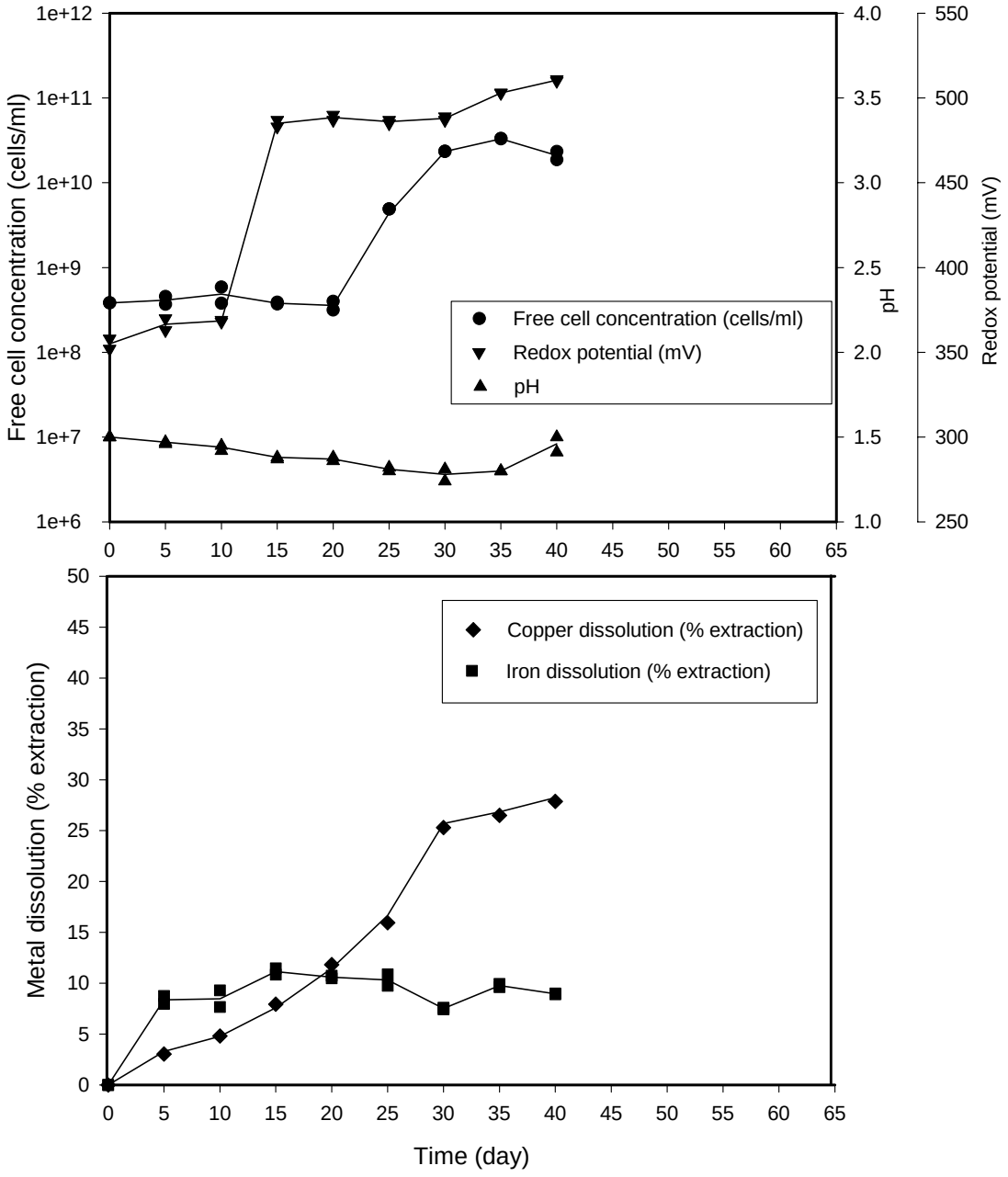

Figure 3.17 The repeat of bioleaching of chalcopyrite concentrate at 5% (w/v) pulp density, +53, -75 µm, initial pH 1.5 and 100 rpm

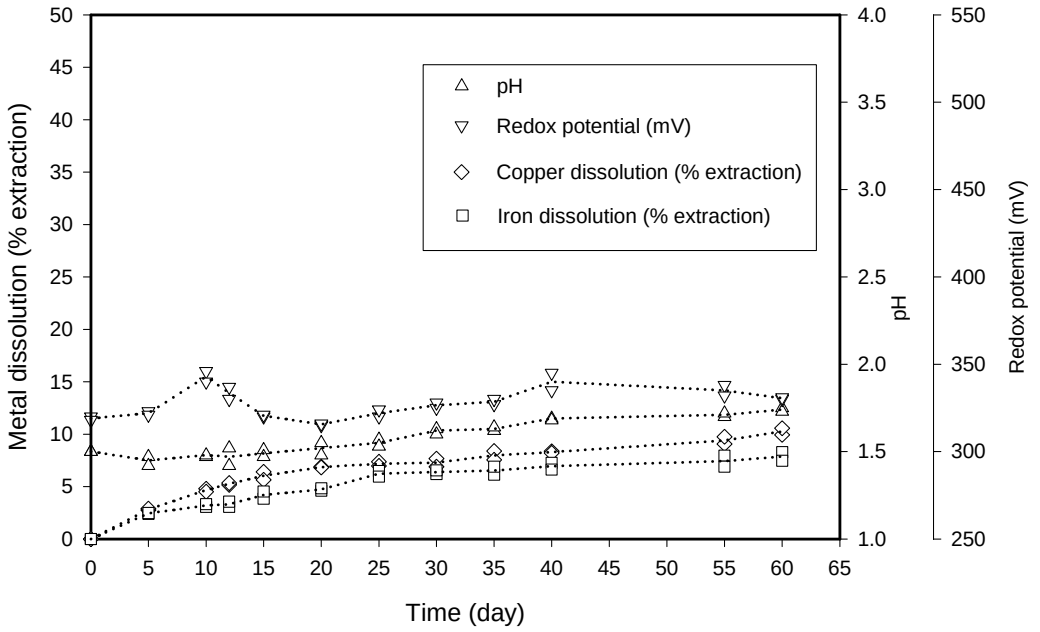

Figure 3.18 Control experiments (in the absence of bacteria) at 5% (w/v) pulp density, +53, -75 μm, initial pH 1.5 and 100 rpm

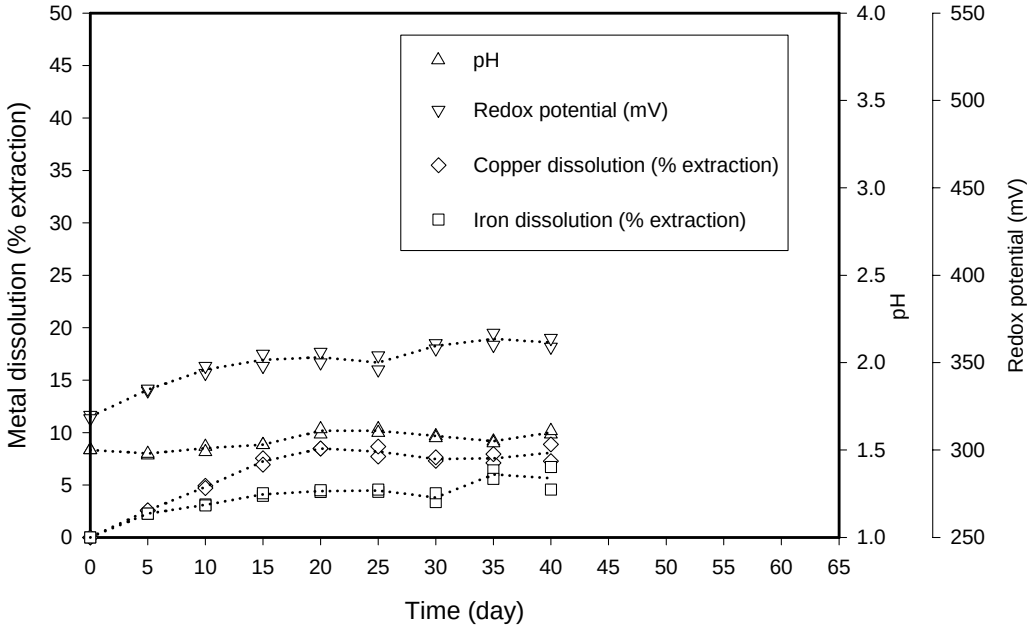

Figure 3.19 The repeat of control experiments (the absence of bacteria) at 5% (w/v) pulp density, +53, -75 μm, intial pH 1.5 and 100 rpm

Overall, a change in the initial pH from 2.8 to 1.5 had a negative effect on the growth rate and the lag phase of this microorganism. This variation in bioleaching kinetics is likely to be due to the inhibition effects of very high acidity, since it would appear from Battaglia *et al*. (1994) that when pH is lower than 1.1, bacterial growth is inhibited. Therefore, it is possible that bacterial growth was relatively slower when the initial pH was reduced to 1.5. This reduction in growth rate is consistent with the following experiment for an initial pH of 2.0.

The growth curve for an initial pH of 2.0 (Figure 3.20) shows a lag phase of about 16 days, which is approximately the same duration as that obtained from the repeat experiment of 17 days (Figure 3.21). The maximum specific growth rates were found to be 0.031 h^{-1} and 0.025 h^{-1}, which gave an mean average of 0.028 h^{-1} for two repeat experiments. The maximum specific growth rate was slightly less than that observed at an initial pH of 2.8. Moreover, the maximum free cell concentration reached was about 1.7 x 10^{11} cells/ml, slightly lower than that obtained for the initial pH 2.8. Although the maximum specific growth rate and the maximum free cell concentration for the initial pH 2.0 have reached approximately the same level as those for the initial pH 2.8, the lag phase increased more than three-fold. Therefore, it seems that the advantage of using an initial pH of 2.8 is to shorten the duration of the lag phase. This pH represents the most suitable condition for bacterial growth amongst those considered because of reduction in the lag phase combined with a high growth rate and maximum free cell concentrations. These results are summarised in Figure 3.23.

3.5.3 Effect of initial pH on the solution pH and redox potential

As can be seen from Figures 3.16 and 3.17, the pH values changed from 1.50 to a minimum value of about 1.27 after 30 days, only a drop of 0.23 in comparison to that of 0.8 for the experiment where the pH was initially 2.8. This was probably due to the lower growth rate and therefore lower copper extraction rate at the lower pH value.

The pH values for an initial pH value of 2.0 (Figures 3.20 and 3.21) showed the same pattern as that for initial pH value of 1.5. The pH values change slightly from 2.0 to a minimum value of about 1.5 after 30 days, and were then followed by an increase in pH to the end of experiments (60 days). Although the solution with an initial pH value of 2.0 contained a greater amount of H^+ ions than the solution at pH 2.8, bacteria appeared to grow at an approximately similar growth rate, notwithstanding a longer lag phase of 16 days.

For the control experiments (Figures 3.18, 3.19, 3.20 b, and 3.21), the pH curves appeared to be roughly constant.

The redox potential curves (Figures 3.16 and 3.17) show a lag of about 10 days, followed by a sharp increase to reach a relatively steady value of about 480 mV after 15 days. These curves showed a rise and levelling off of the redox potential value whilst bacterial growth was still in the lag phase. Interpretation of redox potential data is difficult. The absolute value depends on an oxidising environment such as the increase in the ferric ions concentration during the bacterial oxidation of ferrous ions, but as can be seen is not directly related to cell growth. The redox potential still had a high

positive value even as the free cell concentration appeared to drop. This has also confirmed that the number of cells in solution had no significant effect on the value of the redox potential. In addition the redox potential reaching its maximum and remaining roughly constant was probably due to the fact that the total iron dissolution did not significantly alter after 10 days (Figure 3.16). It was assumed that since total iron dissolved remained roughly constant, the ferric ion concentration remained constant as well. Therefore, the redox potential reached its maximum and remained roughly constant.

3.5.4 Effect of initial pH on metal dissolution

No detectable lag occurred before copper and iron ions were released in solution at an initial pH value of 1.5. Therefore, the rate of copper and iron dissolution was calculated from the beginning to the thirtieth day of the leaching process. The rate of copper dissolution reached 0.12 g/l per day (Figure 3.16) and 0.11 g/l per day (Figure 3.17), giving a mean average rate was 0.12 g/l per day for a series of two repeat experiments. This is a nearly 2.5-fold decrease in the rate of copper dissolution compared to that obtained at the higher initial pH. The copper dissolution rate then began to level off after 30 days and reached a maximum yield of 4.51 g/l after 60 days (Figure 3.16) and 4.08 g/l after 40 days (Figure 3.17).

The iron dissolution data showed (Figures 3.16 and 3.17) that there was quite a high iron release, relative to that of all the previous experiments, this being approximately 1.5 g/l (corresponding to about 10 % Fe dissolution). This caused a nearly 3.5-fold increase in the rate of iron dissolution in comparison to that for the initial pH value of

2.8 (Figures 3.1-3.3). This was presumably because the increased amount of H^+ ions at pH 1.5 had increased iron dissolution. This effect on metal dissolution is consistent with the control experiments for initial pH 1.5 (Figures 3.18 and 3.19).

For the control experiments (Figures 3.18 and 3.19), the amount of copper and iron released also increased, reaching maximum values of 1.48 g/l Cu and 1.14 g/l Fe after 60 days. This increase may confirm the above assumption that the higher H^+ ion concentration in solution has an affect on metal dissolution when compared to the control experiments for the initial pH value of 2.8 (Figures 3.4 and 3.5). Although a low pH had a positive effect on the chemical metal dissolution in the control experiment, overall the rate of copper dissolution and the maximum amount of copper released in the presence of bacteria were lower than those obtained at an initial pH value of 2.8 (Figures 3.1 to 3.3). This was apparently because direct and indirect bacterial leaching was inhibited by the lower pH value.

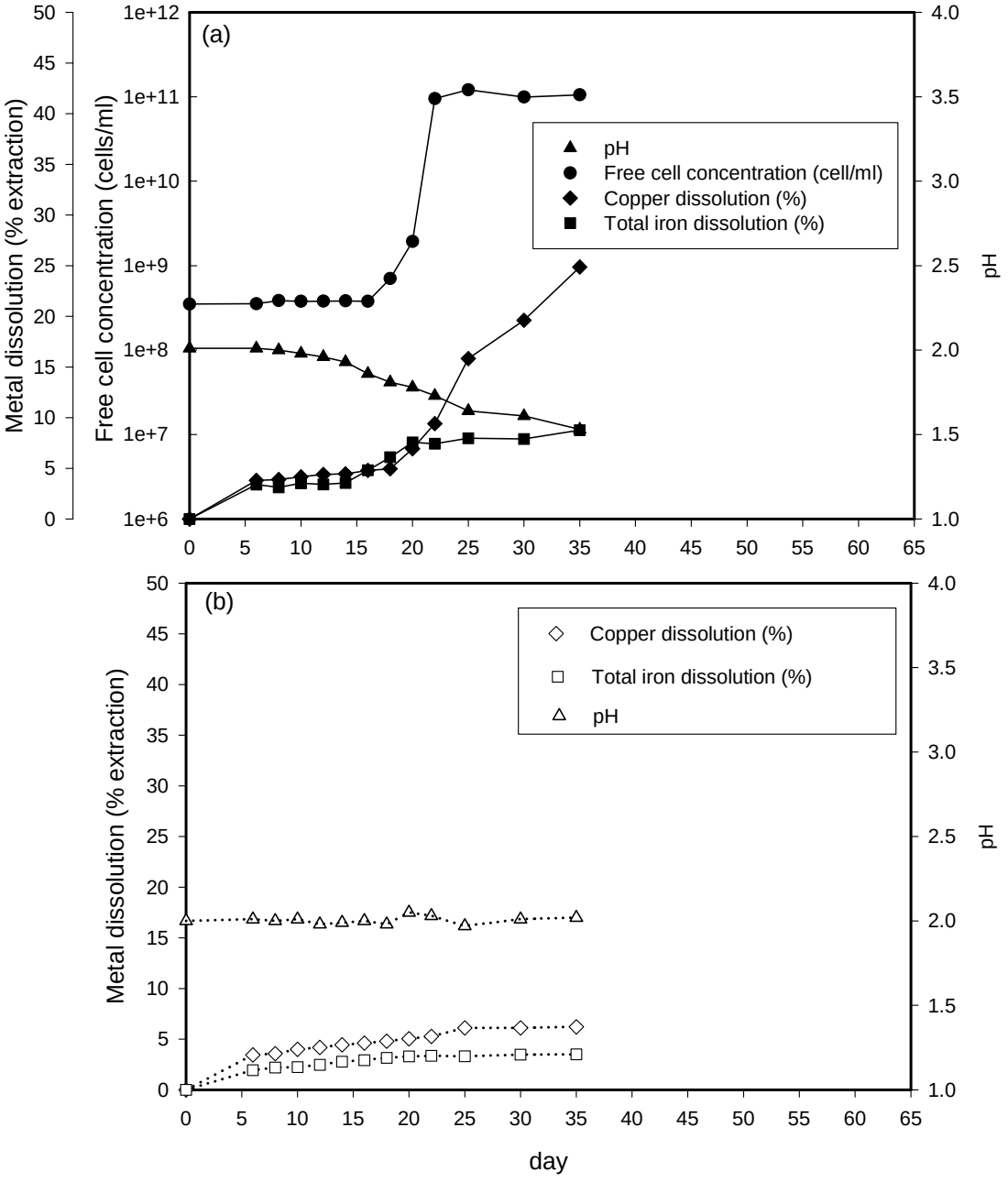

Figure 3.20 (a) Bioleaching of chalcopyrite concentrate and (b) control experiments (in the absence of bacteria) at 5% (w/v) pulp density, +53, -75 µm, initial pH 2.0 and 100 rpm

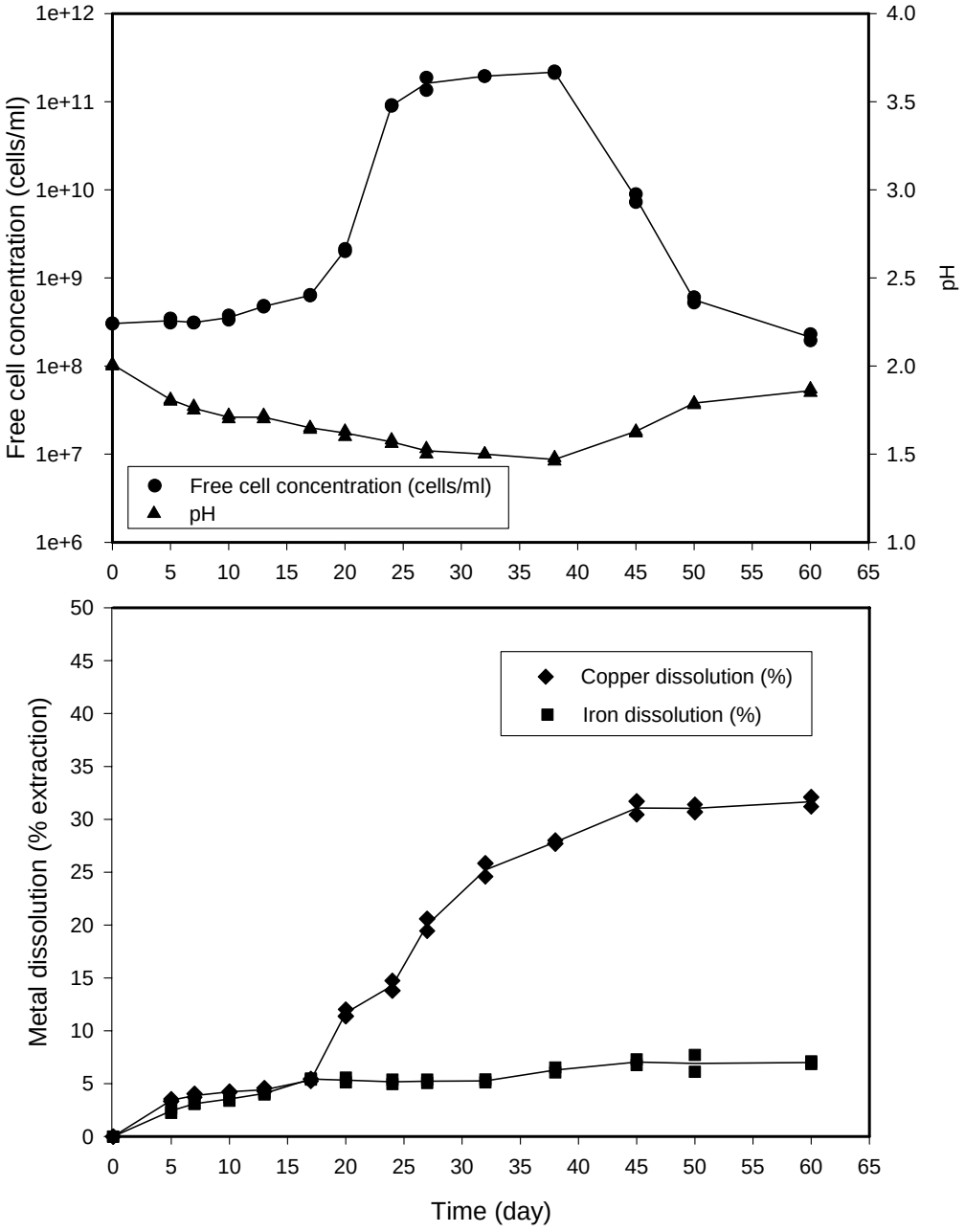

Figure 3.21 The repeat of bioleaching of chalcopyrite concentrate at 5% (w/v) pulp density, +53, -75 µm, initial pH 2.0 and 100 rpm

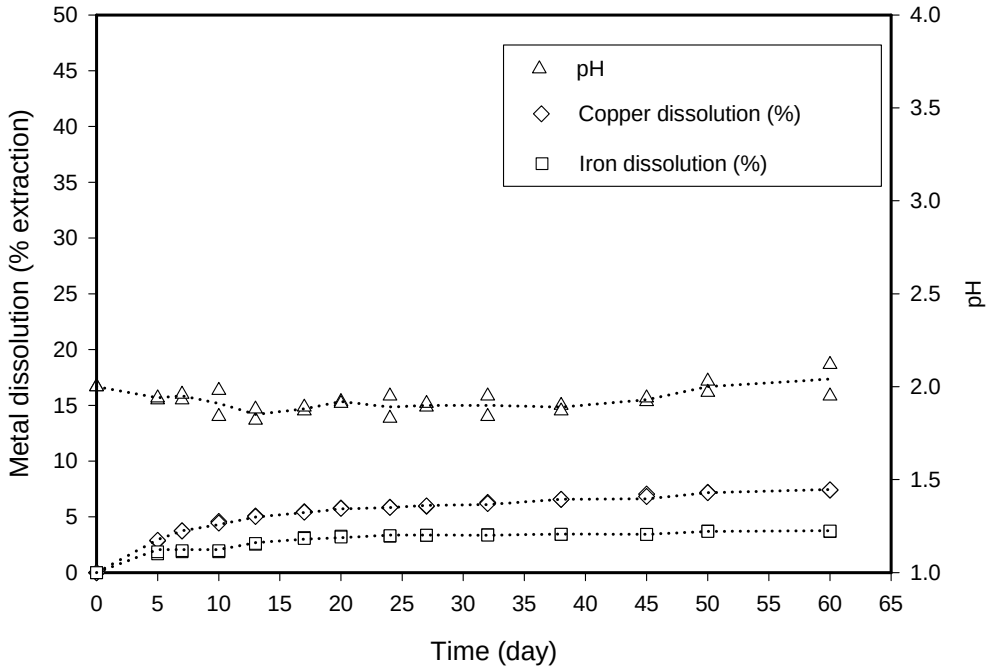

Figure 3.22 The repeat of control experiments (the absence of bacteria) at 5%(w/v) pulp density, +53, -75 μm, initial pH 2.0 and 100 rpm

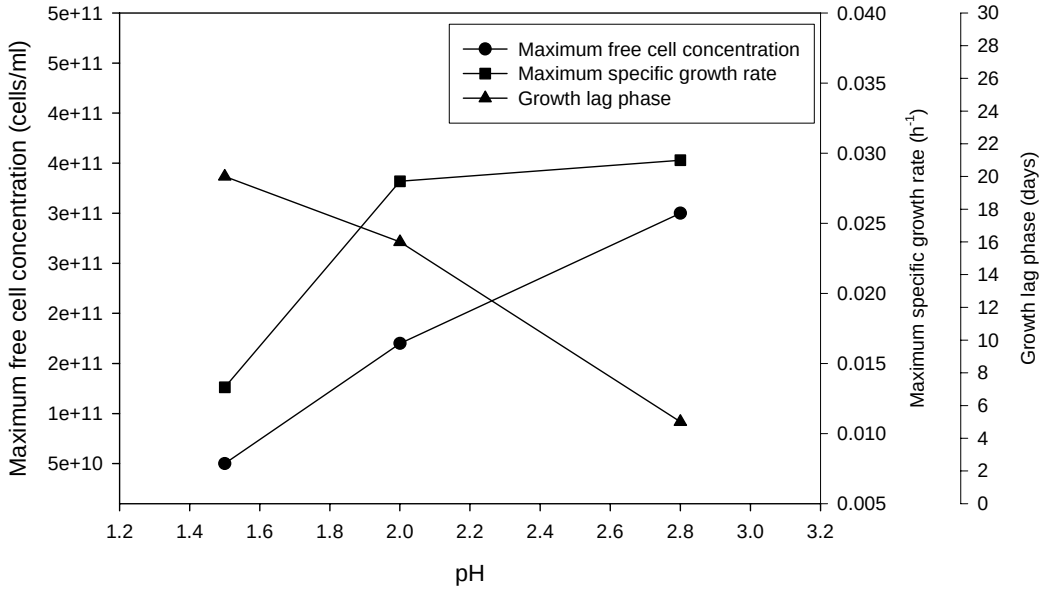

Figure 3.23 Summary of effects pH had on bacterial leaching

Again there was no distinct lag before copper and iron ions were released for experiments at an initial pH value of 2.0 (Figures 3.20 and 3.21). However, the graph of copper dissolution versus time was found to have two distinct features: an initial constant or relatively shallow slope up to the seventeenth day. This was followed by a steeper slope that was observed from the seventeenth day to the thirtieth day. During the initial period copper dissolution proved to be fairly slow, averaging 0.014 g/l per day (Figure 3.20 a) and 0.017 g/l per day (Figure 3.21), giving a mean average rate of 0.016 g/l per day. However, for second part of the curve the copper dissolution rates were found to be 0.173 and 0.186 g/l per day, giving an average rate of copper dissolution of 0.18 g/l per day for a series of two repeat experiments. The initial metal dissolution was caused by chemical leaching, however the increase in leaching kinetics was caused by bacterial activity given the significant increase in the number of cells between the seventeenth to the thirtieth day. In addition, the iron dissolution varied from 4 to 7 % for two repeat experiments, which represent a maximum of a 1.3-fold increase in comparison to that for an initial pH of 2.8.

When compared to the previous experiments when the initial pH was set at a value of 2.8, a 1.6-fold decrease in the rate of copper dissolution was found. However, just before the experiments were terminated at the sixtieth day, the final copper dissolution was 4.57 g/l (corresponding to 31.6 % extraction), slightly lower than that obtained at the initial pH of pH 2.8.

For the control experiments (Figures 3.20 b and 3.22), the copper and iron dissolution slightly increased from the beginning of the experiment. After 30 days they reached a

value of 0.9 g/l Cu and 0.6 g/l Fe. Figure 3.22 shows that final copper and iron extraction after 60 days were found to be 7.41 % and 3.75 % respectively.

3.5.5 Conclusion

These sets of results show a considerable variation in terms of bacterial growth, solution pH, redox potential and metal dissolution when the experiments were carried out at different initial pH values (i.e. 1.5, 2.0, and 2.8). The experiments that were set with an initial pH value of 2.8 gave the best results: the average rate of copper dissolution was found to be 0.29 g/l per day and the average copper extraction percentage was 34.5 % (Figures 3.1-3.3).

3.6 Effect of pulp density on bioleaching of chalcopyrite

3.6.1 Introduction

The effect of pulp density on the bioleaching of ores has been studied by a number of researchers; key papers are shown in Table 3.8. The rate of metal dissolution as reported by several authors was found to decrease with increasing pulp density (Deng *et al*., 2000; Gómez *et al*., 1999 b; Witne and Phillips, 2001). Of the densities tested, Deng *et al*. (2000) reported an optimal pulp density of 10 % (w/v) for iron and arsenic dissolution. Gómez *et al*. (1999 b) also found a significant decrease in metal dissolution when the pulp density was increased from 5 % to 20 % w/v. However, Nemati and Harrison (2000) found that the rates of iron solubilisation were not influenced by an increase in pulp density from 3 to 9 % (w/v), whereas the iron solubilisation at a pulp density of 18 % (w/v) was significantly decreased in comparison to a lower pulp density. Ubaldini *et al*. (2000) reported that the rates of iron dissolution for both experiments (i.e. 10 and 20 % (w/v) pulp density) were found to be similar.

Pulp densities had an influence on bacterial growth as well as metal dissolution rate. Gómez *et al*. (1999 b) found that the greatest cell growth of *Sulfolobus rivotincti* was found at pulp density of 1-3 % (w/v), whereas no cell growth was found above a pulp density of 7 % (w/v). Nemati and Harrison (2000) observed a longer lag phase of cell growth in order of increasing pulp density from 3 to 9 % (w/v). However, Konishi *et al*. (1999) found that the free cell concentration and the rate of copper dissolution for a pulp density of 1 % (w/v) were significantly greater than that for 0.5 % (w/v), due to the fact that the quantity of adsorbed cells increases with the suspension ore content.

Table 3.8 A summary of pulp density studies by independent researchers

Ref.	Minerals	Bacteria	Pulp density (%)	Conditions
Paponetti *et al.*, 1991	Chalcopyrite	*T. ferrooxidans*	10, 20, 30, 35	Shake flask, Particle size <38 μm
Konishi *et al.*, 1992	Sphalerite	*T. ferrooxidans*	1, 2	Shake flask, Initial pH 2.2 Particle size +38, -53 μm
Gómez *et al.*, 1999 (a)	Complex sulphides concentrate	Mixed culture of *T. ferrooxidans, T. thiooxidans* and *L. ferrooxidans*	5, 10, 15, 20	Shake flask, Initial pH 1.8 Particle size <30 μm
Gómez *et al.*, 1999 (b)	Complex sulphides concentrate	*Sulfolobus rivotincti*	1, 2, 3, 5, 7, 10	Shake flask, Initial pH 2
Ubaldini *et al.*, 1997	Arsenopyrite	Mixed culture of *T. ferrooxidans* and *T. thiooxidans*	10, 15, 20	Shake flask, Initial pH 2, 2.25, 2.5 Particle size <75 μm
Konishi *et al.*, 1999	Chalcopyrite	*Acidianus brierleyi*	0.5, 1	Shake flask, Initial pH 1.2 Particle size +38, -53 μm
Deng *et al.*, 2000	Gold sulphide ores	*T. ferrooxidans*	5, 7, 10, 20, 50	Shake flask, Initial pH 1.5 Particle size <150 μm
Nemati and Harrison, 2000	Pyrite	*Sulfolobus metallicus*	3, 6, 9, 12, 15, 18	Bioreactor: 1L capacity Particle size +53, -75 μm
Ubaldini *et al.*, 2000	Pyrrhotite	*Thiobacillus sp.*	10, 20	Shake flask, Initial pH 2 Particle size < 75 μm
Witne and Phillips, 2001	Copper concentrate	*T. ferrooxidans* *Sulfobacillus acidophilus* *Sulfolobus BC65*	3, 10, 20, 30, 40	Bioreactor: 1L capacity Initial pH 1.5-1.7 Particle size < 112 μm

As part of this research project, experiments were undertaken whereby the copper and iron bioleaching were observed at various pulp densities. Pulp densities of 2.5 % and 10 % (w/v) were studied by employing cell suspensions containing 10 % (v/v) inoculum (corresponding to a bacterial concentration of 5×10^9 cells/ml), a particle size of +53, -75 μm and an initial pH of 2.8. The experiments were carried out in shake flasks, which were incubated at 30 °C and agitated at 100 rpm in a rotary shaker. The effects of free cell concentration and the pH were also investigated. The bioleaching results of these experiments and the control experiments (in the absence of bacteria) for different pulp densities are presented in Figures 3.24-3.27. The bioleaching of the chalcopyrite concentrate at pulp density of 2.5 % (w/v) is shown in Figure 3.24, whereas the control

experiment (in the absence of bacteria) at the same pulp density is presented in Figure 3.25. The bioleaching of chalcopyrite concentrate at a pulp density of 10 % (w/v) is shown in Figure 3.26, in comparison to the control experiment for the same pulp density which is shown in Figure 3.27. All the results mentioned above were compared with the results obtained from the previous experiments (Figures 3.1-3.3) at a pulp density of 5 % (w/v).

3.6.2 Effect of pulp density on bacterial growth

As can be seen in Figures 3.1-3.3, 3.24 and 3.26, the initial period of bioleaching exhibited a lag phase in bacterial growth, which was slightly longer at higher pulp densities. The lag phases were found to be 5 days for pulp densities of 2.5 % and 5 % (w/v) and 7 days for 10 % (w/v). This was followed by the exponential phase; the maximum specific growth rates dropped significantly when the pulp density was increased, giving the values of 0.04, 0.03, and 0.02 h^{-1} for 2.5 %, 5 %, and 10 % (w/v) respectively.

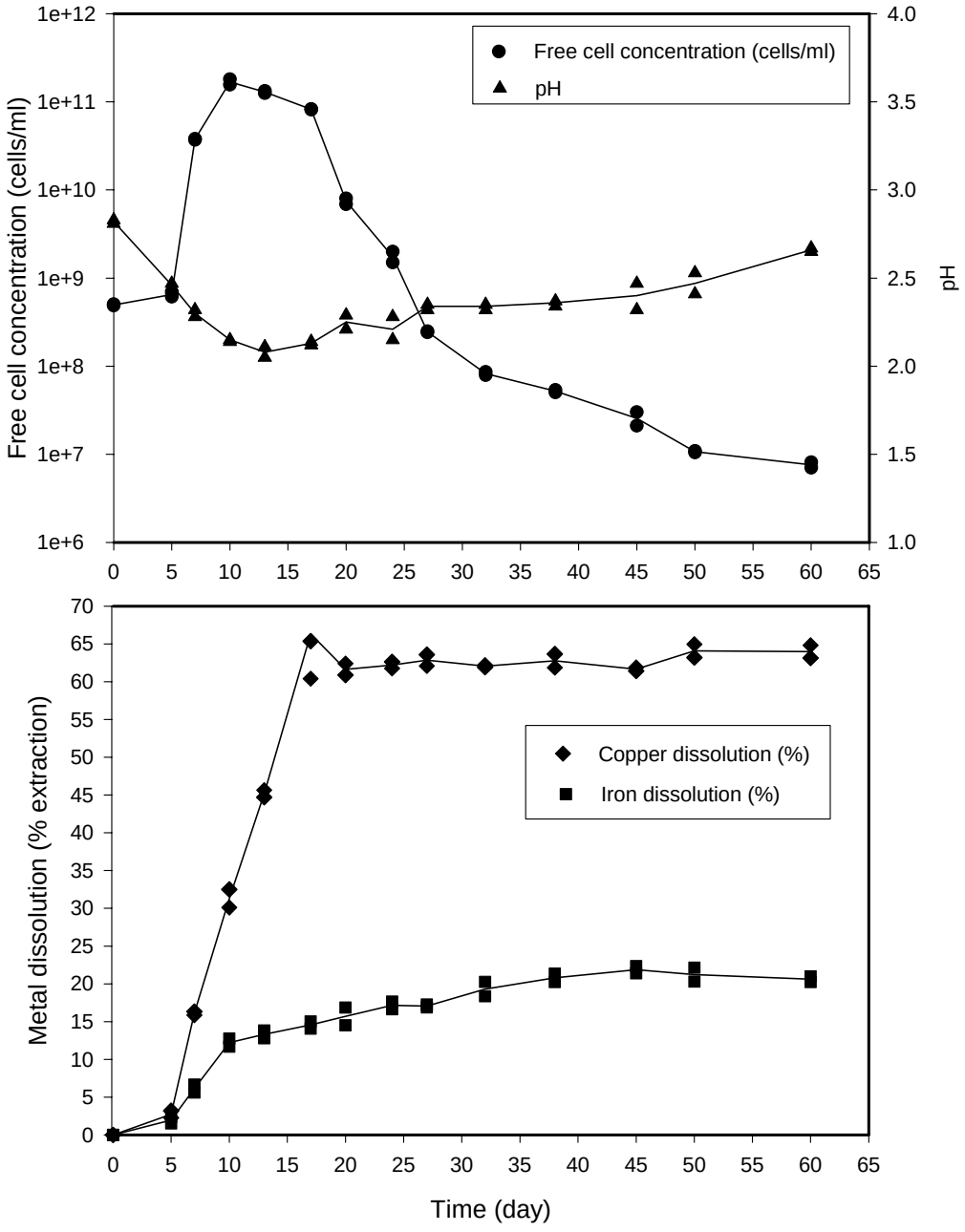

Figure 3.24 Bioleaching of chalcopyrite concentrate at 2.5% (w/v) pulp density, +53, -75 µm, initial pH 2.8 and 100 rpm

Figure 3.24 shows a maximum free cell concentration of about 1.7 x 10^{11} cells/ml. This was followed by a marked decrease in growth curve. This decrease in cell number was probably due to the exhaustion of available chalcopyrite as an energy source. With a pulp density of 10 % (w/v) a larger plateau region in the free cell concentration curve was observed, indicating a stationary phase of bacterial growth (Figure 3.26). The maximum free cell concentration was found to be 9.2 x 10^{10} cells/ml, and therefore lower than at a pulp density of 2.5 % (w/v).

3.6.3 Effect of pulp density on the solution pH

The pH patterns in the experiments with the pulp density of 2.5 % and 10.0 % (w/v) chalcopyrite were similar to one another. Figure 3.24 shows the pH value, which decreased continuously from 2.80 to 2.08 during the first thirteen days, and then increased until the end of the experiments. The final pH of the solution was found to be 2.66. Figure 3.26 shows a gradual decrease of pH value, unlike the pH curve of Figure 3.24. The pH value dropped from 2.80 to 2.09 by day twenty and was followed by a slight reduction in acidity over the next 40 days to reach a pH value of 2.82. For the control experiments (Figures 3.25 and 3.27), the pH remained at a constant 2.8.

3.6.4 Effect of pulp density on metal dissolution

For all the pulp densities there was an initial lag period before copper dissolution occurred. After this lag period the rate of copper dissolution was linear during the exponential phase. Finally the dissolution rate became constant as the cell entered the stationary phase. For a pulp density of 2.5 % and 5.0 % (w/v), the initiation of exponential phase of microbial growth led to a linear increase in copper dissolution,

which levelled off as cells entered the stationary phase (Figures 3.1-3.3 and 3.24). For the 10 % (w/v) concentrate, the onset of copper dissolution was somewhat delayed until approximately half way through the exponential stage. With a pulp density of 2.5 % (w/v), bioleaching of 64 % of the total copper and 20 % of the total iron (corresponding to a maximum concentration of 4.6 g/l Cu and 1.5 g/l Fe) was achieved after 60 days (Figure 3.24). With a pulp density of 10 % (w/v), the extent of copper and iron dissolution observed after 60 days were 16.8 and 3.5 % respectively (Figure 3.26). These percentages correspond to a maximum copper concentration of 4.8 g/l and a total iron concentration of 1 g/l.

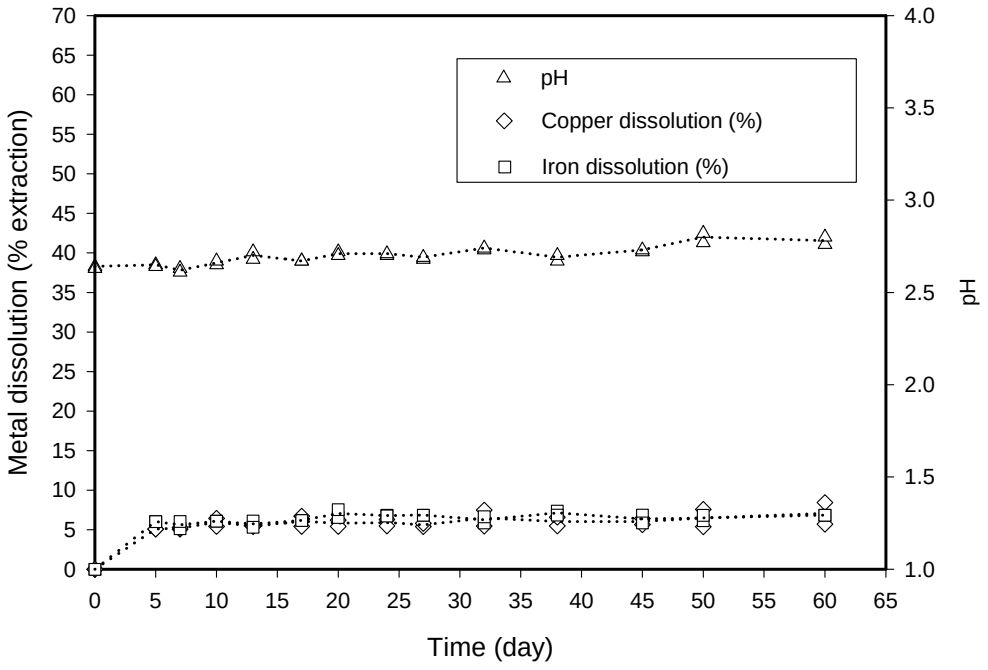

Figure 3.25 Control experiments (the absence of bacteria) at 2.5% (w/v) pulp density, +53, -75 μm, intial pH 2.8 and 100 rpm

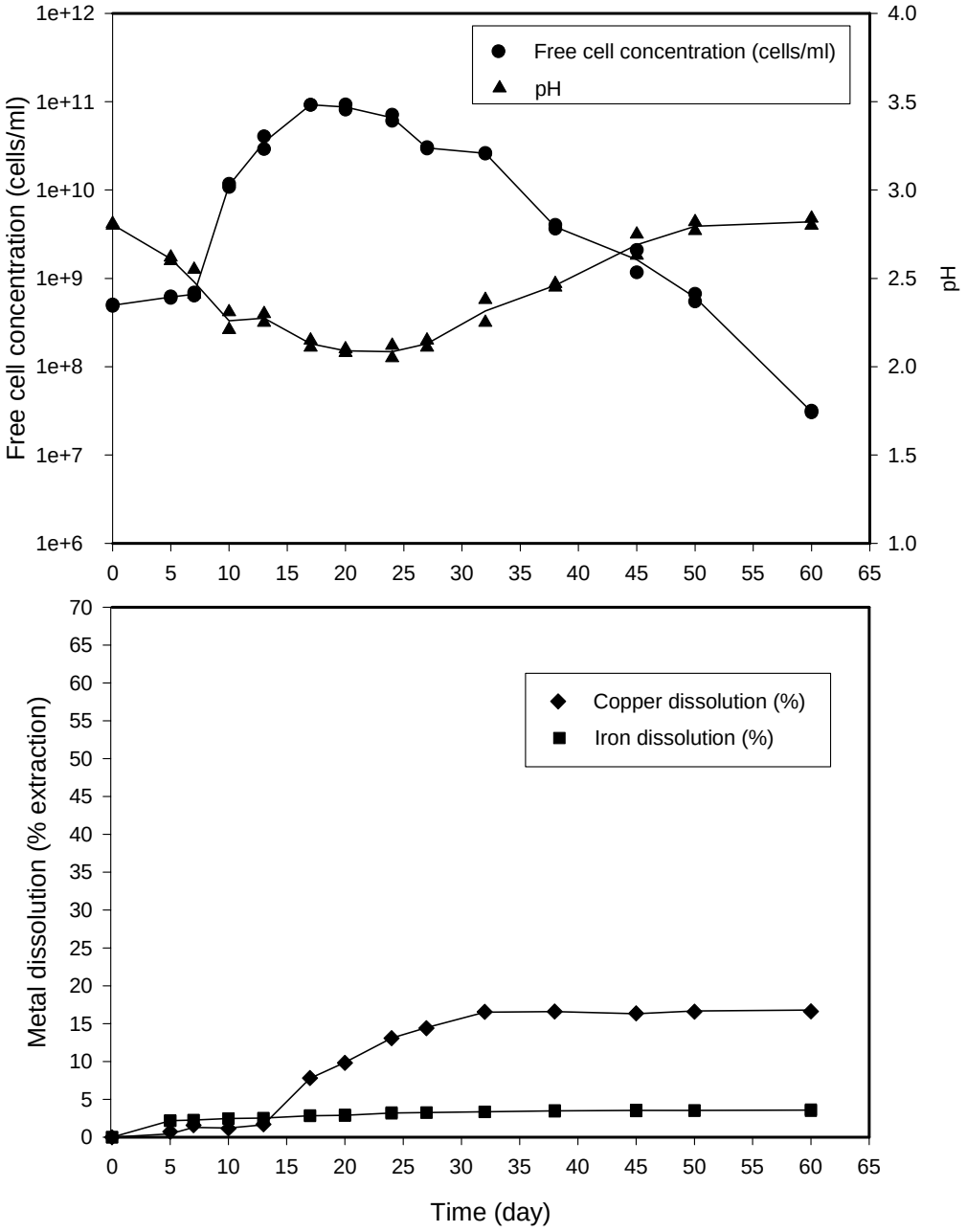

Figure 3.26 Bioleaching of chalcopyrite concentrate at 10% (w/v) pulp density, +53, -75 μm, initial pH 2.8 and 100 rpm

The maximum rate of copper dissolution at a pulp density of 2.5 % (w/v), reached 0.37 g/l per day, whereas at 10 % (w/v) was found to be 0.22 g/l per day. The rate of copper dissolution increased with decreasing pulp density. The results show a good agreement with works of several researchers (Deng *et al*., 2000; Gómez *et al*., 1999 b; Witne and Phillips, 2001). The rates of iron dissolution at a pulp density of 2.5 % and 10 % (w/v) were found to be only 0.027 and 0.015 g/l per day respectively.

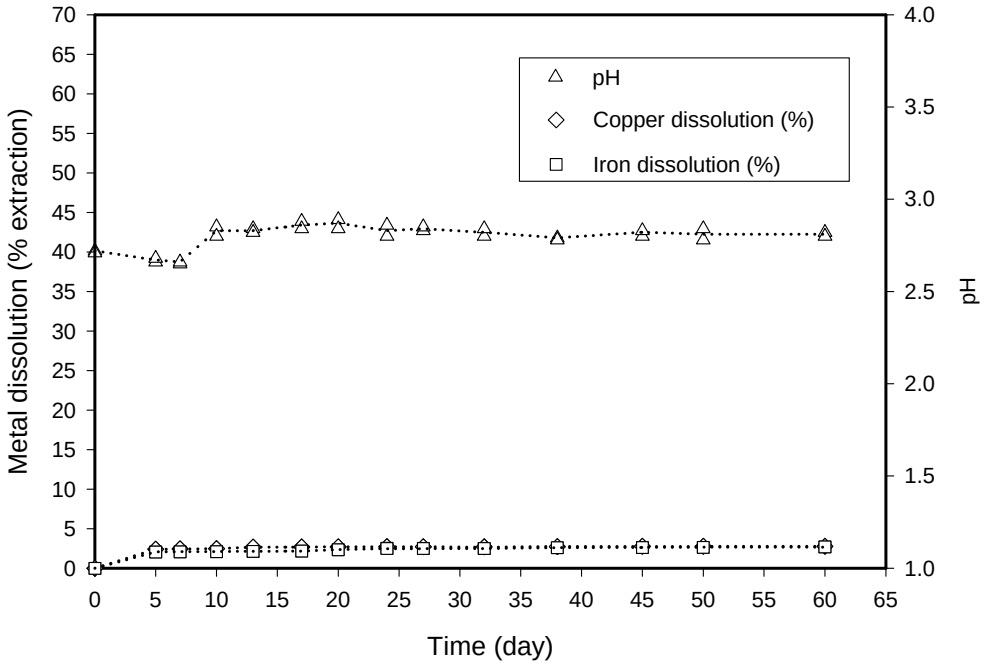

Figure 3.27 Control experiments (the absence of bacteria) at 10% (w/v) pulp density, +53, -75 μm, intial pH 2.8 and 100 rpm

According to the previous experiments (Figures 3.2 and 3.3), with a pulp density of 5 % (w/v), the maximum concentration of metal dissolution was 5 g/l Cu and 0.3 g/l Fe after 60 days. The figure for copper was not significantly different from the results of using 2.5 and 10 % (w/v) pulp density. This is likely to be due to the inhibition effects of a large number of metal ions on bacterial growth, which in turn led to a plateau region in

copper dissolutions. This inhibition in bacterial growth is consistent with the results of Das *et al*. (1997) who studied metal ion tolerance of *T. ferrooxidans*. They found that the toxicity index[1] for *T. ferrooxidans* in the presence of copper concentrations of 5 g/l and 10 g/l were found to be 1.05 and 1.85 respectively. In other words, a presence of copper concentration more than 5 g/l was found to be toxic to the bacterial cells.

As might be expected for the control experiments, the copper and iron dissolved remained constant throughout the experiments (Figure 3.25). For a pulp density of 2.5 % (w/v), values of about 0.5 g/l Cu and about 0.5 g/l Fe (corresponding to about 6-7 % dissolution) were observed. For a pulp density of 10 % (w/v), Figure 3.27 shows that the concentration of copper and iron dissolution were similar to those at 2.5 % (w/v).

3.6.5 Conclusion

Overall, the rates and percentages of copper dissolution increased significantly with decreasing pulp density although the maximum corresponding concentration was relatively constant between 4.6-5 g/l. The copper dissolution reached the stationary phase after 20 days, 25 days, and 32 days for pulp densities of 2.5 %, 5 % and 10 % respectively. The occurrence of those stationary phases is probably due to the inhibition effects of metal ions on bacterial growth.

[1] A toxicity index is defined as the ratio of time required for complete ferrous ion oxidation by a strain in the presence of dissolved metal ion M at concentration X g/l, to that required by wild unadapted strain in the absence of any dissoluted metal ion.

CHAPTER 4 The characterisation of *T. ferrooxidans* on chalcopyrite concentrate

4.1 Introduction

The adsorption and electrophoretic mobility characteristics of *T. ferrooxidans* on a chalcopyrite concentrate were investigated to better understand the effect of shake flask speed on attachment and to confirm that both attachment to and chemical modification of the chalcopyrite surface occurred. Previous studies on various mineral samples show that high concentrations of free cells in the solution, the concentration of adsorbed cells per unit weight of mineral particle approaches a limiting value, indicating that the equilibrium data can be modelled by the Langmuir isotherm (Konishi *et al*., 1994). After *T. ferrooxidans* adsorbed on mineral surfaces, the surface properties of not only the bacterial cells but also those of the minerals are altered. After interaction with each other, sulphur, pyrite and chalcopyrite and *T. ferrooxidans* showed a change in surface charge characteristics as determined by a change in isoelectric points (Devasia *et al*., 1993). Other studies have shown effect of mineral size and concentration on adsorption. In the present work, the effect of shake flask speed has been investigated in order to explain the effects on bioleaching reported in chapter 3, section 3.3.

The present work was undertaken with the objective of studying the adsorption and surface charge characteristics of *T. ferrooxidans* on a chalcopyrite concentrate. Adsorption isotherms of *T. ferrooxidans* on chalcopyrite at a varying shake flask speeds were investigated. Electrophoretic mobilities of *T. ferrooxidans* and of chalcopyrite particles before and after bioleaching were also examined. Experiments were undertaken whereby the culture of *T. ferrooxidans* was grown in the conditions

described in the materials and procedures section of those experiments. Furthermore, the maximum adsorption capacity and electrophoretic mobilities from other studies are compared with this work.

4.2 Adsorption isotherm

4.2.1 Introduction

Adsorption is a surface phenomenon where gas or liquid components are concentrated on the surface of solid particles or at fluid interfaces (Doran, 1998). Adsorption equilibrium, namely the adsorption isotherm is defined as the equilibrium distribution of a given component between an adsorbate and adsorbent. The adsorption isotherm is a useful method of estimating the number of bacteria adsorbed on a mineral surface (Konishi *et al.*, 1992).

The equilibrium isotherm data can be characterised by a model such as the Langmuir equation.

$$\frac{X_L}{X_A} = \frac{X_L}{X_{AM}} + \frac{1}{X_{AM}K_A} \qquad (4.1)$$

where: X_A is the concentration of adsorbed cells per unit weight of chalcopyrite (cell/kg), X_L is the concentration of free cells in the liquid medium (cell/m^3) X_{AM} is the maximum adsorption capacity per unit weight of chalcopyrite (cell/kg), and K_A is the adsorption equilibrium constant (m^3/cell)

Table 4.1 shows the maximum adsorption capacity per unit weight of chalcopyrite (X_{AM}) and the adsorption equilibrium constant (K_A) as determined by various researchers. X_{AM} and K_A are dependent not only on the mineral surface and the

microorganism but also on the many operating conditions of the shake flask being used for the bioleaching, such as particle size, initial pH, and pulp density.

Table 4.1 The maximum adsorption capacity per unit weight of chalcopyrite (X_{AM}) and the adsorption equilibrium constant (K_A) as determined by independent researchers

Ref.	X_{AM} (cell/kg)	K_A (m^3/cell)	Mineral	bacteria	Conditions
Asai *et al*., 1992	6.61E+13	4.68E-15	Pyrite, +25, -44 μm	*T. ferrooxidans*	1% (w/v), pH 2, 30 °C
	2.50E+13	3.58E-15	Pyrite, +53, -63 μm	*T. ferrooxidans*	1% (w/v), pH 2, 30 °C
	1.41E+13	4.03E-15	Pyrite, +63, -88 μm	*T. ferrooxidans*	1% (w/v), pH 2, 30 °C
	9.12E+12	5.29E-15	Pyrite, +149, -177μm	*T. ferrooxidans*	1% (w/v), pH 2, 30 °C
Konishi *et al*., 1992	1.65E+13	5.90E-15	Zinc sulphide, +37, -53 μm	*T. ferrooxidans*	1% (w/v), pH 2.2, 30 °C
Konishi *et al.*, 1994	4.88E+13	2.15E-15	Elemental sulphide, +25, -63 μm	*T. ferrooxidans*	2% (w/v), pH 2, 30 °C
Konishi *et al.*, 1998	8.32E+13	2.43E-15	Pyrite, +25, -44 μm	*A. brierley*	0.5% (w/v), pH 1.5, 65 °C
Konishi *et al*., 1999	3.83E+13	3.28E-15	Chalcopyrite, +38, -53 μm	*T. ferrooxidans*	1% (w/v), pH1.2, 65 °C
Beolchini *et al*., 2000	3.50E+12	4.00E-15	Pyrrfotite, <74 μm	*T. ferrooxidans* + *T. thiooxidans*	10% (w/v), pH 2, 30 °C, 200 rpm

4.2.2 Experimental procedure

A 10 % v/v inoculum of the stock culture (Appendix II) was added to a flask (250 ml) containing 45 ml of ATCC 64 medium at an initial pH of 2.8. The flask was incubated in a rotary shaker at 30 °C and 200 rpm. The cells were harvested after they had reached the late exponential phase (96 hours) and then the culture was filtered through filter paper (Whatman No. 1) to eliminate iron precipitation and other solid particles. The culture was centrifuged at 8000 rpm for 40 minutes to separate the cells and washed three times with the same medium used for growth (ATCC 64 medium without ferrous

ions). The cells were then diluted to a known concentration ($5.1 \times 10^9 - 3.6 \times 10^{10}$ cells/ml) with the medium (without ferrous ions).

All experiments were carried out in a 250 ml shake flask containing 2.5 g of chalcopyrite concentrate particles and 45 ml of ATCC 64 medium (without ferrous ions). A 10 % (v/v) solution of bacteria (previously diluted to a known concentration) was added to a series of flasks. The flasks were then incubated in a rotary shaker at 30°C. Different shaker speeds were used (100, 200 and 300 rpm). Duplicate samples were taken at regular time intervals; 5, 10, 20, 30, 40, 50 and 60 minutes and the free cell concentrations were monitored. The number of cells adsorbed on the mineral surface was determined from the difference between the number of cells in the liquid solution before and after adsorption.

4.2.3 Results and discussion

Figure 4.1 shows representative curves of the adsorption of the bacteria on the chalcopyrite concentrate at three different shake flask speeds expressed as free cell concentration against time. These experiments were set at the same initial free cell concentration of 2.6×10^9 cells/ml. The free cell concentration in the liquid-phase decreased rapidly with time, indicating that the bacteria were being adsorbed on the chalcopyrite concentrate. This figure also shows that the quantity of adsorbed bacteria is dependent of the shake flask speed; the amount of adsorbed bacteria decreases when the shake flask speed increases. The decrease in adsorbed bacteria may be explained by considering an increase in shear rates during mixing (Toma *et al.*, 1991). These conditions interfered with bacterial adhesion on the mineral surfaces and also caused a

significant decrease in free cell growth rate (Chapter 3, section 3.3). Since it would appear from Devasia *et al*. (1993)'s work that adhesion is a necessary event for bacterial growth on sulphur, pyrite, and chalcopyrite, thus a low cell adhesion could induce a slow growth rate.

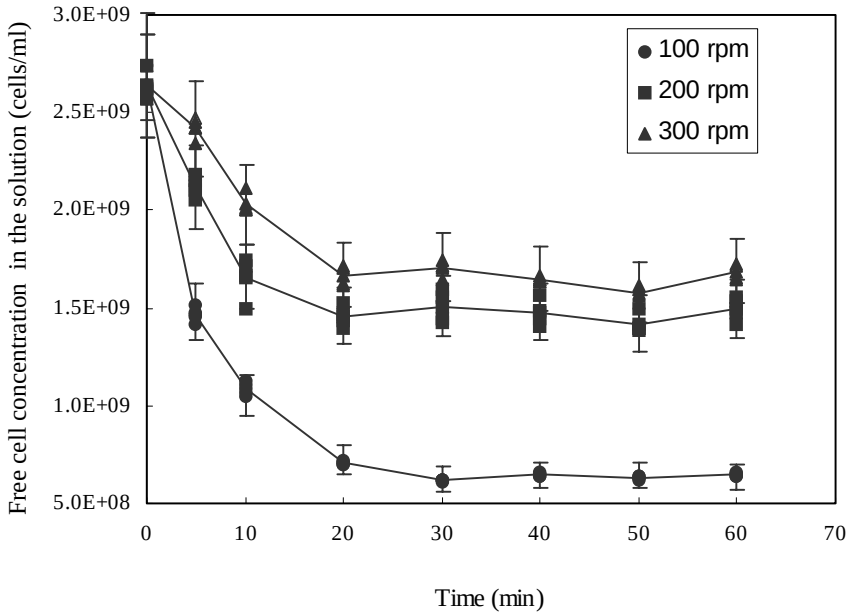

Figure 4.1 Adsorption of *T. ferrooxidans* on the chalcopyrite concentrate at different shake flask speeds; 100, 200, and 300 rpm

Equilibrium adsorption of *T. ferrooxidans* was attained within the first 20 minutes of the experiment for all shake flask speeds investigated. The data beyond 20 minutes approached a limiting adsorption amount, indicating that the data can be modeled by fitting the Langmuir equation (equation 4.1).

The equilibrium adsorption isotherm (Figure 4.2) was based on data obtained by varying the initial total cell concentration between 5×10^8 and 5×10^9 cells/ml. For each

initial cell concentration two values were obtained, X_A (the concentration of adsorbed cells per unit weight of chalcopyrite at t= 20 minutes) and X_L (the concentration of free cells in the liquid medium at t= 20 minutes). In Figure 4.2 equilibrium data for the bacterial adsorption was plotted as X_L/X_A vs X_L, according to the Langmuir isotherm. The two constants X_{AM} and K_A were calculated from the slope ($1/ X_{AM}$) and intercept ($1/ X_{AM}K_A$) of the line.

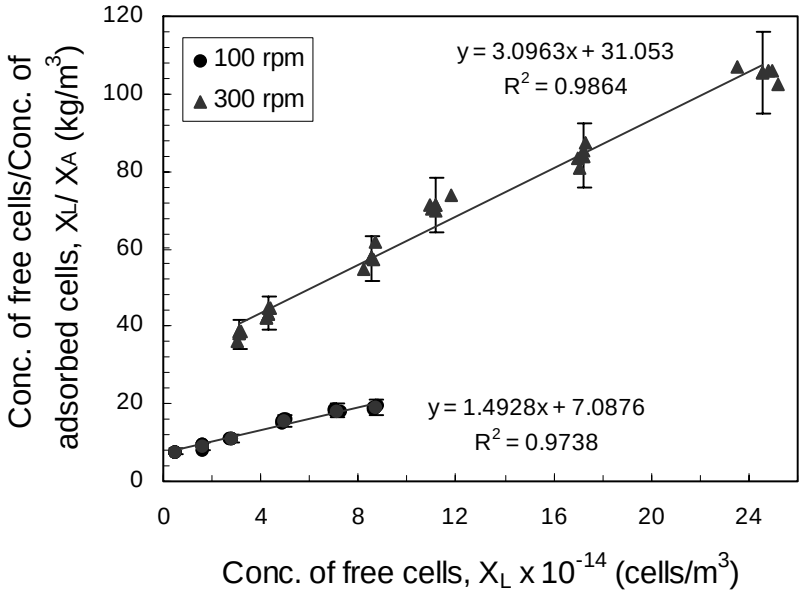

Figure 4.2 Equilibrium data for adsorption of *T. ferrooxidans* on the chalcopyrite concentrate at different shake flask speeds; 100 and 300 rpm

Table 4.2 shows the maximum adsorption capacity per unit weight of chalcopyrite (X_{AM}) and the adsorption equilibrium constant (K_A) from these curves. The correlation coefficient for the fit of equation 4.1 to the data for 100 rpm was 0.97 and for 300 rpm was 0.99, indicating that the equilibrium distribution data conforms to the Langmuir isotherm. The results from this work were found to give reasonable values and were in

reasonable agreement with other work (Table 4.1). The maximum adsorption capacity per unit weight of chalcopyrite (X_{AM}) and the adsorption equilibrium constant (K_A) were found to depend on shake flask speed. Specifically both X_{AM} and K_A appear to decrease with increasing shake flask speed. The decrease in X_{AM} (at a higher shake flask speed) can be explained by lower cell attachment due to the increase in shear rates achieved when employing a higher shake flask speed.

Table 4.2 The maximum adsorption capacity per unit weight of chalcopyrite (X_{AM}) and the adsorption equilibrium constant (K_A) at different shake flask speed

Shake flask speed	Bacteria	Mineral	Conditions	X_{AM} (cell/kg)	K_A (m^3/cell)
100 rpm	*T. ferrooxidans*	Chalcopyrite	5% (w/v), +53, -75 μm, initial pH of 2.8, 30 °C	6.70E+13	2.11E-15
300 rpm	*T. ferrooxidans*	Chalcopyrite	5% (w/v), +53, -75 μm, initial pH of 2.8, 30 °C	3.23E+13	9.97E-16

The percentage of the cells absorbed on the chalcopyrite after 20 minutes (Appendix VIII) was found to vary from 72 to 87 % at 100 rpm and from 36 to 58 % at 300 rpm when an initial total cell concentration between 5 x 10^8 and 5 x 10^9 cells/ml was employed. Santelli *et al*. (2001) suggested that approximately 10-50 % of *T. ferrooxidans* are attached to a fayalite (Fe-silicate mineral) surface based on estimates from the SEM observation after 8 days. Their work mainly concerned employing cell suspensions containing bacterial concentrations between 1.0 x 10^7 cells/ml and shake flask speeds of 120 rpm.

4.3 Electrophoretic mobility

4.3.1 Introduction

The specific chemical species present on a surface determine to a large extent, the interparticle forces acting between colloidal particles in a suspension. In electrolyte solutions particle surface charge can be characterised by the zeta potential, ζ (mV) measurements. In practice the electrophoretic mobility of particles is determined.

The electrophoretic mobility of the chalcopyrite concentrate particles and *T. ferrooxidans* in buffer solutions of different pH but fixed ionic strengths were measured using a Zetamaster (Malvern Instruments Ltd, UK). The pH where the electrophoretic mobility changes sign is called the isoelectric point (IEP). The electrophoretic mobility is positive at pH values below the IEP, but negative for pH values above the IEP. Because of this, the IEP of the particles and the bacterial cells can be determined.

In order to assess any significant changes in surface chemistry resulting from bacteria interactions, electrophoretic mobility measurements were carried out on the cells as well as the chalcopyrite before and after interaction with each other for 10 days at an initial pH of 2.8. Since previous studies had shown that after this time, significant changes in the IEP of mineral particles and bacterial cells could be detected (Devasia *et al*., 1993).

4.3.2 Experimental procedure

4.3.2.1 Particle preparation

The electrophoretic mobility measurements were adapted from previously published studies, in particular Devasia *et al*. (1993), and Santhiya *et al*. (2000), who studied the

surface chemistry of *T. ferrooxidans* in the presence of mineral particles (i.e. sulphur, pyrite, chalcopyrite, galena and sphalerite). The electrophoretic mobility measurements on the chalcopyrite concentrate before interaction with *T. ferrooxidans* were obtained by suspending 1 g/l chalcopyrite concentrate in buffers (i.e. McIIvaine type buffer and HCl-KCl buffer) of varying pH (i.e. pH 1 to pH 4.5) and a constant ionic strength (i.e. 0.1and 0.01 M).

Prior to the electrophoretic mobility measurements, the bacteria was prepared from a 10 % (v/v) of inoculum that was added to ATCC 64 medium (with 20 g/l ferrous sulphate) at an initial pH of 2.8 and incubated at 30 °C in a rotary shaker at 100 rpm for 4 days. The experiments were carried out bacterial suspensions of about 3 x 10^8 cells/ml in 0.01 M HCl-KCl buffer of varying pH.

For the microbe-mineral interaction studies, all experiments were carried out in a 250 ml shake flask containing 5 % (w/v) chalcopyrite concentrate particles (+53, -75 μm) and 45 ml of ATCC 64 medium (without ferrous ions) at an initial pH of 2.8. A 10 % (v/v) of inoculum (3 x 10^9 cells/ml) was added to a series of flasks which were then incubated in a rotary shaker at 100 rpm and 30°C for 10 days. After interaction, the mineral particles were separated from the cells by filtration (Whatman No.1) and were washed 3 times with the medium (ATCC 64 medium without ferrous ions). They were then added to 0.01 M buffers (i.e. McIIvaine type buffer and HCl-KCl buffer) of varying pH to a final concentration of 1 g/l. The electrophoretic mobility of the bacterial cells, as well as the mineral particles were measured separately. The electrophoretic mobility measurements for the bacteria grown on the chalcopyrite were conducted on bacterial

suspensions of about 3 x 10^8 cells/ml in 0.01 M HCl-KCl buffer of varying pH. Measurements were carried out after conditioning the mineral particles or the cells at the required pH for an hour at room temperature (25 °C).

4.3.2.2 Buffer preparation

All the buffers of constant ionic strength used in this experiment were prepared as described in "Data For Biochemical Research (1969)". M^{c}IIvaine type buffers could be prepared at pH between 2.2 and 8.0, whereas HCl-KCl buffers can be set at a pH between 1.11 and 3.11. The compositions of HCl-KCl buffer and M^{c}IIvaine type buffer are shown in Appendix VII. Buffer solutions of varying pH but fixed ionic strength were made up and then diluted with Millipore water to the ionic strength of 0.1 M and 0.01 M. The final pH of these solutions was then accurately measured and recorded prior to their use.

The molar ionic strength (I) of a solution can be calculated from:

$$I = \frac{1}{2}\sum m_i z_i^2 \qquad (4.2)$$

where m_i is the molarity of a particular ion and z_i is its charge. The ionic strengths (I) calculated from equation 4.2 are 0.096 and 0.018 M for ATCC medium in the presence and absence of ferrous sulphate (20 g/l) respectively and, therefore, buffer solutions required for this work were 0.1 M and 0.01 M.

4.3.3 Results and discussion

The electrophoretic mobilities of the chalcopyrite concentrate before interaction with *T. ferrooxidans* are illustrated in Figure 4.3 as a function of pH. The particles were suspended in two different buffers of the same ionic strength. The pH range for HCl-KCl buffers its was between 1.1 and 2.2, whereas that for M^{c}IIvaine type buffers was between 2.2 and 4.35. Each point displayed was the arithmetic mean of 20 measurements. The isoelectric point at pH 1.7 was observed when the particles were suspended in 0.1 M HCl-KCl buffers (Figure 4.3 a). A linear regression was fitted to the data with an R^2 value of 0.98, indicating a good data fit. The electrophoretic mobilities when the particles were suspended in 0.1 M M^{c}IIvaine type buffers were found to be a continuation of the data observed for HCl-KCl buffers, giving a continuous curve.

Preece (1999) measured the electrophoretic mobilities of latex as a function of pH and resulting curve was generally S-shaped. If all the data points were fitted with a second order polynomial regression (Figure 4.3 b), the trend line would achieve R^2 values of 0.99, indicating a very good data fit. From this regression, the IEP for the chalcopyrite concentrate was shown to be about 1.6. Thus, no significant difference was found in the values for the IEP calculated from a linear regression and a second order polynomial regression in Figure 4.3 a, and b.

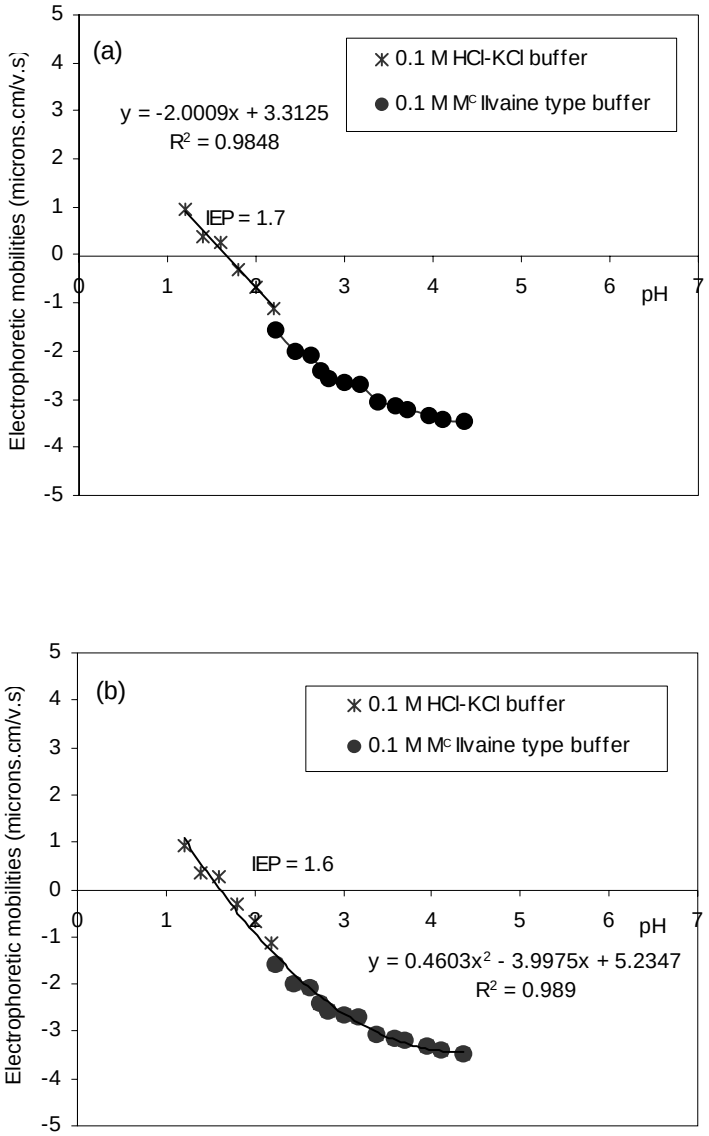

Figure 4.3 Electrophoretic mobilities of the chalcopyrite concentrate as a function of pH at two different buffers; ionic strength 0.1 M

Similar electrokinetic measurements were made with the chalcopyrite concentrate at an ionic strength of 0.01 M; a plot of electrophoretic mobilities versus pH is shown in Figure 4.4. A correlation coefficient for the fit of the linear regression to the data was 0.98 indicating that the equilibrium distribution data conforms to the linear regression. The data observed from two different buffers were found to overlap within the region of pH of 2.2 to 3.1. At the lower ionic strength of 0.01 M, the IEP was observed to be at pH 1.7. Thus, these results show no significant difference in the values for the IEP for the two ionic strengths used. Preece (1999) explained that this is indicative of the buffer system acting as an indiffererent electrolyte, i.e. the ions within the electrolyte do not interact with the chalcopyrite concentrate surface.

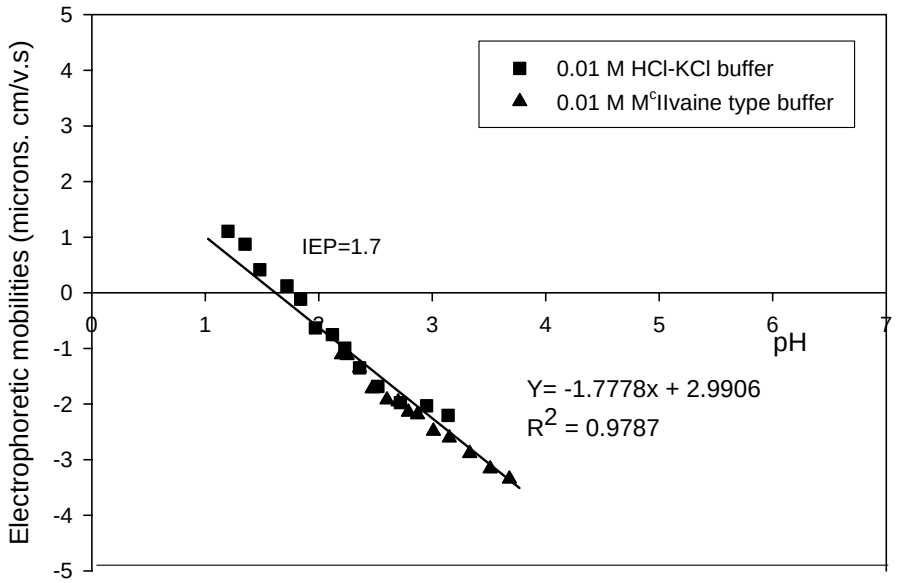

Figure 4.4 Electrophoretic mobilities of the chalcopyrite concentrate as a function of pH at two different buffers; ionic strength 0.01 M

Electrophoretic mobilities of the cells before and after interaction with the chalcopyrite concentrate are shown in Figure 4.5. Before interaction the isoelectric point is located at pH 1.6. The curve had a characteristically gentle slope. This implies that the surface charge of the cell grown on ferrous sulphate did not alter significantly over a relatively broad pH range of 1.1-3.1.

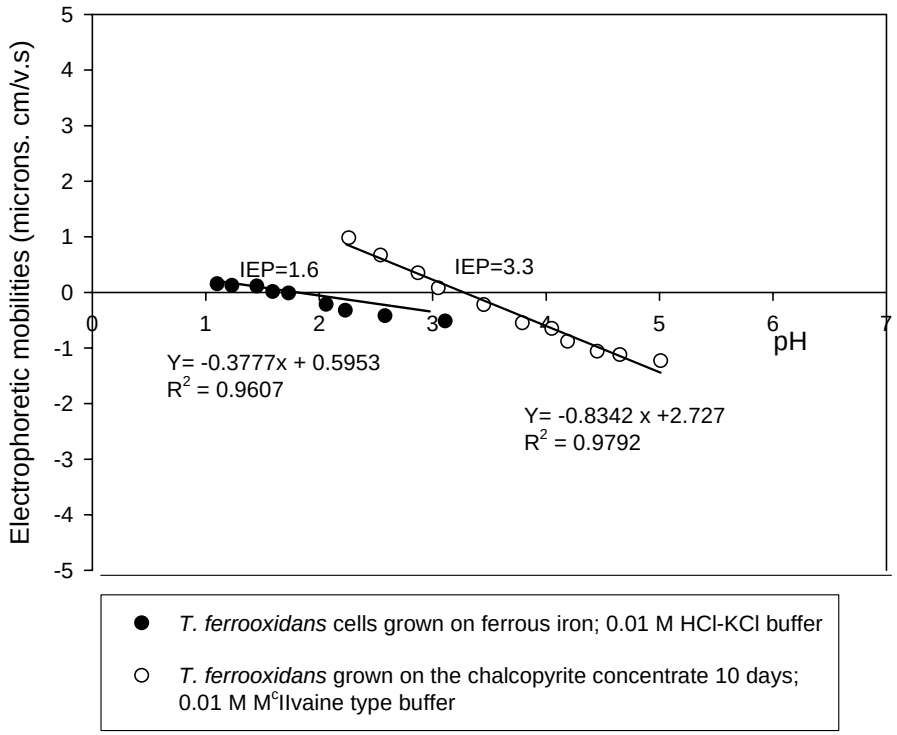

Figure 4.5 Electrophoretic mobilities of *T. ferrooxidans* as a function of pH

When the electrokinetic behavior of the iron-grown cells is compared with that of those grown on the chalcopyrite concentrate, a significant difference was observed. The cells, which were grown on the chalcopyrite concentrate, exhibited an IEP corresponding to a pH of about 3.3. Such an increase in the IEP value of the cells may be attributed to the predominance of the NH_3 group on the surface of chalcopyrite, pyrite and sulphur

minerals (Devasia *et al.*, 1996). Evidence of the presence (determined by Fourier transform infrared spectroscopy) of NH_3, NH_2, NH, CONH, CO, CH3, CH2, CH and COOH functional groups on the cells exposed to sulphide minerals during growth has been proven by several researchers (Devasia *et al.*, 1993; Devasia *et al.*, 1996; Santhiya *et al.*, 2000), and therefore, there is indication that environmentally necessitated changes occur on bacterial cells. Such a surface modification present on sulphide minerals or cells of *T. ferrooxidans* enables their adhesion to mineral surfaces (Devasia

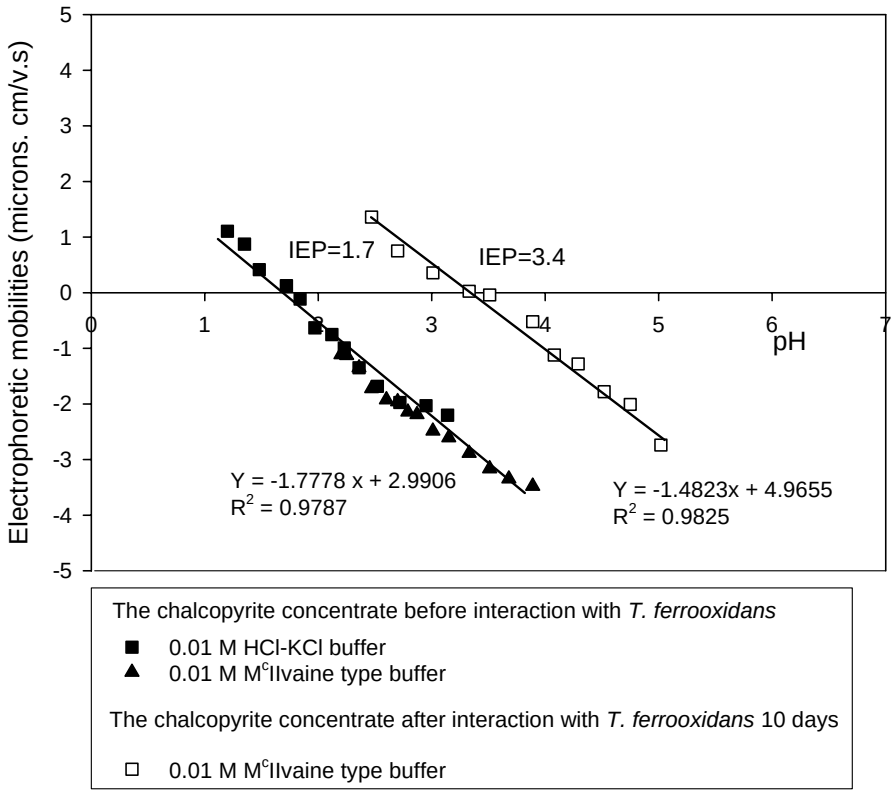

et al., 1996).

Figure 4.6 Electrophoretic mobilities of the chalcopyrite concentrate as a function of pH

The IEP of the chalcopyrite was also observed to be moved towards higher pH values after 10 days of interaction with *T. ferrooxidans*, as shown in Figure 4.6. A sample of chalcopyrite was found to have an IEP at pH 1.7 which moved to pH 3.4 after interaction with the bacteria 10 days. It thus becomes clear that, due to the interaction with mineral particles, the surface properties of not only the bacterial cells but also those of the minerals are altered. Devasia *et al.* (1996) reported that the IEP of the chalcopyrite (at about pH 2.5 in the absence of interaction with bacteria) was moved to higher pH values of 4.5 after interaction with the mineral particles for 24 hours. When compared to the work of Devasia *et al.* (1996), a big difference in the value of IEP before and after interaction with the bacteria can be observed. This difference is probably due to the different nature of the chalcopyrite samples.

The IEP of bacteria and sulphide minerals and the observed shift in the IEP consequent to interaction with sulphide minerals by several researchers are summarised in Table 4.3. Santhiya *et al*. (2000) suggested that the observed shifts in the IEP attest to specific adsorption between the cells and the minerals due to chemical interaction.

Table 4.3 IEP studies by several researchers

Ref.	Bacteria	Buffer	Sulphide minerals	Before interaction with sulphide minerals		After interaction with sulphide minerals	
				IEP of cell	IEP of Sulphide minerals	IEP of cell	IEP of sulphide mineral
Devasia *et al*., 1993 and Devasia *et al*., 1996	*T. ferroxidans*	0.001 M KCL	Chalcopyrite Sulfur Pyrite	2.0 2.0 2.0	2.5 2.2 2.8	3.8 3.8 3.8	4.5 4.2 4.5
Santhiya *et al*., 2001	*T. thioxidans*	0.001 M KNO_3	Galena Sphalerite	3.0 3.0	2.2 2.3	3.6 4.0	3.5 3.3
Deo *et al*., 2001	*Paenibacillus polymyxa*	0.001 M KNO_3	Hematite Corundum Quartz	1.5-1.7 1.5-1.7 1.5-1.7	5.8 7.5 1.75	N.A. N.A. N.A.	N.A. N.A. 3.6
This work	*T. ferroxidans*	0.01 M HCl-KCl and 0.01 M M^{c}Ilvaine type buffer	Chalcopyrite	1.6	1.7	3.3	3.4

4.4 Conclusion

The adsorption results indicated that shake flask speed has an effect on bacterial attachment. The quantity of the cells adsorbed on the chalcopyrite surface is significantly higher at shake flask speeds of 100 rpm than at 200 or 300 rpm. The positive effect on bacterial growth and thus copper dissolution (Chapter 3, section 3.3.4) at the lower shake flask speed may have occurred as a result of the increase bacterial attachment.

In addition, the IEP of the chalcopyrite concentrate and of the cells was shifted to higher pH values after bacterial interaction. This confirms that chemical modification of the chalcopyrite surface and of the cells occurred after interaction with each other. It is therefore demonstrated that the bacterial attachment plays an important role in bioleaching of minerals since the surface modification occurred before the copper dissolution reached its maximum (Figure 3.1-3.3, Chapter 3).

CHAPTER 5 Mechanism of copper dissolution in shake flask cultures of *Thiobacillus ferrooxidans*

5.1 Introduction

The bacterially assisted dissolution of metal sulphides (bioleaching) is often facilitated by bacteria such as *T. ferrooxidans, L. ferrooxidans* and *T. thiooxidans*. Most studies have identified two leaching mechanisms: the direct and the indirect mechanism (Chapter 2, section 2.3). In direct leaching the bacteria are thought to attach to the sulphide surface. Metal sulphides are directly oxidised to soluble metal sulphates. Extracellular polymeric substances (EPS) were found to be involved in cell attachment and biofilm formation (Sand *et al*., 2001). The bioleaching that takes place by an indirect mechanism involves two simultaneous processes, the chemical oxidation of the sulphide by ferric ions and the bacterial regeneration of the ferrous ions produced.

The development and optimisation of leaching processes requires an understanding of the mechanism and kinetics of copper dissolution. Although the process of copper dissolution has been investigated for many years, there is still not a generally accepted published mechanism and the kinetics are not yet defined in terms of rate equations which can be used to predict the performance of the bioreactors used for bioleaching (Hansford and Vargas, 2001). The aim of this work is to study chemical leaching and bioleaching in the presence of ferric sulphate, followed by scanning electron microscope analysis of the chalcopyrite concentrate, which will hopefully lead to an understanding of the chemical and biological basis of the process as well as give some information on the leaching kinetics of the copper dissolution.

5.2 Chemical leaching: Sulphuric acid and ferric sulphate solutions

5.2.1 Introduction

A commercial approach to chalcopyrite concentrate leaching is generally the use of bacterially generated ferric ions in the presence of dilute sulphuric acid solution (Brierley and Brierley, 2001). The chemical stage rate can be enhanced by thermal activation and the use of catalysts (Iglesias and Carranza, 1995). Moderately high temperatures of 60-90 °C are detrimental to a mesophilic bacterial population, which includes *T. ferrooxidans*. Using a proposed separation scheme by Iglesias and Carranza (1995), a high concentration of 10 g/l ferric ions is produced in a separate reactor, heated to about 70 °C and adjusted the initial pH of 1.25 with sulphuric acid, is then brought in contact with the chalcopyrite concentrate (1 % w/v, 82 μm), giving a 90 % copper extraction obtained after 12 days.

As mentioned in the literature review, the bioleaching mechanism proposed by Schippers and Sand (1999), and Sand *et al*. (2001) involves two chemical pathways, depending on the electronic structure of a metal sulphide (i.e. valence bond and molecular orbital theories). Schippers and Sand (1999) stated that “the valence bonds of pyrite, molybdenite, and tungstenite do not contribute to the bonding between metal and sulphur of the metal sulphide; this bonding can only be broken by several oxidation steps with the attacking agent iron (III) hexahydrate ion”. In the case of other metal sulphides (e.g. galena, sphalerite, chalcopyrite), they stated that “protons can remove electrons from the valence bond causing a break of the bonding between the metal and sulphur of the metal sulphide; these metal sulphide are more or less soluble in acid, whereas pyrite, molybdenite, and tungstenite are insoluble”.

Due to their principal solubility in acid (Schippers and Sand, 1999), the first reaction of metal dissolution is thought to be:

$$MS + 2H^{+} \longrightarrow M^{2+} + H_2S \qquad (5.1)$$

In addition, Hansford and Vargas (2001) cite Dutrizac's proposed kinetic equations for chemical leaching of chalcopyrite, which involve only an initial acid attack on the metal sulphide:

$$CuFeS_2 + 2H_2SO_4 \longrightarrow CuSO_4 + FeSO_4 + 2H_2S(aq) \qquad (5.2)$$

$$2H_2S + 2Fe_2(SO_4)_3 \longrightarrow 4FeSO_4 + 2H_2SO_4 + 2S^0 \qquad (5.3)$$

The net result of these two reactions is the same as that of the ferric oxidation of chalcopyrite:

$$CuFeS_2 + 2Fe_2(SO_4)_3 \longrightarrow CuSO_4 + 5FeSO_4 + 2S^0 \qquad (5.4)$$

Much literature reports that metal sulphides can be soluble in a chemical reagent (e.g. sulphuric acid, ferric ions, silver chloride) as shown in Table 5.1. However, the percentage of metal extraction varies from 2-3 % up to 90 %, depending on the interactions of many operating conditions such as the nature of mineral particle, initial pH, temperature, particle size, and pulp density. The objective of this work is to determine whether or not sulphuric acid and ferric ion leaching plays an important role in copper dissolution. With regard to the above kinetic equations proposed, a further objective of the work is to attempt to determine the stoichiometry of the biochemical leaching.

Table 5.1 Previous chemical leaching studies

Refs.	Minerals	Reagent	Conditions
Battaglia *et al*., 1994	Cobaltiferous pyrite	2–35 g/l Ferric ions	10 % (w/v) pulp density, Initial pH 1.7, 35 °C
Iglesias and Carranza, 1995	A copper ore	10 g/l Ferric ions	1 % (w/v) pulp density, Initial pH 1.25, 70 °C
Havlík and Kammel, 1995	Chalcopyrite	1) 0.2 M HCl + 1 M $FeCl_3$ 2) 0.2 M HCl + 1 M $FeCl_3$ + 50 ml CCl_4	1 % (w/v) pulp density, 3.5–80 °C 1 % (w/v) pulp density, 40-90 °C
Breed *et al*., 1997	A pyrite and arsenopyrite concentrate	0.09-0.54 M Ferric ions	1 % (w/v) pulp density, - 75 μm, 40 °C
Hiroyoshi *et al*., 1997	Chalcopyrite	1) 0.1 M H_2SO_4+ 0.01M Ferric ions 2) 0.1 M H_2SO_4+ 0.01M Ferrous ions	1 % (w/v) pulp density, -75 μm, 30 °C
Gómez *et al*., 1997 a	A Spanish complex sulphides ore	6 M NH_4Cl + 0.06 M $CuCl_2$	2.4 % (w/v) pulp density, 95 °C
Carranza *et al*., 1997	A Spanish copper-zinc sulphide concentrate	8-16 g/l Ferric ions + 2 mg Ag^+ / g concentrate	1 % (w/v) pulp density, Initial pH 1.25, 70 °C
Fowler and Crundwell, 1998	Zinc sulphide	2-10 Ferric ions	10 % (w/v) pulp density, Initial pH 1.6, 35 °C,
Carranza and Iglesias, 1998	A zinc sulphide concentrate	12 g/l Ferric ions	1 % (w/v) pulp density, Initial pH 1.25, 70 °C, 80 °C
Fowler *et al*., 1999	Pyrite	1-20 g/l Ferric ions	1 % (w/v) pulp density, Initial pH 1.3, 35 °C
Third *et al*., 2000	Chalcopyrite	1) 0.1 M ferric sulphate 2) 0.1 M ferrous sulphate 3) A sulphuric acid solution of pH 1.5	4 % (w/v) pulp density, a mean particle size of about 45 μm, Initial pH 1.5, 37 °C
Sato *et al*., 2000	Chalcopyrite	0.135-1.33 g/l Silver chloride	4 % (w/v) pulp density
Hiroyoshi *et al*., 2001	Chalcopyrite	0.1 M H_2SO_4+ 0.01- 0.03 M Ferric ions	1 % (w/v) pulp density, -75 μm, 30 °C
Sand *et al*., 2001	Sphalerite, Pyrite	H_2SO_4 solution at pH 1.5, pH 1.9, pH 2.5	2 % (w/v) pulp density, +36, -50 μm,

5.2.2 Experimental procedure

5.2.2.1 Sulphuric acid leaching

A 5 % (w/v) chalcopyrite concentrate (+53, -75 μm) was added to a flask (250 ml) containing 50 ml of either 1 N H_2SO_4 solution or 10 N H_2SO_4 solution. The flask was incubated in a water bath shaker at 100 rpm. This experiment was maintained at 70 °C for the duration of the experiment. Duplicate analysis samples were taken at the following time intervals; 0, 0.5, 1, 2, 4, and 7 days. The leaching solution was filtered through filter paper (Whatman No. 1) and was then diluted with sterile distilled water prior to analysis for copper and total iron by atomic absorption spectrophotometry (AAS).

5.2.2.2 Ferric sulphate leaching

The experimental procedure was the same as for the sulphuric acid leaching experiments, but this study was carried out at different ferric sulphate concentrations and an initial pH of 2.8. The concentrations of ferric sulphate ($Fe_2 (SO_4)_3 \cdot 5H_2O$) were 1, 2, and 10 g/l, corresponding to 0.23, 0.46, and 2.28 g/l ferric ions. Again, a series of flasks were incubated in a water bath shaker at 100 rpm. This experiment was maintained at 30 °C, for comparison reasons with the following experiments of bioleaching in the presence of ferric ions. However, since it has been reported (Iglesias and Carranza, 1995) that the metal dissolution was observed at a moderately high temperature, the other series of flasks where 10 g/l ferric sulphate hydrate were added, was maintained at 70 °C for two different initial pHs (i.e. initial pH of 2.8 and initial pH of 1.5).

5.2.3 Results and discussion

5.2.3.1 Sulphuric acid leaching

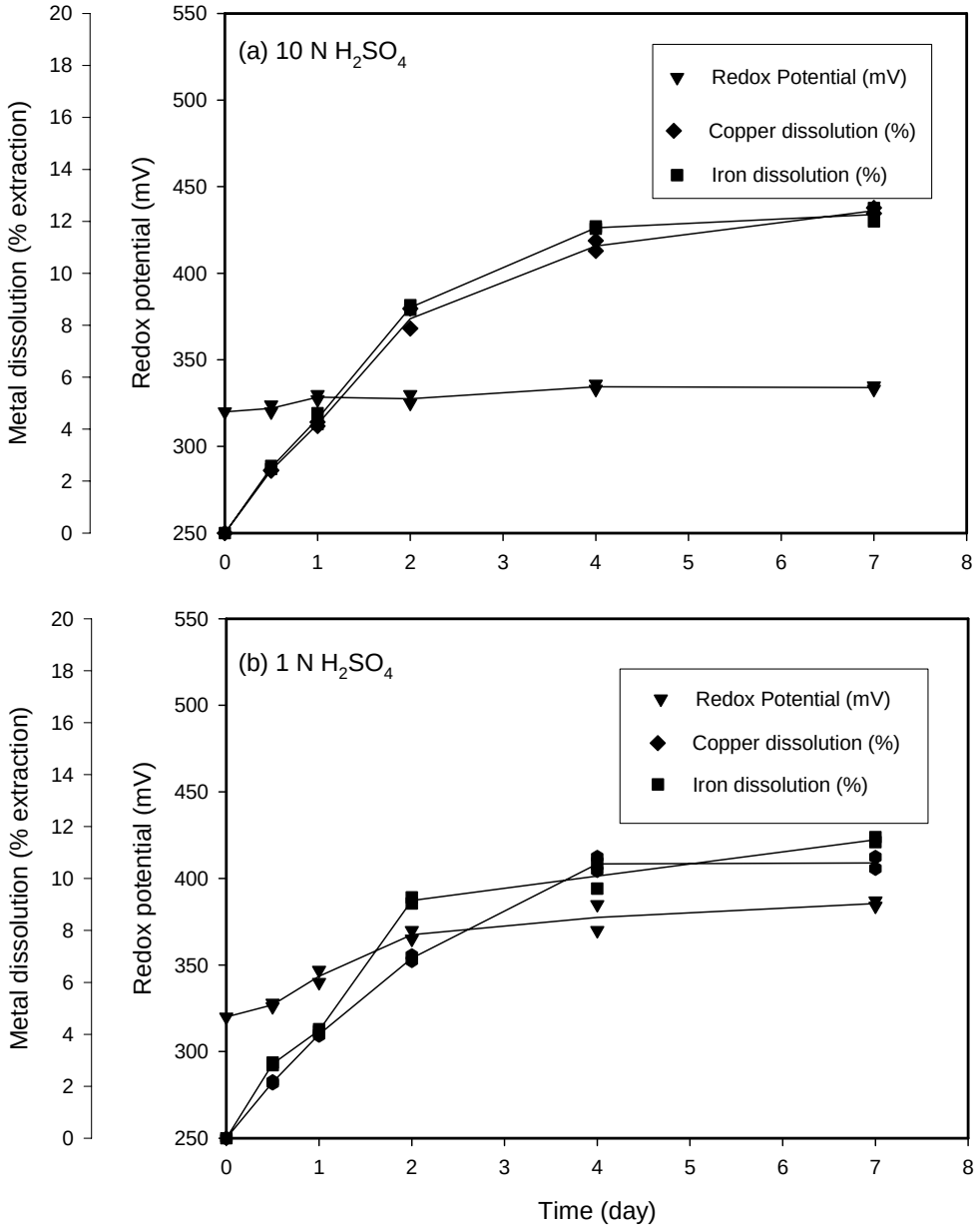

Figure 5.1 Copper and iron dissolution as a function of time for the sulphuric acid leaching of chalcopyrite concentrate at 5 % (w/v) pulp density, +53, -75 µm, and 70°C at different concentrations of sulphuric acid solution

The chalcopyrite concentrate only dissolved slightly in the 1 N sulphuric acid solution and similarly in the 10 N solution. Figure 5.1 a shows that after 7 days, the percentage of copper and iron dissolutions for 10 N sulphuric acid solutions were found to be the same, being about 12 %. These percentages correspond to a maximum copper concentration of 1.79 g/l and a total iron concentration of 1.70 g/l. The maximum rate of copper dissolution, reached 0.450 g/l per day, whereas that of iron dissolution was found to be 0.454 g/l per day.

Figure 5.1 b for 1 N sulphuric acid also shows similar percentages of copper and iron dissolution, giving the rates of copper and iron dissolution of 0.416 and 0.417 g/l per day respectively. The maximum copper concentration after 7 days reached 1.53 g/l, whereas that for iron was found to be 1.58 g/l per day. The final extent of leaching was not dependent on the initial concentration of sulphuric acid solution. The ratio of the molar concentration of produced copper and iron ions was about 1:1. This therefore confirmed that the dissolution of the chalcopyrite concentrate proceeded based on equation 5.2.

From previous experiments (Figures 3.17 and 3.18), the copper and iron dissolutions (in the absence of bacteria) at an initial pH of 1.5 and temperature of 30 °C increased slightly from the starting value, reaching a concentration of 1.0 g/l Cu (7 % extraction) and 0.9 g/l Fe (6 % extraction) after 25 days. These results are summarised in Table 5.2.

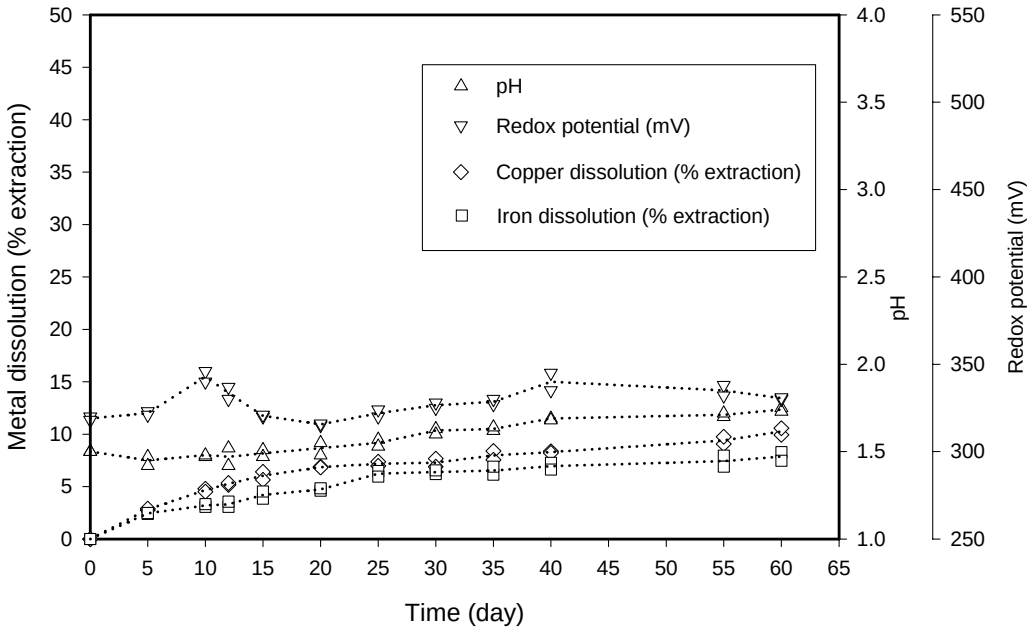

Figure 3.17 Control experiments (in the absence of bacteria) at 5% (w/v) pulp density, +53, -75 μm, initial pH 1.5 and 100 rpm (reprinted from chapter3)

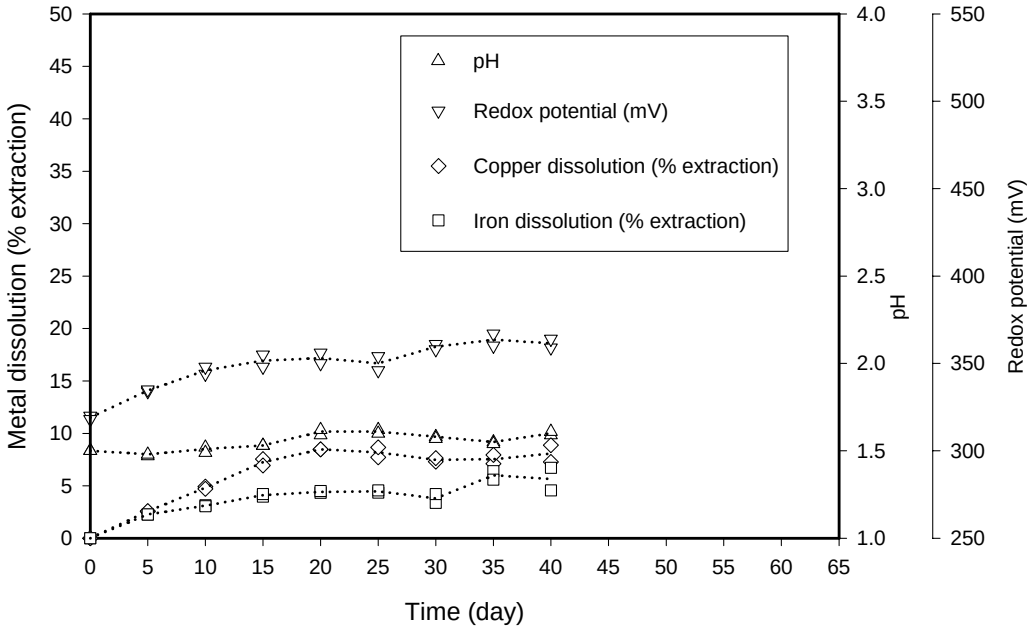

Figure 3.18 The repeat of control experiments (the absence of bacteria) at 5% (w/v) pulp density, +53, -75 μm, intial pH 1.5 and 100 rpm (reprinted from chapter3)

Table 5.2 Summary of acid leaching results

Acid leaching	Temp. (°C)	Time (days)	Copper dissolution			Iron dissolution		
			Rate	Percent Extraction	Concentration g/l	Rate	Percent Extraction	Concentration g/l
sulphuric acid solution at pH 1.5	30	15	0.058 g/l per day, at t=0-15 days	6.0 %	0.87	0.037 g/l per day, at t=0-15 days	4.2 %	0.61
		25	0.017 g/l per day, at t=15-25 days	7.2 %	1.03	0.029 g/l per day, at t=15-25 days	6.2 %	0.90
1N sulphuric acid solution	70	4	0.416 g/l per day, at t=0-4 days	10.6 %	1.53	0.417 g/l per day, at t=0-4 days	10.1 %	1.39
		7	0.002 g/l per day, at t=4-7 days	10.6%	1.53	0.065 g/l per day, at t=4-7 days	11.5%	1.58
10 N sulphuric acid solution	70	4	0.450 g/l per day, at t=0-4 days	11.1%	1.60	0.454 g/l per day, at t=0-4 days	11.7%	1.62
		7	0.066 g/l per day, at t=4-7 days	12.4%	1.79	0.023 g/l per day, at t=4-7 days	12.3%	1.70

The 1N and 10 N sulphuric acid leaching process at 70 °C is faster than the bioleaching process (Figure 5.2). No lag phase was observed, which is to be expected. Metal dissolution was constant in the initial 4 days period, after this time the metal leaching rate reduced significantly (Table 5.2). The decrease in metal dissolution rate was presumably due to the fact that the chalcopyrite surface was covered with mineral deposits, probably ferric ion precipitates (Appendix VI). The 1N and 10 N sulphuric acid leaching was found to be less effective than bioleaching in terms of maximum of copper concentration. The bioleaching experiments (Figure 5.2 a) gave the average copper extraction percentage of 34.5 % and reached a maximum yield of about 4.7 g/l after 25 days, whereas the iron dissolution was observed to be very low (>3 % extraction). Although the bioleaching took longer than acid leaching, the advantage of using bioleaching process lies in maximising copper concentration with respect to iron dissolution and the lower process temperature required (30 °C compared to 70 °C).

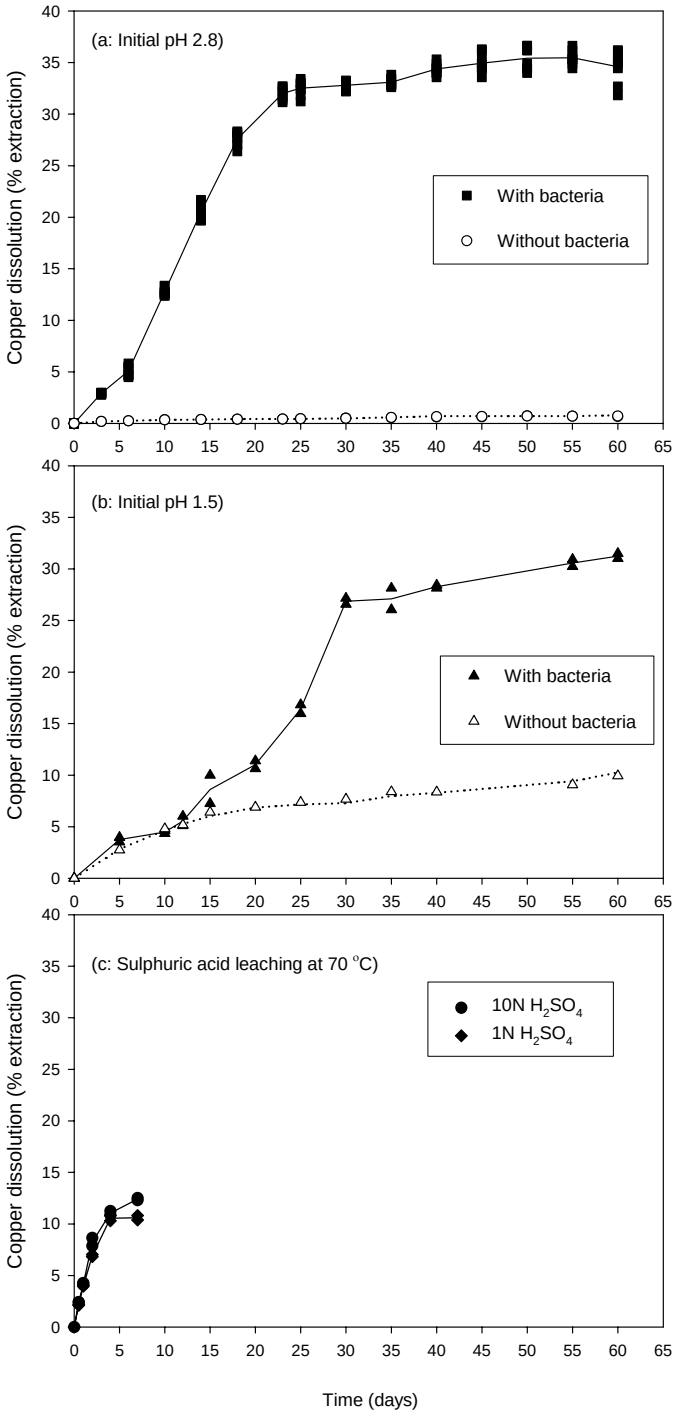

Figure 5.2 Comparison of percent copper extraction obtained in a bacterial leaching test and a control experiment (the absence of bacteria) at 5 % (w/v) chalcopyrite concentrate (+53, -75 μm), 100 rpm, 30 ^{o}C; (a) initial pH 2.8, (b) initial pH 1.5 and (c) 1 N and 10 N H_2SO_4 solution leaching test at 70 ^{o}C

5.2.3.2 Ferric sulphate leaching

The degree of copper released from the chalcopyrite concentrate with regard to time in the ferric sulphate leaching tests are shown in Figure 5.3. The percent copper dissolution increases with increasing concentration of ferric ions, but overall the chalcopyrite concentrate dissolves only slightly in ferric sulphate solution (less than 4 % extraction) for all three different concentrations of ferric sulphate solution. Although there was evidence (Iglesias and Carranza, 1995) that moderately high temperatures could activate copper dissolution, the results obtained in ferric leaching tests carried out at 70 °C showed that there was still less than 5 % extraction (Figure 5.4).

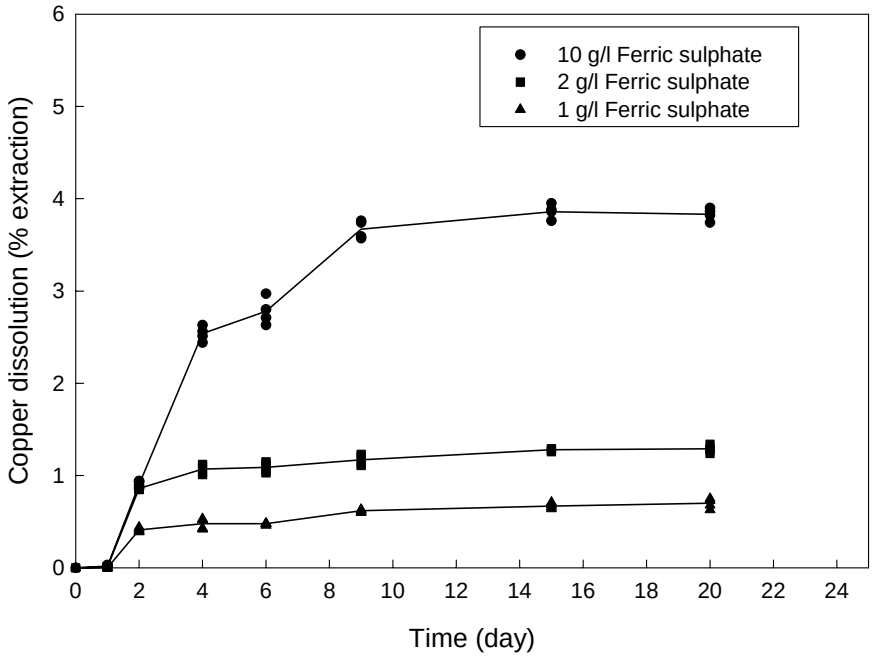

Figure 5.3 Copper dissolution as a function of time for ferric sulphate leaching of chalcopyrite concentrate at 5 % (w/v) pulp density, +53, -75 µm, initial pH of 2.8 and 30 °C at different concentrations of ferric sulphate solution

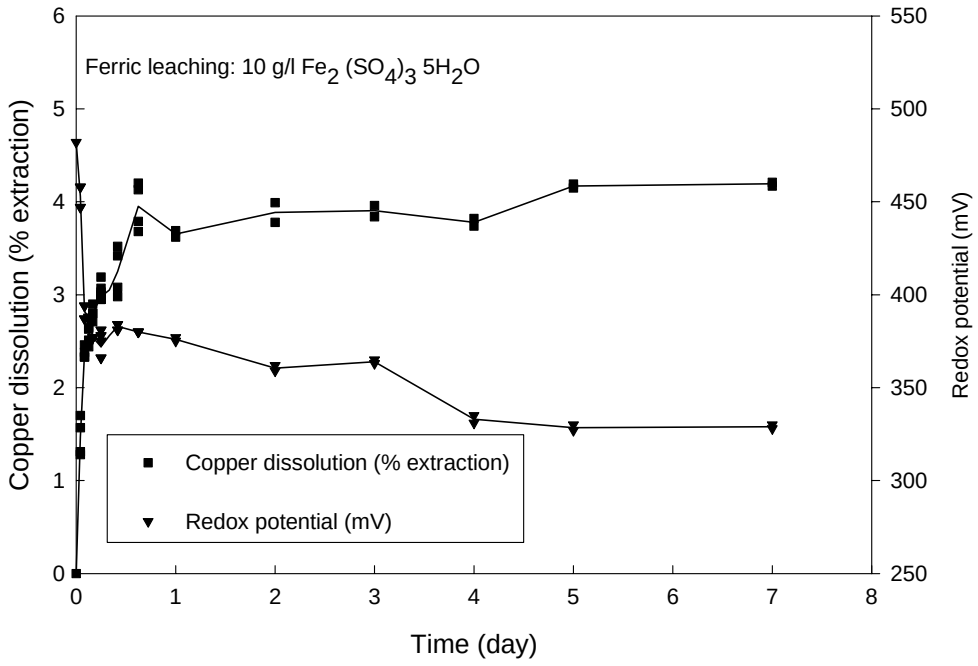

Figure 5.4 Copper dissolution as a function of time for 10 g/l ferric sulphate leaching of chalcopyrite concentrate at 5 % (w/v) pulp density, +53, -75 µm, initial pH of 2.8 and 70 °C

At an initial pH of 2.8, copper extraction was not enhanced by the addition of 10 g/l ferric sulphate either at 30 °C or at 70 °C. Consequently, this result cannot confirm that the dissolution of the chalcopyrite concentrate proceeds via equation 5.4 at this pH.

Iglesias and Carranza (1995) reported that the percent copper extraction was found to be about 90 % after 12 days. However, it should be pointed out that the initial pH of their experimental conditions (Table 5.1) was set at 1.25. The concentration of hydrogen ions can also influence copper dissolution. Therefore the reported copper dissolution was not due to the effect of ferric ions alone. According to the equation (5.5) proposed

by Sand *et al* (2001), the metal dissolution by ferric ions is particularly associated with H^+:

$$MS + Fe^{3+} + 2H^+ \longrightarrow M^{2+} + H_2S^{*+} + Fe^{2+} \qquad (5.5)$$

Considering the above kinetic equation, the kinetic equation (5.6) of chalcopyrite dissolution by ferric ions should be:

$$CuFeS_2 + 2Fe^{3+} + 4H^+ \longrightarrow Cu^{2+} + 3Fe^{2+} + 2H_2S^{*+} \qquad (5.6)$$

The cation radical (H_2S^{*+}) can further be oxidised to elemental sulphur as can be seen in Figure 5.5 below.

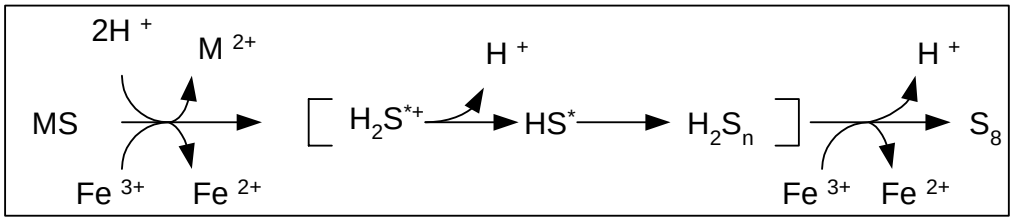

Figure 5.5 Simplified scheme of the polysulphide mechanism (reprinted from Schippers and Sand, 1999).

The experimental results obtained in the ferric leaching tests carried out at 70 °C at an initial pH of 1.5 are shown in Figure 5.6. Copper dissolution increases significantly with the decrease in initial pH value. The graph of copper dissolution versus time was found to have two distinct linear features: the initial part of the curve having a steeper slope was observed from 0-4 hours. The initial copper dissolution rate was found to be 12.05 g/l per day. This was followed by the second part with a shallow slope that was observed from 4 hours to 1 day. During the second period, copper dissolution

proved to be fairly slow, 1.24 g/l per day. The copper dissolution (% extraction) then began to level off after 1 day and reached a maximum copper dissolution of 20 % extraction (corresponding to 2.9 g/l). The metal dissolution by ferric ions is particularly associated with H^+. Thus, it was likely that the dissolution of the chalcopyrite concentrate proceeded via equation 5.6.

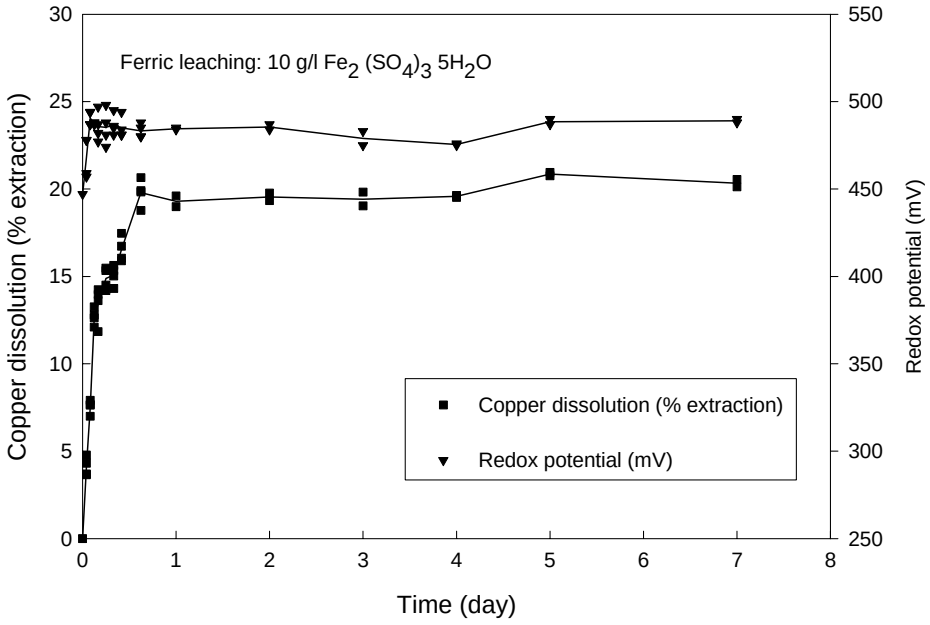

Figure 5.6 Copper dissolution as a function of time for 10 g/l ferric sulphate leaching of chalcopyrite concentrate at 5 % (w/v) pulp density, +53, -75 µm, initial pH of 1.5 and 70 °C

5.3 Effect of ferric sulphate on bioleaching

5.3.1 Introduction

Since Silverman and Lundgren (1959) proposed a bioleaching model with two types of mechanisms (i.e. direct and indirect leaching), these mechanisms of bacterial interaction with metal sulphide are still the subject of much debate and controversy. The direct leaching is a process by which the bacterial membrane directly interacts with the sulphide surface, possibly by the extracellular secretion of an enzyme or by oxidation with an enzyme specific to sulphide minerals present on the cell wall (Fowler *et al*., 1999). Thus, chalcopyrite can be directly oxidised by *T. ferrooxidans* to soluble metal sulphates according to equation 5.7 (Silverman and Lundgren, 1959).

$$4CuFeS_2 + 17O_2 + 2H_2SO_4 \xrightarrow{T.\,ferrooxidans} 4CuSO_4 + 2Fe_2(SO_4)_3 + 2H_2O \qquad (5.7)$$

Following the previous experiments, this work focused on bioleaching in the presence of ferric ions and investigated the effect of the concentration of ferric ions on chalcopyrite leaching with and without bacteria. Ultimately, all the results including the previous experiments (section 5.2) are used to propose a bioleaching mechanism for copper dissolution from the chalcopyrite concentrate.

5.3.2 Materials and Methods

5.3.2.1 Inoculum preparation procedure

A 10 % v/v inoculum of the stock culture (Appendix II) was added to a flask (250 ml) containing 45 ml of ATCC 64 medium of an initial pH of 2.8. The flask was incubated in a rotary shaker at 30 °C and 100 rpm. The cells were harvested after they had reached the late exponential phase (96 hours) and then the culture was filtered through filter

paper (Whatman No. 1) to eliminate iron solids. The culture was centrifuged at 8000 rpm for 40 minutes to separate the cells and washed three times with the same medium used for growth (ATCC 64 medium without ferrous ions). The cells were then diluted to a known concentration (about 5.0 x 10^9 cells/ml) with the medium.

5.3.2.2 Experimental procedure

All experiments were carried out in 250 ml shake flasks containing 45 ml of ATCC 64 medium (without ferrous ions) at an initial pH of 2.8. These flasks were then autoclaved at 121 °C for 15 minutes. Prior to all the experiments, the chalcopyrite concentrate was sterilised. 2.5 g of the chalcopyrite concentrate was added to a tube, which was then autoclaved at 121 °C for 15 minutes. Ferric sulphate ($Fe_2 (SO_4)_3 \cdot 5H_2O$) granules were dissolved in distilled water at pH 2.8 at different concentrations i.e. 1, 2, and 10 g/l ferric sulphate (corresponding to 0.23, 0.46, and 2.28 g/l ferric ions). The ferric sulphate solution was then sterilised by Microfiltration (Clyde filter, 0.2 μm).

A 10 % (v/v) of inoculum (5.0 x 10^9 cells/ml), the sterile chalcopyrite, and ferric sulphate solution were added to a series of flasks using aseptic techniques. The flasks were then incubated in a rotary shaker at 100 rpm and 30°C. The control experiments were set up by preparing a series of flasks with the same composition but the bacteria were absent. Duplicate samples were taken at regular time intervals. After determining the mass of the flasks, the loss of water due to evaporation was compensated by adding sterile distilled water (ASTM E1357-90). The leaching solution was filtered through filter paper (Whatman No. 1) and the filtrate was then used for analysis of the solution pH, redox potential, free cell concentration, total iron and copper concentration.

5.3.3 Effect of initial ferric sulphate on bacterial growth, the solution pH and the redox potential

The bacteria growth curves as a function of the initial ferric ion concentration are shown in Figures 5.7-5.9 and all three sets display the typical pattern seen previously. The lag phase lasted approximately 5 days and was followed by an exponential phase (5-15 days), a stationary phase (15-30 days) and then a death phase (after 30 days). In order to calculate the specific growth rate, ln x was plotted against time. Calculation of the gradient of the line corresponding to exponential phase growth yielded the maximum specific growth rate (μ) in units of h^{-1}. The values obtained were 0.022, 0.025, and 0.025 h^{-1} for 1, 2, and 10 g/l initial ferric sulphate respectively. These growth rates were not significantly different from the growth rate in the absence of initial ferric ions (Figures 3.1-3.3), which was 0.030 h^{-1}.

Moreover, the maximum free cell concentrations reached (Figures 5.7-5.9), was about $3.0 \times 10^{11} - 4.9 \times 10^{11}$ cells/ml for all tests, were about the same level as those in the absence of initial ferric ions. Thus, for a range of 1 to 10 g/l ferric sulphate (corresponding to 0.23 to 2.28 g/l ferric ions) there was no effect on bacterial growth either inhibiting or enhancing. In addition, Dastidar *et al*. (2000) found that in the presence of more than 5 g/l ferric ions no cell growth was observed, indicating inhibition of cell growth. Therefore, when the experiment was set at a range of 0.23 to 2.28 g/l ferric ions, the bacteria were not inhibited by these concentrations. However, this result highlights the fact that adding ferric ions did not enhance bacterial growth.

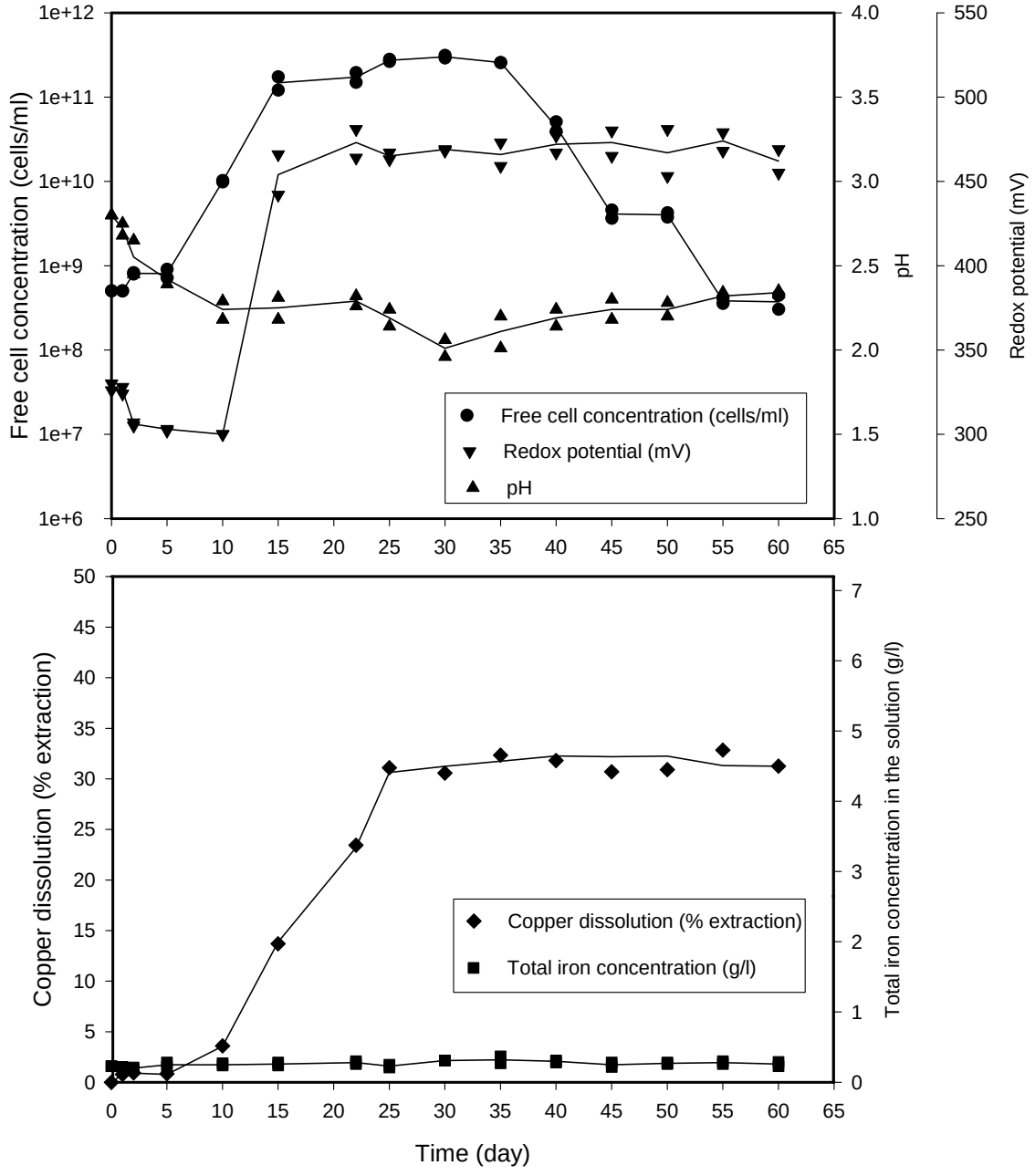

Figure 5.7 Bioleaching of chalcopyrite concentrate at 5 % (w/v) pulp density, +53, -75 μm, initial pH 2.8, 100 rpm and 1 g/l ferric sulphate addition

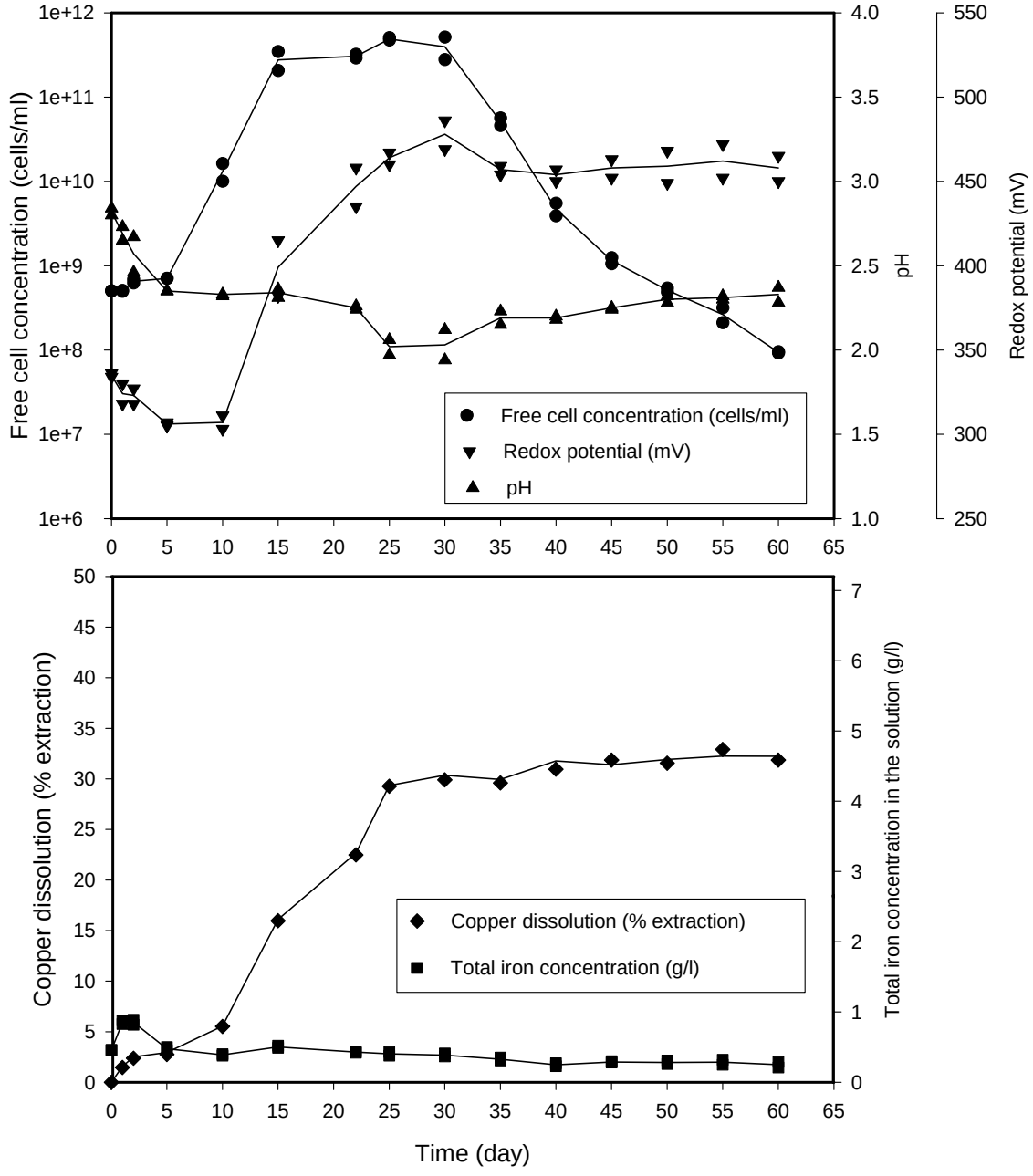

Figure 5.8 Bioleaching of chalcopyrite concentrate at 5 % (w/v) pulp density, +53, -75 μm, initial pH 2.8, 100 rpm and 2 g/l ferric sulphate addition

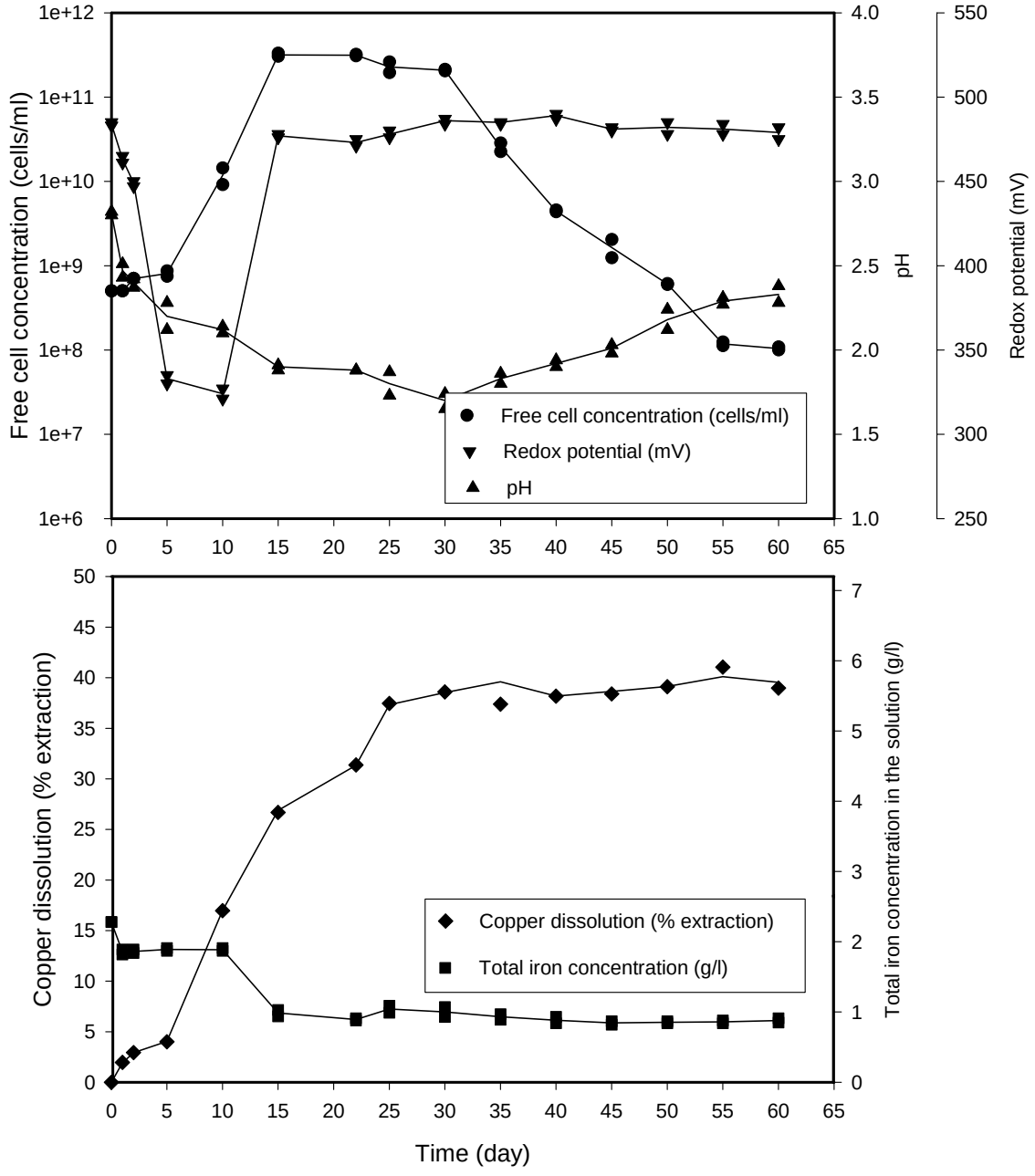

Figure 5.9 Bioleaching of chalcopyrite concentrate at 5 % (w/v) pulp density, +53, -75 μm, initial pH 2.8, 100 rpm and 10 g/l ferric sulphate addition

The pH curves show a drop in pH from 2.8 to about 2.0 after 30, 25, and 15 days for 1, 2, and 10 g/l initial ferric sulphate respectively (Figures 5.7-5.9). The pH curve with the steepest slope was observed when 10 g/l initial ferric sulphate was used. The pH drop was found to occur primarily before the exponential phase of cell growth was observed. This increase in acidity of the solution may not occur due to bacterial oxidation alone. The mechanism related to the H^+ formation in this study was assumed to have two distinct mechanisms (equation 5.8 and 5.9). According to the polysulphide mechanism (Figure 5.5), elemental sulphur is the final product. Silverman and Lundgren(1959) proposed that elemental sulphur was oxidised by *Thiobacillus* sp. (equation 5.8) leading to the formation of H^+.

$$2S^o + 3O_2 + 2H_2O \xrightarrow{Thiobacillus} 4H^+ + 2SO_4^{2-} \qquad (5.8)$$

Moreover, the iron concentration in the solution (Figure 5.9) decreased from the start to 15 days, and then remained constant. This observation was also noted in Figures 5.7 and 5.8. A decrease in iron concentration in the solution indicates ferric ion (Fe^{3+}) precipitation. The formation of ferric hydroxide depends on the pH; at neutral pH in the presence of oxygen, the ferric ions form highly insoluble precipitates (e.g. ferric hydroxide (Brock and Gustafson, 1976). Battaglia *et al*. (1994) reported that at a low pH of 1.7, the initial ferric ions were found to be precipitated at the beginning of their experiments, causing a decrease in ferric ion concentration in the solution. The formation of ferric hydroxide ($Fe(OH)_3$) and jarosites precipitation ($XFe_3(SO_4)_2(OH)_6$) result in the production of protons and, therefore leads to acidification of the solution, according to equation 5.9 (Brock and Gustafson, 1976) and equation 5.10 (Gómez *et al*., 1996 a).

$$Fe^{3+} + 3H_2O \longrightarrow Fe(OH)_3 + 3H^+ \quad (5.9)$$

$$3Fe^{3+} + X^+ + 2HSO_4^- + 6H_2O \longrightarrow XFe_3(SO_4)_2(OH)_6 + 8H^+ \quad (5.10)$$

where $X = K^+,\ Na^+,\ NH_4^+,\ H^+$

Then, after the drop of pH values from 2.8 to 2.0, a slight increase in pH was observed (Figures 5.7-5.9). This increase in pH was presumably due to the fact that when the bacterial growth rate reached the stationary phase, no further cell growth occurred to produce acid ions into the solution, based on equation 5.8. Moreover, the reduction in acidity was more affected when the bacteria reached the dead phase, because of the effects of cell lysis.

From the beginning until the 10th day of the experiments, the redox potential values (Figures 5.7, 5.8) slightly decreased from about 330 to 300 mV and were then followed by a marked increase in the redox potential to reach about 470 mV. After 25 days, the redox potential remained practically constant between 470 ± 5 mV until the end of the experiments. For the 10 g/l ferric sulphate solution (Figure 5.9), the initial redox potential was significantly higher. Nemati and Webb (1997) found that the redox potentials of the solutions varied from about 370 to 550 mV depending on the ratios of ferric to ferrous ions and temperature between 20 and 35 °C.

For the 10 g/l ferric sulphate solution, the redox potential values then dropped from 485 to 324 mV at the 0-10 days period (Figure 5.9). The observed decrease in redox potentials after the start was presumably due to the formation of ferric hydroxide

($Fe(OH)_3$) (equation 5.9), causing a decrease in ferric ions in the solution, which in turn led to a decrease in the redox potential value. This decrease in the redox potential after the start, was also found to be consistent with the control experiment at the same initial ferric sulphate concentration (Figures 5.11-5.13). After 10 days, the redox potential value then increased to about 480 mV and remained constant at 480 ± 5 mV (Figure 5.9). This increase in the redox potential values was mainly due to the bacterial oxidation of ferrous ions to ferric ions.

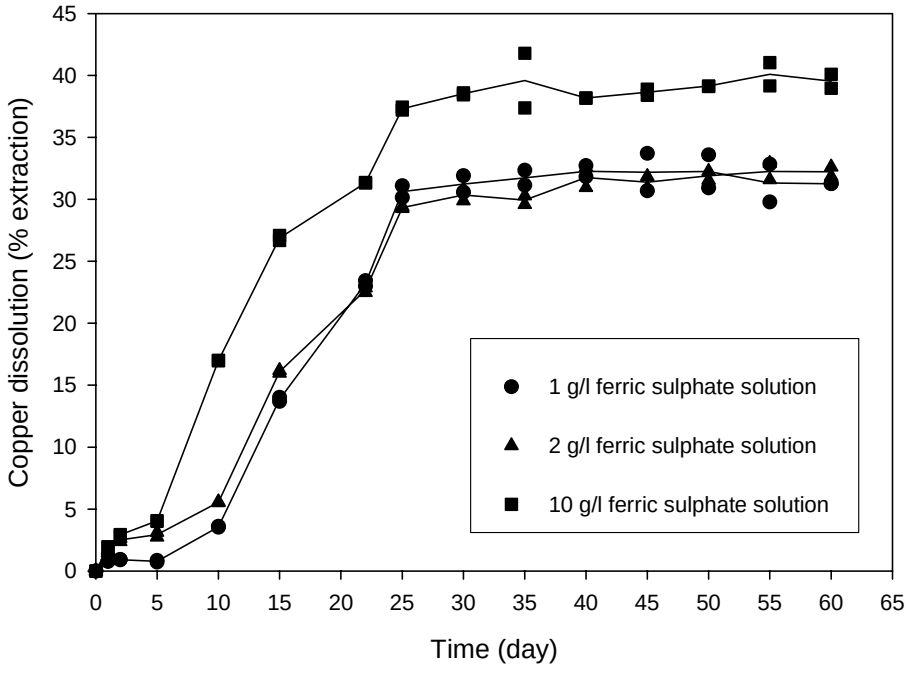

Figure 5.10 Effect of the concentration of ferric ions in the solution on the bioleaching of the chalcopyrite at 5 % (w/v) pulp density, +53, -75 μm, initial pH 2.8, 100 rpm and 30 °C

5.3.4 Effect of initial ferric ion concentration on metal dissolution

The rates of copper dissolution were not significantly increased with increasing ferric sulphate concentration, being 0.219, 0.189 and 0.222 g/l per day in the presence of 1, 2 and 10 g/l of ferric sulphate respectively (Figures 5.7-5.9). After 30 days, copper dissolution in the presence of 1 and 2 g/l ferric sulphate were found to be similar, whilst that of the 10 g/l ferric sulphate was greater than the others (Figure 5.10). These values were 31.2 %, 30.4 % and 38.5 % copper extraction in order of increasing ferric sulphate concentration, corresponding to copper solution concentrations of 4.5, 4.4 and 5.6 g/l. In the presence of 10 g/l ferric sulphate of an extra 8 % extraction can be observed, because of the influence of ferric sulphate, which was also noted in the control experiment especially when 10 g/l ferric sulphate was added (Figure 5.13). These results imply that dissolution in the presence of ferric ions involves only chemical leaching.

For all conditions the copper dissolution reached a steady value after 25 days (Figures 5.7-5.9). This was probably due to the inhibition effects of metal ions on bacterial growth, which is consistent with the finding that an alteration of the bacterial growth curve occurred after 30 days (Figures 5.7-5.9).

5.3.5 Control experiments

For the control experiments in the absence of bacteria (Figures 5.11-5.13), the solution pH values slightly decreased from the initial pH of 2.8 to about pH 2.3, 2.0, and 2.0 in the presence of 1, 2 and 10 g/l ferric sulphate respectively. The redox potential also decreased from the beginning to level off at about 300 mV after 10 days. Both pH and redox potential values did not significantly alter in the next 50 days of the experiments. Copper dissolution (% extraction) appeared to be less than 1, 1.5 and 4 % in order of increasing ferric sulphate concentration. On the other hand, iron concentration in the solution decreased from the initial total iron concentrations of 0.23, 0.46, and 2.28 g/l to that of 0.07, 0.20, and 1.8 g/l after 5 days as seen in Figures 5.11, 5.12, and 5.13 respectively. After 5 days, the iron concentration remained practically constant. These decreases in iron concentration suggest that iron precipitation took place according to equation 5.9.

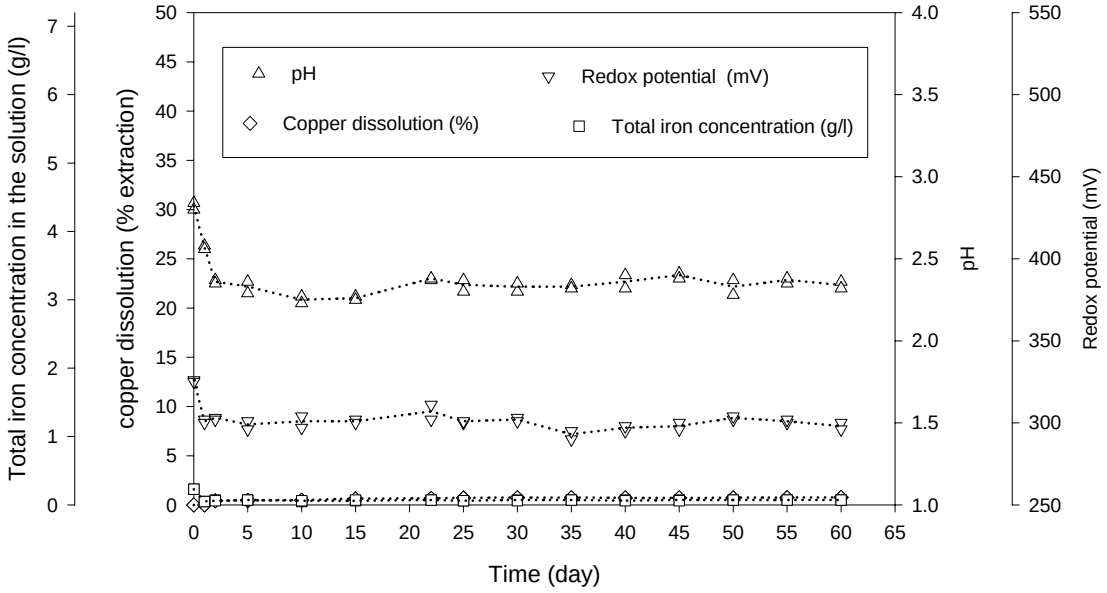

Figure 5.11 Control experiments (in the absence of bacteria) at 5% (w/v) pulp density, +53, -75 μm, initial pH 2.8, 100 rpm and 1 g/l ferric sulphate addition

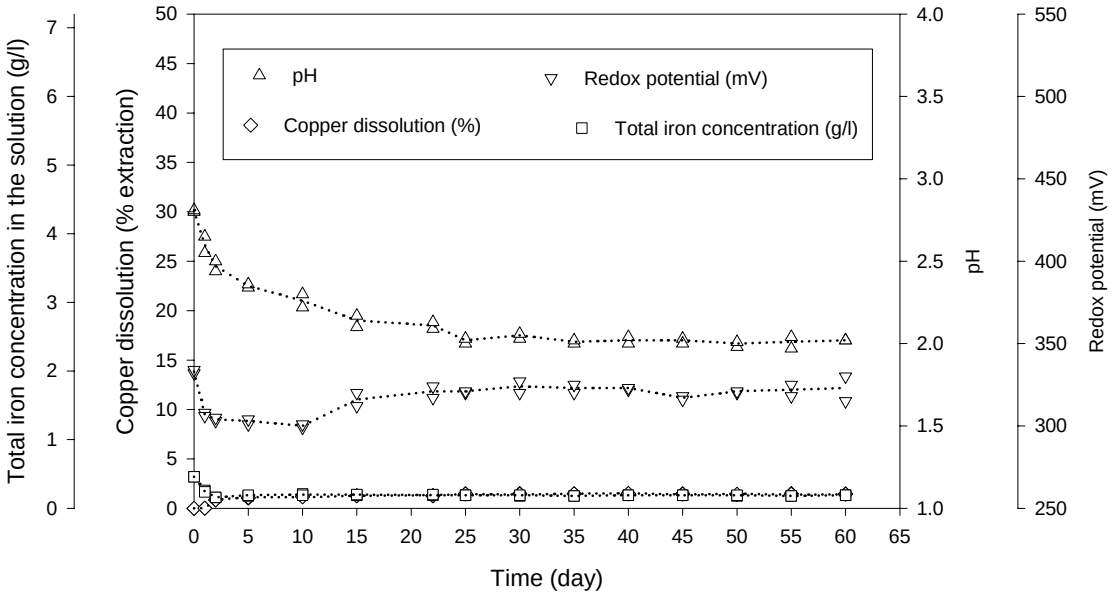

Figure 5.12 Control experiments (in the absence of bacteria) at 5% (w/v) pulp density, +53, -75 μm, initial pH 2.8, 100 rpm and 2 g/l ferric sulphate addition

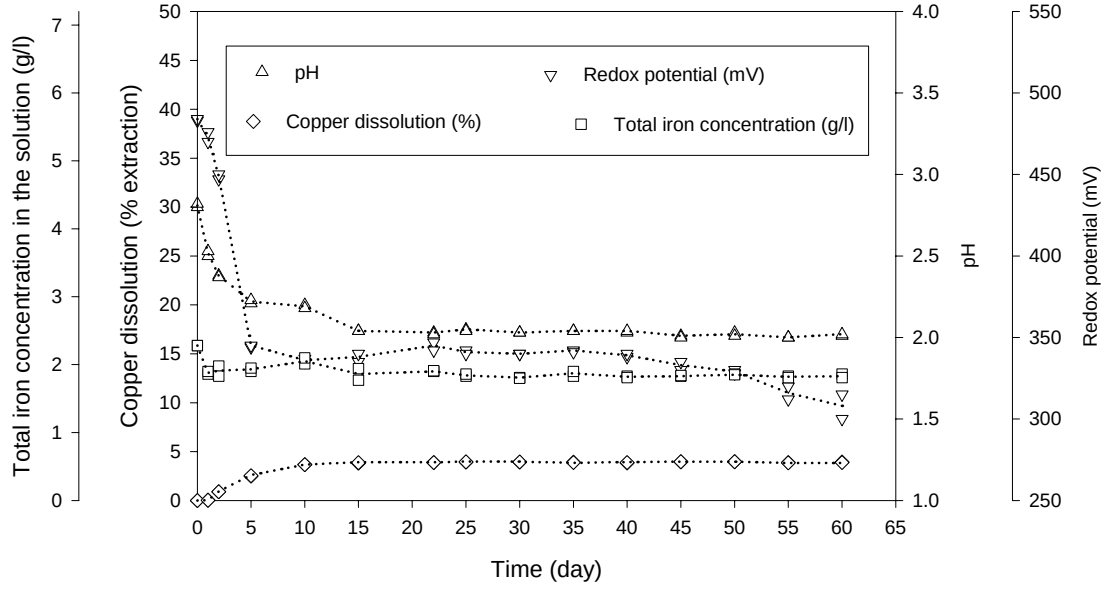

Figure 5.13 Control experiments (in the absence of bacteria) at 5% (w/v) pulp density, +53, -75 μm, initial pH 2.8, 100 rpm and 10 g/l ferric sulphate addition

5.4 Scanning electron microscope (SEM)

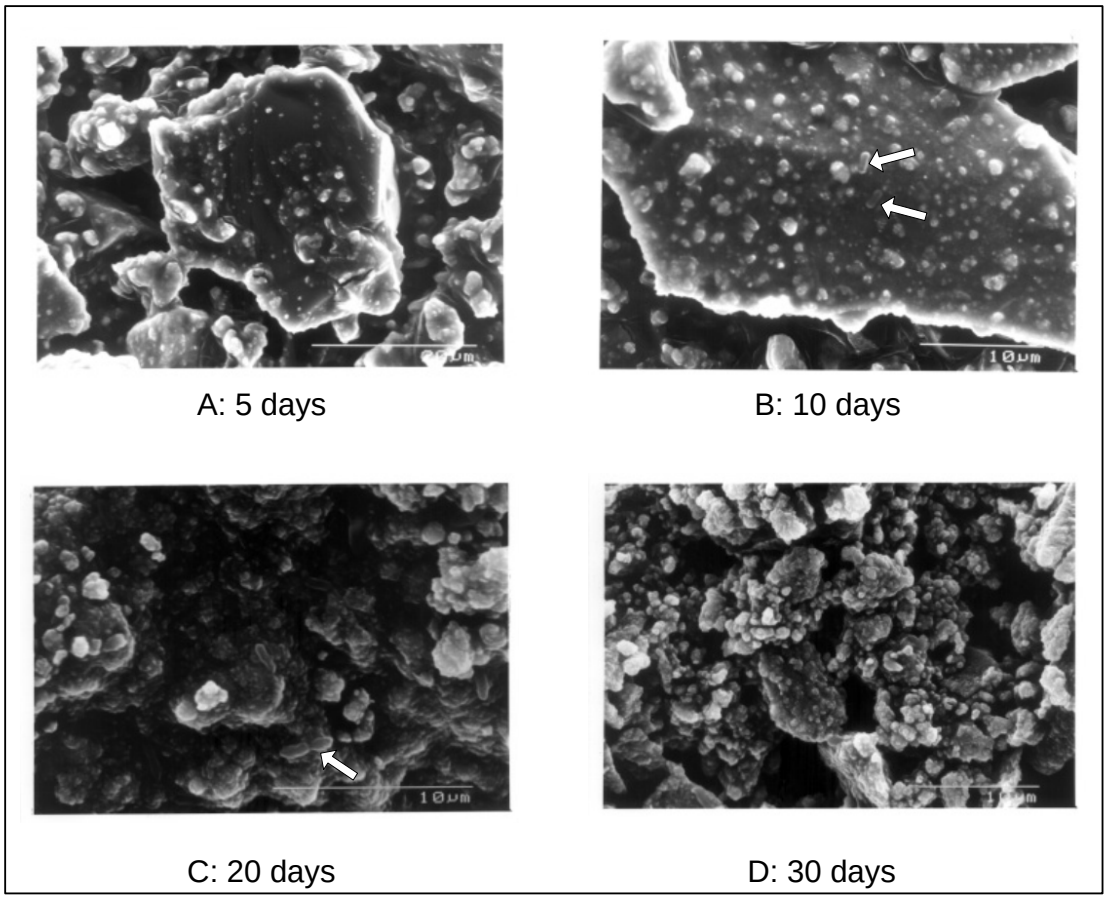

Figure 5.14 SEM images of the chalcopyrite concentrate surface with attached cells of *T. ferrooxidans* (washed with the medium) after interaction for 5, 10, 20 and 30 days; some of the cells are indicated by arrows

The SEM images of the leached chalcopyrite concentrate were obtained by using a scanning electron microscopy (Model S-2300, Hitachi, Japan). For the images of the microbe-mineral interaction studies, all experiments were carried out in a 250 ml shake flask containing 5 % (w/v) chalcopyrite concentrate particles (+53, -75 μm) and 45 ml of ATCC 64 medium (without ferrous ions) at an initial pH of 2.8. A 10 % (v/v) of inoculum (3 x 10^9 cells/ml) was added to a series of flasks, which were then incubated

in a rotary shaker at 100 rpm and 30°C for certain time intervals. After interaction, the mineral particles were separated from the free cells by filtration (Whatman No.1) and were rinsed 3 times with the medium (ATCC 64 medium without ferrous ions). The interacted mineral particles were added to a 0.01 M McIIvaine type buffer of pH 2.0 (the compositions are shown in Appendix VII) in order not to disturb attached cells.

Figure 5.14 shows scanning electron micrographs of the chalcopyrite concentrate after interaction with *T. ferrooxidans* for 5, 10, 20, and 30 days. Although some bacteria were visible on the surface, the adhesion of *T. ferrooxidans* on the chalcopyrite concentrate is not clearly revealed. After interaction for 5 days, the mineral surface became coated with metal precipitation. The chalcopyrite surface was covered by mineral deposits, likely ferric ion precipitates that are commonly associated with *T. ferrooxidans* (Edwards *et al*., 2001).

The observation that the iron concentration in the solution decreased from the start to about 15 days (Figure 5.9) confirmed that iron is deposited onto the mineral surface during the bioleaching (Figure 5.14), which agrees with the findings of Gómez *et al*., 1996 a; Sasaki and Konno, 2000; Edwards *et al*., 2001. It can be seen that hardly any attached cells on the mineral surface are observed. Moreover, it was difficult to obtain accurate cell counts using scanning electron microscopy. An estimate of attached cells from SEM observation is not reliable (Santelli *et al*., 2001).

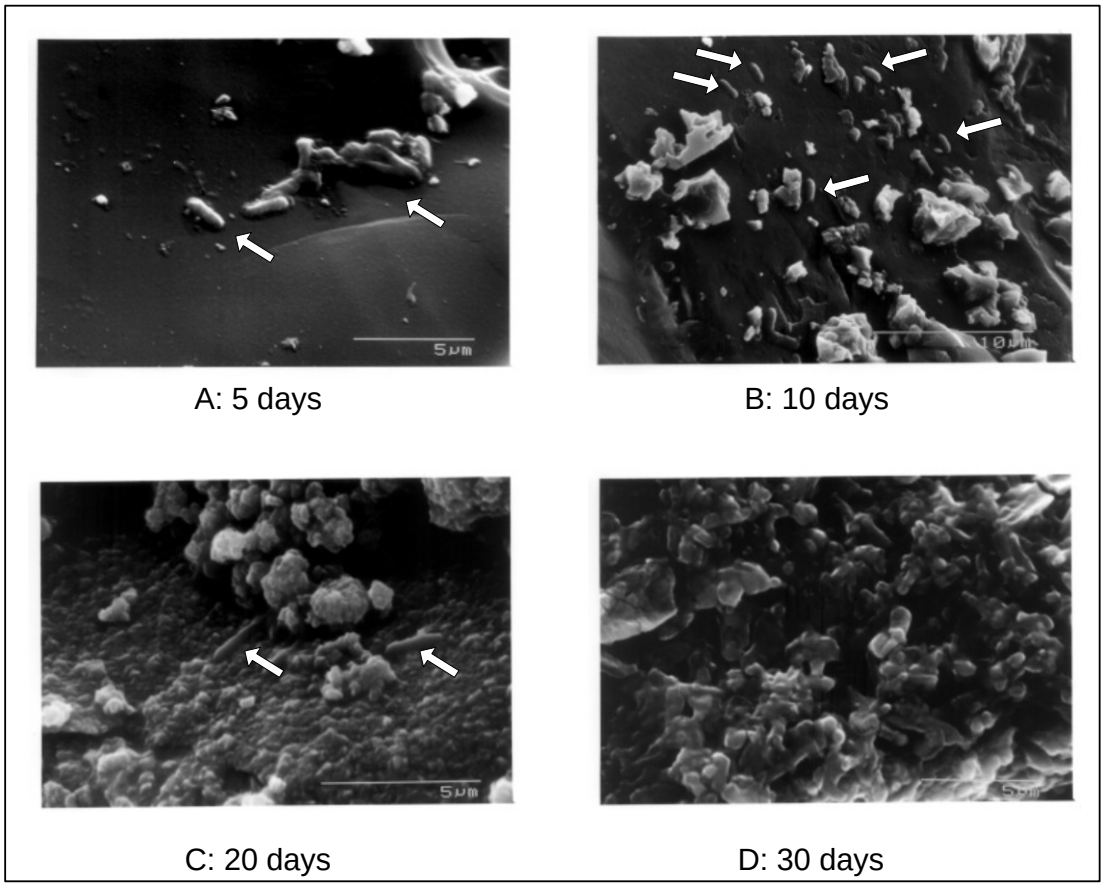

Figure 5.15 SEM images of the chalcopyrite concentrate surface with attached cells of *T. ferrooxidans* (washed with 6 N HCl solution) after interaction for 5, 10, 20 and 30 days; some of the cells are indicated by arrows

Because of problems caused by metal precipitation on the surface of the interacted mineral particles, samples were rinsed thoroughly with 6 N HCl solution once, prior to microscopic examination (Monroy *et al*., 1994). Washing with acid solution succeeded in achieving clear pictures. The strongly-attached cells were observed clearly after interaction for 5 days (Figure 5.15 a) showing an image of *T. ferrooxidans* on the mineral surface, which can occur singly or in pairs. After interaction for 10 days, some attached cells and some metal precipitation can be observed (Figure 5.14 b). In addition, after interaction for 30 days, metal precipitation was found to cover almost

all of the surface. This showed clearly that metal precipitation gathers over a period of time; after 30 days the appearance of the mineral surface could not be recognised. This could be a proof of the observation in Chapter 3 (section 3.3.4) that after more than 30 days of bioleaching process, the copper dissolution was found to reach a maximum extraction yield.

5.5 Conclusion

Overall, these experiments can be summarised in three points: (i) chalcopyrite is soluble in a sulphuric acid solution at a pH of 1.5 because of its mineralogical structure type, however acid leaching is less effective than bioleaching for the given conditions in terms of copper extraction; (ii) copper dissolution by ferric ions proceeds with the addition of sulphuric acid at a pH of 1.5 and is activated by a moderately high temperature; (iii) ferric ions have a slightly positive influence on copper extraction, when 10 g/l ferric sulphate was added for both the bioleaching of the chalcopyrite concentrate and the control experiment.

Based on the results obtained from the bacterial absorption isotherm depending on agitation speed (Chapter 4) and the number of strongly-attached bacteria on the chalcopyrite surface from SEM observation, the influence of the direct bacterial mechanism seems to be the one responsible for metal dissolution. The results obtained from chemical leaching (acid and ferric ions) combined with bioleaching in the presence of ferric ions suggested that overall the chalcopyrite concentrate can be oxidised according to the following bacterial and chemical oxidation mechanism:

Bacterial oxidation mechanism

$$4CuFeS_2 + 17O_2 + 2H_2SO_4 \xrightarrow{T.\,ferrooxidans} 4CuSO_4 + 2Fe_2(SO_4)_3 + 2H_2O$$

Chemical oxidation mechanism

$$CuFeS_2 + 2H_2SO_4 \longrightarrow CuSO_4 + FeSO_4 + 2H_2S\,(aq)$$

$$CuFeS_2 + 2Fe^{3+} + 4H^+ \longrightarrow Cu^{2+} + 3Fe^{2+} + 2H_2S_n$$

After having reached an overview over possible bioleaching mechanisms the above mentioned bacterial oxidation mechanism agrees with Silverman and Lundgren (1959), and the chemical oxidation mechanisms agree with Schippers and Sand (1999), Hansford and Vargas (2001) and Sand *et al* (2001). These findings show that *T. ferrooxidans* enhance the rate of dissolution of chalcopyrite more than that achieved by chemical oxidation with acid and ferric sulphate. Thus, in summary, bioleaching of chalcopyrite is affected by both bacterial and chemical oxidation mechanisms.

CHAPTER 6 Bioleaching of the chalcopyrite concentrate in a 4 L stirred tank bioreactor

6.1 Introduction

Stirred vessels are widely used in industry for blending, suspension and mass transfer operations. The process variables of stirred vessels that affect these operations include: vessel type and general geometry, vessel size (working size), size and number of baffles (if present), air flow rate and agitation speed.

Stirred vessel-bioleaching is a three-phase system, composing incoming air and outlet gas, acidic aqueous liquid, and microbial cells and mineral particles. The complex nature of this slurry makes the attainment of homogeneity especially difficult (Brucato and Brucato, 1998). Agitation has two main purposes: to increase the rate of transfer operations (such as oxygen and carbon dioxide transfer and heat transfer), and to mix the reactor content. Under conditions of insufficient agitation the transfer operations may become limiting and the overall reaction performance will decline because of the appearance of zones in the fluid with insufficient nutrients or inadequate temperature or pH (Acevedo, 2000). Many investigators have studied impellers that specifically enhance oxygen transfer, however it has been suggested that the high shear stress exerted by the disc turbine on the fluid may also produce metabolic stress and cell growth inhibition on *Brevibacterium flavum*, *Trichoderma reesei*, and *Saccharomyces cerevisae* (Toma *et al*., 1991).

Table 6.1 A summary of bioreactor studies by independent researchers

Refs	Vessel								Experimental study			
	Type	Baffle	Types of turbines	Working volume (Litre)	Agitaion speed (rpm)	Air	Air flow rate (VVM)	Temp. (°C)	Bacteria	Mineral particles	Particle size	Pulp density % (w/v)
Ballester *et al.*, 1990	Batch stirred tank bioreactor	n/a	-	0.3	150	Air enriched with 1% CO_2		35	*T. ferooxidans*	A sphalerite concentrate	8.3-74μm	5
Asai *et al.*, 1992	Air-lift reactor	-	-	0.6	-	Air	0.83	30	*T. ferooxidans*	Pyrite	53-63 μm 63-88 μm 149-177μm	1
Nagpal *et al.*, 1993	Continuous stirred tank reactor	n/a	Three Rushton turbine	14	600	Air enriched with 0.04 - 1% CO_2	0.01-0.21	35	*T. ferooxidans*	Pyrite-arsenopyrite ore concentrate	< 75 μm	16
Langhans *et al.*, 1995	Semi-batch stirred tank bioreactor	n/a	n/a	3	200	O_2 =2 mg/l	n/a	30-35	A mixed of autotrophic, acidophilic, iron and sulphide bacteria	An arsenic-bearing refractory gold ore	< 150 μm	10
Clark and Norris, 1996	Air-lift reactor	-	-	0.44	-	Air enriched with 1% CO_2	0.91	30	*T. ferooxidans* (DSM 583), *Sulfobacillus thermosulfidooxidans*, *Sulfolobus* sp.	Pyrite-arsenopyrite ore concentrate	< 75 μm	2, 10
Hugue *et al.*, 1997	Batch stirred tank bioreactor	4 Baffles	Six-vertical flat blades	21	390-450	Air enriched with 1% CO_2	0.3-0.7	35	A mixed culture of *T. ferrooxidnas and T. thiooxidans*	Cobaltiferous pyrite	< 63 μm	20
Konishi *et al.*, 1997	Continuous stirred tank reactor	n/a	Six-blades turbine impellers	10	500	Air	0.2-0.5	65	*Acidianus brierleyi* (DSM 1651)	Pyrite	25-44 μm	5, 10
Nemati *et al.*, 2000	Batch stirred tank bioreactor	n/a	Four pitch blades	1	500-550	Air	1	68	*Sulfolobus metallicus*	Pyrite	25-180 μm	3
Witne and Phillips, 2001	Batch stirred tank bioreactor	4 Baffles	Four vertical flat paddle	1	200	Air, Air+CO_2, Air+ O_2+CO_2	0.2, 0.5, 0.7, 1.0	30	*T. ferooxidans* (DSM 583)	A copper concentrate	<112 μm	3-40
Malik *et al.*, 2001	Batch stirred tank bioreactor	n/a	n/a	20	250	Air	1	30	*T. ferooxidans* (ATCC 13984)	Coal	< 250 μm	n/a
Yahya and Johnson, 2002	Batch stirred tank bioreactor	n/a	n/a	1.5	150	Air	0.33	35	*Sulfolobacillus, T. ferrooxidans*	Pyrite	<20 μm	1

A summary of bioreactor studies by independent researchers can be seen in Table 6.1. Several researchers have studied particle size and pulp density (Asai *et al.*, 1997, Clark and Norris, 1996, Konishi *et al*., 1997, and Witne and Phillips, 2001). Others have studied oxygen & carbon dioxide transfer by varying the percentage of CO_2 and O_2 in air as well as the air flow rate i.e. Nagpal *et al*. (1993), Clark and Norris (1996), Hugue *et al*. (1997), Konishi *et al*. (1997), and Witne and Phillips (2001). Oxygen and carbon dioxide can be provided by ambient air (Nagpal *et al*., 1993). An optimum air flow rate was found to be 0.5 vvm (Witne and Phillips, 2001), while Hugue *et al*. (1997) reported that an optimum air flow rate was found to be about 0.6 vvm, whilst Konishi *et al*. (1997) found that the air flow rate of 0.2-0.5 vvm gave similar results. As a result of their studies, this study used ambient air with an air flow rate of 0.5 vvm.

Previous studies of agitation speeds by Hugue *et al*. (1997) and Nemati *et al*. (2000) employed a mixed culture of *T. ferrooxidans* and *T. thiooxidans*, and a thermophile culture of *Sulfolobus metallicus* respectively and used a range of relatively high agitation speeds (i.e. 390-450 rpm and 500-550 rpm). The present work has therefore examined a range of agitation speeds; 50, 100, 150 and 200 rpm.

As stated in chapter 3 and 4, shake flask speed was found to have an influence on cell growth, metal dissolution and cell adsorption ratio. This work was extended to consider an agitated vessel for the purpose of scale up, and how the same parameters can influence cell growth and metal dissolution.

6.2 Materials and Methods

6.2.1 Bioreactor

The batch stirred bioreactor experiments were conducted in a cylindrical 4-litre (working volume) or 5-litre (total volume) bioreactor (Figure 6.1) fitted with flat stainless steel top and bottom plates. The base of the vessel was connected with heating and cooling systems in order to maintain a constant operating temperature (30 ± 1 °C). Air was passed through an air-filter to purge the medium and the exit gas was forced to pass though a condenser and an air-filter before being released to the atmosphere. The condenser used for this work was designed so it prevented the loss of water due to evaporation.

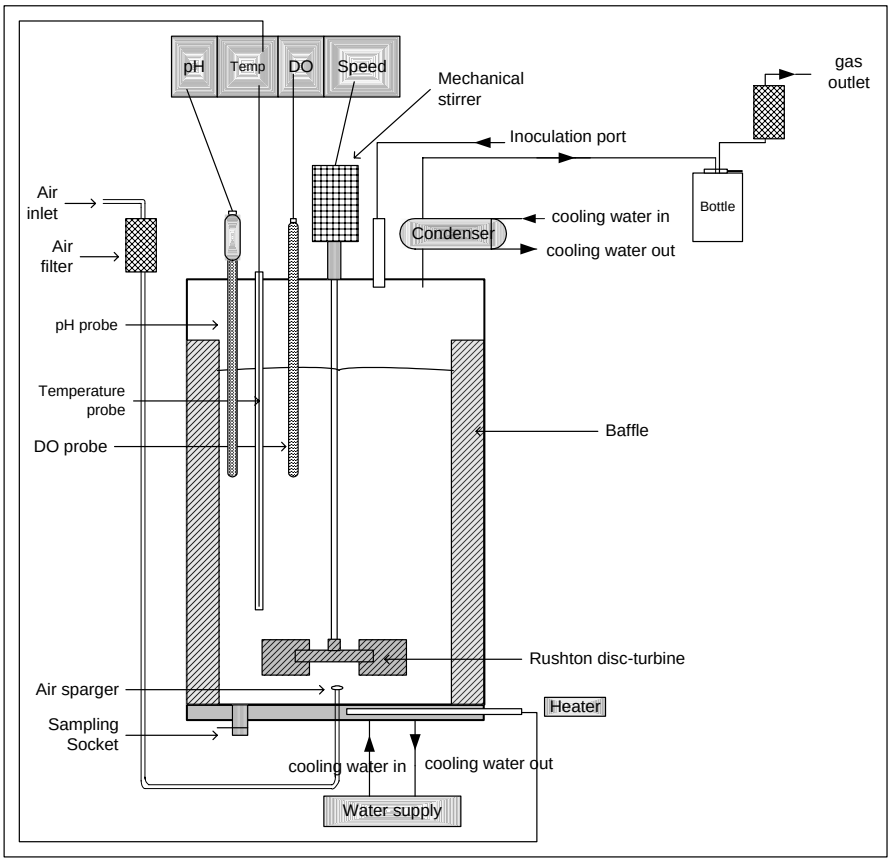

Figure 6.1 Simplified scheme of the laboratory bioreactor

The dimensions of the bioreactor's components are shown in Table 6.2. The vessel was equipped with a Rushton disc-turbine and four equi-spaced vertical baffles. It was also fitted with a pH probe (Broadley-James, UK), a dissolved oxygen probe (galvanic type) and a temperature probe while the latter was connected to a control unit (the two probes and the control unit were made 'in-house' in the Department of Chemical Engineering, The University of Birmingham, UK). The slurry was agitated by a mechanical stirrer at different agitation speeds for this study.

Table 6.2 The dimensions of the laboratory bioreactor

Reactor Parts	Bioreactor dimensions (mm)
Vessel diameter	157
Baffle width	17
Impeller diameter	76
Width of impeller blade	25
Thickness of impeller blade	1.6
Distance of impeller from the base of the vessel	29

6.2.2 Experimental procedure

6.2.2.1 Preparation of inoculum

A 10 % v/v inoculum of the stock culture (Appendix II) was added to a flask (2000 ml) containing 400 ml of ATCC 64 medium at an initial pH of 2.8. The flask was incubated in a rotary shaker at 30 °C and 100 rpm. The cells were harvested after they had reached the late exponential phase (96 hours) and then the culture was filtered through filter paper (Whatman No. 1). The culture was centrifuged at 8000 rpm for 40 minutes in order to separate the cells, and washed three times with the same medium used for growth (ATCC 64 medium without ferrous ions). The cells were then diluted to a known concentration (about 5.0 x 10^9 cells/ml) with the medium (ATCC 64 medium

without ferrous ions). This was then used as inoculum for the bioreactor studies (section 6.2.2.3).

6.2.2.2 Calibration of pH probe, dissolved oxygen probe and temperature probe

The pH probe was immersed into a standard reference buffer pH of 7. The reading indicated from the pH module was then checked and adjusted until the desired reading was achieved. The pH probe was again checked with a standard reference buffer of pH 4. The pH probe was rechecked with a standard reference buffer of pH 7.

The dissolved oxygen probe was immersed into the bioreactor containing about 4 litres of tap water, which had been aerated and agitated for about 30 minutes and was considered to be saturated with dissolved oxygen. The reading indicated at the DO module was checked and adjusted until the desired reading (100 % DO) was achieved. The air valve was then turned off, and the nitrogen gas valve was turned on. The water was thus constantly purged with nitrogen gas and agitated. The dissolved oxygen reading gradually decreased from 100 to 0 % DO. After the desired reading was achieved, the nitrogen gas valve was turned off and the air valve was turned on. The dissolved oxygen reading was increased in turn to give a reading of 100 ± 5 % DO.

A temperature probe was placed into a pocket in the bioreactor that contained about 4 litres of tap water. The temperature of the water was checked with another temperature probe. The temperature set point was set at 30 ± 0.5 °C.

6.2.2.3 Preparation of bioleaching of the chalcopyrite concentrate

After the probes had been calibrated, 200 g of the chalcopyrite concentrate (+53, -75 μm) and 3.6 litres of ATCC 64 medium (in the absence of ferrous ions) were added into the bioreactor. The initial pH of the slurry was adjusted to 2.8 and the bioreactor was then autoclaved at 121 °C for 30 minutes. The vessel and contents were allowed to cool to a constant temperature of 30 ± 0.5 °C.

400 ml of the inoculum as described in Section 6.2.2.1 was added to the 3.6 litres of the sterilised ATCC 64 medium in the bioreactor. Aseptic techniques were used throughout. The gas supply system was designed to accommodate ambient air only (0.03 % (v/v) CO_2). Gómez *et al*. (1999 a) have reported no significant effect on bacterial leaching rates by the supplementation of ambient air with carbon dioxide. The air flow rate was controlled at 0.5 vvm (corresponding to 2 l/min). The optimal air flow rate was found to be 0.5 vvm for bioleaching of OK Tedi copper concentrate by *T. ferrooxidans* (Witne and Phillips, 2001). The aim of this work was to study the bioleaching of the chalcopyrite concentrate by *T. ferrooxidans* at a range of agitation speeds, i.e. 50, 100, 150 and 200 rpm were considered.

Samples were taken at regular time intervals. The pH and % DO were recorded. The leaching solution was filtered through filter paper (Whatman No. 1) in order to separate solid and liquid phases and the filtrate was then used to analyse for the solution pH, redox potential, free cell concentration, total iron and copper concentration.

6.2.2.4 Preparation of *T. ferrooxidans* grown on ferrous ions

The experimental procedure was the same as that used in the bioleaching of the chalcopyrite concentrate experiments except that instead of chalcopyrite it used ferrous sulphate (20 g/l $FeSO_4 \cdot 7H_2O$). Ferrous sulphate (240 g) was dissolved in 400 ml of distilled water and 4 ml of 1N H_2SO_4 solution. The ferrous sulphate solution was then sterilised by Microfiltration (Clyde filter, 0.2 μm). Prior to the experiments, 3.2 litres of the ATCC 64 medium were added to the bioreactor and then sterilised by autoclaving. The ferrous sulphate solution was added into the bioreactor using aseptic techniques; the pH in the bioreactor after sterilisation was about 2.8, but was adjusted if necessary. 400 ml of the inoculum as described in Section 6.2.2.1 was inoculated and added to the bioreactor, which was run at an agitation speed of 200 rpm. The air flow rate was controlled at 0.5 VVM (corresponding to 2 l/mim). Samples were taken at regular time intervals (i.e. 24, 32, 48, 56, 72, 78, 96, 120, 144, and 168 h.).

In order to investigate whether the presence of solid particles had a significant influence on cell growth, an experiment was set up by preparing a bioreactor as described above and adding 5 % (w/v) Zirconium[1], $ZrSiO_4$ (+53, -75 μm). Zirconium was chosen as an inert solid particle for this study. The results are presented in section 6.4.2.

[1] Zirconium is an inert mineral particle alloyed with iron, silicon and tungsten with specific gravity of 4.6-4.7.

6.3 Bioleaching of the chalcopyrite concentrate

6.3.1 Agitation speed of 50 rpm

Preliminary experiments showed that the minimum speed to prevent solid deposition at the base of the vessel (at the start of the experiment) was 50 rpm. Figures 6.2 and 6.3 show cell growth and metal dissolution for two experiments at 50 rpm. The bacteria growth curve displayed the usual pattern; the lag phase lasted approximately 5 days and was followed by a rapid exponential phase and a stationary phase until the end of the experiment. However, the maximum free cell concentration obtained from these graphs was found to be only about 3×10^9 - 4×10^9 cells/ml for the two experiments. The maximum specific growth rate was 0.03 h^{-1}. The maximum free cell concentration obtained from this graph was much lower than that found from previous experiments conducted in shake flasks using the same initial cell concentration for the latter cell concentration was about 3×10^{11} cells/ml for the 100 rpm test. These two experiments suggested that bacterial growth was limited at this agitation speed.

Because the 5 % (w/v) chalcopyrite concentrate had been shown to provide enough substrate for bacterial growth to reach free cell concentrations as high as 3×10^{11} cells/ml (chapter 3, section 3.3.2), the reduced cell concentration at 50 rpm was not considered to be due directly to substrate limitation. Instead, after a few days most of the solid phase was observed to settle on the base of the vessel. This may have been due to the precipitation of ferric ion on the particle surface resulting in an increase in size and change in surface area leading to coagulation. The settled material provides a lower free surface area for bacteria and nutrients are less able to diffuse to cells within the settled mass.

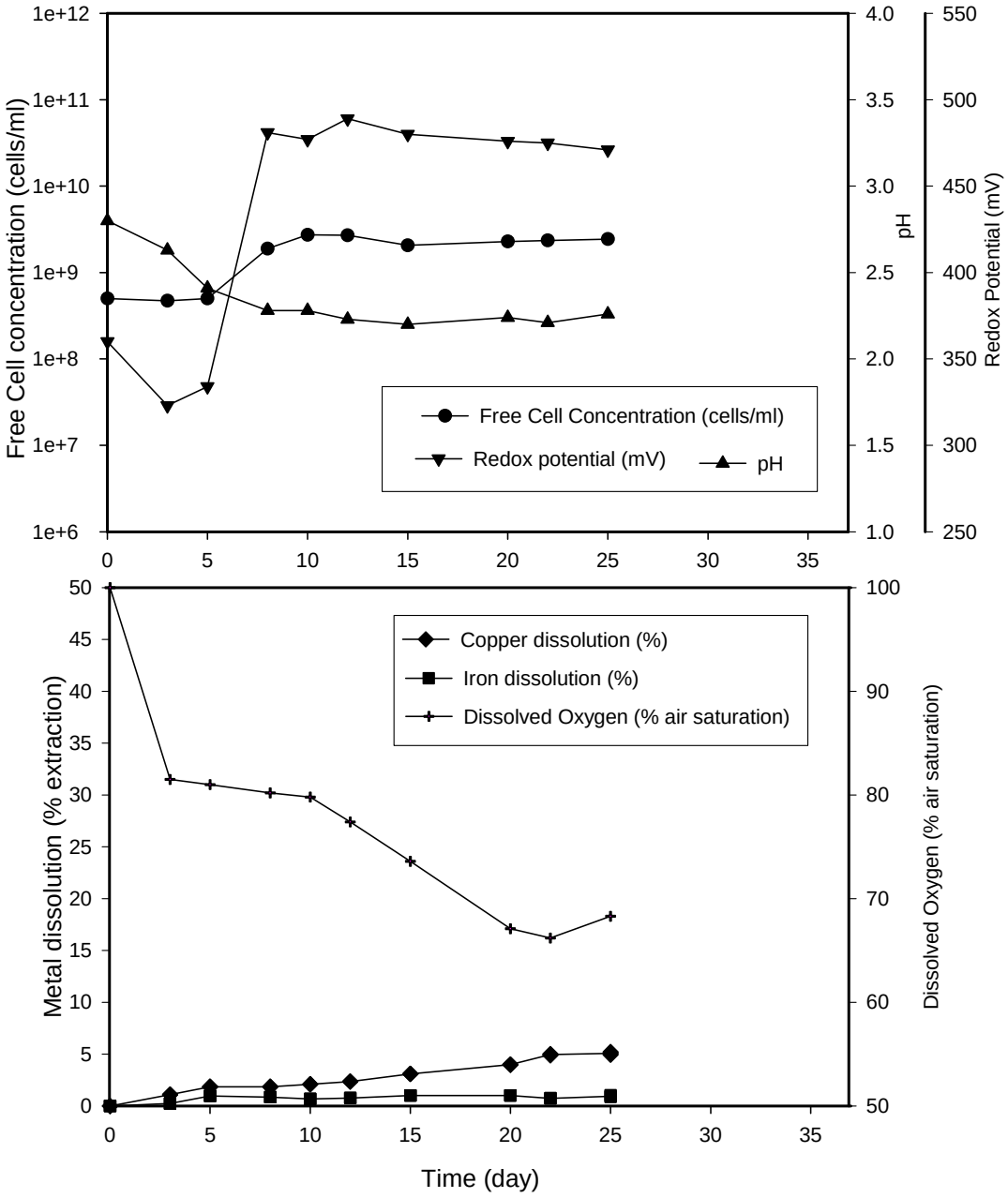

Figure 6.2 Bioleaching of the chalcopyrite concentrate in the bioreactor at 5 % (w/v) pulp density, +53, -75 μm, initial pH 2.8 and 50 rpm

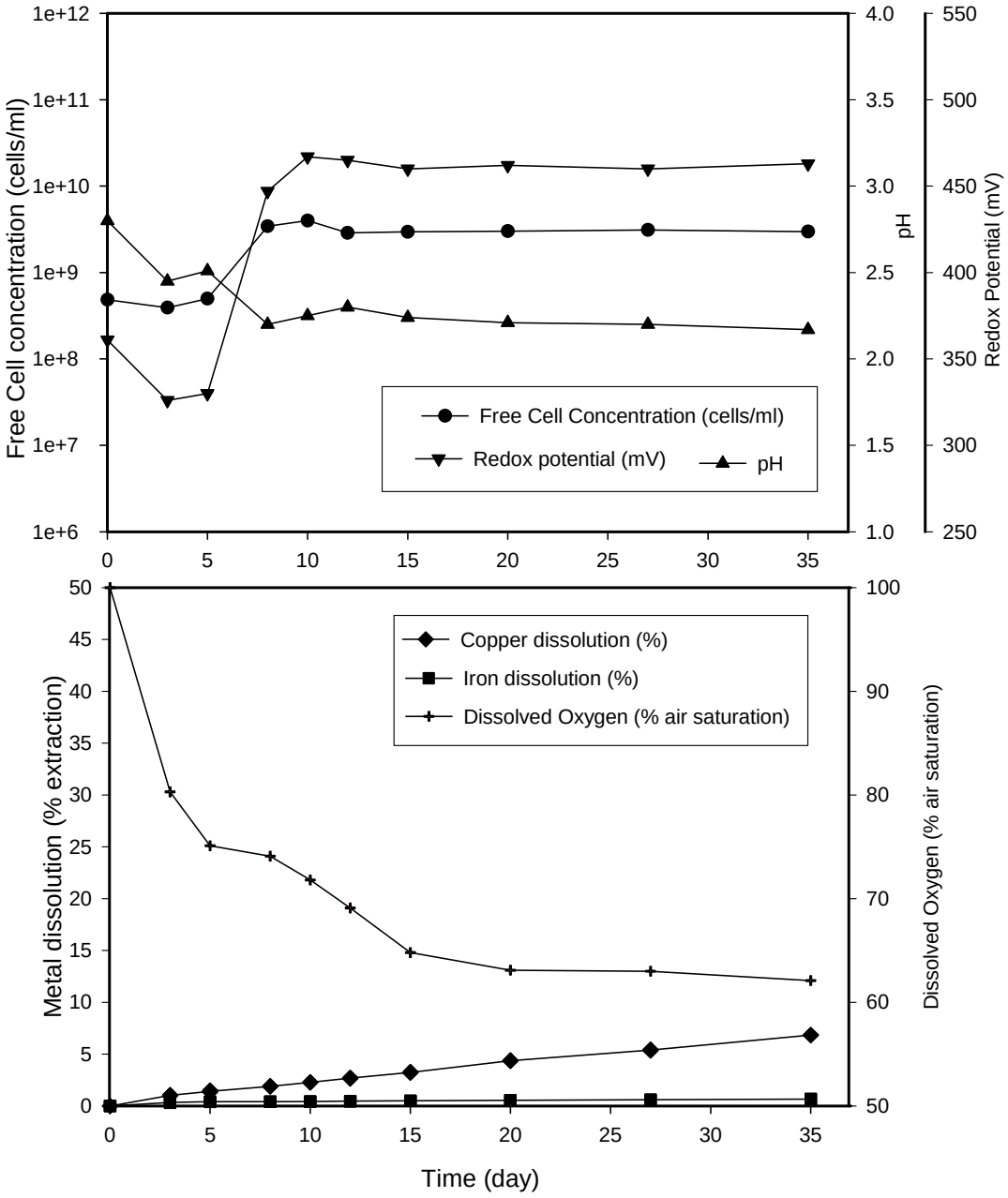

Figure 6.3 The repeat of bioleaching of the chalcopyrite concentrate in the bioreactor at 5 % (w/v) pulp density, +53, -75 μm, initial pH 2.8 and 50 rpm

From Figures 6.2 and 6.3 the dissolved oxygen curve shows a drop in percentage of air saturation from 100 to about 60-70 after 20 days. The fall in solution pH was fairly gradual; the pH values dropped from 2.8 to 2.2 after 8 days and remained relatively constant until the end of the experiment. The redox potential showed an increase in value from 360 mV to a maximum of 480 mV after 8 days (Figure 6.2) and 467 mV after 10 days (Figure 6.3). The percentage of metal solubilisation in the bioreactor proved to be very low, being less than 5 % Cu and 1 % Fe extraction (0.57 g/l Cu and 0.14 g/l Fe) for 20 days (Figure 6.2). The metal dissolution curves of Figure 6.3 also showed a similar trend; the final copper dissolution after 35 days was found to be 7 % Cu and 1 % Fe extraction (1 g/l Cu and 0.09 g/l Fe). Overall, the copper dissolution at 50 rpm was very poor in comparison to that of previous experiments in the shake flask at 100 rpm (Figures 3.1-3.3).

Although the redox potential was found to be quite high in this experiment (480 mV), the copper dissolution (% extraction) was still low. This was thought to be related to the observed aggregate deposition on the base of the bioreactor as a result of poor agitation. In the absence of oxygen, acid attack on chalcopyrite causes the solubilisation of iron (II), the evolution of hydrogen sulphide and leaves the copper in the solid state as CuS using equation 6.1 below (Barrett *et al.*, 1993).

$$FeCuS_2 + 2H^+ \rightarrow Fe^{2+} + CuS_{(s)} + H_2S \qquad (6.1)$$

In addition, the formation of Fe^{3+} polymers, e.g. iron hydroxides, oxyhydroxides and jarosite, (equation 6.2) have been observed by several researchers (Fernadez *et al.*, 1995; Loan *et al.*, 2002; Pogliani and Donati, 2000). Even if the experiment was set at a low pH (initial pH 2.0), the jarosite was still found to be strongly bound on the

chalcopyrite surface as characterised by using X-ray diffraction, and scanning electron microscopy/elemental analysis (Stott *et al.*, 2000).

$$3Fe^{3+} + 2SO_4^{2-} + 6H_2O \rightarrow Fe_3(SO_4)_2(OH)_6^- + 6H^+ \quad (6.2)$$

Therefore, a layer of metal precipitation (mainly iron and copper ions) would hinder greater copper extraction by restricting the flow of bacteria, nutrients, oxidants and reaction products to and from the mineral surface.

6.3.2 Agitation speed of 100 rpm

The experimental data (Figure 6.4) demonstrates that the free cell concentration, copper dissolution, iron dissolution and pH are markedly affected by agitation speed. The lag phase of the cell growth curve decreased significantly at 100 rpm from 5 days to 3 days. The maximum specific growth rate calculated from the gradient of the line that was plotted using the natural logarithm of cell population against time was 0.039 h^{-1} (Figure 6.4). The maximum free cell concentration obtained from this graph was much higher than that of the 50 rpm test, being 5.2 x 10^{10} cells/ml after 8 days, compared to about 4.0 x 10^9 cells/ml after 10 days for the 50 rpm test.

When this data was compared to the lag phase data from shake flask tests obtained at the same agitation speed (Chapter 3), a difference of a few days can be observed. The maximum specific growth rate during the exponential phase increased more than 1.32-fold from 0.0295 h^{-1} (the average maximum specific growth rate from Figures 3.1-3.3). This achievement was probably due to the promotion of the gas liquid interfacial mass transfer in the bioreactor.

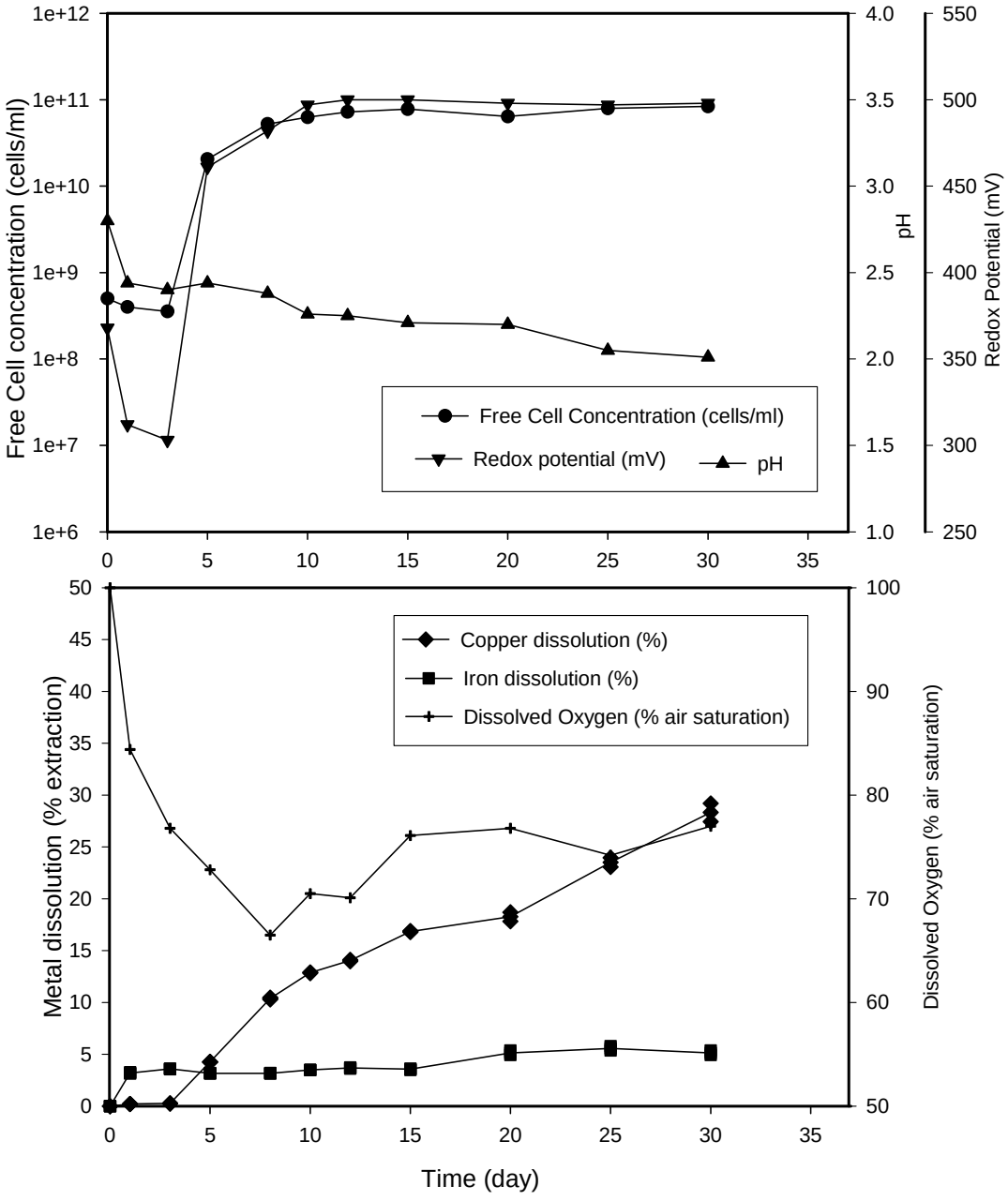

Figure 6.4 Bioleaching of the chalcopyrite concentrate in the bioreactor at 5 % (w/v) pulp density, +53, -75 μm, initial pH 2.8 and 100 rpm

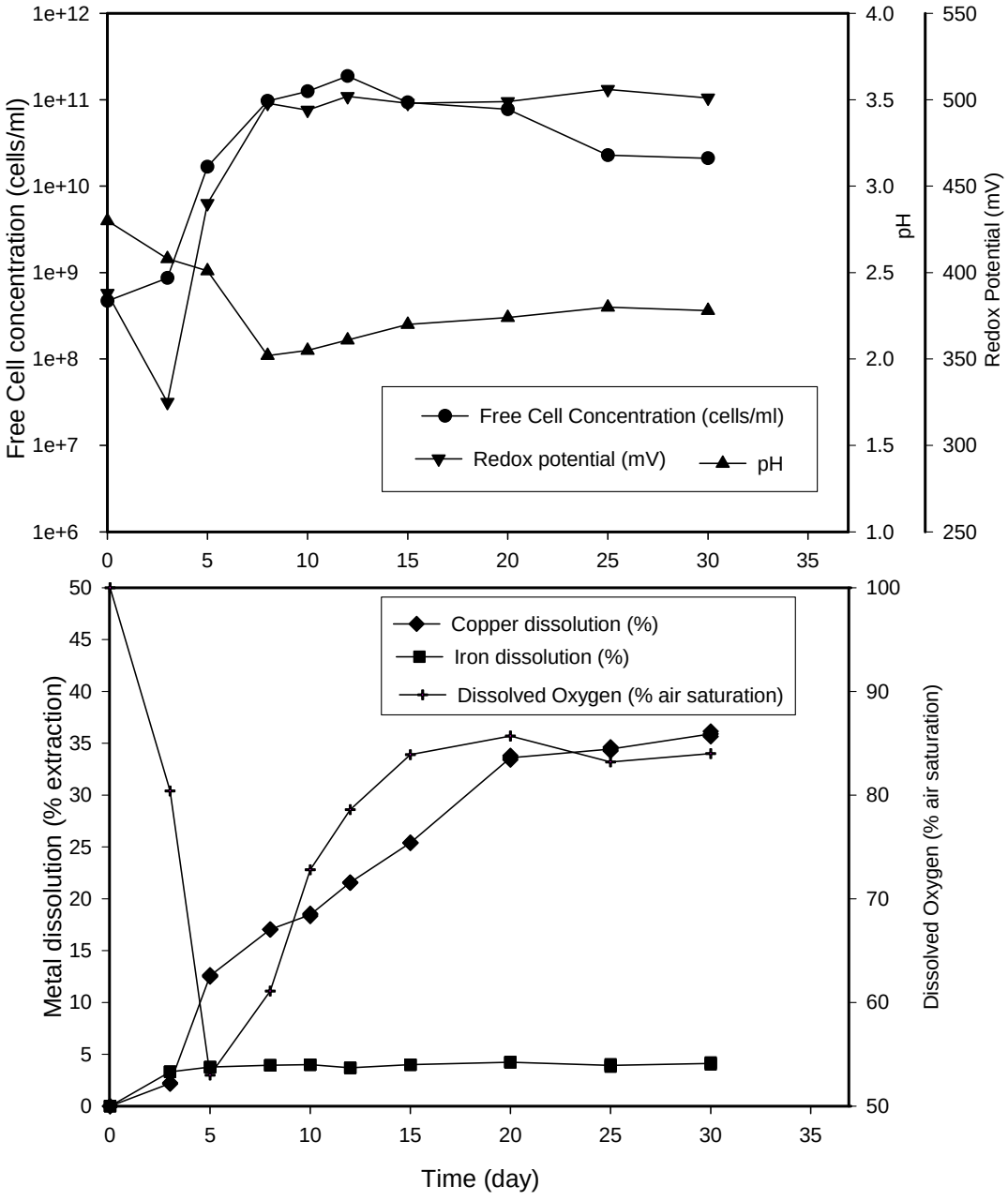

Figure 6.5 Bioleaching of the chalcopyrite concentrate in the bioreactor at 5 % (w/v) pulp density, +53, -75 μm, initial pH 2.8 and 150 rpm

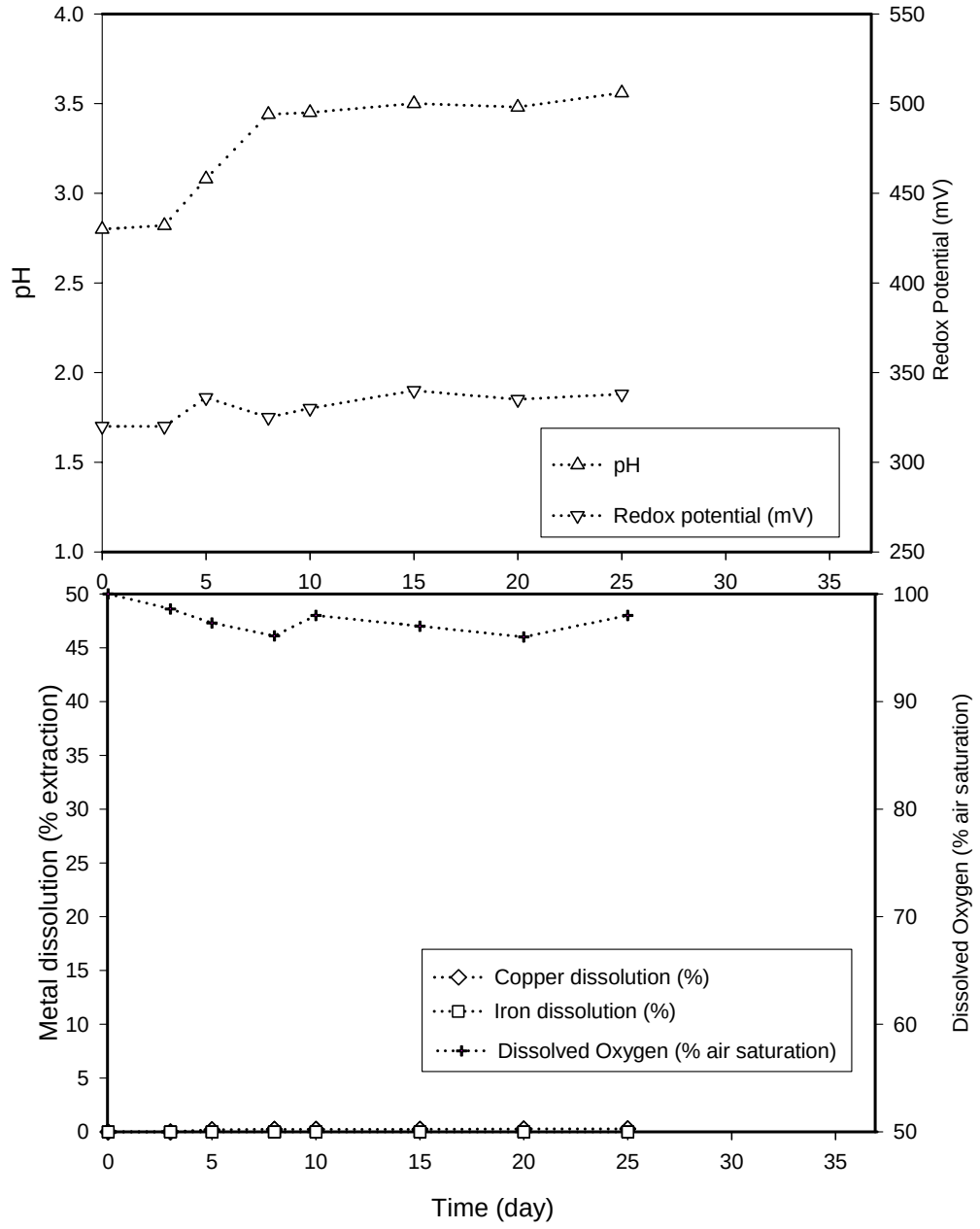

Figure 6.6 Control experiments (in the absence of bacteria) at 5 % (w/v) pulp density, +53, -75 μm, initial pH 2.8 and 150 rpm

The solution pH values decreased from the initial pH of 2.8 to about 2.4 after 3 days (Figure 6.4). This was followed by a slight decrease in the pH values until the end of the experiment where pH reached a value of approximately 2.0. The redox potential curve of Figure 6.4 shows that the value decreased from 368 mV to 303 mV after 3 days; this was followed by a sharp increase in the redox potential value to 461 mV during the next 2 days. The redox potential after 5 days remained roughly constant at about 490-500 mV. The dissolved oxygen curve shows the drop in percentage of air saturation from 100 % to about 66 % after 8 days (i.e. during the lag and exponential phases), which was then followed by a slight increase in the value as the culture entered stationary phase.

The lag phase of copper dissolution at 100 rpm was only 3 days (as shown in Figure 6.4). The rate of copper dissolution was 0.12 g/l per day and there was no leveling off before the experiment was finished, after 30 days. The final total copper dissolution was 28.3 % extraction after 30 days. However, the iron dissolution remained constant at about 4.5 ±1 % extraction until the end of experiment. The final yield of total copper solubilised after completion of leaching (30 days) was 4.09 g/l, a significantly greater value than that observed for the 50 rpm test.

6.3.3 Agitation speed of 150 rpm

At an agitation speed of 150 rpm, the growth curve (Figure 6.5) showed a lag phase of about 3 days, this was followed by an exponential phase of about 5 days with a maximum specific growth rate of 0.04 h^{-1}. Not only was the lag phase of the same duration with those obtained at the agitation speed of 100 rpm (Figure 6.4), but also the maximum specific growth rate was similar. However, the maximum free cell concentration reached was 1.9 x 10^{11} cells/ml, i.e. greater than that obtained at 100 rpm.

The solution pH values (Figure 6.5) dropped from 2.8 to 2.02 after 8 days. This was followed by a slight increase in pH towards the end of the experiments. The final pH of the solution was about 2.3 after 30 days, a rise of 0.28 from the minimum value.

The dissolved oxygen curve shows a sharp drop in percentage of air saturation from 100 % to about 53 % after 5 days (Figure 6.5), which was then followed by an increase in the value over the next 25 days to reach about 80 % of air saturation. This sharp decrease in dissolved oxygen implies oxygen consumption by bacteria, especially when they start to grow during the early exponential phase.

The lag phase prior to copper dissolution lasted approximately 3 days (Figure 6.5), after which the rate of copper dissolution reached 0.24 g/l per day. The copper dissolution graph shows that there was a slight increase in copper solubilisation after 20 days. The copper dissolution increased to about 34 % at 20 days and was then followed by a slight increase over the next 10 days to reach 36 % (corresponding to a maximum yield of 5.29 g/l).

The rate of iron dissolution was found to be only 0.11 g/l per day (Figure 6.5), which was significantly lower than the copper dissolution rate. Iron dissolution levelled off at about 0.55 g/l and gave a total iron dissolution percentage of approximately 4 %. The graph shows no increase in the amount of total iron concentration before the experiment was terminated. This observation may be due to preferential iron precipitation during the leaching process.

A control experiment was conducted at 150 rpm in the absence of bacteria (Figure 6.6). An increase in the solution pH value was observed from 2.8 to about 3.5, which then remained constant at pH values of 3.5. The redox potential began to level off at about 320 – 340 mV from the beginning of this experiment. The redox potential values did not significantly alter during the duration of the experiment (25 days).

Copper dissolution appeared to be lower than 1 % (<0.1 g/l), iron dissolution was also found to be lower than 1 %(<0.1 g/l) in the absence of bacteria (Figure 6.6). As expected the percentage of copper dissolution obtained from the experiment in the presence of bacteria (Figure 6.5) was much greater than in the control experiments. In contrast to the bioleaching experiment, the dissolved oxygen curve remained constant at about 95 % of air saturation (Figure 6.6). During bioleaching the dissolution of the chalcopyrite concentrate by *T. ferrooxidans* proceeded according to equation 5.7, Chapter 5 ($4CuFeS_2 + 17O_2 + 2H_2SO_4 \xrightarrow{T.\,ferrooxidans} 4CuSO_4 + 2Fe_2(SO_4)_3 + 2H_2O$).

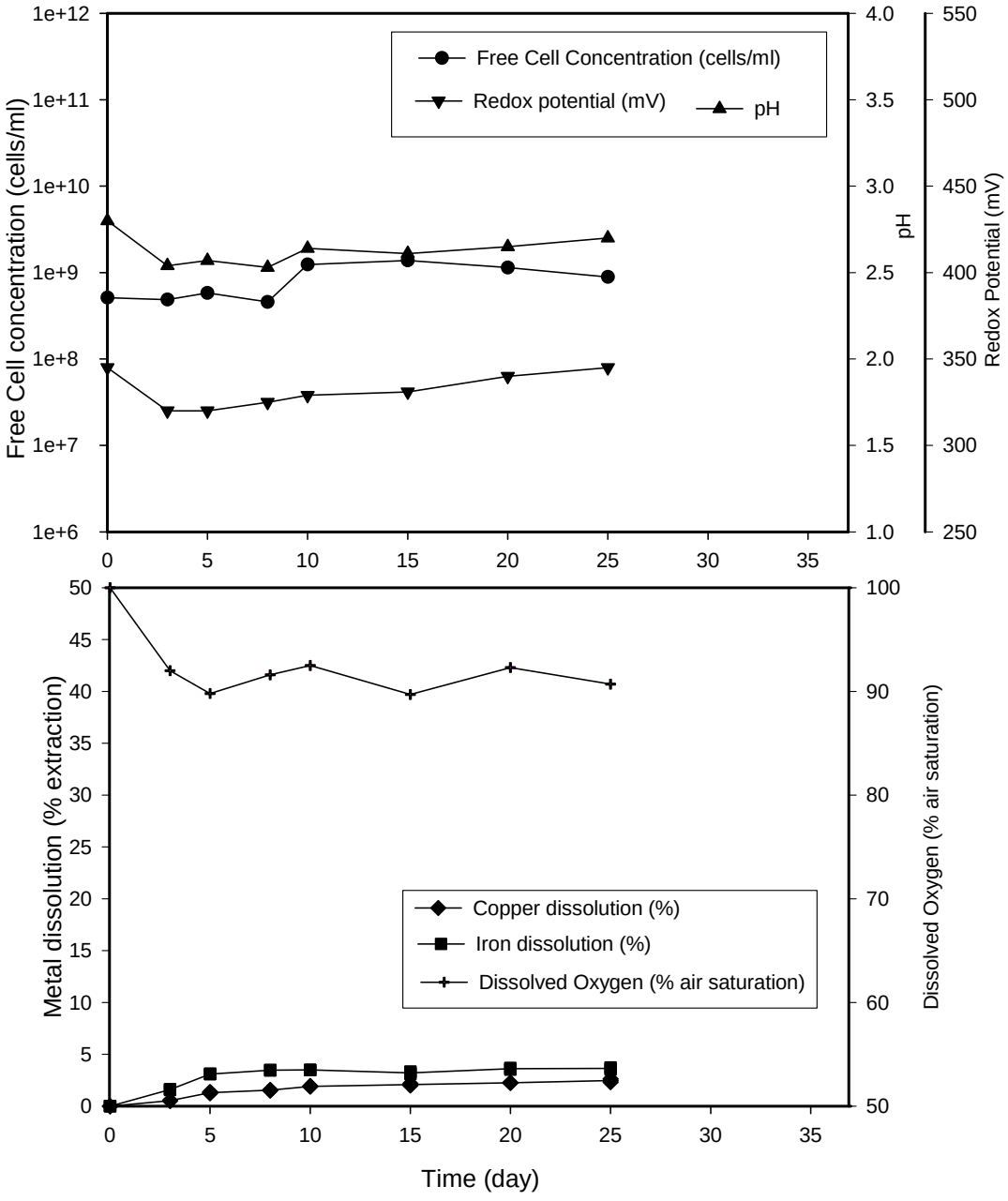

Figure 6.7 Bioleaching of the chalcopyrite concentrate in the bioreactor at 5 % (w/v) pulp density, +53, -75 μm, initial pH 2.8 and 200 rpm

6.3.4 Agitation speed of 200 rpm

No growth curve was observed at 200 rpm and overall there was little change in free cell concentration between 4.56 x 10^8 – 1.38 x 10^9 cells/ml (Figure 6.7). The solution pH values decreased slightly from an initial pH of 2.8 to about 2.54 after 3 days. This was followed by a slight increase in the pH values until the end of the experiment where the pH was about 2.7. The redox potential values did not significantly alter during the duration of the experiments. The dissolved oxygen curve dropped from the start to about 90 % air saturation and remained constant at about 90 % of air saturation. This minor alteration in oxygen consumption supports the fact that little change in free cell concentration was observed at this agitation speed.

The copper dissolution was found to be lower than 3 % extraction (corresponding to about 0.3 g/l). The iron dissolution was also similar to copper dissolution; it was found to be lower than 4 % extraction. Overall, the percentage of copper dissolution at 200 rpm was very poor in comparison to that at 100 and 150 rpm (Figures 6.4 and 6.5 respectively).

6.3.5 Conclusion

The experimental work in this chapter addresses the effect of agitation speed on bioleaching in a stirred bioreactor in the range of 50 to 200 rpm. The control experiment (in the absence of bacteria) was performed at 150 rpm. These results are summarised in Table 6.3.

Table 6.3 Experimental results in agitation speed tests using 4 L stirred tank bioreactor

Figure	Condition	Free cell concentration At t=0 day	Agitation speed (rpm)	Experimental results				
				Free cell concentration at late exponential phase (t=10 days), cells/ml	Copper dissolution at t=25 days		Total iron dissolution at t=25 days	
					g/l	Percentage	g/l	Percentage
6.2	Bacteria	5.00E+08	50	2.73E+09	0.73	5.1	0.13	0.9
6.3	Bacteria	4.84E+08	50	3.99E+09	0.70	5.0	0.81	0.5
6.4	Bacteria	5.00E+08	100	6.26E+10	3.40	23.5	0.77	5.6
6.5	Bacteria	4.69E+08	150	1.25E+11	4.98	34.6	1.04	7.5
6.6	No Bacteria	-	150	-	0.04	0.3	0	0
6.7	Bacteria	5.12E+08	200	1.24E+09	0.36	2.5	0.50	3.6

The optimum agitation speed was found to be 150 rpm since this gave the highest value of copper dissolution coupled with the lower value of iron dissolution. At the low agitation speeds (i.e. N = 50 rpm) it is possible that a poor solids suspension regime resulting in either poor oxygen transfer to the cells attached to the surface or a reduction in attachment sites may have caused the low copper dissolution. Although, faster stirring has a positive effect on the oxygen transfer, a significant decrease in copper dissolution was observed at 200 rpm.

In this case, the agitation speed of 200 rpm may have produced detrimental fluid stresses and particle collisions. Work done by Hewitt *et al*. (1998) suggests that *E. Coli* is very resistant to mechanical damage even at 1200 rpm and it is likely that *T. ferrooxidans* would therefore be resistant to rupture at 200 rpm. However, it was found that the outer polysaccharide layer on the *E. Coli* cell wall was stripped away. It is possible that at higher agitation speeds the extracellular polymeric substances (EPS) that have been found to be involved in cell attachment of *T. ferrooxidans* (Sand *et al*.,

2001) was also stripped away causing a decrease in cell attachment between the bacteria and the mineral ore and therefore a reduction in copper dissolution.

According to Doran (1998), collision between cells, collision of cells with the impeller, and collision of cells with stationary surfaces in the vessel may cause cell damage. In addition, at higher agitation speeds the probability of collisions increases. Such damage has largely been observed with animal cells, which are inherently weaker than bacteria. However, particle friction may reduce the microbial attachment to mineral surface and therefore reduces the rate of bioleaching (Chong *et al*, 2002).

6.4 *T. ferrooxidans* grown on ferrous ions

From the previous section it was unclear why copper dissolution decreased at 200 rpm. One possible reason was the effect of particle collisions at the higher speed. To test this, *T. ferrooxidans* growth on ferrous ions was compared in the absence and the presence of inert solid particles of zirconium of the same size range, roughly the same specific gravity and at the same concentration of the chalcopyrite used in the previous experiments.

6.4.1 Growth curve of *T. ferrooxidans*

A growth curve was plotted in terms of cell concentration against time after inoculation (Figure 6.8). The lag phase was found to extend to about 32 hours after inoculation. Exponential growth occurred between 32 and 56 hours followed by the stationary phase, which was between 56 and 78 hours, and the death phase at about 78 hours after inoculation. In order to calculate the specific growth rate, natural logarithm of cell concentration was plotted against time. Calculation of the gradient of the line corresponding to exponential phase growth yielded the specific growth rate (μ) in units of h^{-1}. The value obtained was 0.22 h^{-1} and the generation time was 3.12 hours. The maximum cell concentration was found to be 1.7×10^{11} cells/ml after 56 hours.

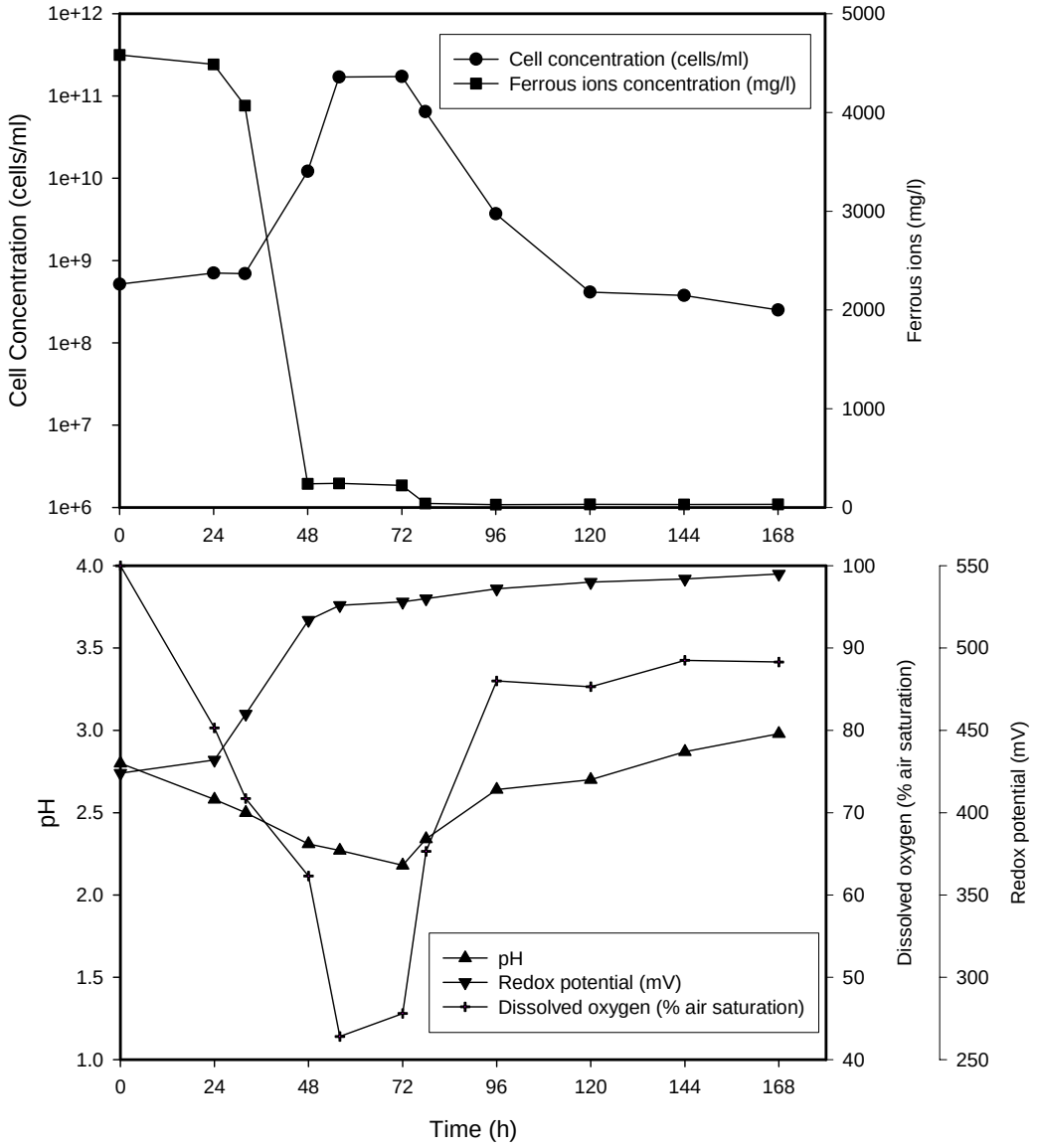

Figure 6.8 *T. ferrooxidans* grown on 20 g/l ferrous sulphate in ATCC 64 medium in the bioreactor at initial pH 2.8 and 200 rpm

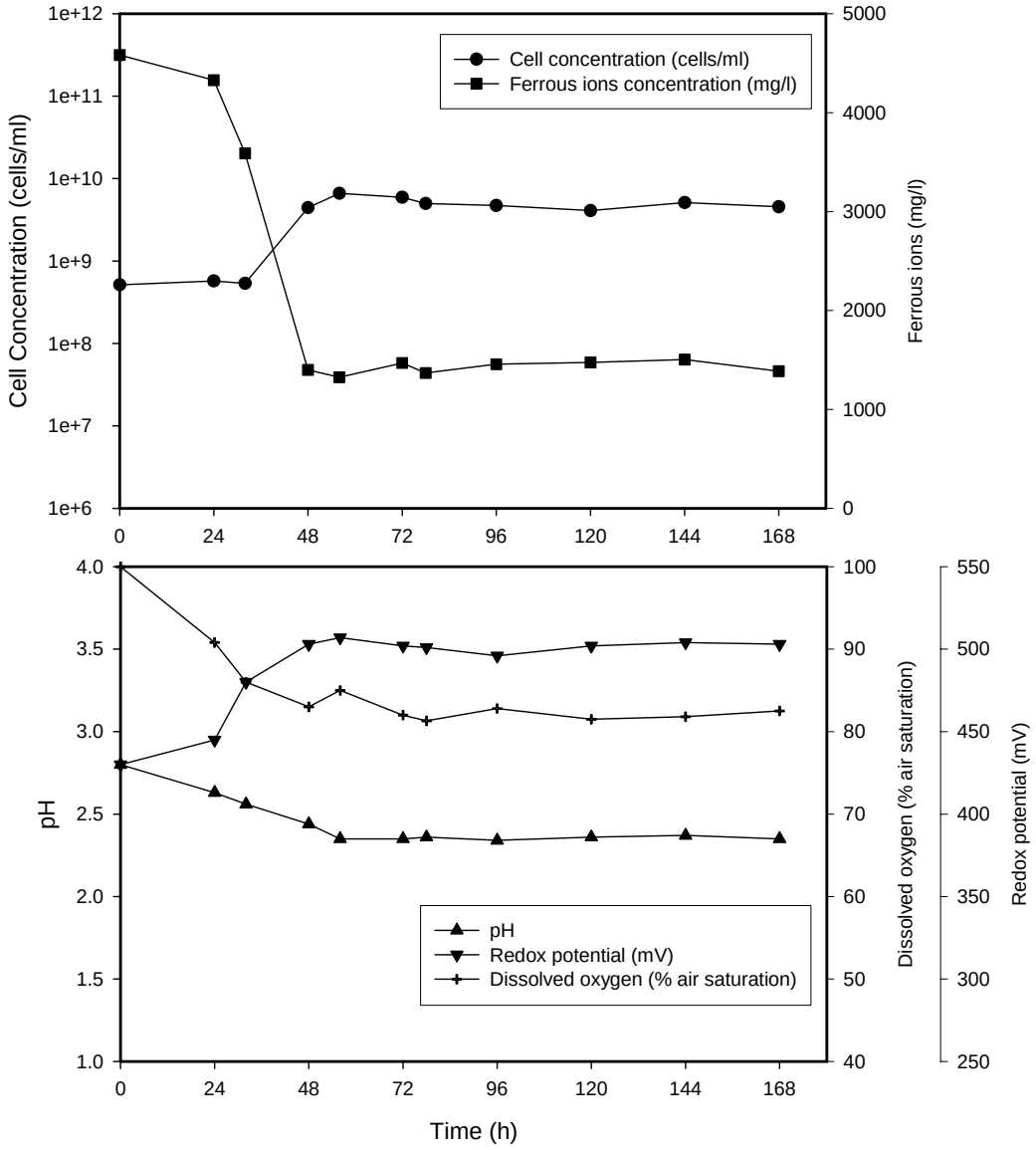

Figure 6.9 *T. ferrooxidans* grown on 20 g/l ferrous sulphate in ATCC 64 medium in the bioreactor at initial pH 2.8, 200 rpm and 5 % (w/v) zirconium

During the exponential phase, a sharp decrease in substrate concentration (ferrous ions) was observed. This is consistent with a marked drop in dissolved oxygen (% air saturation) and the pH values. Moreover, the redox potential increased from 424 to 526 mV after 56 hours, and remained constant until the end of the experiment. This followed, in turn, a rise in the pH values and dissolved oxygen (% air saturation) during the death phase of the growth curve. The following table (Table 6.4) summarises the results given from this growth curve and those results obtained from the shake flask experiment (Appendix I). The bacterial growth rate on ferrous ions in the bioreactor turned out to be more than two-fold higher than that in a shake flask using the same medium at an agitation speed of 200 rpm. Moreover, it was approximately 10 times higher than that obtained in a bioreactor using chalcopyrite and ATCC 64 medium at 200 rpm (Table 6.5).

Table 6.4 The results of the growth of *Thiobacillus ferrooxidans* at 200 rpm

Results	Shake flask			4L bioreactor
	Experiment I	Experiment II	Experiment III	
Maximum specific growth rate, μ_m (h^{-1})	0.0946	0.0984	0.0952	0.2218
Generation time (h)	7.33	7.04	7.23	3.12
Lag phase (h)	0-64	0-40	0-48	0-32
Exponential phase (h)	64-96	40-72	48-96	32-56
Stationary phase (h)	96-136	72-88	96-128	56-78
Death phase (h)	After 136	After 88	After 128	After 78

6.4.2 Growth curve of *T. ferrooxidans* in the presence of zirconium

In the presence of 5 % (w/v) zirconium (+53, -75 μm), the growth curve (Figure 6.9) showed a lag phase of about 32 hours, this was then followed by an exponential phase of about 24 hours with a maximum specific growth rate of 0.11 h^{-1}, i.e. half that obtained without particles. Moreover, the maximum cell concentration was found to be only 6.6 x 10^9 cells/ml after 56 hours.

Table 6.5 The results of the growth of *Thiobacillus ferrooxidans* on different substrates and agitation speed using 4 L stirred tank bioreactor

Figure	Agitation speed (rpm)	Substrate	Lag phase	The maximum cell concentration (cells/ml)	Maximum specific growth rate, μ_m (h^{-1})
6.2	50	5 % (w/v) the chalcopyrite concentrate + ATCC 64 medium (in the absence of ferrous ions)	5 days	4 x 10^9	0.027
6.4	100	5 % (w/v) the chalcopyrite concentrate + ATCC 64 medium (in the absence of ferrous ions)	3 days	5.2 x 10^{10}	0.039
6.5	150	5 % (w/v) the chalcopyrite concentrate + ATCC 64 medium (in the absence of ferrous ions)	3 days	1.88 x 10^{11}	0.038
6.7	200	5 % (w/v) the chalcopyrite concentrate + ATCC 64 medium (in the absence of ferrous ions)	8 days	1.38 x 10^9	0.021
6.8	200	20 g/l ferrous sulphate + ATCC 64 medium	32 hours	1.69 x 10^{11}	0.222
6.9	200	20 g/l ferrous sulphate + ATCC 64 medium + 5 % (w/v) zirconium	32 hours	6.6 x 10^9	0.109

6.5 Conclusion

Although the precise mechanism remains unclear it appears that the presence of particles at a relatively high agitation speed significantly reduces growth rate and maximum cell concentration (Table 6.5, comparison between Figures 6.10 and 6.11). This would suggest that particle collision or abrasion may at least be in part responsible for the reduced metal dissolution.

Table 6.6 shows the effectiveness of thermophiles for bioleaching a copper concentrate ore in comparison to the mesophile (*T. ferrooxidans*). In general, bioleaching with thermophiles was very fast and copper extraction levels of about 80 % are obtained. However, this advantage is countered by the higher levels of iron dissolution.

Table 6.6 A comparison of copper extraction between thermophiles and mesophiles based on bioreactor studies

Ref.	Ore minerals	Minerals content	Microrganism	Conditions								Results	
				Vessel type	Working volume (litre)	Agiation Speed (rpm)	Air flow rate (vvm)	Temp.	pH	Pulp density	Particle size	Rate	% extraction
Witne and Phillips, 2001	Copper concentrate	20 % Cu 17 % Fe 18 % S	*T. ferrooxidans* (DSM 583)	Batch stirred tank reactor	1	200	0.2-1.0	30	1.5-1.8	3 % (w/v)	A size distribution of 90 % passing 112 μm	10.3 mg Cu/l/hr	86 % Cu, 5-6 days at 0.5 vvm air flow rate
			Sulfobacillus acidophilus					50				12.6 mg Cu/l/hr	81 % Cu, 5-6 days at 0.5 vvm air flow rate
			Sulfolobus strain BC65					70				13.6 mg Cu/l/hr	88 % Cu, 5-6 days at 0.5 vvm air flow rate
Konishi *et al*., 1999	Chalcopyrite concentrate	30 % Cu 29 % Fe 4 % Zn 1 % Pb	A. brierleyi	Batch stirred tank reactor	0.8	500	1.25	65	2	0.5% (w/v)	+38, -53 μm	N/A	90 % Cu, 7 days 80 % Fe, 7 days
Gericke *et al*., 2001	Chalcopyrite concentrate	24 % Cu 30 % Fe 8 % SiO_2	An extremely thermophilic isolated from a hot sulphur-rich coal dump near Witbank, South Africa	Batch stirred tank reactor	12	220	N/A	70	2.2	7.5 % (w/v)	d_{90} = 10 μm	N/A	98 % Cu, 10 days 96 % Fe, 10 days
Duarte, *et al*., 1993	Low-grade copper	33 % Fe 1.2 % Cu 16 % SiO_2	A thermophilic isolated from sulphurous thermal springs	Air-lift reactor	N/A	-	1.5	70	N/A	1 % (w/v)	An average particle size of 13.5 μm	N/A	80 % Cu, 4 days
This work	Chalcopyrite concentrate	29 % Cu 27 % Fe	*T. ferrooxidans* (ATCC 19859)	Batch stirred tank reactor	4	150	0.5	30	2.8	5 % (w/v)	+53, -75 μm	12 mg Cu/l/hr	34 ± 1 % Cu, 20 days 4 % Fe, 20 days

CHAPTER 7 Bioleaching of low-grade copper ores in shake flask cultures of *Thiobacillus ferrooxidans*

7.1 Introduction

Extraction of copper from low-grade ores using bioleaching techniques is becoming increasingly important, as pyrometallurgical processes have an unfavourable environmental pollution impact as well as a high production cost (Barrett *et al*., 1993). Industrial scale dump and heap leaching processes are especially suited for low-grade copper ores (Ahonen and Tuovinen, 1995). Copper ions and other metal ions are dissolved from mineral ores in varying concentrations catalysed by bacterial reaction. In this work, only results dealing with copper and iron dissolution into the leachate solution are considered. Previous chapter have considered bioleaching of chalcopyrite concentrate. The experiments in this chapter deal with the leaching of low-grade copper ores in shake flask. Acid leaching of low-grade ores from Palabora mine, South Africa was studied by using either 1N or 10N H_2SO_4 solution. Bioleaching experiments were also undertaken whereby the culture of *T. ferrooxidans* was grown with the same mineral ores.

7.2 Sulphuric acid leaching of low-grade copper ore

7.2.1 Materials and Methods

A low-grade copper ore, originating from the Palabora mine, South Africa and supplied by Rio Tinto, Research & Development Division, Bristol (UK) was used in this study. Appendix V contains a mineralogical description of the low-grade copper ore. Copper and total iron assays were obtained by digesting the ore in a concentrated HNO_3-HCl

solution as described in Standard Methods for Examination of Water and Wastewater (Greenberg *et al*, 1992). The metal content of the supernatant (solubilised metal) was determined by using a Flame Atomic Adsorption Spectrophotometer. The percentage of copper and total iron concentration in the low-grade copper ores were found to be 1.0 and 10.2 % respectively.

A 5 % (w/v) low-grade copper ore (+53, -75 μm) was added to a shake flask (250 ml) containing 50 ml of either 1 N H_2SO_4 solution or 10 N H_2SO_4 solution. The flask was incubated in a water bath shaker at 100 rpm. This experiment was maintained at 70 °C which corresponds to an average of a moderately high temperature (50-90 °C) bacterial leaching test. Duplicate samples were taken at various time intervals; 0, 1, 2, 5, 7, 10 and 15 days. The leaching solution was filtered through filter paper (Whatman No. 1) to eliminate iron precipitation and other solid particles, and the described metals in the filtrate were determined by atomic absorption spectrophotometry (AAS).

7.2.2 Results and discussion

The low-grade copper ores dissolved significantly in the 1N and 10N sulphuric acid solution (Figure 7.1 a and b). After 7 days the percentage of copper and iron dissolution for the 10N sulphuric acid solution were found to be 25.6 % and 15.1 % respectively (Figure 7.1 a). These percentages correspond to a copper concentration of 0.13 g/l and a total iron concentration of 0.76 g/l. The maximum rate of copper dissolution, reached 0.023 g/l per day, whereas that of iron dissolution was found to be 0.09 g/l per day.

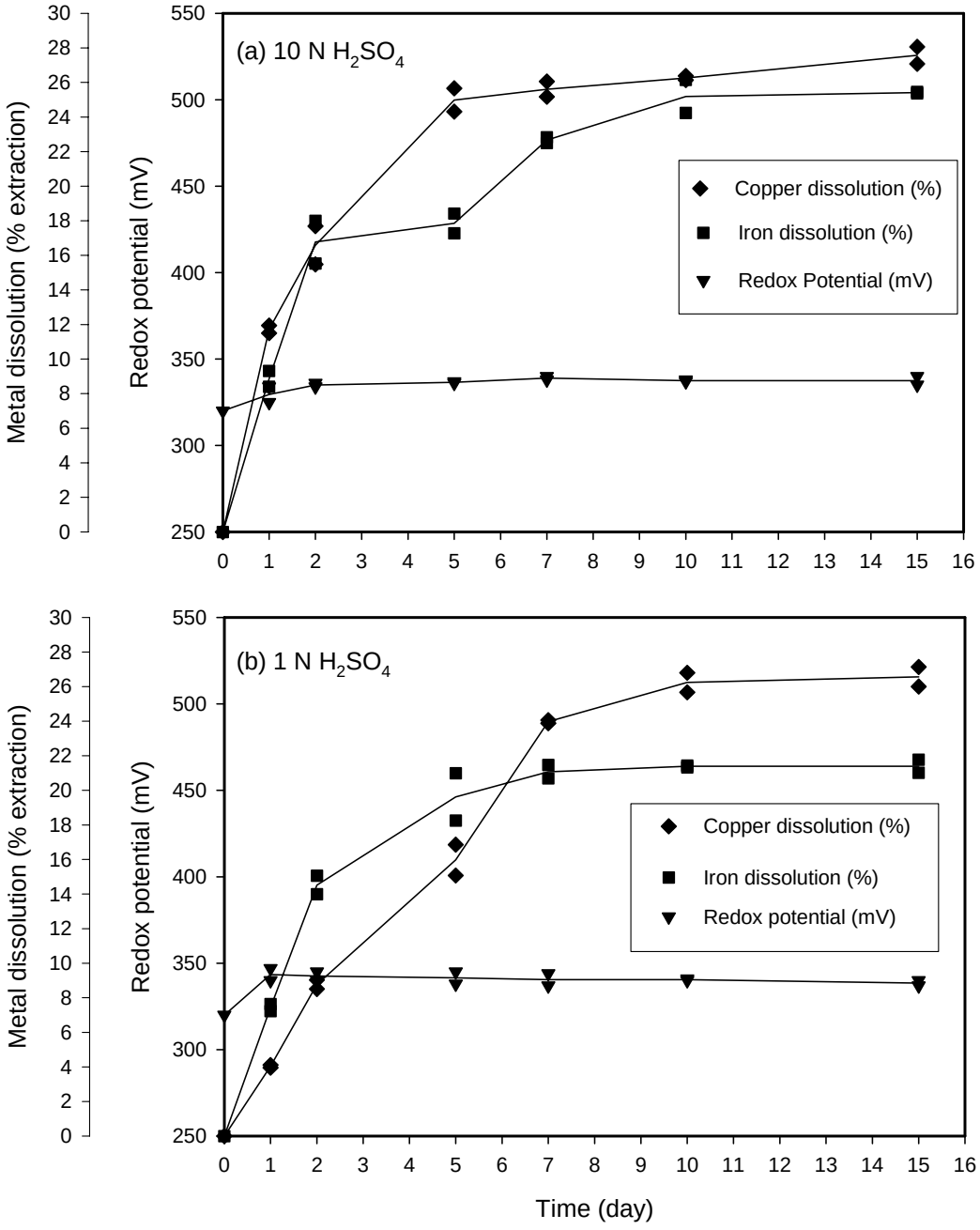

Figure 7.1 Copper and iron dissolution as a function of time for sulphuric acid leaching of low-grade copper ores at 5 % (w/v) pulp density, +53, -75 µm, and 70°C at different concentrations of sulphuric acid solution

The percentage of copper and iron dissolutions obtained from the 1N sulphuric acid solution (Figure 7.1 b) were slightly less than those obtained from the 10N sulphuric acid solution (Figure 7.1 a), giving copper and iron dissolution rates of 0.014 and 0.09 g/l per day respectively.

Overall, the rate of copper dissolution was found to be slightly higher with the stronger acid, as opposed to the rate of iron dissolution, which was found to be about the same for the acid concentrations tested. However, the rates of copper and iron dissolution were markedly lower than those values observed when the sulphuric acid leaching of the chalcopyrite concentrate was carried out (Chapter 5). These results are summarised in Table 7.1.

Table 7.1 Summary of acid leaching results at 70 °C

Source	Sulphuric acid solution	Time (days)	Copper dissolution			Iron dissolution		
			Rate (g/l per day)	Percent Extraction	Concentration (g/l)	Rate (g/l per day)	Percent Extraction	Concentration (g/l)
Low-grade copper ore	10N	7	0.023	25.6	0.13	0.090	15.1	0.76
	1N	7	0.014	24.0	0.12	0.092	14.1	0.70
Chalcopyrite concentrate (Chapter 5)	10N	7	0.416	10.6	1.56	0.417	11.5	1.60
	1N	7	0.450	12.4	1.81	0.454	12.3	1.72

7.3 Bioleaching of low-grade copper ore

7.3.1 Materials and Methods

7.3.1.1 Inoculum preparation procedure

A 10 % v/v inoculum of the stock culture (Appendix II) was added to a flask (250 ml) containing 45 ml of ATCC 64 medium at an initial pH of 2.8. The flask was incubated in a rotary shaker at 30 °C and 100 rpm. The cells were harvested after they had reached the late exponential phase (96 hours) and then the culture was filtered through filter

paper (Whatman No. 1) to eliminate iron precipitation and other solid particles. The culture was centrifuged at 8000 rpm for 40 minutes to separate the cells and washed three times with the same medium used for growth (ATCC 64 medium without ferrous ions). The cells were then diluted to a known concentration (about 5.0 x 10^9 cells/ml) with the medium.

7.3.1.2 Experimental procedure

All experiments were carried out in a 250 ml shake flask containing 45 ml of ATCC 64 medium (without ferrous ions) of an initial pH of 2.8. These flasks were then autoclaved at 121 °C for 15 minutes. Prior to all experiments, the low-grade copper ores were sterilised. 2.5 g of the low-grade copper ores (+53, -75 μm) were added to a tube, which was then autoclaved at 121 °C for 15 minutes. A 10 % (v/v) inoculum of bacteria (5.0 x 10^9 cells/ml) and the sterile low-grade copper ores were added to a series of flasks using aseptic techniques. The flasks were then incubated in a rotary shaker at 100 rpm and 30°C. Duplicate samples were taken at regular time intervals (5, 10, 15, 20, 25, 30, 35, 40, 50 and 60 days. After determining the mass of the flasks, the loss of water due to evaporation was compensated by adding sterilised distilled water (ASTM E1357-90). The leaching solution was filtered through filter paper (Whatman No. 1) in order to separate solid and liquid phases and the filtrate was then used to analyse the solution pH, redox potential, free cell concentration, total iron and copper concentration.

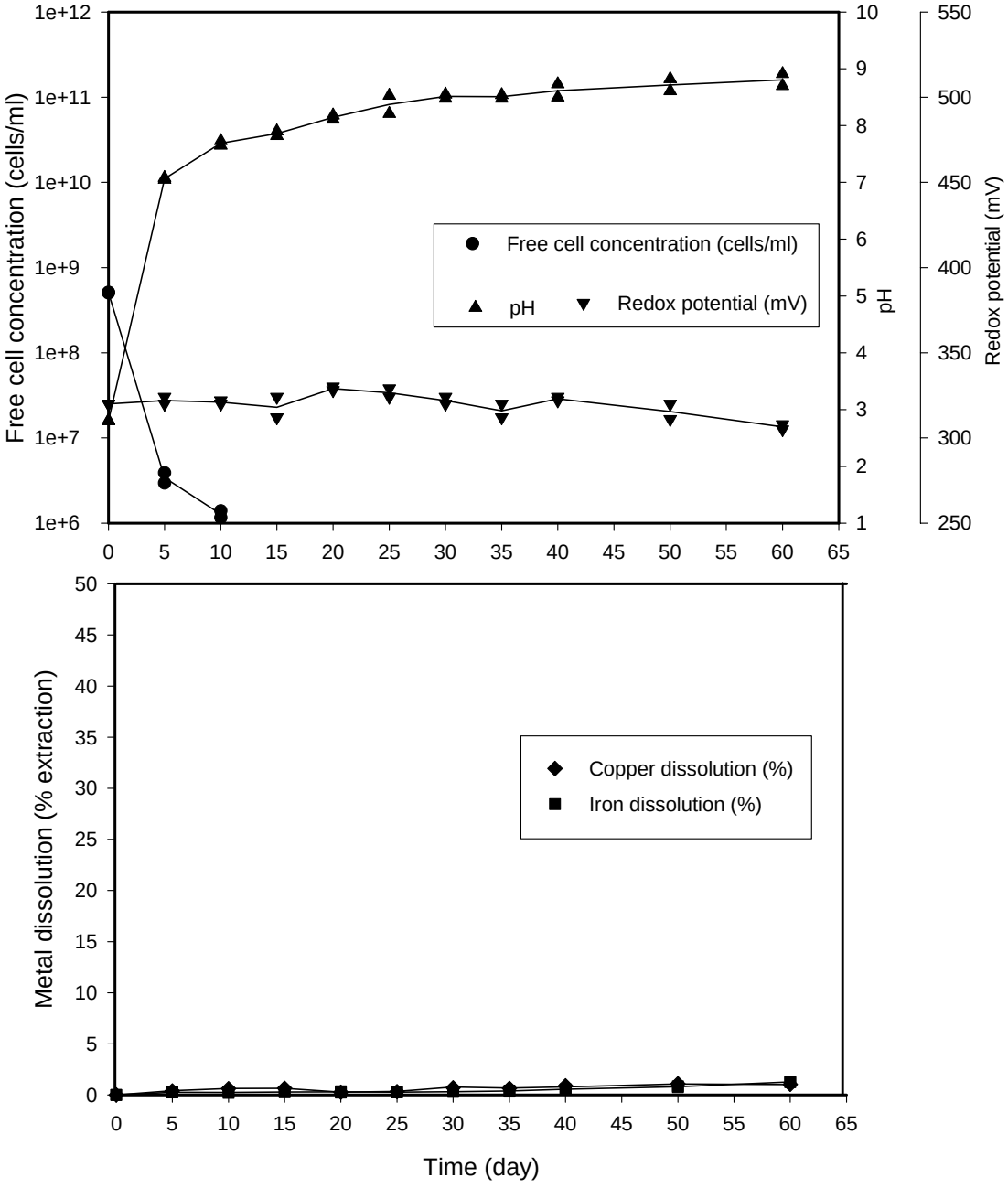

Figure 7.2 Bioleaching of low-grade copper ore at 5% (w/v) pulp density, +53, -75 µm, initial pH 2.8 and 100 rpm

7.3.2 Results and discussion

For bioleaching of low-grade copper ores, no growth curve was observed and overall, there was a drop in free cell concentration from the beginning of the experiment (Figure 7.2). The pH curve showed a notable increase from an initial pH of 2.8 to 7.1 after 5 days followed by a slight increase until the end of the experiment, reaching a maximum value of 8.8 after 60 days. The redox potential values did not significantly alter during the duration of the experiments (320 ±10 mV). The percentages of copper and iron dissolution obtained were very low; copper dissolution appeared to be about 1 % extraction (0.005 g/l) after 60 days, whereas iron dissolution was found to be about 1 % extraction (0.06 g/l) after 60 days. This demonstrates that the copper dissolution did not take place since no bacterial growth was observed under these conditions.

According to the low-grade copper ore (palabora) mineralogy report (Appendix V), this sample was characterised by the presence of minor amounts of Cu-bearing sulphide minerals, which are associated with one or more of magnetite sulphides and transparent gangue minerals. Copper sulphide ores in which the copper is encapsulated by other minerals is not readily extracted hydrometallurgically because of their inaccessibility.

In addition, the sample was dominated by the presence of significant amounts of carbonate minerals (i.e. calcite ($CaCO_3$) and dolomite ($CaMg(CO_3)_2$)). Ehrlich (1995) suggested that “sulphide ores that contain significant amounts of carbonate are also not bioleachable by acidophilic bacteria unless the carbonate is first removed”. This is due to the neutralising action of carbonate, which creates an environment in which the pH is too high for the acidophilic bacteria to grow. All the pH results obtained after 5 days

were found to be higher than 7.0 (Figure 7.2). As mentioned in the literature review section 2.4.5, the optimum pH for the cell growth of acidophilic is in a pH range of 1.5 to 3.0. Therefore, such a high pH therefore resulted in no bacterial growth observed under this condition.

Overall, this test suggested that bioleaching by using *T. ferrooxidans* resulted in an ineffective copper extraction. Thus, the percentage of copper extraction could be improved, possibly either by selecting another bacterial culture that grows at neutral pH values (e.g. *T. thioparus* and *T. dentrificans*) or by eliminating the carbonate minerals from the ores before bioleaching. Ehrlich (1995) stated that removal of carbonate by carbonate-solubilising microorganism is technically feasible, but published reports of commercial exploitation of this technology are lacking in this aspect.

7.4 Conclusion

After a number of trials the low-grade copper ores solubilised by acid leaching were found to give a slow leaching rate and a low metal concentration in the leachate solution. From the initial bioleaching, it was found that *T. ferrooxidans* could not leach copper and iron from the low-grade copper ores due to its chemical composition. In order to achieve copper dissolution from a low-grade copper ore using *T. ferrooxidans*, the carbonate minerals present in the ore should be removed before bioleaching take place.

CHAPTER 8 Conclusion and recommendations for future work

8.1 Conclusion

Bioleaching of the chalcopyrite concentrate is an extraction method which consists of solubilising copper sulphide minerals to copper sulphate. This work has examined the bioleaching of chalcopyrite concentrate by *Thiobacillus ferrooxidans* ATCC 19859 in the absence of added ferrous ions. The initial experiments were carried out in a shake flask in order to investigate the effects of experimental factors such as initial pH, particle size, pulp density and shake flask speed on cell growth, as well as copper and iron dissolution as a function of time.

It was found that an increase in percent extraction of copper dissolution was observed when the free cell concentration increased. The rates of copper dissolution were found to depend on the shaker speed; agitation above 100 rpm was detrimental to bacterial growth, thus affecting negatively the rate of copper dissolution. For the size fractions of +38, -53 μm, +53, -75 μm, +75, -106 μm and +106 -150 μm, the rates and percentages of copper dissolution increased significantly with decreasing particle size due to the fact that finer particle sizes have a larger surface area and greater chalcopyrite ($CuFeS_2$) exposed surface area. The experiments were then carried out at different initial pH values (i.e. 1.5, 2.0, and 2.8), these set of results showed a considerable amount of variation in bacterial growth, redox potential and copper and iron dissolution rates. The experiments that were set at an initial pH value of 2.8 gave the most positive results: the average rate of total copper dissolution was found to be 0.29 g/l per day and the average total copper extraction percentage was 34.5 % after 30 days. In addition,

the rate and percentage of total copper dissolution increased significantly with decreasing pulp density (i.e. 2.5 %, 5 % and 10 % (w/v)). However, the concentration of copper dissolution for all pulp densities reached its maximum at a concentration of 4.8 ± 0.2 g/l, giving a copper recovery of 35 ± 1% from the chalcopyrite concentrate after 30 days leaching time. This indicted that copper dissolution has a limited solubility; this may be because the chalcopyrite particle surface was covered by mineral and bacterial deposits over the period of bioleaching time as described in the SEM analysis of the bioleaching surface.

The characterisation of *T. ferrooxidans* adsorption on the chalcopyrite concentrate surface was examined by investigating the adsorption isotherm of *T. ferrooxidans* and the electrophoretic mobility of chalcopyrite particles before and after bioleaching. Adsorption studies indicate that the quantity of the cells adsorbed on the chalcopyrite surface is significantly higher at shake flask speeds of 100 rpm rather than 200 or 300 rpm. Furthermore, the isoelectric point (IEP) of the chalcopyrite concentrate was shifted to higher pH values after bacterial interaction. A similar shift in the IEP of the cells towards higher pH values was observed after interaction with the mineral particles. These findings were evidence that the changes in surface chemistry resulted from bacterial interactions on the mineral surface.

Based on the above data, a mechanism of copper dissolution was proposed by employing relevant experiments including the chemical leaching of chalcopyrite by sulphuric acid and ferric sulphate, bioleaching of chalcopyrite in the presence of added ferrous ions, and observation of cell attachment by scanning electron microscopy.

Chalcopyrite concentrate is soluble in a sulphuric acid solution at a pH of 1.5, however improved leaching was obtained with 1 N and 10 N added sulphuric acid solution. Overall, acid leaching is less effective than bioleaching in terms of copper extraction. The copper dissolution by ferric ions takes place in an environment in which the pH is low and it is activated by a moderate high temperature. Furthermore, ferric ions have a slight positive influence on copper extraction, as it was observed when 10g/l ferric sulphate was added for both the bioleaching of the chalcopyrite concentrate and the control experiment. The results obtained from the above experiments suggested that, overall, the chalcopyrite concentrate can be oxidised according to the following bacterial and chemical oxidation mechanism:

Bacterial oxidation mechanism

$$4CuFeS_2 + 17O_2 + 2H_2SO_4 \xrightarrow{T.\,ferrooxidans} 4CuSO_4 + 2Fe_2(SO_4)_3 + 2H_2O$$

Chemical oxidation mechanism

$$CuFeS_2 + 2H_2SO_4 \longrightarrow CuSO_4 + FeSO_4 + 2H_2S\,(aq)$$

$$CuFeS_2 + 2Fe^{3+} + 4H^+ \longrightarrow Cu^{2+} + 3Fe^{2+} + 2H_2S_n$$

Following the above, the work then focused on the bioleaching in a stirred tank bioreactor for the purpose of investigating the effects of agitation speeds when employing the following experimental conditions: i) a 4L (157mm diameter) vessel reactor with 4 vertical baffles; ii) 0.5 VVM air flow rate; iii) chalcopyrite concentrate ore (+53, -75 μm) at 5 % w/v; and iv) initial free cell concentration of about $5.0 \times 10^8 \pm$ 10 % cells/ml.

An agitation speed of 50 rpm had no significant influence on increasing copper dissolution. This was due to the poor mixing conditions since solids deposition was observed after incubation for a few days, and thus the solids aggregate imposed an additional difficultly in obtaining a homogeneous slurry. A significant decrease in copper dissolution was also observed at 200 rpm, compared to stirring at 150 rpm. At 25 days, the percentage of copper dissolution decreased from 34.4 % to 2.5 % when stirring at 150 and 200 rpm respectively. It was thought increased fluid stresses and particle friction or abrasion at the higher speed may have reduced cell attachment to the mineral surface. Overall, the bioleaching experiment at 150 rpm represents the most suitable conditions for bacterial growth and the percent extraction of copper dissolution amongst those considered (50, 100, 150 and 200 rpm), proving that agitation speed plays an important factor for bacterial growth, which in turn enhances copper dissolution.

Ultimately this work tried to apply the bioleaching techniques to extract copper from low-grade ore. However, initial bioleaching proved that *T. ferrooxidans* could not leach copper and iron from the low-grade copper ores due to the fact that the sample is dominated by the presence of significant amounts of carbonate minerals causing an environment in which the pH is too high for the acidophilic bacteria to grow.

8.2 Recommendations for future work

There is a great deal of future work that could expand upon the findings of this project, with particular attention to the increase in percentage of copper extraction. As

mentioned earlier, metal precipitation (mainly iron precipitates) was the major cause of the undesired termination of the bioleaching process by *T. ferrooxidans*, after the copper concentration reached its maximum (about 5 g/l copper). The percentage of copper in residues was found to be more than 60 %, thus retaining a high copper content. It is possible for these residues to be used for the subsequent bioleaching.

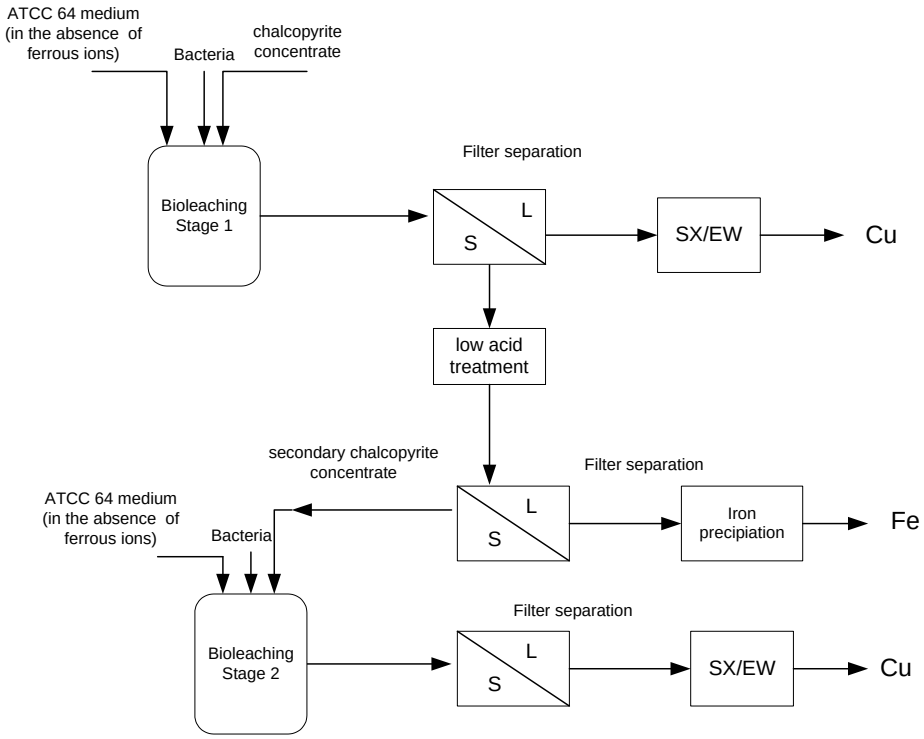

Figure 8.1 Representative flowsheet of a proposed bioleaching process for chalcopyrite concentrate

Figure 8.1 shows a representative flowsheet of a proposed bioleaching process for the chalcopyrite concentrate employing multi-stage batch stirred tank bioreactors. The chalcopyrite concentrate goes through the first stage of bioleaching, which consists of a medium (ATCC 64 medium in the absence of ferrous ions) and *T. ferrooxidans*.

After solid-liquid separation, the liquid is fed to the solvent extraction and electro-winning (SX / EW) units to deliver a high-grade copper cathode, where the solid residue is treated with a low acid solution in order to remove the mineral deposits. At the end of the acid treatment and solid-liquid separation, the liquid is then passed to the iron precipitation unit, while the solid leach residue is then used in the second stage of bioleaching in order to solubilise more copper from the secondary chalcopyrite concentrate. The aim of this proposed bioleaching process is to re-treat chalcopyrite concentrate until it has achieved an almost complete copper extraction (more than 90%). Since there is a decrease in exploitable ore reserves, a complete extraction is desired. However there should be a compromise between the number of bioleaching stages and the cost of extraction process.

In addition, in this work only *T. ferrooxidans* have been studied, therefore any future work should try to study thermophiles (such as *Sulfolobus acidocaldarius* and *Acidianus brierleyi*) in order to compare the effectiveness of copper extraction from chalcopyrite concentrate to this work. According to previously published literature, a comparative study of different types of microorganisms is sometimes conflicting. For example, Konishi *et al*. (2001) have shown that extreme thermophiles (*Acidianus brierleyi*) at 65 °C can significantly increase the rate of bioleaching in the case of chalcopyrite in comparison to *T. ferrooxidans*. On the other hand, Yahya and Johnson (2002) reported that the rate of pyrite concentrate oxidation obtained from *T. ferrooxidans* was faster than that of *Sulfobacillus* sp. Therefore, a comparative study could be done by completing a bioleaching test programme with a thermophile.

Finally, the copper extraction of bioleaching from low-grade copper ores did not succeed. However, this does not solely depend on the growth of *T. ferrooxidans*, but also the nature of the mineral ores. If a mineral ore contains some elements (e.g. carbonates, silica) that interfere with bioleaching process, those elements should be removed prior to bioleaching. Therefore, future work should try to remove carbonates, possibly by using carbonate-solubilising microorganisms (Ehrlich, 1995). The use of carbonate-solubilising microorganisms in removing carbonates from low-grade copper ores is a practicable technique, known as biobeneficiation. After removing the carbonates, the low-grade copper ores could allow for an increase in *T. ferrooxidans* growth.

Reference

Acevedo, F. (2000) 'The use of reactors in biomining processes', *Electronic Journal of Biotechnology*, 3 (3), 1-12.

Agatzini, S. and Tzeferis, P. (1997) 'Bioleaching of nickel-cobalt oxide ores', *The AusIMM Proceedings*, 1, 9-15.

Ahonen, L. and Tuovinen, O.H. (1991) 'Temperature effects on bacterial leaching of sulfide minerals in shake flask experiments', *Applied and Environmental Microbiology*, 57 (1), 138-145.

Ahonen, L. and Tuovinen, O.H. (1995) 'Bacterial leaching of complex sulfide ore samples in bench-scale column reactors', *Hydrometallurgy*, 37, 1-21.

Anthony, M., Flett, D.S., and Hanson, A. (2002) *Future changes for metals recovery-outlook through 2010* [Online]. Available from http://www.sbcs.freeuk.com/ sulphurpaper.pdf [Accessed 27 July 2002].

Asai, S., Konishi, Y., and Yoshida, K. (1992) 'Kinetic model of batch bacterial dissolution of pyrite particles by *Thiobacillus ferroxidans*', *Chemical Engineering Science*, 47 (1), 133-139.

Bállester, A., González, F., Blázquez, M.L., and Mier, J.L. (1990) 'The influence of various ions in the bioleaching of metal sulphides', *Hydrometallurgy*, 23, 221-235.

Barrett, J., Hughes, M.N., Karavaiko, G.I., and Spencer, P.A. (1993) *Metal extraction by bacteria oxidation of minerals*. New York: Ellis Horwood.

Battaglia, F., Hugues, P., Cabral, T., Cezac, P., Garcia, J.L., and Morin, D. (1998) 'The mutual effect of mixed *Thiobacilli* and *Leptospirilli* populations on pyrite bioleaching', *Minerals Engineering*, 11, 195-205.

Battaglia, F., Morin, D., and Ollivier, P. (1994) 'Dissolution of cobaltiferous pyrite by *Thiobacillus ferrooxidans* and *Thiobacillus thiooxidans*: factors influencing bacterial leaching efficiency', *Journal of Biotechnology*, 32, 11-16.

Beolchini, F., Nardini, A., and Veglió, F. (2000) 'Development of a direct count method by factorial experiments and application in sorption of *Thiobacilli* on pyrrhotite ore particles', *Resource an Environmental Biotechnology*, 3, 23-38.

Bhattacharya, P., Sarkar, P., and Mukherjea, R. N. (1990) 'Reaction kinetics model for chalcopyrite bioleaching using *Thiobacillus ferrooxidans*', *Enzyme Microbiology Technology*, 12, 873-875.

BHP Copper (1996) *How do they: make copper* [Online]. Available from http:// www.innovations.copper.org/how/howdo3.htm [Accessed 9 July 2001].

Biegler, T. and Horne, M.D. (1985) 'The electrochemistry of chalcopyrite', *Journal of Electrochemical Society*, 132, 1363-1369.

Billiton (2001) *Creating Value through innovation biotechnology in mining* [Online]. Available from http://www.imm.org.uk/gilbersonpaper.htm [Accessed 3 September 2001].

Biswas, A.K. and Davenport, W.G. (1994) *Extractive metallurgy of copper*, 3 rd ed. Oxford: Pergamon.

Blancarte-Zurita, M.A., Branion, R.M.R., and Lawrence, R.W. (1986) 'Particle size effects in the microbiological leaching of sulfide concentrates by *Thiobacillus ferrooxidans*', *Biotechnology and Bioengineering*, 28, 751-755.

Blight, K., Ralph, D.E., and Thurgate, S. (2000) 'Pyrite surfaces after bio-leaching: a mechanism for bio-oxidation', *Hydrometallurgy*, 58, 227-237.

Boon, M. and Heijnen, J.J. (1998) 'Chemical oxidation kinetics of pyrite in bioleaching processes', *Hydrometallurgy*, 48, 27-41.

Boon, M., Meeder, T.A., Thöne, C., and Ras, C. (1999) 'The ferrous iron oxidation kinetics of *Thiobacillus ferrooxidans* in continuous cultures', *Applied Microbiology and Biotechnology*, 51, 820-826.

Bosecker, K. (1997) 'Bioleaching: metal solubilisation by microorganisms', *FEMS Microbiology Reviews*, 20, 591-604.

Boswell, C.D., Nienow, A.W., and Hewitt, C.J. (2002) 'Studies on the effect of mechanical agitation on the performance of brewing fermentation: fermentation rate, yeast physiology, and development of flavor compounds', *American Society of Brewing Chemists*, 60 (3), 101-106.

Braddock, J.F., Luong, H.V., and Brown, E.J. (1984) 'Growth kinetics of *Thiobacillus ferroxidans* isolated from arsenic mine drainage', *Applied and Environmental Microbiology*, 48 (1), 48-55.

Brandl, H. (2001) 'Microbial leaching of metals', in Rehm, H.J. (ed.) *Biotechnology volume 10*, New York: Wiley.

Breed, A.W., Harrison, S.T.L., and Hansford, G.S. (1997) 'Technical note a preliminary investigation of the ferric leaching of a pyrite/arsenopyrite flotation concentrate', *Minerals Engineering*, 10 (9), 1023-1030.

Brickett, L.A., Hammack, R.W., and Edenborn, H.M. (1995) 'Comparison of methods used to inhibit bacterial activity in sulfide ore bioleaching studies', *Hydrometallurgy*, 39, 293-305.

Brierley, J.A. and Brierley, C.L. (2001) 'Present and future commercial applications of biohydrometallurgy', *Hydrometallurgy*, 59, 233-239.

Brock, T.D. (1978) *Thermophilic microorganisms and life at high temperatures*. New York: Springer-Verlag.

Brock, T.D. and Gustafson, J. (1976) 'Ferric iron reduction by sulfur-and iron-oxidizing bacteria', *Applied and Environmental Microbiology*, 32, 567-571.

Brucato, A. and Brucato, V. (1998) 'Unsuspended mass of solid particles in stirred tanks', *The Cannadian Journal of Chemical Engineering*, 76, 420-427.

Büchs, J (2001) 'Introduction to advantages and problems of shaken cultures', *Biochemical Engineering Journal*, 7, 91-98.

Büchs, J., Maier, U., Milbradt, C., and Zoels, B. (2000) 'Power consumption in shaking flasks on rotary shaking machines: I Power consumption measurement in unbaffled flasks at low liquid viscosity', *Biotechnology and Bioengineering*, 68 (6), 589-593.

Büchs, J., Maier, U., Milbradt, C., and Zoels, B. (2000) 'Power consumption in shaking flasks on rotary shaking machines: II nondimensional description of specific power consumption and flow regimes in unbaffled flasks at elevated liquid viscosity', *Biotechnology and Bioengineering*, 68 (6), 594-601.

Cardone, P., Ercole, C., Breccia, S., and Lepidi, A. (1999) 'Fractal analysis to discriminate between biotic and abiotic attacks on chalcopyrite and pyrolusite', *Journal of Microbiological Methods*, 36, 11-19.

Carranza, F. and Iglesias, N. (1998) 'Technical note application of IBES process to a Zn sulphide concentrate: effect of Cu^{2+} ion', *Minerals Engineering*, 11, (4), 385-390.

Carranza, F., Palencia, I., and Romero, R. (1997) 'Silver catalyzed IBES process: application to a Spanish copper-zinc sulphide concentrate', *Hydrometallurgy*, 44, 29-42.

Castro, I.M., Fietto, J.L.R., Vieira, R.X., Trópia, M.J.M., Campos, L.M.M., Paniago, E.B., and Brandão, R.L. (2000) 'Bioleaching of zinc and nickel from silicates using *Asperillus niger* cultures', *Hydrometallurgy*, 57, 39-49.

Chan, G. (2001) *Isolate (33)* [Online]. Available from http://epsc.wustl.edu/~chan/download/Iceland.pdf [Accessed 17 July 2002].

Chong, N., Karamanev, D.G., and Margaritis, A. (2002) 'Effect of particle-particle shearing on the bioleaching of sulfide minerals', *Biotechnology and Bioengineering*, 80, 349-357.

Clark, D.A. and Norris, P.R. (1996) 'Oxidation of mineral sulphides by thermophilic microorganisms', *Minerals Engineering*, 9, 1119-1125.

Copper Organisation (2001 a) *Copper in the USA: bright future-glorious past* [Online]. Available from http://www.copper.org/general/g_fact.htm [Accessed 9 July 2001].

Copper Organisation (2001 b) *Copper production from ore to finished products* [Online]. Available from http://www.copper.org/general/g_prod.htm [Accessed 9 July 2001].

Cote, R.M.A. (1984) American Type Culture Collection Media Handbook, New Tork, Marcel Dekker

Curutchet, G., and Donati, E (2000) 'Iron-oxidizing and leaching activities of sulphur-grown *Thiobacillus ferrooxidans* cells on other substrates: effect of culture pH', *Journal of Bioscience and Bioengineering*, 90, 57-60.

Das, A., Modak, J.M., and Natarajan, K.A. (1997) 'Technical note studies on multi-metal ion tolerance of *Thiobacillus ferroxidans*', Minerals Engineering, 10 (7), 743-749.

Dastidar, M.G., Malik, A., and Roychoudhury, P.K. (2000) 'Biodesulphurization of Indian (Assam) coal using *Thiobacillus ferrooxidans* (ATCC 13984)', *Energy Conversion and Management*, 41, 375-388.

Dawson, R.M.C., Elliott, D.C., Elliott, W.H., and Jones, K.M. (1969) *Data for biochemical research*, 2 rd ed. Clarendon Press.

Deng, T.L., Liao, M.X., Wang, M.H., Chen, Y.W., and Belzile, N. (2000) 'Investigations of accelerating parameters for the biooxidation of low-grade refractory gold ores', *Minerals Engineering*, 13 (14), 1543-1553.

Derksen, J.J., Buist, K., Van Weert, G., and Reuter, M.A. (2000) 'Oxygen transfer in agitated silica and pyrite slurries', *Minerals Engineering*, 13 (1), 25-36.

Devasia, P., Natarajan, K.A., and Rao, G.R. (1996) 'Role of bacterial growth conditions and adhesion in the bioleaching of chalcopyrite by *Thiobacillus ferrooxidans*', *Minerals and Metallurgical Processing*, 13 (2), 82-86.

Devasia, P., Natarajan, K.A., Sathyanarayana, D.N., and Ramananda Rao, G. (1993) 'Surface chemistry of *Thiobacillus ferroxidans* relevant to adhesion on mineral surfaces', *Applied and Environmental Microbiology*, 59 (12), 4051-4055.

Donati, E., Pogliani, C., and Boiardi, J.L. (1997) 'Anaerobic leaching of covellite by *Thiobacillus ferrooxidans*', *Applied Microbiology and Biotechnology*, 47, 636-639.

Dopson, M., and Lindstrom, E.B. (1999) 'Potential role of *Thiobacillus caldus* in arsenopyrite bioleaching', *Applied and Environmental Microbiology*, 65, 36-40.

Doran, P.M. (1998) *Bioprocess engineering principles*. London: Academic Press.

Dresher, W.H. (2001) *How hydrometallurgy and the SX/EW process made copper the green metal* [Online]. Available from http://www.innovations.copper.org /2001/08/hydrometallurgy.html [Accessed 28 July 2002].

Duarte, J.C., Estrada, P.C., Pereira, P.C., and Beaumont, H.P. (1993) ' Thermophilic vs. mesophilic bioleaching process performance', FEMS Microbiology Reviews, 11, 97-102.

Edwards, K.J., Hu, B., Hamers, R.J., and Banfield, J.F. (2001) 'A new look at microbial leaching patterns on sulfide minerals', *FEMS Microbiology Ecology*, 34, 197-206.

Ehrlich, H.L. (1990) *Geomicrobiology*, 2 nd ed. New York: Marcel Dekker.

Ehrlich, H.L. (1995) *Microbial leaching of ores*, in Brooks, R.R., Dunn, C.E., Hall, G.E.M. (eds) *Biological systems in mineral exploration and processing*. Hertfordshire: Ellis Horwood.

Ehrlich, H.L. (2001) 'Past, present and future of biohydrometallurgy', *Hydrometallurgy*, 59, 127-134.

Eichrom (2002) *Iron control process for copper electrolyte* [Online]. Available from http://www.eichrom.com/process/apps/ironcontrol.html [Accessed 25 July 2002].

Elzeky, M. and Attia, Y.A. (1995) 'Effect of bacterial adaptation on kinetics and mechanisms of bioleaching ferrous sulfides', *The Chemical Engineering Journal*, 56, B115-B124.

Escobar, B., Jedlicki, E., Wiertz, J., and Vargas, T. (1996) 'A method for evaluating the proportion of free and attached bacteria in the bioleaching of chalcopyrite with *Thiobacillus ferrooxidans*', *Hydrometallurgy*, 40, 1-10.

Espejo, R.T. and Ruiz, P. (1987) 'Growth of free and attached *Thiobacillus ferrooxidans* in ore suspension', *Biotechnology and Bioengineering*, 30, 586-592.

Fernandez, M.G.M., Mustin, C., Donato, P., Barres, O., Marion, P., and Berthelin, J. (1995) 'Occurrences at mineral-bacteria interface during oxidation of arsenopyrite by *Thiobacillus ferrooxidans*', *Biotechnology and Bioengineering*, 46, 13-21.

Fowler, T.A. and Crundwell, F.K. (1998) 'Leaching of zinc sulfide by *Thiobacillus ferrooxidans*: experiments with a controlled redox potential indicate no direct bacterial mechanism', *Applied and Environmental Microbiology*, 64, 3570-3575.

Fowler, T.A., Holmes, P.R., and Crundwell, F.K. (1999) 'Mechanism of pyrite dissolution in the presence of *Thiobacillus ferrooxidans*', *Applied and Environmental Microbiology*, 65 (7), 2987-2993.

Fowler, T.A., Holmes, P.R., and Crundwell, F.K. (2001) 'On the kinetics and mechanism of the dissolution of pyrite in the presence of *Thiobacillus ferrooxidans*', *Hydrometallurgy*, 59, 257-270.

Gericke, M., Pinches, A., and Van Rooyen, J.V. (2001) 'Bioleaching of a chalcopyrite concentrate using an extremely thermophilic culture', *International Journal of Mineral Processing*, 62, 243-255.

Giaveno, A. and Donati, E. (2001) 'Bioleaching of heazelwoodite by *Thiobacllus* sp.', *Process Biochemistry*, 36, 955-962.

Golterman, H.L., Clymo, R.S., and Ohnstad, M.A.M. (1978) *Methods for physical and chemical analysis of fresh waters*, 2 nd ed. Oxford: Blackwell Scientific Publications.

Gómez, C., Blázquez, M.L., and Ballester, A. (1999 a) 'Bioleaching of a Spanish complex sulphide ore bulk concentrate', *Minerals Engineering*, 12 (1), 93-106.

Gómez, C., Figueroa, M., Muñoz, J., Blázquez, M.L., and Ballester, A. (1996 b) 'Electrochemistry of chalcopyrite', *Hydrometallurgy*, 43, 331-344.

Gómez, C., Limpo, J.L., De Luis, A., Blázquez, M.L., González, F., and Ballester, A. (1997 a) 'Hydrometallurgy of bulk concentrates of spanish complex sulphides: chemical and bacterial leaching', *Canadian Metallurgical Quarterly*, 36 (1), 15-23.

Gómez, C., Roman, E., Blázquez, M.L., and Ballester, A. (1997 b) 'SEM and EDS of chalcopyrite bioleaching in the presence of catalytic ions', *Minerals Engineering*, 10, 825-835.

Gómez, E., Ballester, A., Blázquez, M.L., and González, F. (1999 c) 'Silver-catalysed bioleaching of a chalcopyrite concentrate with mixed cultures of moderately thermophilic microorganisms', *Hydrometallurgy*, 51, 37-46.

Gómez, E., Ballester, A., González, F.,and Blázquez, M.L. (1999 b) 'Leaching capacity of a new extremely thermophilic microorganism, *Sulfolobus rivotincti*', *Hydrometallurgy*, 52, 349-366.

Gómez, E., Blázquez, M.L., Ballester, A., and González, F. (1996 a) 'Study by SEM and EDS of chalcopyrite bioleaching using a new thermophilic bacteria', *Minerals Engineering*, 9, 985-999.

Gómez, J.M. and Cantero, D. (1998) 'Modelling of ferrous sulphate oxidation by *Thiobacillus ferroxidans* in discontinous culture: influence of temperature, pH and agitation rate', *Journal of Fermentation and Bioengineering*, 86 (1), 79-83.

Greenburg, A.E., Clesceri, L.S., and Eaton, A.D. (1992) *Standard methods for the examination of water and wastewater*, 18 th ed. Washington: American Public Health Association.

Grotefend, B. (2001) *ANL spinoff continues growth* [Online]. Available from http://www.itd.anl.gov/highlights/8-1/eichrom.html [Accessed 9 July 2001].

Gulley, V. (1999) *Metallosphaera prunae* [Online]. Available from http://web.umr.edu/~microbio/bio221_1999/m_pruae.html [Accessed 17 July 2002].

Haddadin, J., Dagot, C., and Fick M. (1995) 'Models of bacterial leaching', *Enzyme and Microbial Technology*, 17 (4), 290-305.

Halfmeier, H., Schäfer-Treffenfeldt, W., and Reuss, M. (1993) 'Potential of *Thiobacillus ferrooxidans* for waste gas purification: part1 kinetics of continuous ferrous iron oxidation', *Applied Microbiology and Biotechnology*, 40, 416-420.

Hallick, R.B. (2001) *Biosynthesis of carbohydrates* [Online]. Available from http://www.blc.arizona.edu/courses/181gh/rick/photosynthesis/Calvin.html [Accessed 17 July 2002].

Han, C.J. and Kelly, R.M. (1998) 'Biooxidation capacity of the extremely thermoacidophlic archaeon *Metallosphaera sedula* under bioenergetic challenge', *Biotechnology and Bioengineering*, 58 (6), 617-624.

Hansford, G.S. and Vargas, T. (2001) 'Chemical and electrochemical basis of bioleaching processes', *Hydrometallurgy*, 59, 135-145.

Havlík, T. and Kammel, R. (1995) 'Leaching of chalcopyrite with acidified ferric chloride and carbon tetrachloride addition', *Minerals Engineering*, 8, 1125-1134.

Hewitt, C.J., Boon, L.A., McFarlane, C.M., and Nienow, A.W. (1998) 'The use of flow cytometry to study the impact of fluid mechnical stress on Escherichia coli W3110 during continous cultivation in an agitation bioreactor', *Biotechnology and Bioengineering*, 59, 612-620.

Hiroyoshi, N., Hirota, M., Hirajima, T., and Tsunekawa, M. (1997) 'A case of ferrous sulfate addition enhancing chalcopyrite leaching', *Hydrometallurgy*, 47, 37-45.

Hiroyoshi, N., Hirota, M., Hirajima, T., and Tsunekawa, M. (1999) , 'Inhibitory effect of iron-oxidizing bacteria on ferrous-promoted chalcopyrite leaching', *Biotechnology and Bioengineering*, 64 (4), 478-483.

Hiroyoshi, N., Miki, H., Hirajima, T., and Tsunekawa, M. (2001) 'Enhancement of chalcopyrite leaching by ferrous ions in acidic ferric sulfate solutions', *Hydrometallurgy*, 60, 185-197.

Holmes, D.S. and Debus, K.A. (1991) *Opportunities for biological metal recovery* in Smith, R.W., and Misra, M. (eds) *Mineral bioprocessing*. California: The minerals, Metals&Materials Society.

Hugues, P., Cezac, P., Cabral,T., Battaglia, F., Truong-Meyer, X.M., and Morin, D. (1997) 'Bioleaching of a cobaltiferous pyrite: a continuous laboratory-scale study at high solids concentration', *Minerals Engineering*, 10 (5), 507-527.

Iglesias, N. and Carranza, F. (1995) 'Bacterial leaching of a copper ore rich in gold and silver: study of the chemical stage', *Minerals Engineering*, 8 (10), 1089-1096.

Johnson, D.B. (2001) 'Importance of microbial ecology in the development of new mineral technologies', *Hydrometallurgy*, 59, 147-157.

Jones, C.A. and Kelly, D.P. (1983) 'Growth of *Thiobacillus ferrooxidans* on ferrous iron in chemostat culture: influence of product and substrate inhibition', *Journals of Chemical Technology and Biotechnology*, 33 B, 241-261.

Jordan, M.A., McGinness, S., and Phillips, C.V. (1996) 'Acidophilic bacteria-their potential mining and environmental applications', *Minerals Engineering*, 9, 169-181

Ju, L.K. and Kankipati, P. (1998) 'Toxicity of dibenzothiophene to thermophile *Sulfolobus acidocaldarius* grown in sucrose medium', *Journal of Biotechnology*, 63, 219-227.

Konishi, Y., Asai, S., and Tokushige, M. (1999) 'Kinetics of the bioleaching of chalcopyrite concentrate by acidophilic thermophile *Acidianus brierleyi*', *Biotechnology Progress*, 15, 681-688.

Konishi, Y., Kogasaki, K., and Asai, S. (1997) 'Bioleaching of pyrite by *Acidianus brierleyi* in a continuous-flow stirred-tank reactor', *Chemical Engineering Science*, 52, 4525-4532.

Konishi, Y., Kubo, H., and Asai, S. (1992) 'Bioleaching of zinc sulfide concentrate by *Thiobacillus ferroxidans*', *Biotechnology and Bioengineering*, 39, 66-74.

Konishi, Y., Takasaka, Y., and Asai, S. (1994) 'Kinetics of growth and elemental sulfur oxidation in batch culture of *Thiobacillus ferroxidans*', *Biotechnology and Bioengineering*, 44 (6), 667-673.

Konishi, Y., Tokushiko, M., Asai, S., and Susuki, T. (2001) 'Copper reovery from chalcopyrite concentrate by acidophilic thermophile *Acidianus brierleyi* in batch and continous-flow stirred tank reactor', *Hydrometallurgy*, 59, 271-282.

Konishi, Y., Yoshida, S., and Asai, S. (1998) 'Effect of yeast extract supplementation in leach solution on bioleaching rate of pyrite by acidophilic thermophile *Acidianus brierleyi*', *Biotechnology and Bioengineering*, 58 (6), 663-667.

Langhans, D., Lord, A., Lampshire, D., Burbank, A., and Baglin, E. (1995) 'Biooxidation of an arsenic-bearing refractory gold ore', *Minerals Engineering*, 8, 147-158.

Loan, M., Parkinson, G., Newman, M., and Farrow, J. (2002) 'Iron oxy-hydroxide crystallization in a hydrometallurgical residue', *Journal of Crystal Growth*, 235, 482-488.

Lorenzo, P., Gómez, E., Isabel de Silóniz, M., Ballester, A., and Perera, J. (1997) 'Chalcopyrite bioleaching and thermotolerance of three acidophilic, ferrous-oxidising bacterial isolates', *Biotechnology Letters*, 19, 1197-1200.

Malik, A., Dastidar, M.G., and Roychoudhury, P.K. (2001) 'Biodesulphurization of coal: effect of pulse feeding and leachate recycle', *Enzyme and Microbial Technology*, 28, 49-56.

Marczenko, Z. (1976) *Spectrophotometric determination of elements*. Sussex: Ellis Horwood.

McDaniel, L.E. and Bailey, E.G. (1969) 'Effect of shaking speed and type of closure on shake flask cultures', *Applied Microbiology*, 17, 286-290.

Mier, J.L., Ballester, A., Blázquez, M.L., González, F., and Muñoz, J.A. (1995) 'Influence of metallic ions in the bioleaching of chalcopyrite by Sulfolobus BC: experiments using pneumatically stirred reactors and massive samples', *Minerals Engineering*, 8, 949-965.

Miller, P.C., Rhodes, M.K., Winby, R., Pinches, A., and Staden, P.J. (1999) 'Commercialization of bioleaching for base-metal extraction', *Minerals and Metallurgical Processing*, 16 (4), 42-50.

Modak, J.M., Natarajan, K.A., and Mukhopadhyay, S. (1996) 'Development of temperature-tolerant strains of *Thiobacillus ferrooxidans* to improve bioleaching kinetics', *Hydrometallurgy*, 42, 51-61.

Monroy, M.G., Dziurla, M.A., Lam, B.T., Berthelin, J., and Marion, P. (1994) 'A laboratory study on the behavior of *Thiobacillus ferrooxidans* during pyrite bioleaching in percolation columns', *Advances in Bioprocess Engineering*, 509-517.

Moody, R. (2001) *The problems with copper* [Online]. Available from http://www.miningwatch.ca/documents/burmaAppendices.pdf [Accessed 3 October 2001].

Nagpal, S., Dahlstrom, D., and Oolman, T. (1993) 'Effect of carbon dioxide concentration on the bioleaching of a pyrite-arsenopyrite', *Biotechnology and Bioengineering*, 41, 459-464.

Nakazawa, H., Fujisawa, H., and Sato, H. (1998) 'Effect of activated carbon on the bioleaching of chalcopyrite concentrate', *International Journal of Mineral Processing*, 55, 87-94.

Namita, D., Natarajan, K.A., and Somasundaran, P. (2001) 'Mechanisms of adhesion of *Paenibacillus polymyxa* onto hematite, corundum and quartz', *International Journal of Mineral Processing*, 62, 27-39.

Nemati, M. (1996) *An evaluation of ferrous sulphate oxidation using immobilized Thiobacillus ferrooxidans*, Unpublished thesis, UMIST

Nemati, M. and Harrison, S.T.L. (2000) 'Effect of solid loading on thermophilic bioleaching of sulphide minerals', *Journals of Chemical Technology and Biotechnology*, 75, 526-532.

Nemati, M. and Webb C. (1997) 'A kinetic model for biological oxidation of ferrous iron by *Thiobacillus ferrooxidans*', *Biotechnology and Bioengineering*, 53 (5), 478-486.

Nemati, M., Harrison, S.T.L., Hansford, G.S., and Webb, C. (1998) 'Biological oxidation of ferrous sulphate by *Thiobacillus ferrooxidans*: a review on the kinetic aspects', *Biochemical Enginerring Journal*, 1, 171-190.

Nemati, M., Lowenadler, J., and Harrison, S.T.L. (2000) 'Particle size effects in bioleaching of pyrite by acidophilic thermophile *Sulfolobus metallicus* (BC)', *Applied Microbiology and Biotechnology*, 53, 173-179.

Nicolau, P.B. and Johnson D.B. (1999) 'Leaching of pyrite by acidophilic heterotrophic iron-oxidizing bacteria in pure and mixed cultures', *Applied and Environmental Microbiology*, 65 (2), 585-590.

Norris, P.R. (1990) *Acidophilic Bacteria and their activity in mineral sulfide oxidation*, in Ehrlich, H. L. and Brierley, C. L. (eds.) *Microbial Mineral Recovery*. New York: Mc Graw-Hill.

NRCan Biotechnology (2002) *Biotechnology Applications in the Mining Industry* [Online]. Available from http://www.nrcan.gc.ca/cfs/bio/fact2.shtml [Accessed 3 April 2002].

Orr, R. (2000) *$CDN 2.0 million financing secured* [Online]. Available from http://www.unscrambled.com/bactech/pressarticle.cfm?ID=8 [Accessed 28 June 2002].

Pagella, C., Perego, P., and Zilli, M. (1996) 'Biotechnological H_2S gas treatment with *Thiobacillus ferrooxidans*', *Chem.Eng.Technol*, 19, 79-88.

Paponetti, B.A., Veglió, F., and Toro, L. (1991) *Biotechnology of a chalcopyrite concentrate by Thiobacillus ferrooxidans*, in Smith, R.W., Misra, M. (eds) *Mineral bioprocessing*. California: The Minerals, Metals&Materials Society.

Pinches, T. (2001) 'Peñoles bioleach process and Mintek/Noranda in heap bioleaching agreement', *Mintek Bulletin*, 131, 1-2.

Pogliani, C. and Donati, E. (2000) 'Immobilisation of *Thiobacillus ferrooxidans*: importance of jarosite precipitation', *Process Biochemistry*, 35, 997-1004.

Porro, S., Ramírez, S., Reche, C., Curutchet, G., Alonso-Romanowski, S., and Donati, E. (1997) Bacterial attachment: its role in bioleaching processes, *Process Biochemistry*, 32 (7), 573-578.

Preece, J.M. (1999) *The influence of aggregation conditions on aggregate size, fractal dimension and susceptibility to disruption in capillary flow*, Thesis, The University of Birmingham.

Rawlings, D.E. (1997) *Biomining: theory, microbes and industrial processes*. Texas: Springer.

Rawlings, D.E., Tributsch, H., and Hansford, G.S. (1999) 'Reason why '*Leptospirillum*'-like species rather than *Thiobacillus ferrooxidans* are the dominant iron-oxidising bacteria in many commercial processes for the biooxidation of pyrite and related ores', *Microbiology*, 145, 5-13.

Rezza, I., Salinas, E., Elorza, M., Sanz de Tosetti, M., and Donati, E. (2001) 'Mechanisms involved in bioleaching of an aluminosilicate by heterotrophic microorganisms', *Process Biochemistry*, 36, 495-500.

Rojas-Chapana, J.A, Bärtels, C.C., Pohlmann, L., and Tributsch, H. (1998) 'Co-operative and chemotaxis of thiobacilli studied with spherical sulphur/sulphide substrates', *Process Biochemistry*, 33, 239-248.

Rojas-Chapana, J.A. and Tributsch, H. (2000) 'Bio-leaching of pyrite accelerated by cysteine', *Process Biochemistry*, 35, 815-824.

Romano, P., Blázquez, M.L., Alguacil, F.J., Muñoz, J.A., Ballester, A., and González, F. (2001) 'Comparative study on the selective chalcopyrite bioleaching of a molybdenite concentrate with mesophilic and thermophilic bacteria', *FEMS Microbiology Letters*, 196, 71-75.

Ryan, B. (2002) *Titan reports big improvement in BioHeap TM trials, in Biotechnology: Latest News* [Online].Available from http://www.min-eng.com/biotech_ recent.html [Accessed 27 July 2002].

Sampson, M.I., Phillips, C.V., and Ball, A.S. (2000 b) 'Investigation of the attachment of *Thiobacillus ferrooxidans* to mineral sulfides using scanning electron microscopy analysis', *Minerals Engineering*, 13 (6), 643-656.

Sampson, M.I., Phillips, C.V., and Blake II, R.C. (2000 a) 'Influence of the attachment of acidophilic bacteria during the oxidation of mineral sulfides', *Minerals Engineering*, 13 (4), 373-389.

Sand, W., Gehrke, T., Jozsa, P.G., and Schippers, A. (2001) 'Biochemistry of bacterial leaching-direct vs. indirect bioleaching', *Hydrometallurgy*, 59, 159-175.

Santelli, C.M., Welch, S.A., Westrich, H.R., and Banfield, J.F. (2001) 'The effect of Fe-oxidizing bacteria on Fe-silicate mineral dissolution', *Chemical Geology*, 180, 99-115.

Santhiya, D., Subramanian, S., and Natarajan, K.A. (2000) 'Surface chemical studies on galena and sphalerite in the presence of *Thiobacillus thiooxidans* with reference to mineral beneficiation', *Minerals Engineering*, 13 (7), 747-763.

Sasaki, K. and Konno, H. (2000) 'Morphology of jarosite-group compounds precipitated from biologically and chemically oxidized Fe ions', *The Canadian Mineralogist*, 38, 45-56.

Sato, H., Nakazawa, H., and Kudo, Y. (2000) 'Effect of silver chloride on the bioleaching of chalcopyrite concentrate', *International Journal of Mineral Processing*, 59, 17-24.

Schippers, A. and Sand, W. (1999) 'Bacterial leaching of metal sulfides proceeds by two indirect mechanisms via thiosulfate or via polysulfides and sulfur', *Applied and Environmental Microbiology*, 65, 319-321.

Shrihari, Kumar, R., Graghi, K.S., and Natarajan, K.A. (1991) ‘Role of cell attachment in leaching of chalcopyrite mineral by *Thiobacillus ferrooxidans*’, *Applied Microbiology and Biotechnology*, 36, 278-282.

Shrihari, Modak, J.M., Kumar, R., and Gandhi, K.S. (1995) ‘Dissolution of particles of pyrite mineral by direct attachment of *Thiobacillus ferroxidans*’, *Hydrometallurgy*, 38, 175-187.

Silverman, M.P. and Lundgren, D.G. (1959) ‘Studies on the chemolithotrophic iron bacterium *Ferrobacillus ferrooxidans*: an improved medium and a harvesting procedure for securing high cell yields’, *Journal of Bateriology*, 77, 642-647.

Stott, M.B., Watling, H.R., Franzmann, P.D., and Sutton, D. (2000) ‘The role of iron-hydroxy precipitates in the passivation of chalcopyrite during bioleaching’, *Minerals Engineering*, 13, 1117-1127.

Sukla, L.B., Chaudhury, G.R., and Das, R.P. (1990) ‘Effect of silver ion on kinetics of biochemical leaching of chalcopyrite concentrate’, *Trans. Instn Min. Metall.*, 99, C43-C46.

Suzuki, I. (2001) ‘Microbial leaching of metals from sulfide minerals’, *Biotechnology Advances*, 19, 119-132.

Third, K.A., Cord-Ruwisch, R., and Watling, H.R. (2000) ‘The role of iron-oxidzing bacteria instimulation or inhibition of chalcopyrite bioleaching’, *Hydrometallurgy*, 57, 225-233.

Third, K.A., Cord-Ruwisch, R., and Watling, H.R. (2002) ‘Control of the redox potential by oxygen limitation improves bacterial leaching of chalcopyrite’, *Biotechnology and Bioengineering*, 78, 433-441.

Toma, M.K., Ruklisha, M.P., Vanags, J.J., Zeltina, O.M., Leite, M.P., Galinina, N.I., Viesturs, U.E., and Tengerdy, R.P. (1991) 'Inhibition of microbial growth and metabolism by excess turbulence', *Biotechnology and Bioengineering*, 38, 552-556.

Torma, A.E., Walden, C.C, Duncan, D.W., and Branion, R.M.R. (1972) 'The effect of carbon dioxide and particle surface area on the microbiological leaching of a zinc sulphide concentrate', *Biotechnology and Bioengineering*, 14, 777-786.

Tributsch, H. (2001) 'Direct versus indirect bioleaching', *Hydrometallurgy*, 59, 177-185.

Tributsch, H. and Rojas-Chapana, J.A. (2000) 'Metal sulfide semiconductor electrochemical mechanisms induced by bacterial activity', *Electrochimica Acta*, 45, 4705-4716.

Tuovinen, O.H. (1990) *Biological fundaments of minerals of mineral leaching processes*, in Ehrlich, H. L. and Brierley, C. L. (eds) *Microbial Mineral Recovery*. New York: Mc Graw-Hill.

Tuovinen, O.H. and Kelly, D.P. (1973) 'Studies on the growth of *Thiobacillus ferrooxidans*', *Archiv fur Mikrobiologie*, 88, 295-298.

Ubaldini, S., Veglió, F., Beolchini, F., Toro, L., and Abbruzzese, C. (2000) 'Gold recovery from a refractory pyrrhotite ore by biooxidation', *International Journal of Mineral Processing*, 60, 247-262.

Ubaldini, S., Veglió, F., Toro, L., and Abbruzzese, C. (1997) 'Biooxidation of arsenopyrite to improve gold cyanidation: study of some parameters and comparison with grinding', *International Journal of Mineral Processing*, 52, 65-80.

Valix, M., Usai, F., and Malik, R. (2001) 'Fungal bio-leaching of low grade laterite ores', *Minerals Engineering*, 14, 197-203.

Vasan, S.S., Modak, J.M., and Natarajan, K.A. (2001) ‘Some recent advances in the bioprocessing of bauxite’, *International Journal of Mineral Processing*, 62, 173-186.

Veglió, F., Beolchini, F., and Ubaldini, S. (1998) ‘Empirical models for oxygen mass transfer: a comparison between shake flask and lab-scale fermentor and appilcation to manganiferous ore bioleaching’, *Process Biochemistry*, 33 (4), 367-376.

Veglió, F., Beolchini, F., Nardini, A., and Toro, L. (2000) ‘Bioleaching of a pyrrothite ore by a sulfooxidans strain: kinetic analysis’, *Chemical Engineering Science*, 55, 783-795.

Wentzel, E. (2001) *Thiobacillus* [Online]. Available from http://www.bsi.vt.edu/biol_4684 / Microbes/Thiobacillus.html [Accessed 17 September 2001].

Witne, J.Y. and Phillips, C.V. (2001) ‘Bioleaching of OK Tedi copper concentrate in oxygen-and carbon dioxide-enriched air’, *Minerals Engineering*, 14, 25-48.

Yahya, A. and Johnson, D.B. (2002) ‘Bioleaching of pyrite at low pH and low redox potentials by novel mesophilic Gram-positive bacteria’, *Hydrometallurgy*, 63, 181-188.

Yuehua, H., Guanzhou, Q., Jun, W., and Dianzuo, W. (2002) ‘The effect of silver-bearing catalysts on bioleaching of chalcopyrite’, *Hydrometallurgy*, 64, 81-88.

Appendix I: The growth of *Thiobacillus ferrooxidans*

1.1 Introduction

A batch process for microbial growth is a closed culture system, which contains an initial, limited amount of substrate. A typical growth curve has four main stages, which include the lag phase, log phase (or exponential phase), stationary phase and death phase. After inoculation there is a period, in which there is no apparent growth; this period is referred to as the lag phase. The following period in which the cells grow at a constant rate is know as the log or exponential phase. The stationary phase is the next period where the growth rate has declined to zero. Finally, the dead phase is a period in which the number of viable cells decreases due to the toxicity of waste products and/or limited amount of substrate. This appendix addresses the growth of *T. ferrooxidans* (ATCC 19859) by showing a growth curve, calculates the maximum specific growth rate (μ_m, h^{-1}) during the exponential phase, and observes the late exponential period when the cell density is at its highest, therefore the culture is theoretically at its most suitable stage for being the active inoculum for further experiments.

The rate of growth during the log phase can be expressed according to equation 1,

$$r_x = \mu x \qquad (1)$$

where μ is the specific growth rate, s^{-1},

x is viable cell concentration with units of ,for example, $kg\ m^{-3}$,

and r_x is the volumetric rate of biomass production with units of, for example, $kg\ m^{-3}\ s^{-1}$,

In a closed system where growth is the only factor affecting cell concentration, $r_x = \frac{dx}{dt}$.

If μ is constant, then equation 1 can be integrated with the initial condition of $x = x_0$ at $t = 0$ as follows,

$$x = x_0 e^{\mu t} \quad (2)$$

where x_0 is the viable cell concentration at time zero.

Taking natural logarithms, equation 2 can be expressed as follows,

$$\ln x = \ln x_o + \mu t \quad (3)$$

and a plot of ln x versus t can be used to determine the specific growth rate.

Cell growth rate can also be expressed in terms of the doubling time t_d:

$$t_d = \frac{\ln 2}{\mu} \quad (4)$$

Table I.1 The maximum specific growth rate, μ_m (h^{-1}) as determined by independent researchers

Reference	μ_m (h^{-1})	System and conditions
Boon *et al.,* 1999	0.096	Chemostat, pH 1.8 to 1.9, temp. 30°C, 0.21 mol/l Fe^{2+} (11.7 g/l)
Pagella *et al.,* 1996	0.091	Batch, pH 2.5, temp. 30°C, 22 g/l $FeSO_4 \cdot 7H_2O$
	0.065	Batch, pH 2.5, temp. 30°C, 44 g/l $FeSO_4 \cdot 7H_2O$
	0.068	Batch, pH 2.5, temp. 30°C, 88 g/l $FeSO_4 \cdot 7H_2O$
	0.051	Batch, pH 2.5, temp. 20°C, 44 g/l $FeSO_4 \cdot 7H_2O$
Modak *et al*., 1996	0.048	Shake flask, 240 rpm, pH 2.0, temp. 30 °C, 9 g/l Fe^{2+}
	0.035	Shake flask, 240 rpm, pH 2.0, temp. 35 °C, 9 g/l Fe^{2+}
	0.028	Shake flask, 240 rpm, pH 2.0, temp. 40 °C, 9 g/l Fe^{2+}
	0.012	Shake flask, 240 rpm, pH 2.0, temp. 42 °C, 9 g/l Fe^{2+}
Halfmeier *et al.,* 1993	0.12	Chemostat, pH 1.3, temp. 30°C, 9 g/l Fe^{2+}
Braddock *et al.,* 1984	0.070	Chemostat, pH 1.9, temp. 22.5°C, 2.5 to 6.5 g/l $FeSO_4 \cdot 7H_2O$
	0.089	Shake flask , pH 1.9, temp. 22.5°C, 5 to 30 g/l $FeSO_4 \cdot 7H_2O$
Jones and Kelly, 1983	1.25 – 1.78	Chemostat, pH 1.6, temp. 30°C, 22 g/l $FeSO_4 \cdot 7H_2O$

Bacterial growth depends on different parameters such as, energy sources, other

required nutrients, and a permissive range of physical conditions such as dissolved oxygen concentration, temperature, and pH. The maximum specific growth rate of *T. ferrooxidans* is referred to in a range of literature based on its pattern of growth under various chemical (nutritional) and physical conditions (Table I.1).

1.2 Growth curve of *T. ferrooxidans*

1.2.1 Experimental procedure

Once a suitable stock culture had been prepared, the organism was subcultured to determine the growth curve at regular time intervals. A 10 % v/v inoculum of the stock culture (Appendix II) was added to a flask (250 ml) containing 45 ml of ATCC 64 medium. The flask was incubated in a rotary shaker at 30 °C for 5 days. In order to obtain sufficient data points for the growth curve, twenty-four or more identical shake flasks were set up. Two flasks were removed to provide duplicate samples for each data point. A 10% v/v inoculum comprising of the 5 day old culture was then subcultured in 50 ml of ATCC 64 medium in those 250 ml flasks at 30 °C and 200 rpm. Samples were taken at regular time intervals and then were filtered through filter paper (Whatman No. 1) to separate solid and liquid phases. The filtrate was used for analysis of the solution pH, cell concentration, total iron and ferrous ions.

A pH probe that was connected to a pH module was used to monitor the pH. Before monitoring, the pH probe was calibrated with two standard reference buffer solutions (i.e. standard reference buffer pH 4 and pH 7). The cells were then diluted to a known

concentration with the medium (ATCC 64 medium without ferrous ions) and counted under a phase-contrast microscope using a Helber bacterial counting chamber. Total iron content of the solution was determined by atomic absorption spectrophotometry (AAS). Calibration curves for each metal were determined using standardised metal solutions. Ferrous ion concentration was determined with 1, 10–phenanthroline. Ferrous ion reacts with o-phenanthroline to form an orange-red complex $[(C_{12}H_8N_2)_3Fe]^{2+}$ (Marczenko, 1976). The ferric ion concentration was calculated by subtracting the ferrous ion concentrations from the total iron (Golterman, 1978). The analyses followed those as described in Standard Methods for Examination of Water and Wastewater (Greenberg *et al*, 1992).

1.2.2 Results and discussion

Thirty-two hours after inoculation and every subsequent hour until 160 hours, samples were taken and solution pH, cell concentration, ferrous ions and total iron measured. A growth curve was plotted in terms of cell concentration against time after inoculation (Figure I.1). The lag phase was found to extend to about 64 hours after inoculation. Exponential growth occurred between 64 and 96 hours followed by the stationary phase between 96 and 136 hours, and the death phase at about 136 hours after inoculation. Late exponential phase cells harvested 96 hours (4 days) after inoculation were used as the inoculum for the next stage of testwork (Chapter 3).

In order to calculate the specific growth rate, natural logarithm of cell concentration

was plotted against time (Figure I.2). Calculation of the gradient of the line corresponding to exponential phase growth yielded the specific growth rate (μ) in units of h^{-1}. The value obtained was 0.0946 h^{-1} and the generation time was 7.33 h. The growth curve experiment was repeated twice and the samples followed sequentially during the lag phase at the exponential phase (Figures I.3 and I.5). The maximum specific growth rates from the repeat experiments were 0.0984 and 0.0952 h^{-1} (Figures I.4 and I.6). The generation times were 7.04 and 7.23 h. The following table (Table I.2) summarises the results given from those growth curves. Those results showed an identical maximum specific growth rate (μ_m) of 0.09 h^{-1}. Whilst the lag phases differ (i.e 64, 40 and 48 h.), presumably because of bacterial variation in storage time, the culture used in experiment II tended to grow more quickly than that of the other experiments. Two experiments showed an identical late exponential phase of 96 h after inoculation. Those experiments confirms when the culture was ready for harvesting. Therefore, the 96 h cell culture could be employed in the further experiments.

Table I.2 The results of the growth of *Thiobacillus ferrooxidans*

Results	Experiment I	Experiment II	Experiment III
Maximum specific growth rate, μ_m (h^{-1})	0.0946	0.0984	0.0952
Generation time (h)	7.33	7.04	7.23
Lag phase (h)	0-64	0-40	0-48
Exponential phase (h)	64-96	40-72	48-96
Stationary phase (h)	96-136	72-88	96-128
Death phase (h)	After 136	After 88	After 128

Table I.3 shows the maximum specific growth rate of *T. ferrooxidans* from this work in comparison with values found in the literature. Overall, there is significant variation in the value of μ_m reported (0.012-1.78 h^{-1}) which probably reflects differences in mode of

culture, culture conditions and substrate concentration. The maximum specific growth rate (μ_m) was particularly high between 0.70 and 1.78 h^{-1} when the pH of the growth media was lower than 2.0. The growth rate decreased with increasing substrate from 22 to 88 g/l $FeSO_4 \cdot 7H_2O$ (Pagella *et al.*, 1996). Increasing the temperature from 30 to 40°C did not enhance the growth rate (Modak *et al*., 1996). The results from this work were found to be in good agreement with the values quoted by Pagella *et al*. (1996) and Boon *et al*. (1999). In comparison with other shake flask experiments much higher values were obtained in the present work.

Table I.3 The maximum specific growth rate, μ_m (h^{-1}) as determined by the independent researchers

Reference	μ_m (h^{-1})	System and conditions
Boon *et al*., 1999	0.096	Chemostat, pH 1.8 to 1.9, temp. 30°C, 0.21 mol/l Fe^{2+}
Pagella *et al*., 1996	0.091	Batch, pH 2.5, temp. 30°C, 22 g/l $FeSO_4 \cdot 7H_2O$
	0.065	Batch, pH 2.5, temp. 30°C, 44 g/l $FeSO_4 \cdot 7H_2O$
	0.068	Batch, pH 2.5, temp. 30°C, 88 g/l $FeSO_4 \cdot 7H_2O$
	0.051	Batch, pH 2.5, temp. 20°C, 44 g/l $FeSO_4 \cdot 7H_2O$
Modak *et al*., 1996	0.048	Shake flask, 240 rpm, pH 2.0, temp. 30 °C, 9 g/l Fe^{2+}
	0.035	Shake flask, 240 rpm, pH 2.0, temp. 35 °C, 9 g/l Fe^{2+}
	0.028	Shake flask, 240 rpm, pH 2.0, temp. 40 °C, 9 g/l Fe^{2+}
	0.012	Shake flask, 240 rpm, pH 2.0, temp. 42 °C, 9 g/l Fe^{2+}
Halfmeier *et al.,* 1993	0.12	Chemostat, pH 1.3, temp. 30°C, 9 g/l Fe^{2+}
Braddock *et al*., 1984	0.070	Chemostat, pH 1.9, temp. 22.5°C, 2.5 to 6.5 g/l $FeSO_4 \cdot 7H_2O$
	0.089	Shake flask , pH 1.9, temp. 22.5°C, 5 to 30 g/l $FeSO_4 \cdot 7H_2O$
Jones and Kelly, 1983	1.25 - 1.78	Chemostat, pH 1.6, temp. 30°C, 22 g/l $FeSO_4 \cdot 7H_2O$
This work	0.095-0.098	Shake flask, 200 rpm, pH 2.8, temp. 30 °C, 20 g/l $FeSO_4 \cdot 7H_2O$

1.3 Conclusion

After a number of trials *T. ferrooxidans* supplied by ATCC was found to give a reasonable growth curve. The culture was grown in ATCC 64 medium with 20 g/l ferrous sulphate in a rotary shaker at 200 rpm, a temperature of 30 °C and an initial pH of 2.8. The average maximum specific growth rate (μ_m) during the exponential phase was found to be 0.095 h^{-1} and the average generation time was 7.20 h for a series of three repeat experiments.

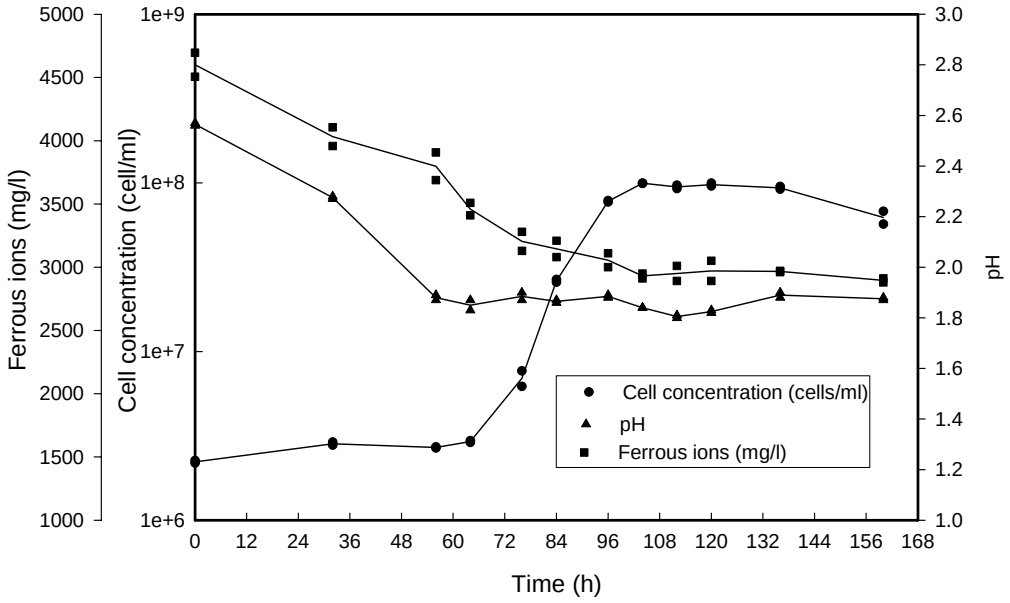

Figure I.1 Growth curve of *T. ferrooxidans*

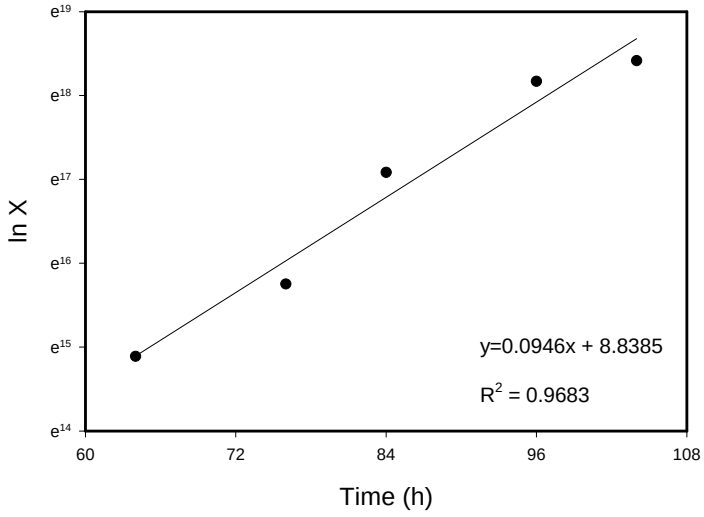

Figure I.2 Specific growth rate of *T. ferrooxidans*

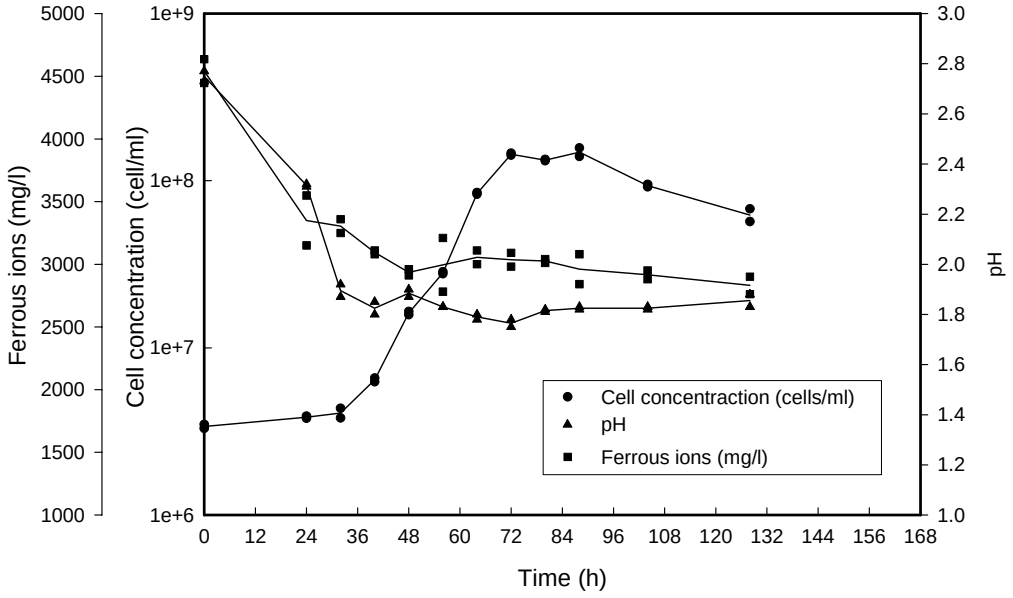

Figure I.3 The first repeat growth curve of *T. ferrooxidans*

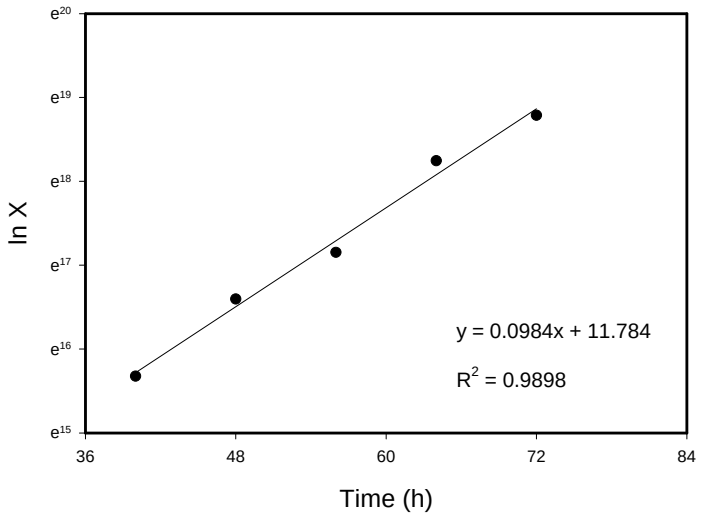

Figure I.4 The first repeat specific growth rate of *T. ferrooxidans*

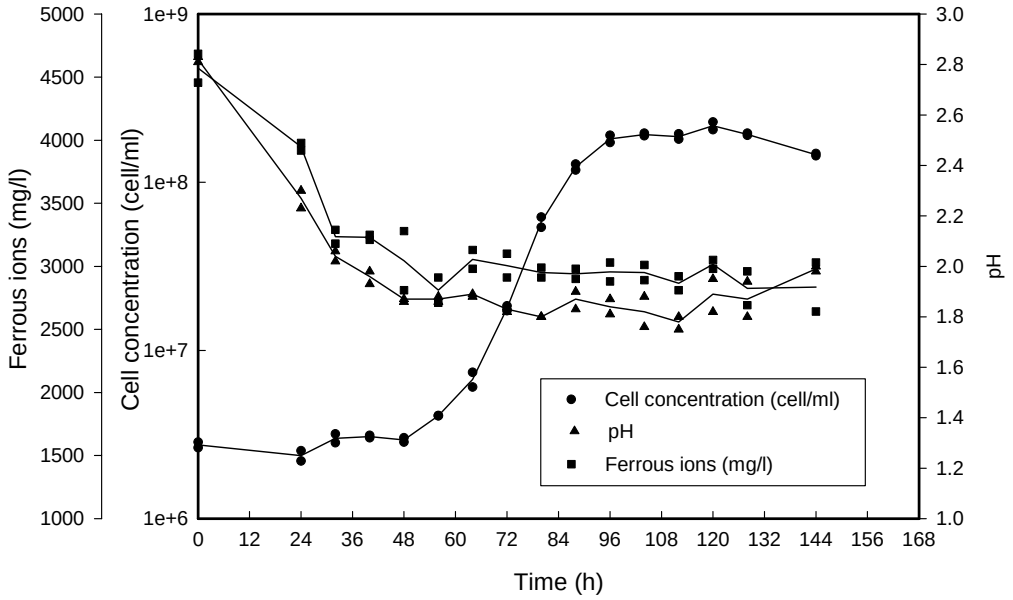

Figure I.5 The second repeat growth curve of *T. ferrooxidans*

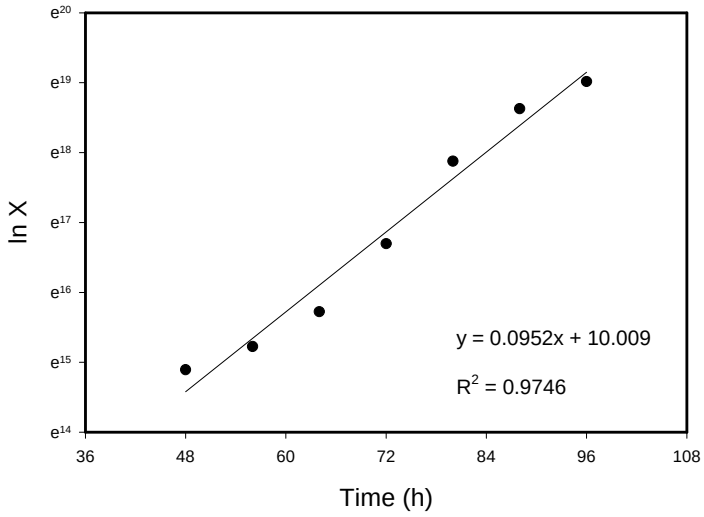

Figure I.6 The second repeat specific growth rate of *T. ferrooxidans*

Appendix II: Culture preparation

A series of preliminary experiments were conducted to determine appropriate conditions for the growth of *Thiobacillus ferrooxidans*. Different media have been used for growing *T. ferrooxidans*. The main components of these media are phosphate, magnesium and ammonium ions, although the different media contain different amounts of these elements. The media that have been used in this study were Tuovinen and Kelly (1973) medium, *Thiobacillus ferrooxidans* medium, ATCC 2093 medium, 9K medium and ATCC 64 medium which have different initial pHs. The components of these media are shown in Appendix III.

Because of problems in achieving sufficient growth, different stock cultures and conditions were tested. These results are summarised in Table II.1. Aseptic techniques were used throughout the study. *Thiobacillus ferroxidans* (NCIMB 9490) was ordered from National Collection of Industrial and Marine Bacteria, Scotland (NCIMB). In experiments 1 and 2, the culture, which was received in lyophilised form, was subcultured in Tuovinen and Kelly (1973) medium (Appendix III). The starter culture (10 % v/v inoculum) was transferred to 10 and 15 ml tubes containing 2 and 5 ml of medium respectively with 33.4 g/l ferrous sulphate and grown at 25 °C in a static incubator. The growth was first assessed by colour changing from cream to brick-red. The culture generally needs 7 days to grow at most, but unfortunately in this case even after it was left for 40 days, it did not grow at all (experiment 1, Table II.1).

Table II.1 Summary of experimental conditions and results of culture preparation

Experiment	Collection company	Culture	Medium	Growth condition				Incubation time (day)	Results
				pH	Temp. (°C)	Inoculum (% v/v)	Agitation		
1	NCIMB	Lyophilized form	Tuovinen and Kelly, 1973	2.0	25	10	Static culture	40	No growth
2	NCIMB	Lyophilized form	Tuovinen and Kelly, 1973	2.0	25	30	Static culture	30	No growth
3 a	NCIMB	Viable cell	Tuovinen and Kelly, 1973	2.0	25	2	200 rpm	35	No growth
3 b	NCIMB	Viable cell	Thiobacillus ferroxidans	2.0	25	2	200 rpm	35	No growth
3 c	NCIMB	Viable cell	ATCC 2093	2.3	25	2	200 rpm	35	No growth
3 d	NCIMB	Viable cell	ATCC 2093	2.3	25	10	200 rpm	35	No growth
3 e	NCIMB	Viable cell	9K medium	2.0	25	2	200 rpm	12	Growth
4	NCIMB	9 K medium	Tuovinen and Kelly, 1973	2.0	25	10	200 rpm	20	No growth
5 a	ATCC	Viable cell	ATCC 64	2.8	25	20	200 rpm	7	Growth
5 b	ATCC	Viable cell	ATCC 64	2.8	25	20	Static culture	30	No growth
6 a	ATCC	ATCC 64	ATCC 64	2.8	25	15	200 rpm	10	Growth
6 b	ATCC	ATCC 64	ATCC 64	2.8	30	15	200 rpm	7	Growth
7	ATCC	ATCC 64	ATCC 64	2.8	30	10	200 rpm	5	Growth

After this initial experiment another lyophilised culture was ordered from NCIMB. The same medium was used to grow the new culture. This time a 30 % (v/v) inoculum was used in a 15 ml medical bottle (experiment 2). Otherwise the growth conditions were the same as that of the first culture. The second culture was kept for 30 days, but again there was no growth.

A third sample from NCIMB (experiment 3) was obtained in a viable form (liquid culture). This culture was suspended in 250 ml Erlenmeyer flasks each containing 50 ml of the different media and incubated at 25 °C in a rotary shaker at 200 rpm. The experimental conditions are shown in Table II.1. In this case there was only one experiment where growth was observed, i.e., when the 9K medium was used and this occurred after an incubation time of 12 days. Subsequently experiment 4 was carried out to subculture these cells (experiment 3e) in the Tuovinen and Kelly (1973) medium (Appendix III). A 10 % v/v inoculum was used and the culture was again incubated at 25 °C and 200 rpm.

T. ferrooxidans uses ferrous ion (Fe^{2+}) as a energy source. However, after autoclaving the 9K medium, the ferrous ion (Fe^{2+}) was oxidised to ferric ion (Fe^{3+}) as observed by a change in colour from cream to brick-red. Since the aim of the project is to use chalcopyrite as a substrate, which contains ferrous ion, growth on a ferric based medium was not considered relevant. Therefore, the Tuovinen and Kelly (1973) medium was used instead since this could be filtered rather than autoclaved thus retaining a high ferrous ion content. Unfortunately, no growth was observed in the Tuovinen and Kelly (1973) medium within 20 days.

For experiment 5 (Table II.1) *Thiobacillus ferrooxidans* (ATCC 19859) was obtained from the American Type Culture Collection (ATCC). A new medium was prepared as suggested by ATCC (see Appendix III). The cells were first subcultured in ATCC 64 medium using a 20 % (v/v) inoculum and then incubated at 25 °C in a static incubator and in a rotary shaker at 200 rpm. It was found that the organism could only grow in the 25 °C rotary shaker. Then the culture was further subcultured (experiments 6 and 7). In experiment 6 the inoculum volume was reduced to 15 % v/v and the temperature was increased from 25 °C to 30 °C in order to determine whether this would reduce incubation time. In experiment 7, the inoculum volume was further reduced to 10 % v/v at a temperature of 30 °C. Using the ATCC 64 medium growth was observed under all the conditions. The best combination of the growth conditions was found to be at 30 °C and inoculum volume of 10 % v/v.

A stock culture was then prepared from experiment 7. The cells were first subcultured in ATCC 64 medium using a 10 % (v/v) inoculum and then incubated at 30 °C and 200 rpm. The culture was then harvested (after 4 days) and filtered through filter paper (Whatman No.1) to eliminate iron precipitation. The suspension was centrifuged at 8000 rpm for 40 minutes and washed three times with the same medium without iron. The cells were then diluted to approximately 5×10^8 cell/ml. A 20 % v/v glycerol was used and the cells (1 ml) were added in a cryogenic vial. The cryogenic vials were kept in the freezer at a temperature of –20 °C.

Appendix III: Medium

1. Tuovinen and Kelly (1973) medium

Solution A:

K_2HPO_4	0.125 g
$(NH_4)_2SO_4$	0.5 g
$MgSO_4 \cdot 7H_2O$	0.5 g
15 N H_2SO_4	5 ml
Dissolved in 1 L distilled water	

Solution B:

$FeSO_4 \cdot 7H_2O$	167 g
15 N H_2SO_4	50 ml
Dissolved in 1 L distilled water	

Sterilise (A) separately and sterilise (B) by filtration

Added 4 parts of (A) to 1 part of (B) aseptically

2. Thiobacillus ferrooxidans medium

Solution I:

K_2HPO_4	0.5 g
$(NH_4)_2SO_4$	0.5 g
$MgSO_4 \cdot 7H_2O$	0.5 g
15 N H_2SO_4	5 ml
Distilled water	1 L

Solution II:

$FeSO_4 \cdot 7H_2O$	167 g
15 N H_2SO_4	50 ml
Distilled water	1 L

Autoclave solution I at 121 °C/15 min and sterilise solution II by filtration. After sterilisation 2 parts of solution I are added to 1 part of solution II.

3. ATCC medium 2093 (Cote, 1984)

Solution A:

$(NH_4)_2SO_4$	0.8 g
$MgSO_4 \cdot 7H_2O$	2.0 g
K_2HPO_4	0.4 g
Wolfe's Mineral Solution	5.0 ml
Distilled water	800 ml

Adjust solution A to pH 2.3 with H_2SO_4

Filter-sterilise.

Solution B:

$FeSO_4 \cdot 7H_2O$	20.0 g
Distilled water	200.0 ml

Stir Solution B to dissolve and quickly filter-sterilise.

Aseptically combine solution A and B.

Wolfe's Mineral Solution:

Nitrilotriacetic acid, 1.5 g

$MgSO_4 \cdot 7H_2O$, 3.0 g

$MnSO_4 \cdot H_2O$, 0.5 g

NaCl, 1.0 g

$FeSO_4 \cdot 7H_2O$, 0.1 g

$CoCl_2 \cdot 6H_2O$, 0.1 g

$CaCl_2$, 0.1 g

$ZnSO_4 \cdot 7H_2O$, 0.1 g

$CuSO_4 \cdot 5H_2O$, 0.01 g

$AlK(SO_4)_2 \cdot 12H_2O$, 0.01 g

H_3BO_3, 0.01 g

$Na_2MoO_4 \cdot 2H_2O$, 0.01 g

Distilled water, 1.0 L

Add Nitrilotriacetic acid to approximately 500 ml of water and adjust to pH 6.5 with KOH to dissolve the compound. Bring volume to 1.0 L with remaining water and add remaining compounds one at a time

4. 9K medium (Cote, 1984)

Solution A:

$(NH_4)_2SO_4$	3.0 g
KCl	0.1 g
K_2HPO_4	0.5 g
$MgSO_4 \cdot 7H_2O$	0.5 g
$Ca(NO_3)_2$	10 mg
10 N H_2SO_4	1 ml
Distilled water	700 ml

Solution B:

$FeSO_4 \cdot 7H_2O$	44 g
Distilled water	300 ml

Prepare solutions A and B separately. Dispense A as 70 ml in 250 ml screw-capped bottles, and B as 30 ml amounts in 1 oz screw-capped bottles. Autoclave A and B separately at 121 °C/15min. Immediately before use add B aseptically to A.

5. ATCC medium 64 (Cote, 1984)

Solution A:

$(NH_4)_2SO_4$	0.4 g
KH_2PO_4	0.2 g
$MgSO_4 \cdot 7H_2O$	0.08 g
Distilled water	400 ml

Solution B:

$FeSO_4 \cdot 7H_2O$	10.0 g
1N H_2SO_4	1 ml
Distilled water	100 ml

Autoclave solution A at 121 °C/15 min and sterilise solution B by filtration. After sterilisation solution A is aseptically added to solution B. pH should be about 2.8

Appendix IV: Chalcopyrite mineralogy report

Two size fractions (>150 μm and <38 μm) of a chalcopyrite-rich flotation concentrate were characterised using a combination of reflected light microscopy and SEM-based techniques. Both size fractions consist largely of chalcopyrite, but are also characterised by the presence of subordinate amounts of transparent gangue mineral and a wide range of accessory ore minerals that are present in minor to trace amounts. The overall mineralogy of both size fractions is basically similar although the degree of liberation and relative proportions of individual minerals varies. A general mineralogical description that is applicable to both size fractions is therefore provided with the differences between the two sub-samples being described separately.

The copper concentrate consists largely of chalcopyrite, a high proportion of which is present in the form of cleanly liberated fragments that are relatively more abundant in the <38 μm fines than in the >150 μm size fraction (Figure IV.1 a-b). Relatively small amounts of transparent gangue minerals (largely quartz, sericite and K-feldspar) are present as impurities together with a wide range of accessory ore minerals, the most common of which include wolframite, cassiterite, pyrite, arsenopyrite, sphalerite and stannite. In addition, a significant number of other ore minerals are present in trace amounts including, galena, various Bi-bearing minerals (emplectite, russellite and bismuthinite), covellite, stolizite or raspite ($PbWO_4$), molybenite and at least two Ag-bearing Bi-sulphides. Brief descriptions of these various minerals are provided, but it is generally not possible to provide much information on their larger-scale textural relationships, associations and/or spatial relationships because of the relatively fine grain size of the concentrate.

Copper Sulphides (Chalcopyrite and Rare Covellite)

Chalcopyrite (ideally $CuFeS_2$) represents the dominant Cu-sulphide mineral in both concentrates where it is present largely as cleanly liberated grains and fragments (Figures IV.1 a-b). A relatively small proportion of the chalcopyrite grains, (notably in the >150 μm size fraction) may, however, be present in the form of incompletely liberated composite grains in which they remain intergrown with one or more of the associated ore and gangue minerals. The chalcopyrite commonly forms simple intergrowths with stannite (ideally Cu_2FeSnS_4) with this phase also commonly being present as inclusions within the chalcopyrite (Figures IV.2 a-b). The chalcopyrite very occasionally shows incipient to a minor degree of replacement by covellite (ideally CuS), particularly at places where it is intergrown with stannite (Figures IV.2 b and IV.3 a). Qualitative energy dispersive electron microbeam analyses of the chalcopyrite serve to indicate that it is close to the theoretical $CuFeS_2$ end member composition.

Pyrite

Small amounts of pyrite are present in both size fractions where it normally occurs as cleanly or extensively liberated grains and fragments (Figure IV.5 a). The pyrite may show the development of cubic crystal outlines and is most commonly found in association with small amounts of intergrown chalcopyrite (Figure IV.5 a). The overall pyrite content of the concentrate is very low (Figure IV.1 a) and it is unlikely that additional cleaning can reduce it further.

Arsenopyrite

Very small amounts of arsenopyrite are also present in both size fractions where it also occurs as both cleanly and extensively liberated grains and fragments (Figure IV.5 a). It

occasionally forms composite grains in which it remains intergrown with subordinate amounts of chalcopyrite. Arsenopyrite is also present as a rare intergrown phase with wolframite (Figure IV.5 b).

The >150 μm Size Fraction

This represents a relatively clean, chalcopyrite-rich concentrate that contains relatively minor amounts of impurities (Figure IV.1 a). The overall degree of liberation of the chalcopyrite (and associated ore and gangue minerals) is generally very high with the incompletely liberated composite grains consisting largely of intergrowths between chalcopyrite-stannite (Figures IV.2 a-b and IV.3 a), chalcopyrite-sphalerite (Figures IV.3 b and IV.4 a) and chalcopyrite-Bi-minerals and/or arsenopyrite (Figures IV.4 b and IV.6 a-b). The overall content of transparent gangue minerals is very low and composite grains consisting of intergrowths between transparent gangue and sulphides are relatively rare. It is unlikely that the overall liberation will be improved significantly with finer grinding.

The < 38 μm fines Fraction

This sample differs markedly from the previous coarser product in that it contains a significant component of cleanly liberated transparent gangue mineral fragments (Figure IV.1 b). These consist largely of quartz, sericite and K-feldspar and may represent as much as 20-25 percent by volume of this product. Considerable scope therefore exists for the rejection of at least some of these impurities by further cleaning should this be warranted.

In other respects, the ore mineralogy of the concentrate is also dominated by chalcopyrite and is essentially similar to that of the coarser size fraction. The overall degree of liberation is also somewhat better as might be expected with composite grains being relatively rare. The most common composite grains consist of intergrowths between chalcopyrite and stannite as well as between chalcopyrite and various Bi-minerals. Most of the other forms of intergrowth have been eliminated.

Discussion

Both size fractions of this concentrate consist largely of chalcopyrite that generally exhibit a high degree of liberation that increases somewhat in the fines fraction. The mineralogy of the concentrate is, however, complex with a wide range of other ore and gangue minerals being present in small amounts. The overall proportion of cleanly liberated transparent gangue contaminants increases significantly in the fines fraction and significant scope exists for reducing this by further cleaning. Most of the cassiterite and wolframite contaminants are present as cleanly liberated grains and fragments that are potentially recoverable by simple gravity concentration should their overall abundance warranted.

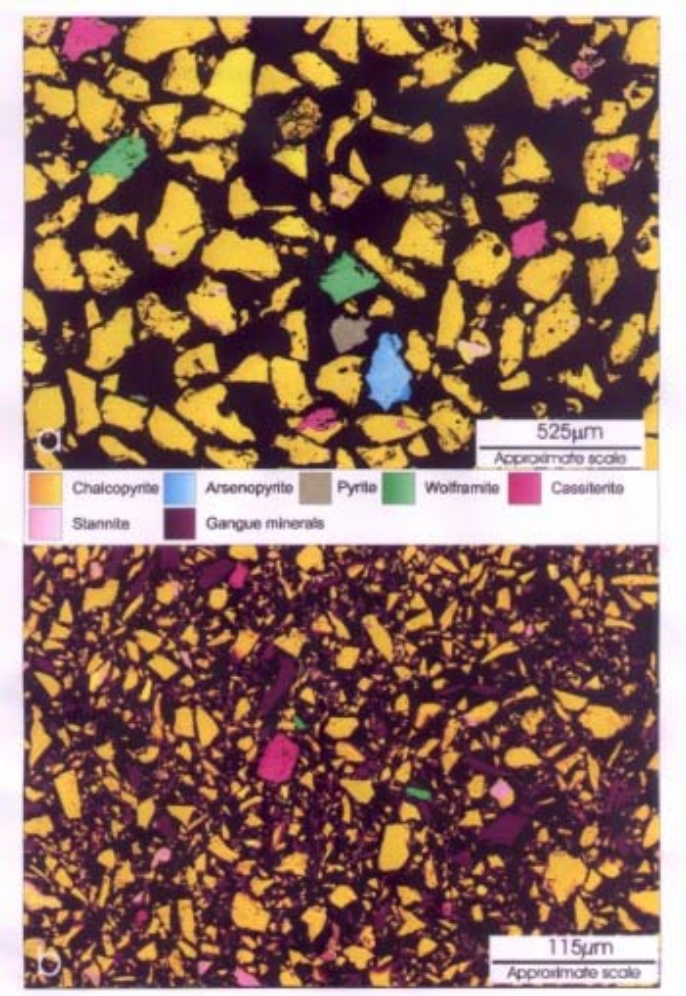

Figure IV.1 Copper concentrate: False colour, backscattered electron images illustrating (a) A typical area of the 150 µm size fraction showing the abundance and nature of the chalcopyrite (yellow). Other minor contaminant phases include stannite (light pink), pyrite (khaki), arsenopyrite (light blue), cassiterite (dark pink) and wolfamite (green). Note the generally high degree of liberation of all phases except stannite. (b) A typical area of the < 38 µm fines fraction at much higher magnification. Note the relative abundance of cleanly liberated, transparent gangue minerals (mauve). Chalcopyrite (yellow) is therefore less abundant. The minor phases are the same as in (a).

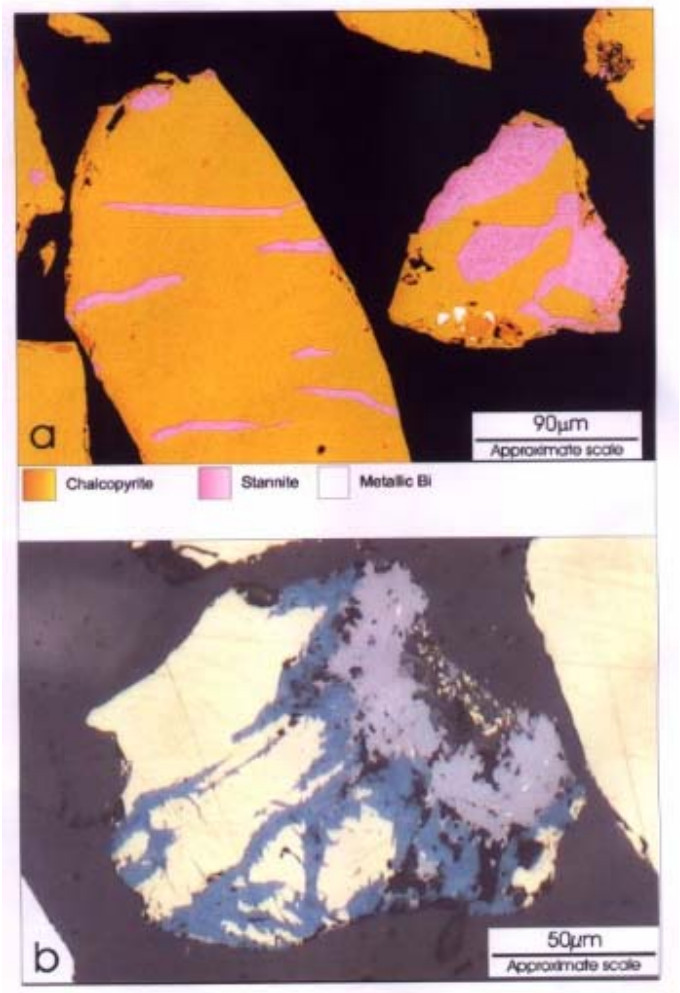

Figure IV.2 Copper concentrate: (a) A false colour, backscattered electron image illustrating the nature and appearance of stannite (light pink) intergrowths in chalcopyrite (yellow). Note the presence of traces of metallic Bi (white). (b) A reflected light photomicrograph illustrating the nature and appearance of a chalcopyrite grain that shows moderate degrees of supergene alteration and replacement by covellite (blue shades). Note that the chalcopyrite also forms a relatively simple intergrowth with stannite (brownish grey).

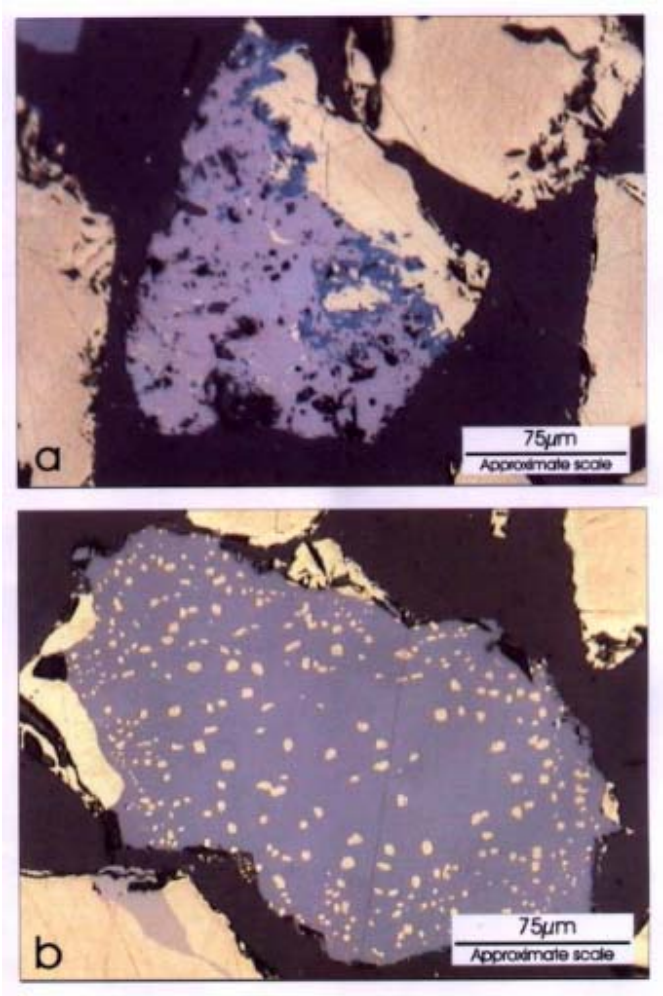

Figure IV.3 Copper concentrate: Reflected light photomicrographs illustrating (a) the nature and appearance of another chalcopyrite grain that shows moderate degrees of supergene alteration and replacement by covellite (blue shades). Note that in this case, the chalcopyrite forms a more complex intergrowth with stannite (brownish grey). (b) The nature and appearance of a typical sphalerite grains (grey) that hosts numerous tiny bodies of chalcopyrite (yellow). These types of intergrowth are commonly referred to as chalcopyrite disease.

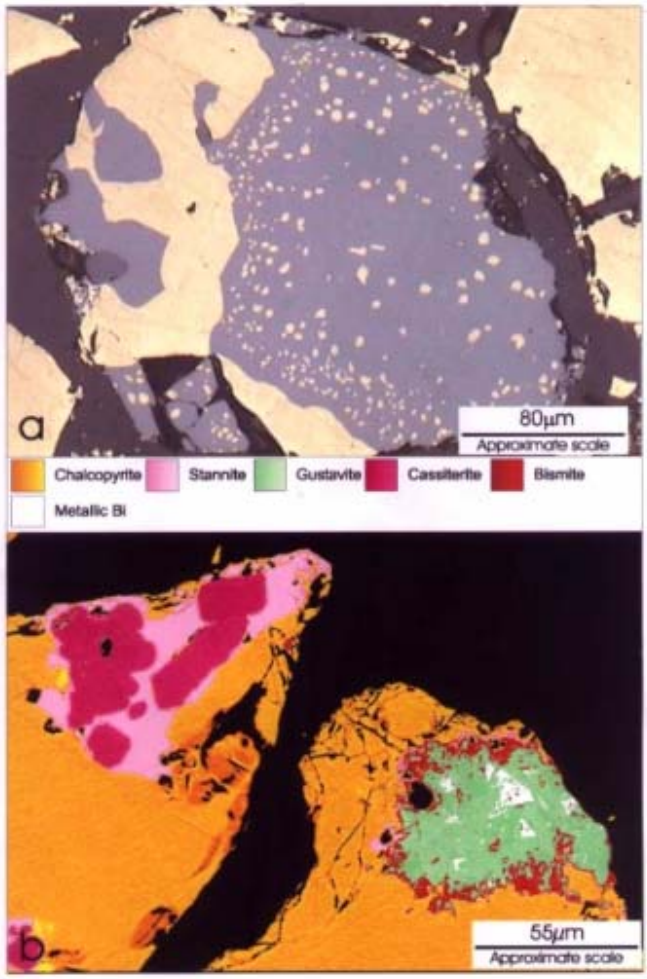

Figure IV. 4 Copper concentrate: (a) A reflected light photomicrographs illustrating the nature and appearance of composite grain consisting of intergrowths between chalcopyrite (yellow) and sphalerite (grey). Note that the sphalerite also exhibits chalcopyrite disease as illustrated in Figure IV.3 b. (b) False colour, backscattered electron images illustrating the nature of some of the phases that form intergrowths with chalcopyrite (yellow). The left-hand grain shows the presence of small cassiterite crystals (dark pink) that are intergrown with stannite (light pink). The right hand grain shows the presence of a complex inclusion that consists largely of the Ag-bearing, Bi-Pb sulphide (gustavite, light green) and minor metallic Bi (white). Note the localized development of small amounts of the Bi-W oxide, russellite (light pink) and bimite (red) at places near to margin of the sulphide grain.

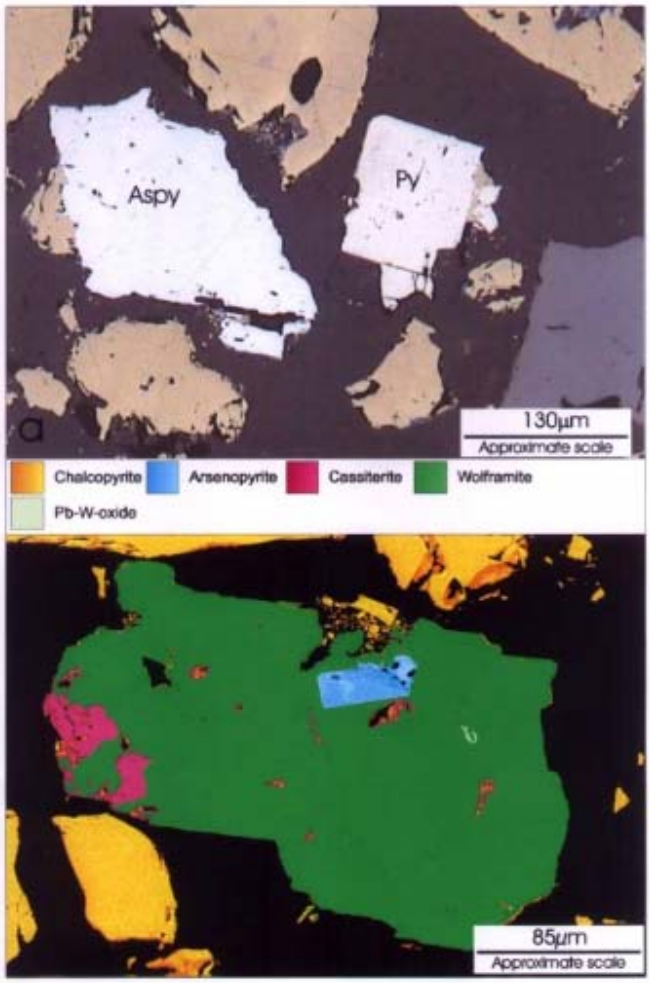

Figure IV.5 Copper concentrate: (a) A reflected light photomicrographs illustrating the nature and appearance of an area of the concentrate showing the presence of chalcopyrite fragments (yellow), some of which host small inclusions of sphalerite (grey). Note the presence of discrete grains or fragments of arsenopyrite (white, rhomb-shaped), pyrite (pale cream, cubic) and wolfamite (green). (b) False colour, backscattered electron images illustrating the nature and appearance of a grain of wolfamite (green) that hosts inclusions of cassiterite (dark pink), arsenopyrite (light blue) and the Pb-W-oxide stolzite or raspite (mauve).

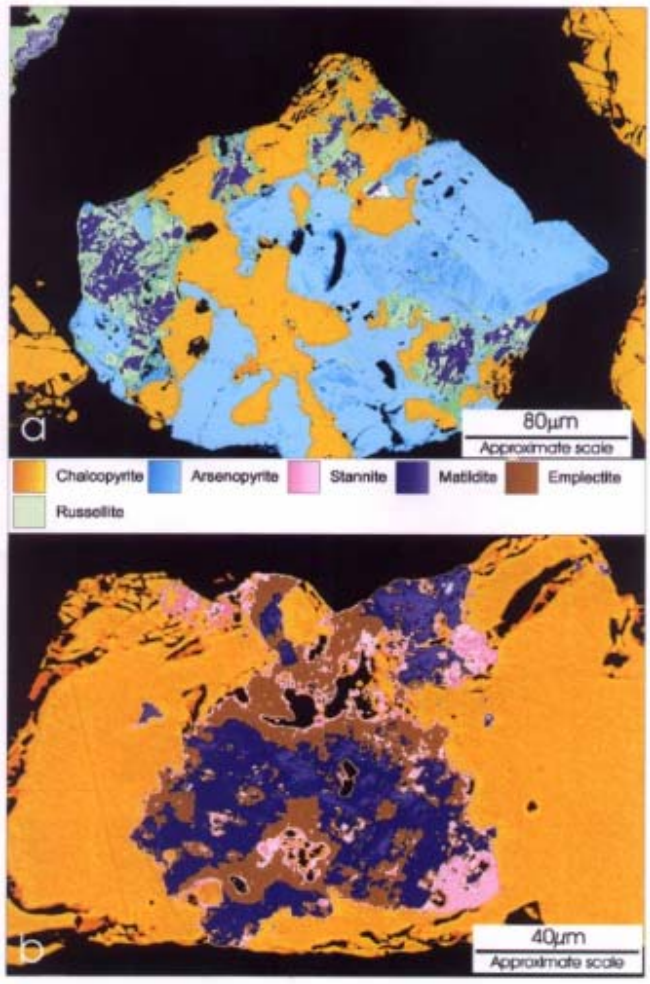

Figure IV.6 False colour, backscattered electron images illustrating (a) the nature and appearance of a complexly intergrown composite grain of chalcopyrite (yellow) and arsenopyrite (light blue) that also host small intergrowths of Bi minerals, notably the Bi-Ag-sulphide matildite (dark blue), metallic Bi (white) and the Bi-W-oxide, russellite (green). (b) the nature and appearance of a composite grain consisting of intergrowths between chalcopyrite (yellow), emplectite (light brown), stannite (light pink) and matildite (dark blue).

Appendix V: Low-grade copper ore (Palabora) mineralogy report

The run of mine ore sample is reported to contain approximately 25 percent magnetite and 1 percent copper sulphide. Examination of the polished sections prepared from the size fractions confirms that this sample consists predominantly of transparent gangue minerals together with subordinate amounts of magnetite. Minor amounts of chalcocite, bornite, chalcopyrite, cubanite, valleriite and pyrite are also present.

Transparent Gangue

The sample is dominated by the presence of significant amounts of transparent gangue. Qualitative SEM analysis of the transparent gangue minerals confirms that they consist of one or more of calcite (ideally $CaCO_3$), dolomite (ideally $CaMg(CO_3)_2$), apatite (ideally $Ca_5(PO_4)_3$ (F, Cl, OH)), Olivine (ideally $(Fe,Mg)_2SiO_4$), phlogopite (ideally $KMg_3AlSi_3O_{10}(F, OH)_2$), serpentine (ideally $Mg_3Si_2)_5(OH)_4$), pyroxene and plagioclase feldspar. Minor amounts of brucite (ideally $Mg(OH)_2$) are also present.

Carbonate minerals are abundant and consist predominantly of calcite and dolomite. The calcite and dolomite typically occur as intergrowths with one or more of magnetite, sulphides and transparent gangue. The dolomite may form complex intergrowths with calcite, occurring as sub-rounded inclusions that probably reflect the exsolution of these two phases during crystallisation. Qualitative SEM analysis of the dolomite confirms that it consists predominantly of Ca, Mg, C and O together with minor amounts of Fe.

Apatite is abundant and represents the dominant P-bearing mineral in the head sample. The apatite largely occurs as rounded or sub-rounded grains associated with one or

more of magnetite, transparent gangue and sulphide minerals. The apatite is commonly traversed by numerous fractures. These fractures may be filled or partially filled by magnetite and serpentine. Qualitative SEM analysis of the apatite confirms that it consists predominantly of Ca, P and O together with minor amounts of Cl.

Olivine is present in moderate amounts in the polished sections. The great bulk of the olivine has been partially or extensively replaced by serpentine. Serpentine is a common alteration product of olivine and is also present in moderate amounts in this sample. The serpentine typically forms fine-grained aggregates that may fill or partially fill fractures in magnetite and apatite. Qualitative SEM analysis of the serpentine confirms that it consists predominantly of Si, Mg and O together with minor amounts of Fe. The olivine is Mg-rich (forsterite) and typically contains minor amounts of Fe.

Phlogopite, a Mg-rich mica, is a common accessory mineral and typically occurs as flake-like aggregates associated with one or more of transparent gangue minerals, magnetite and to a lesser extent sulphide minerals. Brucite is present in very minor amounts. Brucite is secondary in origin, occurring predominantly along fractures associated with magnetite, apatite and other transparent gangue minerals.

Microgabbro rock fragments

This sample is characterised by the presence of a small number of rock fragments that consist predominantly of plagioclase feldspar, pyroxene and skeletal crystals of magnetite. These aggregates represent fragments of microgabbro (dolerite) that are present as intrusives within the ore body. The plagioclase feldpar occurs as lath-like

crystals and as fine interstitial grains that are intimately intergrown with pyroxene. Qualitative analysis of the plagioclase confirms that it consists predominantly of Si, O, Al, Ca and Na. The pyroxene is Ca-rich and probably represents the mineral diopside (ideally $MgCaSi_2O_6$). The diopside occurs as anhedral grains and as fine interstitial grains that are intimately intergrown with plagioclase. Minor amounts of ilmenite may also occur within these aggregates.

Magnetite

Magnetite is abundant in this sample. The magnetite occurs largely as discrete liberated grains and to a lesser extent as intergrowths with transparent gangue. Cu-bearing sulphide minerals may also occur along the margins of the magnetite grains. Qualitative SEM analysis of the magnetite confirms that it consists predominantly of Fe and O with Mg and Ti generally being present below the detection limits for this technique (~0.5%). A significant proportion of the magnetite contains abundant spinel inclusions (ideally $MgAl_2O_4$). The spinel typically exhibits euhedral morphologies with discrete crystals rarely exceeding 30 μm in size. The great bulk of the spinel crystals are less than a 10 μm in size. The spinel represents the exsolution of Mg and Al from the magnetite during cooling of the magmatic body from which these phases crystallised. Ilmenite is also intimately associated with the magnetite, occurring as granular intergrowths, laths, fine-grained lamellae and inclusions. The textures observed between ilmenite and magnetite result from the oxidation of a former magnetite-ulvöspinel solid solution. The magnetite grains are commonly traversed by numerous fractures that are particular abundant in the coarser size fractions.

Magnetite may also occur along fractures and grain boundaries, often associated with one or more of the Cu-bearing sulphide aggregates. The magnetite associated with the Cu-bearing sulphides may have formed as a result of the oxidation of Fe from the Cu-sulphides during crystallisation and/or sub-solidus cooling. This late-stage magnetite is typically granular in nature and may also occur along fractures in earlier formed phases, including apatite, baddelyite and other transparent gangue minerals. A relatively small proportion of the magnetite occurs as Ti-bearing, skeletal magnetite that is present within the pyroxene-and plagioclase- rich microgabbro fragments that are present in relatively minor amounts in this sample.

Ilmenite

Ilmenite is a common accessory mineral and hosts a significant proportion of the Ti present in this sample. Qualitative SEM analysis of the ilmenite confirms that it consists predominantly of Fe, Ti, O and Mg. The ilmenite is particularly Mg-rich and exhibits a relatively low reflectivity when observed using reflected light microscope techniques. The ilmenite typically occurs along the grain boundaries of magnetite grains and as penetrating laths that extend into the magnetite. These textures are commonly observed in ores of this type and represent the contemporaneous oxidation-exsolution ilmenite from the magnetite during cooling.

Micrometre-sized inclusions of Ti-rich bodies are often finely disseminated throughout the magnetite grains. These Ti-rich bodies represent fine-grained, exsolved ilmenite and become less abundant towards the margins of the larger ilmenite grains. This is largely due to the migration of the exsolved ilmenite from the magnetite into the ilmenite grain,

also reflecting changes that occur during the cooling of the host rock. Fine-grained ilmenite lamellae may also be observed in a number of the magnetite grains. The ilmenite lamellae are not particularly abundant in this sample, but they also present the products of contemporaneous oxidation-exsolution. A relatively small proportion of the ilmenite occurs within the pyroxene- and plagioclase-rich microgabbro fragments that are present in relatively minor amounts in this sample.

Sulphide minerals

This sample is characterised by the presence of minor amounts of Cu-bearing sulphide minerals. These include cubanite (ideally $CuFe_2S_3$), chalcopyrite (ideally $CuFeS_2$), bornite (ideally Cu_5FeS_4) and chalcocite (ideally Cu_2S). Valleriite (ideally 4(Fe, Cu)S.3(Mg, Al)$(OH)_2$) is also an important Cu-bearing sulphide and occurs as porous, flake-like aggregates that typically occur along fractures and grain boundaries associated with other Cu-bearing sulphides and one or more of magnetite and transparent gangue. Valleriite is an alteration product that has formed, at least in part, as a result of the alteration of one or more of the Cu-bearing sulphide minerals. Relict chalcopyrite and bornite are commonly present within the valleriite aggregates. Common mineral associations with valleriite in other ore deposits include magnetite, chalcopyrite, cubanite and serpentine. These minerals are all present in this sample.

The bulk of the chalcopyrite is present as intergrowths with bornite and to a lesser extent chalcocite and cubanite. The chalcopyrite may form simple grain boundary relationships with other Cu-bearing sulphides or more typically occur as lamellae within bornite and/or chalcocite grains. Bornite hosts a significant proportion of the Cu content

of this sample, occurring as discrete liberated grains and as intergrowths with one or more of chalcocite, chalcopyrite, transparent gangue and magnetite. Valleriite may partially or significantly replace the bornite. Chalcocite is present in lesser, but nevertheless significant amounts, largely occurring as intergrowths with one or more of chalcopyrite, bornite and valleriite.

Accessory Minerals

Baddelyite is a common accessory mineral, occurring as rounded grains or euhedral crystals that commonly exhibit some degree of fracturing. The baddelyite is often associated with a discrete U-Th-bearing oxide, probably uranothorianite (ideally (U, Th)O_2) and rare-earth-bearing minerals including monazite (ideally (Ce, La, Nd, Th)PO_4). Other accessory minerals observed in minor amounts include pyrite, siderite and rutile.

Appendix VI: Metal precipitation

The aim of this work was to examine the copper and iron precipitation during the bioleaching of the chalcopyrite concentrate when different initial pHs were used (i.e. pH 1.5 and pH 2.8). All experiments were carried out in a 250 ml shake flask containing 45 ml of ATCC 64 medium (without ferrous ions). These flasks were then autoclaved at 121 °C for 15 minutes. The experiments were done by employing cell suspensions containing 10 % inoculum (corresponding to bacterial concentration of about 2.5 x 10^9- 3.8 x 10^9 cells/ml), pulp density of 5 % (w/v) chalcopyrite concentrate (+53, -75 μm) and a variety of initial pH values. These shake flasks were incubated at 30 °C and 100 rpm in a rotary shaker. The control experiments were set up by preparing a series of flasks with the same composition but without any bacteria. Two flasks were removed to provide duplicate samples for each data point. After determining the mass of the flasks, the loss of water due to evaporation was compensated by adding sterilised distilled water (ASTM E1357-90). The leaching solution was then filtered through filter paper (Whatman No. 1) to separate the solid phase from the liquid phase and the filtrate was then used to analyse the total iron and copper concentration.

The solids were left to dry in an oven at 45 °C for 1 day, and after that their weight was measured. Each sample was washed by 50 ml of 1N H_2SO_4 solution; the solution was then filtered through filter paper (Whatman No. 1) to separate the solid phase from the liquid phase and the filtrate was then used to analyse the total iron and copper concentration for metal precipitation.

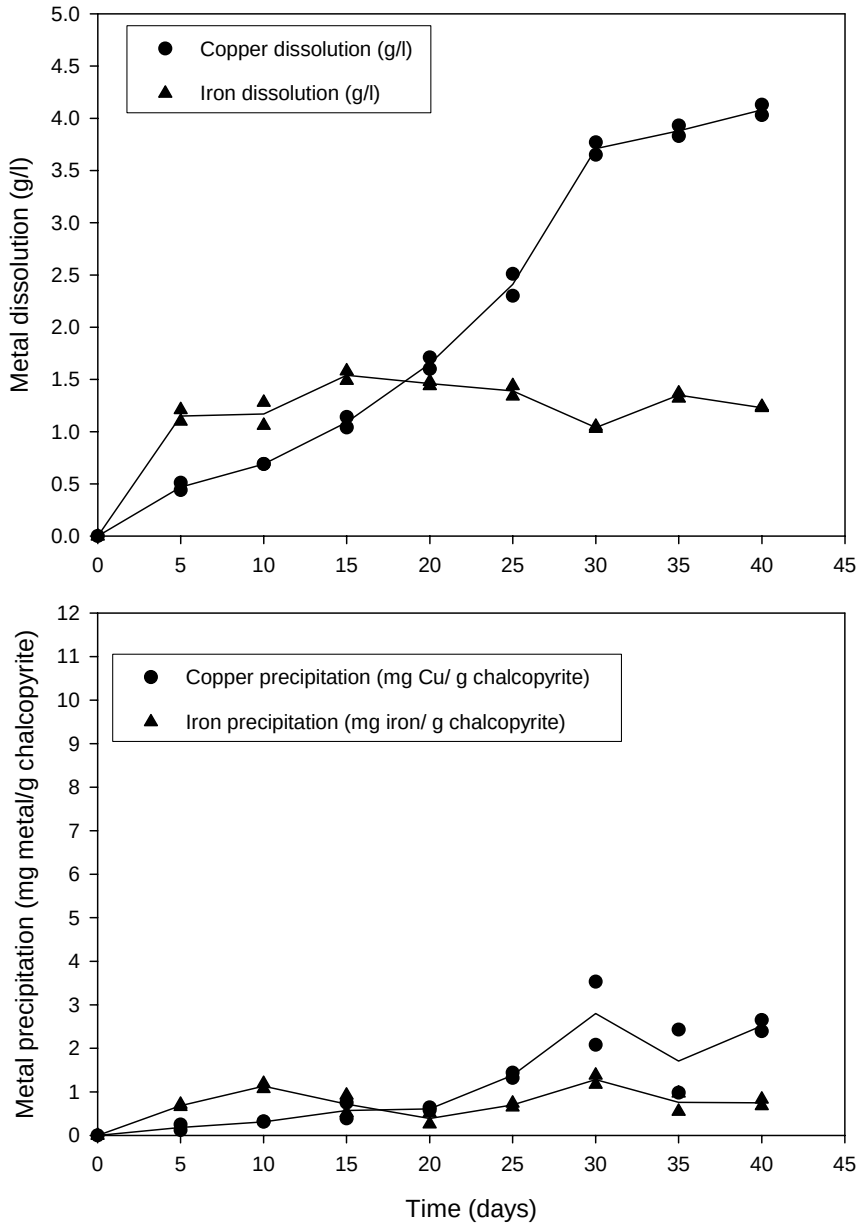

Figure IV.1 Bioleaching of chalcopyrite concentrate at 5% (w/v) pulp density, +53, -75 µm, initial pH 1.5 and 100 rpm

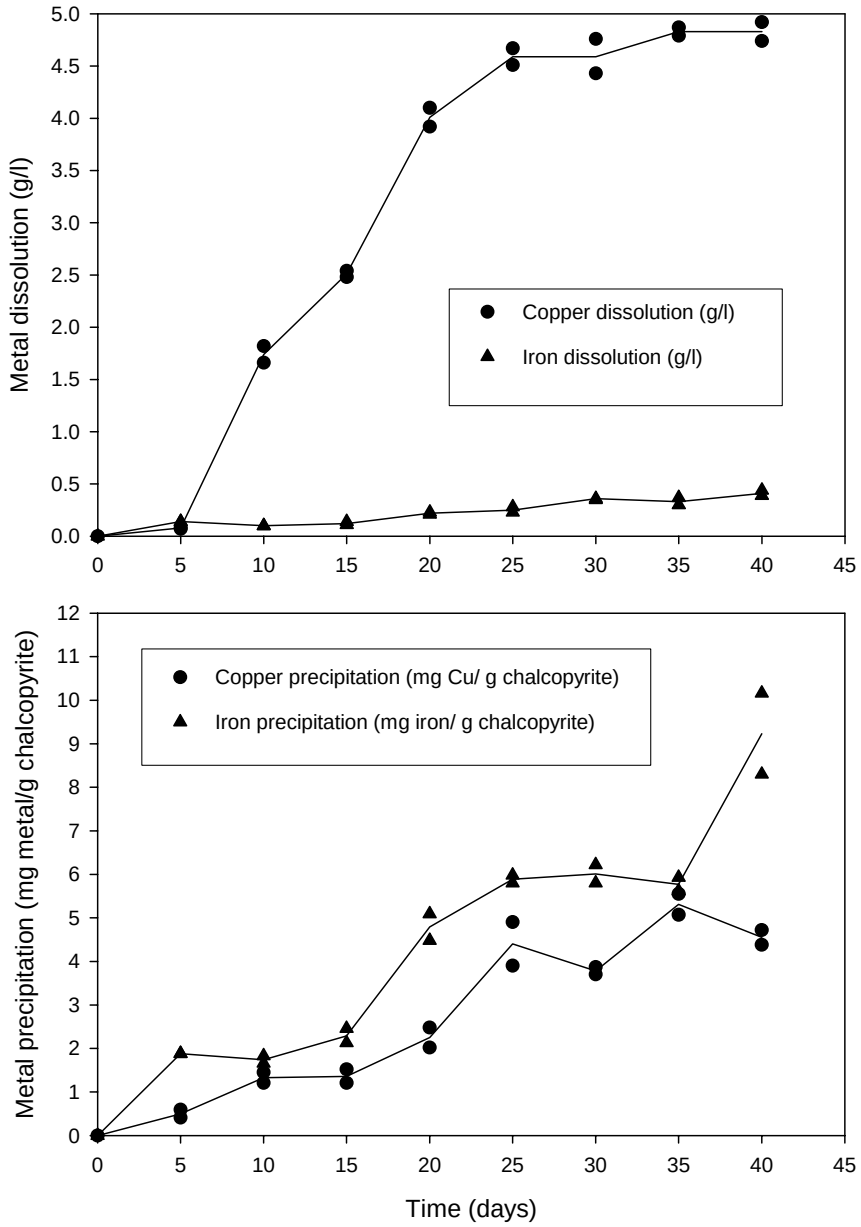

Figure IV.2 Bioleaching of chalcopyrite concentrate at 5% (w/v) pulp density, +53, -75 µm, initial pH 2.8 and 100 rpm

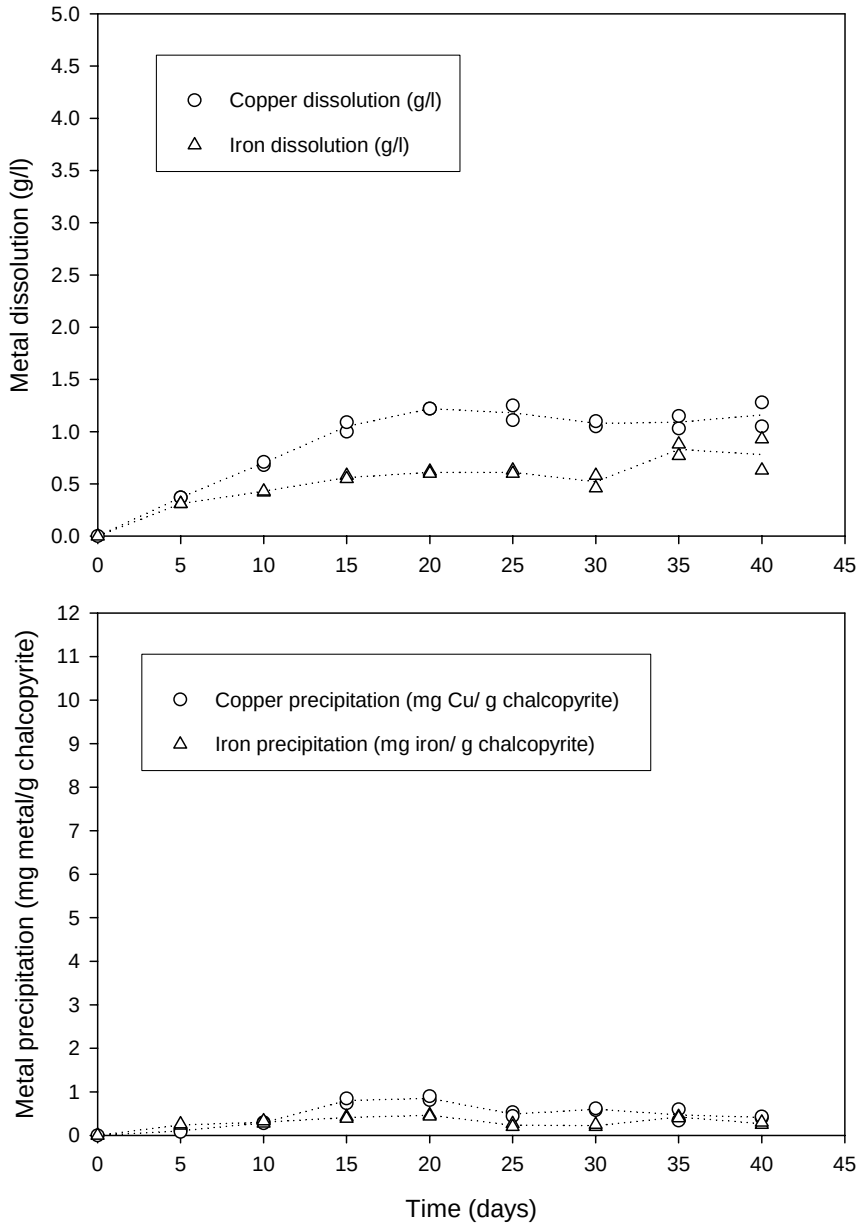

Figure IV.3 The control experiments (in the absence of bacteria) at 5% (w/v) the chalcopyrite concentrate, +53, -75 μm, initial pH 1.5 and 100 rpm

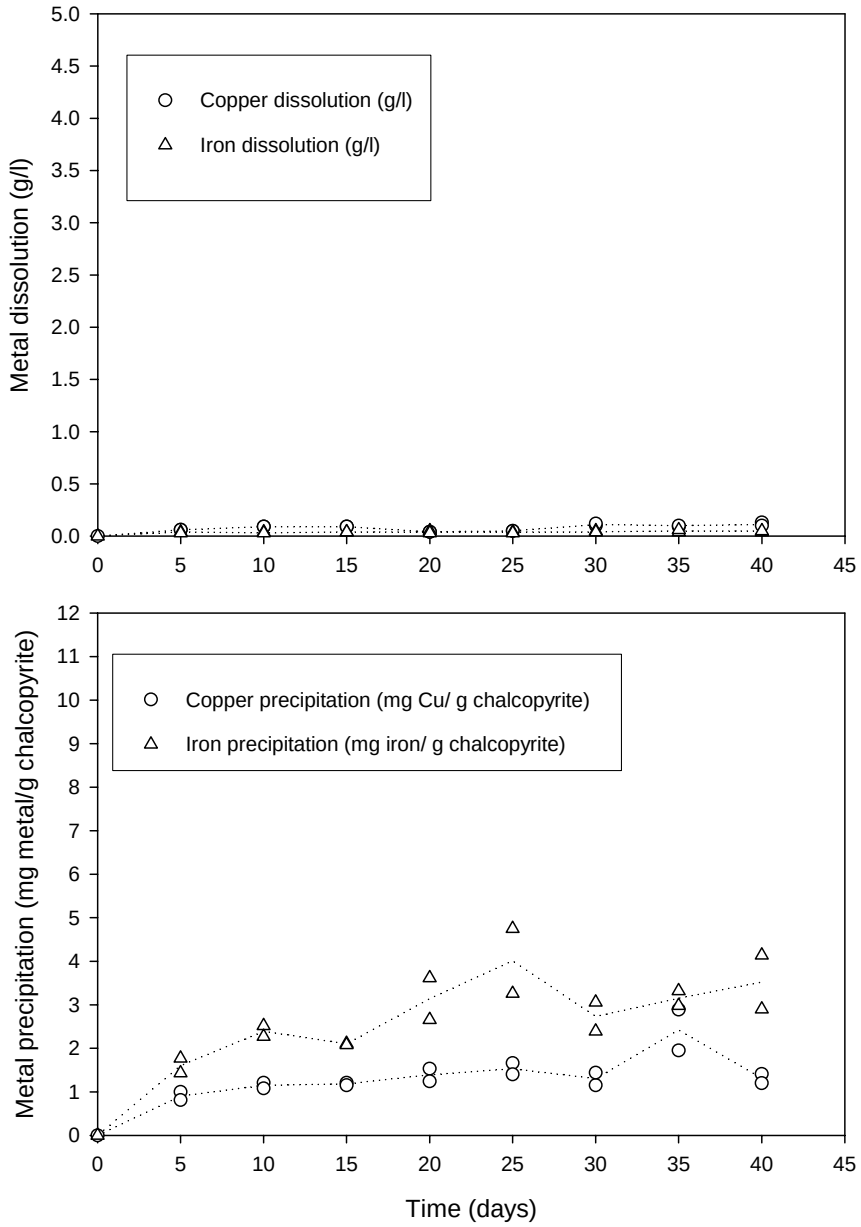

Figure IV.4 The control experiments (in the absence of bacteria) at 5% (w/v) the chalcopyrite concentrate, +53, -75 μm, initial pH 2.8 and 100 rpm

The bioleaching results and the control experiments (in the absence of bacteria) for different initial pHs are presented in Figures IV.1- IV.4. The bioleaching of chalcopyrite concentrate at an initial pH of 1.5 is shown in Figure IV.1, whilst the control experiments (in the absence of bacteria) at the same initial pH are presented in Figure IV.3. In addition, the bioleaching of chalcopyrite concentrate at the initial pH of 2.8 is shown in Figure IV.2, while the control experiment (in the absence of bacteria) is shown in Figure IV.4.

Overall, copper and iron precipitation was observed in all of the experiments including the control experiments. After bioleaching, the copper and iron precipitates were found to have similar trends for all pHs, however, the accumulation, for both copper and iron, after 40 days had greatly increased compared to the 5 day accumulation of metal precipitate. The initial pH of 2.8 had a very negative effect on the copper and iron precipitation (compared to the initial pH of 1.5); iron precipitation, especially, was found to be considerably greater, compared to its content in the solution. This was due to the fact that the formation of ferric hydroxide depends on the pH; at neutral pH and in the presence of oxygen, the ferric ion forms highly insoluble precipitates e.g. ferric hydroxide (Brock and Gustafson, 1976). Battaglia *et al*. (1994) also reported that at a low pH of 1.7, initial ferric ions were found to be precipitated at the beginning of their experiments.

In addition, the copper ions can precipitate to insoluble copper sulphide (CuS) (Stott *et*

al., 2000). The copper precipitation appeared to be slightly reduced from its metal dissolution, however, this finding resulted in a reduced percentage of copper extraction during the bioleaching process.

Since, the initial calculations of percent metal extraction were based solely on filtration without taking into account the metal precipitate, the percentage of metal extraction was underestimated. However, table VI.1 shows that the underestimations of copper and iron extraction were not significant enough to re-calculate the data of this work.

Table VI.1 A summarised version of the underestimations of copper and iron extraction

Time (days)	Initial pH 1.5				Initial pH 2.8			
	The underestimation of copper extraction (%)		The underestimation of iron extraction (%)		The underestimation of copper extraction (%)		The underestimation of iron extraction (%)	
	With bacteria	Without bacteria	With bacteria	Without bacteria	With bacteria	Without bacteria	With bacteria	Without bacteria
5	0.06	0.03	0.25	0.09	0.17	0.31	0.68	0.58
10	0.11	0.10	0.41	0.11	0.46	0.40	0.63	0.87
15	0.20	0.28	0.26	0.15	0.47	0.41	0.83	0.76
20	0.21	0.30	0.14	0.17	0.78	0.48	1.74	1.14
25	0.48	0.17	0.25	0.09	1.52	0.53	2.14	1.45
30	0.97	0.21	0.46	0.08	1.31	0.45	2.18	0.99
35	0.59	0.16	0.28	0.15	1.84	0.84	2.10	1.14
40	0.87	0.14	0.27	0.10	1.57	0.45	3.35	1.28

Appendix VII: Buffer

Table VII.1 HCl-KCl buffer of constant ionic strength (Dawson *et al*., 1969)

pH desired (at 25 °C)	Ionic strength of 0.1 M	
	Molarity of HCl	Molarity of KCl
1.11	0.10	0
1.15	0.09	0.01
1.20	0.08	0.02
1.26	0.07	0.03
1.33	0.06	0.04
1.41	0.05	0.05
1.50	0.04	0.06
1.63	0.03	0.07
1.80	0.02	0.08
2.11	0.01	0.09
2.41	0.005	0.095
2.8	0.002	0.098
3.11	0.001	0.099

Table VII.2 M^{c}IIvaine type buffer of constant ionic strength (Dawson *et al*., 1969)

pH desired (at 25 °C)	Composition g/l		g KCl added per litre of solution to produce ionic strength of	
	$Na_2HPO_4 \cdot 12\ H_2O$	Citric acid $\cdot\ H_2O$	1.0 M	0.5 M
2.2	1.43	20.6	74.5	37.2
2.4	4.44	19.7	72.7	35.4
2.6	7.80	18.7	71.5	34.2
2.8	11.35	17.7	70.2	32.9
3.0	14.7	16.7	68.7	31.4
3.2	17.7	15.8	67.6	30.3
3.4	20.4	15.0	66.2	28.9
3.6	21.5	14.2	64.9	27.6
3.8	25.4	13.6	64.0	26.7
4.0	27.6	12.9	62.8	25.5
4.2	29.7	12.3	61.7	24.4
4.4	31.6	11.7	60.4	23.1
4.6	33.4	11.2	58.9	21.6
4.8	35.3	10.7	57.2	19.9
5.0	36.9	10.2	55.5	18.2
5.2	38.4	9.75	53.8	16.5
5.4	40.0	9.29	52.1	14.8
5.6	41.5	8.72	50.6	13.3
5.8	43.3	8.32	49.5	12.2
6.0	45.2	7.74	48.9	11.6
6.2	47.5	7.12	47.9	10.6
6.4	49.6	6.47	46.9	9.62
6.6	52.1	5.72	45.8	8.50
6.8	55.4	4.79	44.5	7.23
7.0	58.9	3.70	42.7	5.44
7.2	62.3	2.74	40.4	3.10
7.4	65.0	1.91	38.2	0.488
7.6	67.2	1.35	36.0	-
7.8	68.6	0.893	34.3	-
8.0	69.6	0.589	32.9	-

Appendix VIII: Adsorption results

100 rpm			
Int. Cell (cells/m3)	Free cell XL (cells/m3)	Adsorbed cell (cells/m3)	% Adsorption
2.57E+15	7.02E+14	1.87E+15	73
2.63E+15	7.05E+14	1.93E+15	73
2.74E+15	7.22E+14	2.02E+15	74
2.62E+15	7.03E+14	1.92E+15	73
2.64E+15	7.08E+14	1.93E+15	73
9.80E+14	1.57E+14	8.23E+14	84
1.02E+15	1.59E+14	8.61E+14	84
1.12E+15	1.58E+14	9.62E+14	86
9.60E+14	1.56E+14	8.04E+14	84
1.02E+15	1.58E+14	8.63E+14	85
1.55E+15	2.78E+14	1.27E+15	82
1.54E+15	2.77E+14	1.26E+15	82
1.53E+15	2.75E+14	1.26E+15	82
1.54E+15	2.75E+14	1.27E+15	82
1.54E+15	2.76E+14	1.26E+15	82
3.12E+15	8.63E+14	2.26E+15	72
3.22E+15	8.65E+14	2.36E+15	73
3.11E+15	8.74E+14	2.24E+15	72
3.15E+15	8.68E+14	2.28E+15	72
3.15E+15	8.68E+14	2.28E+15	72
2.08E+15	4.90E+14	1.59E+15	76
2.12E+15	4.87E+14	1.63E+15	77
2.03E+15	4.91E+14	1.54E+15	76
2.05E+15	5.02E+14	1.55E+15	76
2.07E+15	4.93E+14	1.58E+15	76
5.20E+14	6.72E+13	4.53E+14	87
5.17E+14	6.81E+13	4.49E+14	87
5.05E+14	6.76E+13	4.37E+14	87
5.02E+14	6.71E+13	4.35E+14	87
5.11E+14	6.75E+13	4.44E+14	87

300 rpm			
Int. Cell (cells/m3)	Free cell XL (cells/m3)	Adsorbed cell (cells/m3)	% Adsorption
2.77E+15	1.71E+15	1.06E+15	38
2.73E+15	1.72E+15	1.01E+15	37
2.72E+15	1.73E+15	9.90E+14	36
2.72E+15	1.70E+15	1.02E+15	38
2.74E+15	1.72E+15	1.02E+15	37
9.26E+14	4.37E+14	4.89E+14	53
9.20E+14	4.20E+14	5.00E+14	54
9.15E+14	4.32E+14	4.83E+14	53
9.34E+14	4.26E+14	5.08E+14	54
9.24E+14	4.29E+14	4.95E+14	54
1.60E+15	8.55E+14	7.40E+14	46
1.58E+15	8.72E+14	7.08E+14	45
1.61E+15	8.59E+14	7.51E+14	47
1.58E+15	8.22E+14	7.53E+14	48
1.59E+15	8.52E+14	7.38E+14	46
3.45E+15	2.35E+15	1.10E+15	32
3.68E+15	2.50E+15	1.18E+15	32
3.65E+15	2.48E+15	1.17E+15	32
3.75E+15	2.52E+15	1.23E+15	33
3.63E+15	2.46E+15	1.17E+15	32
1.92E+15	1.12E+15	8.00E+14	42
1.85E+15	1.09E+15	7.63E+14	41
1.88E+15	1.10E+15	7.80E+14	41
1.98E+15	1.18E+15	8.00E+14	40
1.91E+15	1.12E+15	7.86E+14	41
7.30E+14	3.18E+14	4.12E+14	56
7.27E+14	3.06E+14	4.21E+14	58
7.15E+14	3.12E+14	4.03E+14	56
7.12E+14	3.10E+14	4.02E+14	56
7.21E+14	3.12E+14	4.10E+14	57

Int. = Intial